# Laboratory Medicine

November 2022 Vol 53 No 6 Pgs 543–651

labmedicine.com

*Laboratory Medicine* (ISSN 0007-5027), is published 6 times per year (bimonthly). Periodicals Postage paid at Chicago, IL and additional mailing offices. POSTMASTER: Send address changes to *Laboratory Medicine*, Journals Customer Service Department, Oxford University Press, 2001 Evans Road, Cary, NC 27513-2009.

**SUBSCRIPTION INFORMATION:** Annually for North America, $173 (electronic) or $225 (electronic and print); single issues for individuals are $29 and for institutions $64. Annually for Rest of World, £112/€159 (electronic) or £144/€206 (electronic and print); single issues for individuals are £19/€27 and for institutions £40/€57. All inquiries about subscriptions should be sent to Journals Customer Service Department, Oxford Journals, Great Clarendon Street, Oxford OX2 6DP, UK, Tel: +44 (0) 1865-35-3907, e-mail: jnls.cust.serv@oup.com. In the Americas, please contact Journals Customer Service Department, Oxford Journals, 2001 Evans Road, Cary, NC 27513. Tel: 800-852-7323 (toll-free in USA/Canada) or 919-677-0977, e-mail: jnlorders@oup.com.

**MEMBERSHIP INFORMATION:** The ASCP membership fees for pathologists are as follows: fellow membership is $349; fellow membership plus 1-year unlimited online CE is $519; 2-year fellow membership is $675; and 2-year fellow membership plus 2-year unlimited online CE is $1,015. The ASCP membership fees for laboratory professionals are as follows: newly certified membership is $49; annual membership is $99; annual membership plus 1-year unlimited online CE is $129; 3-year membership is $349. All inquiries about membership should be sent to American Society for Clinical Pathology, 33 West Monroe Street, Suite 1600, Chicago, IL 60603, Tel: 312-541-4999, e-mail: ascp@ascp.org.

**CLAIMS:** Publisher must be notified of claims within four months of dispatch/ order date (whichever is later). Subscriptions in the EEC may be subject to European VAT. Claims should be made to Laboratory Medicine, Journals Customer Service Department, Oxford University Press, 2001 Evans Road, Cary, NC 27513, Tel: 800-852-7323 (toll-free in USA/Canada) or 919-677-0977, e-mail: jnlorders@oup.com.

*Laboratory Medicine* is published bimonthly by Oxford University Press (OUP), on behalf of the ASCP, a not-for-profit corporation organized exclusively for educational, scientific, and charitable purposes. Devoted to the continuing education of laboratory professionals, *Laboratory Medicine* features articles on the scientific, technical, managerial, and educational aspects ofthe clinical laboratory. Publication of an article, column, or other item does not constitute an endorsement by the ASCP of the thoughts expressed or the techniques, organizations, or products described therein. *Laboratory Medicine* is indexed in the following: MEDLINE/PubMed, Science Citation Index, Current Contents—Clinical Medicine, and the Cumulative Index to Nursing and Allied Health Literature.

*Laboratory Medicine* is a registered trademark. Authorization to photocopy items for internal and personal use, or the internal and personal use of specific clients, is granted by ASCP Press for libraries and other users registered with the Copyright Clearance Center (CCC) Transactional Reporting Service, provided that the base fee of USD 15.00 per copy is paid directly to the CCC, 222 Rosewood Drive, Danvers, MA 01923, 978.750.8400. In the United States prior to photocopying items for educational classroom use, please also contact the CCC at the address above.

**Printed in the USA**









ASCP
**Laboratory Medicine**
33 West Monroe Street, Suite 1600
Chicago, IL 60603
T: 312-541-4999
F: 312-541-4750

Laboratory Medicine

November 2022
Vol 53, No 6
p. 543-651

## OVERVIEW



## SCIENCE



## CORRECTION



*The following are online-only papers that are available as part of Issue 53(6) online.*




**ON THE COVER:** Historically, RNA was thought to exclusively provide a template for the synthesis of proteins. However, it is becoming increasingly clear that RNA has an essential role in regulating gene expression. About 3 decades ago, small noncoding fragments of single-stranded RNA consisting of approximately 22 nucleotides each were discovered and given the name "micro-RNA," customarily abbreviated miRNA. Since then, research has demonstrated that these RNA fragments bind to complementary sequences in messenger RNA to halt transcription, thereby regulating gene expression. A host of miRNAs have been characterized, and dysregulation of miRNA expression has been associated with numerous diseases, catalogued in an online database, miR2Disease. This has proved to be fertile ground in the hunt for biochemical markers of disease, and *Laboratory Medicine* receives many manuscripts on the subject. One such paper, in this issue, explores the relationship between a miRNA designated miR-149 and progression of hepatocellular carcinoma.

OVERVIEW

# Metabolomics: A New Tool to Reveal the Nature of Diabetic Kidney Disease

*Guoqing Huang,[1,2] Mingcai Li, PhD,[2] Yan Li, PhD,[1,2,a] Yushan Mao, PhD[1,*,a]*

[1]Department of Endocrinology, The Affiliated Hospital of Medical School, Ningbo University, Ningbo, China, [2]School of Medicine, Ningbo University, Ningbo, China; *To whom correspondence should be addressed. maoyushan@nbu.edu.cn [a]Yushan Mao and Yan Li contributed equally to this work.

**Keywords:** metabolomics, diabetic kidney disease, biological markers, early diagnosis, disease prognosis, pathogenesis

**Abbreviations:** DKD, diabetic kidney disease; DM, diabetes mellitus; ESRD, end-stage renal disease; eGFR, estimation of glomerular filtration rate; UACR, urine albumin creatinine ratio; NMR, nuclear magnetic resonance; LC/GC, liquid chromatography/gas chromatography; MS, mass spectrometry; PLS-DA, partial least squares-discriminant analysis; PCA, principal component analysis; VIP, variable importance of projection; NO, nitric oxide; T1DM, type 1 diabetes mellitus; OAT, organic anion transporter; HR, hazard ratio

*Laboratory Medicine* 2022;53:545–551; https://doi.org/10.1093/labmed/lmac041

## ABSTRACT

Metabolomics is a field of systems biology that draws on the scientific methods of other groups to qualitatively or quantitatively characterize small molecule metabolites in organisms, revealing their interconnections with the state of the organism at an overall relative macroscopic level. Diabetic kidney disease (DKD) is well known as a chronic metabolic disease, and metabolomics provides an excellent platform for its clinical study. A growing number of metabolomic analyses have revealed that individuals with DKD have metabolic disturbances of multiple substances in their bodies. With the continuous development and improvement of metabolomic analysis technology, the application of metabolomics in the clinical research of DKD is also expanding. This review discusses the recent progress of metabolomics in the early diagnosis, disease prognosis, and pathogenesis of DKD at the level of small molecule metabolites in vivo.

Diabetes mellitus (DM) is one of the chronic noncommunicable diseases that seriously endangers human life and health, affects the quality of life of patients, and increases the economic burden of countries. According to the latest data from the International Diabetes Federation, there were about 463 million people with DM worldwide in 2019, and it was expected to reach 700 million by 2045.[1] Diabetic kidney disease (DKD) is not only one of the most common chronic microvascular complications of diabetes but is also an important cause of end-stage renal disease (ESRD). Some research shows that about 30% to 50% of ESRD worldwide is due to DKD.[2] Alicic et al[3] revealed that the prevalence of DKD in diabetic patients to be 40%. Current clinical indicators used to diagnose DKD include estimation of glomerular filtration rate (eGFR) and urine albumin creatinine ratio (UACR), although they have limited high sensitivity and specificity. The eGFR decreases significantly only when severe renal damage occurs in patients with DKD because the blood creatinine, which is used to calculate the eGFR, drops significantly only when the eGFR is below 50% of normal. Increased UACR is considered a characteristic manifestation of renal damage, but some studies have shown that a significant proportion of DKD patients do not have albuminuria.[4,5] In terms of treatment, despite the fact that the number of patients with DM and DKD is increasing annually, there are very limited therapies available to slow down or reverse the progression. The main therapeutic strategies for DKD include strict blood pressure and glycemic control, antidiabetic drugs, etc; however, these measures only slow down the progression of DKD, and there is no way to reverse DKD so far. This requires us to examine DKD from a new perspective, deepen the mechanism research, discover more biomarkers that can help early diagnosis, and develop new treatment strategies.

DKD is a chronic metabolic disease that often causes metabolic disorders of water, electrolytes, proteins, and lipids in the body. The dynamics of small molecule metabolites (relative molecular mass <1000) in an organism reflect the physiological or pathological state of the organism in real time. Metabolomics gives us a new perspective on DKD, which would help us to deepen our mechanistic studies, discover more biological markers for early diagnosis, and develop new therapeutic strategies.

## Metabolomics

Metabolomics originated in the 1970s,[6] when Professor Nicholson[7] proposed the concept of "metabolomics" and drew up a metabolic fingerprint by scanning body fluids through nuclear magnetic resonance (NMR) techniques. With the completion of the sequencing of the Human Genome Project marking the advent of the postgenomic era, more and more research is focusing on the functional analysis of genomes. The emergence of metabolomics bridges the gap between genes and disease phenotypes and provides a possibility for the functional analysis of genomes. Metabolomics mainly focuses on the quantitative

analysis of small molecule metabolites in organisms by following the research ideas of genomics to find the relationship between metabolites and physiological/pathological changes in the organism. Currently, metabolomics, genomics, transcriptomics, and proteomics have become important components of systems biology. The core concept of metabolomics is to use the metabolic state of the organism to reflect its overall functional status. It allows a comprehensive analysis of the dynamics of endogenous and exogenous compounds in the body and systematically reflects the expression levels of genes and proteins in the body in response to various stimuli. Many metabolic substances in the body have been maintained in a relatively balanced and stable state for a long time, which is regulated and influenced by genes, diet, environmental factors, and intestinal microorganisms; once this balance is disrupted, it would herald the onset or development of disease.[8] Metabolomics, as an emerging omics discipline, has a wide range of applications in the fields of plants, food, disease diagnosis, and microbiology.[9] Meanwhile, it has a multidisciplinary intersection and is closely related to organic chemistry, analytical chemistry, chemometrics, informatics, and biology.[10,11] Metabolomics is positioned downstream of proteomics and belongs to the continuation of the central dogma, which allows the mapping of body fluids (plasma, urine, tissue fluids, etc) and metabolic profiles to dynamically reflect the function and state of the organism. Compared with transcriptomics and proteomics, metabolomics has its own unique advantages: (1) as a continuation of the central dogma, it can amplify small changes at the gene level; (2) as the end product of gene expression and body metabolism, the number of metabolites in the body is much smaller than the number of genes and proteins; (3) as a relatively macroscopic representation of the body's state, metabolomics is closer to the phenotype of disease and allows us to visualize the current physiological or pathological state of the organism; (4) the chemical composition of metabolites is similar across species, and the metabolomic analysis techniques used are more generalizable.[12]

In general, the main processes of metabolomics research include sample collection and preparation, sample testing, metabolic data collection, and data analysis. Currently, the samples used for metabolomics are mainly from blood, urine, and tissue fluids, and a sufficient number of representative samples are usually required to reduce individual differences. Different analysis platforms require different sample preparation processes; for example, nuclear magnetic resonance (NMR) does not require much processing of the sample and is noninvasive and nondestructive,[13] while liquid chromatography/gas chromatography (LC/GC) coupled with mass spectrometry (MS) may require derivatization to increase the volatility of the sample.[14] Data analysis is the most critical part of performing metabolomics studies. The sample testing process would generate a large amount of fragmented data. In order to extract potentially valuable information from these data, it is necessary to reduce the dimensionality of the data with the help of some multivariate mathematical statistical analysis methods. Partial least squares-discriminant analysis (PLS-DA), principal component analysis (PCA), neural networks, cluster analysis, and support vector machines are the most commonly used data analysis methods in metabolomics.[12,15] The appropriate data analysis method is selected according to the specific experimental design scheme as well as the experimental results. For example, PCA can be chosen when the results are more different between groups, while PLS-DA is preferred when the results are less different between groups and the sample size is more different between groups.[15] On the basis of PLS-DA, characteristic variables of diseases is then screened out by the variable importance of projection (VIP), with the screening criterion of VIP >1.[16] In turn, this would then be used to construct machine learning models and regression models for early identification and diagnosis of diseases. In addition, metabolic pathway enrichment analysis based on characteristic variables can find the specific metabolic pathways associated with diseases, which would contribute to the study of pathogenesis. MetaboAnalyst (4.0), the R-code-based online analysis tool for metabolomics, provides a convenient one-stop shop for metabolomics data analysis (screening of characteristic markers, cluster analysis, and enrichment of metabolic pathways), interpretation, and integration with other omics data.[17] The basic flow chart of metabolomics research is shown (**FIGURE 1**).

## Metabolomics Analysis Platform

Given that metabolomics requires the detection of large samples, high-throughput analytical platforms play a crucial role in this. Currently, metabolomics typically employs NMR, MS, LC/GC, and coupling of various analytical platforms to analyze and map metabolites.[18] The coupling of these techniques can improve the resolution, sensitivity, and selectivity during sample analysis and help to map more metabolic profiles. Different metabolomics analysis platforms have their own unique features[14,19–22]; the characteristics of the main metabolomics analysis platforms are shown in **TABLE 1**.

## Early Diagnosis of DKD Based on Metabolomics

Although DKD still faces great challenges in terms of treatment, early diagnosis of DKD has become a promising research direction. The gold standard for the diagnosis of DKD is renal puncture biopsy, but this invasive test is difficult for patients to accept in the clinical setting. At present, DKD is mostly diagnosed clinically, and the main diagnostic criteria are eGFR and UACR. As mentioned above, eGFR and UACR still have some limitations as diagnostic criteria for DKD, which forces us to search for biological markers with higher sensitivity and specificity. Metabolomics, with its high-throughput detection technology and unique data processing methods, is uniquely positioned to find specific biological markers (**TABLE 2**).[23–36]

Currently, most of the biological markers identified based on metabolomics that contribute to the early diagnosis of DKD are focused on fatty acids, amino acids, lipids, and nucleotide metabolites. Fatty acids have an important impact on the metabolism of the body, and fat mobilization can increase the level of nitric oxide (NO) accumulation in the matrix, ultimately leading to increased glomerulosclerosis.[37] Some studies have shown that pathologically elevated saturated fatty acids have a strong toxic effect on cells,[34] which in turn promotes the development and progression of diabetes.[28] The role of unsaturated fatty acids in DKD is still a controversial topic. Some studies have shown that oleic acid ameliorates palmitic acid-induced endoplasmic reticulum stress, inflammation, and insulin resistance[38,39]; however, other researchers suggested that high levels of oleic acid cause endoplasmic reticulum stress and apoptosis, causing proliferation or damage to glomerular thylakoid cells.[40,41] Phospholipids are key components of the phospholipid bilayer of biological membranes, which includes glycerophospholipids and sphingolipids. Peng et al[42] showed that the expression levels of phosphatidylethanolamine ($m/z$ = 750), phosphatidylglycerol ($m/z$ = 747), and phosphatidylcholine ($m/z$ = 802) were lower in DKD

**FIGURE 1.** Basic flow chart of metabolomics research. PLS-DA, partial least squares-discriminant analysis.

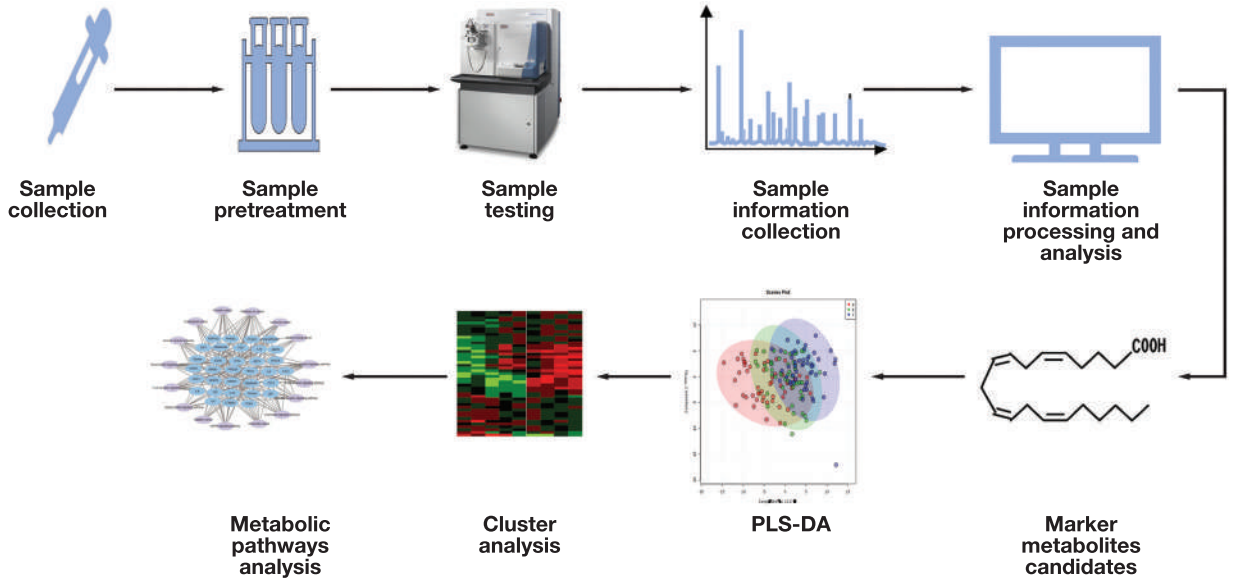


**TABLE 1.** The Characteristics of the Main Metabolomics Analysis Platforms

| Analysis Platform | Advantages | Disadvantages |
|---|---|---|
| NMR | Simple handling of samples; noninvasive and unbiased detection and analysis; lower cost | High investment in equipment; relatively low detection sensitivity; narrow dynamic detection range; difficult to detect metabolic small molecules with relatively large differences in concentration simultaneously |
| MS | Excellent repeatability and objectivity; high sensitivity and wide detection range; rapid analysis and identification of multiple chemicals simultaneously | Preparation of large quantities of samples; relatively high daily costs; requires some knowledge of the metabolic small molecules being tested |
| LC-MS | High sensitivity; no need for high temperature; no derivatization of the sample is required; relatively simple sample preparation compared to GC-MS | Poor repeatability; database not yet robust |
| GC-MS | High precision, sensitivity and durability; excellent performance in the analysis of volatile substances; library of standard spectra available | Sample derivatization; more cumbersome sample preparation; difficult to use for difficult volatiles |

*GC-MS, gas chromatography-mass spectrometry; LC-MS, liquid chromatography–mass spectrometry; MS, mass spectrometry; NMR, nuclear magnetic resonance.*

patients than in healthy controls. In addition, Zhu et al[29] identified plasma phospholipids in T2DM and DKD patients based on an HPLC-ESI/MS platform and screened 18 phospholipids (VIP >1, $P < .05$) as potential biomarkers by PLS-DA data analysis, including 2 novel biomarkers, phosphatidylinositol ($m/z$ = 909) and sphingomyelin ($m/z$ = 801). Several amino acid metabolic abnormalities were also observed in DKD individuals. Glutamate has an important role in regulating insulin secretion and maintaining glucose homeostasis in the body,[43] which has been suggested as a potential biological marker for early diagnosis of DKD.[34] In addition, plasma tryptophan levels were found to be positively correlated with estimated glomerular filtration rate in studies,[31] while its metabolite, kynurenine, was negatively correlated with eGFR.[30]

## Prognostic Risk Assessment for DKD Based on Metabolomics

Metabolites in the organism are constantly changing dynamically in response to internal and external factors, and fluctuations in the metabolic profile suggest changes in the physiological/pathological state of the organism. By mapping and analyzing the metabolic profile of the organism, the disease progression and prognosis would be better assessed. Tavares et al[44] investigated the role of plasma metabolites in the assessment of DKD prognosis by an untargeted metabolomics approach. The results of the research showed that an adverse event (death, doubling of blood creatinine, or dialysis treatment) occurred in 30.3% of DKD patients during 2.5 years of follow-up; univariate Cox regression analysis showed that 1,5-anhydroglucitol (hazard ratio (HR): 0.10, 95% CI: 0.02–0.63, $P$ =.01), norvaline (HR: 0.01, 95% CI: 0.001–0.4, $P$ =.01), and aspartic acid (HR: 0.12, 95% CI: 0.02–0.64, $P$ =.01) were negatively associated with the occurrence of DKD adverse events. Niewczas et al[45] conducted a prospective study with 158 patients with type 1 diabetic kidney disease followed up for a long period of time (median follow-up, 11.5 years). During the follow-up period, 99 patients (63%) progressed to ESRD; for the shorter the duration of diabetes, the younger the age, and the poorer the glycemic control, the faster the decline in renal function.[45] To further find the independent risk factors for the progression of DKD, they examined the serum of patients by high-throughput metabolomics technology, and the results revealed that 7 modified metabolites, including C-glycosyltryptophan, pseudouridine, O-sulfotyrosine, N-acetylthreonine, N-acetylserine, N6-carbamoylthreonyladenosine, and N6-acetyllysine, were independent risk factors for the progression of DKD to ERSD.[45] Another comprehensive study of plasma metabolic profiles in patients with type 2 diabetes mellitus showed that certain

**TABLE 2. Biological Markers in the Early Diagnosis of Diabetic Kidney Disease (DKD)**

| Researchers | Country | Platform | Species | Sample | Major Differential Metabolites | Metabolic Pathways |
|---|---|---|---|---|---|---|
| Peng et al[23] | China | LC-MS | Human | Plasma | 5-HET, LTB4, 5,6-DHET, 14,15-DHET, and 9,10-diHOME | Lipoxygenase metabolites and cytochrome P450s metabolic pathway |
| Devi et al[24] | India | HPLC-MS | Human | Plasma | Acyl ethanolamides, acetylcholine, monoacylglycerols, and cortisol | |
| Gordin et al[25] | USA | LC-MS | Human | Plasma | Sorbitol, aconitate, and fumarate | Glycolytic, polyol, and tricarboxylic acid cycle pathways |
| Liu et al[26] | China | HPLC-MS | Human | Urine | 5-Hydroxyindoleacetic acid, deoxycholic acid, nutriacholic acid | Tryptophan metabolism, bile acid metabolism, and glycine metabolism pathway |
| Ng et al[27] | Singapore | GC-MS | Human | Urine | Octanol, oxalic acid, phosphoric acid, benzamide, creatinine, and N-acetylglutamine | |
| Tan et al[28] | Singapore, | LC-MS | Human | Plasma | Glutamine, phenylacetylglutamine, 3-indoxyl sulfate, xanthine, and dimethyluric acid | |
| Zhu et al[29] | China | NPLC-TOF/MS | Human | Plasma | LPC (C18:2), PE (C16:0/18:1), PE (pC18:0/20:4), PI (C18:0/22:6), PS (C18:0/18:0), SM (dC18:0/20:2) | |
| Hirayama et al[30] | Japan | CE-TOF/MS | Human | Serum | Creatinine, aspartic acid, γ-butyrobetaine, citrulline, and symmetric dimethylarginine | |
| Zhang et al[31] | China | HPLC-MS | Human | Serum | L-Tryptophan, 5-hydroxyindoleacetic acid, indole-3-acetamide | Tryptophan metabolism pathway |
| Shao et al[32] | China | GC-TOF/MS | Human | Serum and urine | Serum: benzoic acid, fumaric acid, erythrose, fructose 6-phosphate, taurine, and L-glutamine.<br>Urine: D-glucose, L-valine, L-histidine, sucrose, gluconic acid, glycine, and oxalic acid | Serum: 9 metabolic pathways<br>Urine: 12 metabolic pathways |
| Zhang et al[33] | China | UPLC-MS | Human | Serum | Hexadecanoic acid (C16:0), linolelaidic acid (C18:2N6T), linoleic acid (C18:2N6C), piperidine, and azoxystrobin acid | linoleic acid metabolism, aminoacyl-tRNA biosynthesis, and arginine metabolism |
| Du et al[34] | China | GC/LC–MS | Rat | Plasma | Oleic acid, glutamate, and guanosine | |
| Ma et al[35] | China | UPLC-MS | Human | Urine | Dihydrouracil, ureidopropionic acid, and pantothenic acid | Pantothenate and coenzyme A biosynthesis pathway |
| Dai et al[36] | China | UPLC-TOF/MS | Rat | Serum and urine | Serum: guanosine triphosphate, lysoPC(18:1), retinyl ester, etc<br>Urine: aminoadipic acid, adenine, and 2-oxo-4-methylthiobutanoic acid, etc | Serum: purinem, alanine, aspartate, and glutamate metabolism<br>Urine: purine, lysine degradation, and sphingolipid metabolism |

*GC-MS, gas chromatography-mass spectrometry; HPLC-MS, high performance liquid chromatography-mass spectrometry; LC-MS, liquid chromatography–mass spectrometry.*

metabolites (amino acids and their derivatives) predicted the onset of ESRD approximately 10 years earlier and independent of baseline albuminuria and renal function.[46] Tofte et al[47] illustrated that alterations in plasma metabolites (particularly polyols and branched-chain amino acids) were associated with future renal impairment in the type 1 diabetes mellitus (T1DM) population; ribonucleic acid was associated with a higher risk, while the amino acids isoleucine, leucine, and valine were associated with a lower risk of combined renal endpoint (≥30% decline in eGFR, ESRD, and all-cause mortality). Acylcarnitine is essential for intracellular energy metabolism and plays an essential role in the β-oxidation metabolism of fatty acids. Research has shown impaired fatty acid oxidation in patients with DKD; the abnormal plasma acylcarnitine levels could be a reflection of the degree of disease progression.[48,49] It has also been shown that metabolites such as uremic toxin and carnitine were strongly associated with the progression of microproteinuria in patients with T1DM.[50] Looker et al[51] showed that 14 markers, such as symmetrical dimethylarginine, uracil, acylcarnitine, and hydroxyproline, were associated with a rapid decline in renal function in patients with T2DM, suggesting that their combination might greatly improve the prediction of renal function in the future (**TABLE 3**).[44–47,49–51]

## Study of the Pathogenesis of DKD on Metabolomics

Metabolic profiles represent the complete collection of metabolites in an organism, and perturbations in metabolic profiles may help to reveal the pathogenesis of the disease early. The convergence of multiple omics plays an important role in the study of DKD pathogenesis. Recent studies have shown that a novel oral hypoglycemic agent (SGLT-1) could act as a renoprotective agent by inhibiting glucose reabsorption and reducing renal tubular energy expenditure,[52–54] which laterally suggested an energy imbalance in the renal tissues of DKD patients. Sharma et al,[55] through urinary metabolomics studies in DKD patients, identified 13 metabolites whose expression was significantly reduced, and the reduction in organic anion expression was associated with the downregulation of the expression of the organic anion transporter (OAT) gene in DKD patients. Bioinformatics analysis revealed that 12 of the 13 differentially expressed metabolites were associated with mitochondrial metabolism and that the expression of PGC1α, a major regulator of mitochondrial activity, was significantly lower in the renal tissue of DKD patients (overall inhibition of mitochondrial activity).[55] Multiple metabolic pathways (pentose phosphate, purine and pyrimidine metabolism, hexosamine biosynthesis, and tricarboxylic acid cycle) were overactivated, and mitochondrial complex 1 activity was enhanced in DKD mouse models (streptozotocin-induced),

**TABLE 3. Prognostic Markers in Diabetic Kidney Disease**

| Researchers | Country | Platform | Species | Sample | Major Differential Metabolites |
|---|---|---|---|---|---|
| Tavares et al[44] | Brazil | GC-MS | Human | Plasma | 1,5-anhydroglucitol, norvaline, and aspartic acid |
| Niewczas et al[45] | USA | GC/LC-MS | Human | Serum | C-glycosyltryptophan, pseudouridine, O-sulfotyrosine, N-acetylthreonine, N-acetylserine, N6-carbamoylthreonyladenosine and N6-acetyllysine |
| Niewczas et al[46] | USA | Metabolon | Human | Plasma | Essential amino acids and their derivatives, acylcarnitines |
| Tofte et al[47] | Denmark | GC-TOF/ MS | Human | Serum | Ribonic acid, myo-inositol, hydroxy butyrate 3,4-dihydroxybutanoic acid, and branched chain amino acids |
| Afshinni et al[49] | USA | MS | Human | Serum | Polyunsaturated triacylglycerols and C16-C20 acylcarnitines |
| Haukka et al[50] | Finland | UPLC-MS | Human | Serum | Erythritol, 3-phenylpropionate, and N-trimethyl-5-aminovalerate |
| Looker et al[51] | UK | LC-MS | Human | Serum | Symmetrical dimethylarginine, uracil, acylcarnitine, and hydroxyproline |

*GC-MS, gas chromatography-mass spectrometry; GC/LC-MS, gas chromatography/liquid chromatography-mass spectrometry; UPLC-MS, ultra-high performance liquid chromatography-mass spectrometry.*

while specific mitochondrial complex 1 inhibitors were effective in reducing glomerular and tubular injury through modulation of the body's metabolic state and oxidative stress.[56] Some scholars have reported abnormalities in fatty acid metabolism in DKD.[33] Saulnier et al[57] showed a correlation between urinary metabolites and renal structure in patients with DKD, where short-chain fatty acids in urine were associated with structural destruction of endothelial cells in the early stages of DKD. In addition, other studies have shown that defects in fatty acid oxidation play a key role in the development of renal fibrosis.[48] Multi-omics studies in DKD have revealed that accumulation of extracellular matrix, abnormal activation of the inflammatory microenvironment, and metabolic disturbances contributed to the development of glomerulosclerosis and tubulointerstitial fibrosis. Further integrative analysis revealed that linoleic acid metabolism and fatty acid β-oxidation are significantly inhibited in the pathogenesis and progression of DKD.[58] Carnitine is an important substance in the oxidative metabolism of fatty acids and protects against cellular oxidative stress from various sources[59]; indeed, Devi et al[24] showed abnormal carnitine metabolism in patients with DKD. The role of NADPH oxidase 4 in the development and progression of DKD is poorly understood. You et al[60] demonstrated the presence of abnormal tricarboxylic acid cycle-related metabolites in DKD mice and that NADPH oxidase 4 could cause an increase in ferredoxin levels. This in turn led to endoplasmic reticulum oxidative stress and increased expression of HIF-1α and TGF-β. Chinese medicines are increasingly used in the treatment of DKD, but the mechanism of action is not well understood. Studies in network pharmacology combined with metabolomics have shown that herbal medicines (shenyankangfu tablets) may improve insulin resistance by regulating the biosynthesis of unsaturated fatty acids and the metabolism of starch and sucrose.[61] Epigenetics has become more widely accepted in the pathogenesis of DKD.[62] High glucose conditions may alter the histone amino acid modification status (methylation, acetylation), causing changes in chromatin structure, facilitating the binding of transcription factors, and ultimately leading to the expression of genes associated with inflammation and fibrosis.[63] Epigenetic markers could not only lead to abnormal expression of metabolism-related genes[64] but may also predispose offspring to metabolic abnormalities and shortened lifespan.[65] A prospective cohort study by Niewczas et al[45] demonstrated that circulating levels of 7 modified metabolites (C-glycosyltryptophan, pseudouridine, O-sulfotyrosine, N-acetylthreonine, N-acetylserine, N6-carbamoylthreonyladenosine, and N6-acetyllysine) were associated with the rate of decline in renal function and the risk of ESRD. It has also been observed that elevated levels of serum modified amino acid metabolites (O-sulfotyrosine) were highly correlated with chronic decompensation of renal function.[66]

## Conclusion

Metabolomics, as an important component of systems biology, is expanding its application in DKD clinical research. Numerous small molecule metabolites (such as amino acids and lipids) in the body have been screened and are expected to become biological markers for the early diagnosis of DKD. The evolution of the metabolic profile with the disease course gives us enough opportunities to evaluate the prognosis of DKD, enabling us to make early interventions. Metabolomics as a new tool gives us a new perspective through which to look at the pathogenesis of DKD. Powered by information biology techniques, we have understood that there are disorders of mitochondrial energy metabolism within individuals with DKD, which severely compromise the structure and function of the kidney. Epigenetics plays an important role in the pathogenesis of DKD, and an increasing number of researches show the presence of abnormal modified metabolites in DKD patients. In addition, metabolomics also has given herbal medicine an arena to demonstrate its efficacy. In the future, with the innovation of high-throughput analysis platforms, cross-fertilization of multi-omics, and comprehensive infiltration of information biotechnology, we will be further exposed to the nature of DKD, which is necessary if we are to overcome it.


## Funding

Grant of Zhejiang Medicine and Health Technology Project, China (No. 2018ZH029, 2020KY871), the Major Project for Science & Technology Innovation 2025 in Ningbo, China (No. 2019B10035), and Grant of Ningbo Social Development, China (No. 2019C50080).


## REFERENCES


1. Saeedi P, Petersohn I, Salpea P, et al. Global and regional diabetes prevalence estimates for 2019 and projections for 2030 and 2045: results from the International Diabetes Federation Diabetes Atlas, 9th edition. *Diabetes Res Clin Pract.* 2019;157:107843. doi:10.1016/j.diabres.2019.107843.
2. Ruiz-Ortega M, Rodrigues-Diez RR, Lavoz C, Rayego-Mateos S. Special issue "Diabetic nephropathy: diagnosis, prevention, and treatment." *Clin Med.* 2020;9(3):8–13.

3. Alicic RZ, Rooney MT, Tuttle KR. Diabetic kidney disease: challenges, progress, and possibilities. *Clin J Am Soc Nephrol.* 2017;12(12):2032–2045.
4. Parving H-H, Chaturvedi N, Viberti G, Mogensen CE. Does microalbuminuria predict diabetic nephropathy? *Diabetes Care.* 2002;25(2):406–407. doi:10.2337/diacare.25.2.406.
5. Vistisen D, Andersen GS, Hulman A, Persson F, Rossing P, Jørgensen ME. Progressive decline in estimated glomerular filtration rate in patients with diabetes after moderate loss in kidney function—even without albuminuria. *Diabetes Care.* 2019;42(10):1886–1894. doi:10.2337/dc19-0349.
6. Gates SC, Sweeley CC. Quantitative metabolic profiling based on gas chromatography. *Clin Chem.* 1978;24(10):1663–1673.
7. Nicholson JK, Lindon JC, Holmes E. Metabonomics: understanding the metabolic responses of living systems to pathophysiological stimuli via multivariate statistical analysis of biological NMR spectroscopic data. *Xenobiotica.* 1999;29(11):1181–1189.
8. Beger RD, Dunn W, Schmidt MA, et al. Metabolomics enables precision medicine: "a white paper, community perspective." *Metabolomics.* 2016;12(10):149.
9. Costa Dos Santos G, Renovato-Martins M, de Brito NM. The remodel of the "central dogma": a metabolomics interaction perspective. *Metabolomics.* 2021;17(5):48.
10. Pinu FR, Villas-Boas SG. Extracellular microbial metabolomics: the state of the art. *Metabolites.* 2017;7(3):43.
11. Ott K-H, Araníbar N, Singh B, Stockton GW. Metabonomics classifies pathways affected by bioactive compounds: artificial neural network classification of NMR spectra of plant extracts. *Phytochem.* 2003;62(6):971–985.
12. Taylor J, King RD, Altmann T, Fiehn O. Application of metabolomics to plant genotype discrimination using statistics and machine learning. *Bioinformatics.* 2002;18(Suppl 2):S241–S248.
13. Beckonert O, Keun HC, Ebbels TMD, et al. Metabolic profiling, metabolomic and metabonomic procedures for NMR spectroscopy of urine, plasma, serum and tissue extracts. *Nat Protocols.* 2007;2(11):2692–2703.
14. Zhang A, Sun H, Wang P, Han Y, Wang X. Modern analytical techniques in metabolomics analysis. *Analyst.* 2012;137(2):293–300.
15. Liu R, Yang Z. Single cell metabolomics using mass spectrometry: techniques and data analysis. *Anal Chim Acta.* 2021;1143:124–134.
16. Olsson M, Hellman U, Wixner J, Anan I. Metabolomics analysis for diagnosis and biomarker discovery of transthyretin amyloidosis. *Amyloid.* 2021;28(4):234–242.
17. Chong J, Soufan O, Li C, et al MetaboAnalyst 4.0: towards more transparent and integrative metabolomics analysis. *Nucleic Acids Res.* 2018;46(W1):W486–W494.
18. Li B, He X, Jia W, Li H. Novel applications of metabolomics in personalized medicine: a mini-review. *Molecules.* 2017;22(7):1173.
19. Wishart DS. Emerging applications of metabolomics in drug discovery and precision medicine. *Nat Rev Drug Discov.* 2016;15(7):473–484.
20. Beale DJ, Pinu FR, Kouremenos KA, et al. Review of recent developments in GC-MS approaches to metabolomics-based research. *Metabolomics.* 2018;14(11):152.
21. Pasikanti KK, Ho PC, Chan ECY. Gas chromatography/mass spectrometry in metabolic profiling of biological fluids. *J Chromatogr B Analyt Technol Biomed Life Sci.* 2008;871(2):202–211.
22. Gika HG, Theodoridis GA, Plumb RS, Wilson ID. Current practice of liquid chromatography-mass spectrometry in metabolomics and metabonomics. *J Pharm Biomed Anal.* 2014;87:12–25.
23. Peng L, Sun B, Liu Y, et al. Increased lipoxygenase and decreased cytochrome P450s metabolites correlated with the incidence of diabetic nephropathy: potential role of eicosanoids from metabolomics in type 2 diabetic patients. *Clin Exp Pharmacol Physiol.* 2021;48(5):679–685.
24. Devi S, Nongkhlaw B, Limesh M, et al. Acyl ethanolamides in diabetes and diabetic nephropathy: novel targets from untargeted plasma metabolomic profiles of South Asian Indian men. *Sci Rep.* 2019;9(1):18117.
25. Gordin D, Shah H, Shinjo T, et al. Characterization of glycolytic enzymes and pyruvate kinase M2 in type 1 and 2 diabetic nephropathy. *Diabetes Care.* 2019;42(7):1263–1273.
26. Liu Y, Chen X, Liu Y, et al. Metabolomic study of the protective effect of Gandi capsule for diabetic nephropathy. *Chem Biol Interact.* 2019;314:108815.
27. Ng DPK, Salim A, Liu Y, et al. A metabolomic study of low estimated GFR in non-proteinuric type 2 diabetes mellitus. *Diabetologia.* 2012;55(2):499–508.
28. Tan YM, Gao Y, Teo G, et al. Plasma metabolome and lipidome associations with type 2 diabetes and diabetic nephropathy. *Metabolites* 2021;11(4):228.
29. Zhu C, Liang Q-l, Hu P, Wang Y-m, Luo G-a. Phospholipidomic identification of potential plasma biomarkers associated with type 2 diabetes mellitus and diabetic nephropathy. *Talanta* 2011;85(4):1711–1720.
30. Hirayama A, Nakashima E, Sugimoto M, et al. Metabolic profiling reveals new serum biomarkers for differentiating diabetic nephropathy. *Anal Bioanal Chem.* 2012;404(10):3101–3109.
31. Zhang F, Guo R, Cui W, et al. Untargeted serum metabolomics and tryptophan metabolism profiling in type 2 diabetic patients with diabetic glomerulopathy. *Ren Fail.* 2021;43(1):980–992.
32. Shao M, Lu H, Yang M, et al. Serum and urine metabolomics reveal potential biomarkers of T2DM patients with nephropathy. *Ann. Transl. Med.* 2020;8(5):199.
33. Zhang H, Zuo J-J, Dong S-S, et al. Identification of potential serum metabolic biomarkers of diabetic kidney disease: a widely targeted metabolomics study. *J Diabetes Res.* 2020;2020:3049098.
34. Du Y, Xu B-J, Deng X, et al. Predictive metabolic signatures for the occurrence and development of diabetic nephropathy and the intervention of Ginkgo biloba leaves extract based on gas or liquid chromatography with mass spectrometry. *J Pharm Biomed Anal.* 2019;166:30–39.
35. Ma T, Liu T, Xie P, et al. UPLC-MS-based urine nontargeted metabolic profiling identifies dysregulation of pantothenate and CoA biosynthesis pathway in diabetic kidney disease. *Life Sci.* 2020;258:118160.
36. Dai X, Su S, Cai H, et al. Protective effects of total glycoside from leaves on diabetic nephropathy rats via regulating the metabolic profiling and modulating the TGF-β1 and Wnt/β-catenin signaling pathway. *Front Pharmacol.* 2018;9:1012.
37. Toyama T, Shimizu M, Furuichi K, Kaneko S, Wada T. Treatment and impact of dyslipidemia in diabetic nephropathy. *Clin Exp Nephrol.* 2014;18(2):201–205.
38. Sargsyan E, Artemenko K, Manukyan L, Bergquist J, Bergsten P. Oleate protects beta-cells from the toxic effect of palmitate by activating pro-survival pathways of the ER stress response. *Biochim Biophys Acta.* 2016;1861(9 Pt A):1151–1160.
39. Sommerweiss D, Gorski T, Richter S, Garten A, Kiess W. Oleate rescues INS-1E β-cells from palmitate-induced apoptosis by preventing activation of the unfolded protein response. *Biochem. Biophys. Res.* 2013;441(4):770–776.
40. Yao F, Li Z, Ehara T, et al. Fatty acid-binding protein 4 mediates apoptosis via endoplasmic reticulum stress in mesangial cells of diabetic nephropathy. *Mol Cell Endocrinol.* 2015;411:232–242.
41. Benito-Vicente A, Jebari-Benslaiman S, Galicia-Garcia U, Larrea-Sebal A, Uribe KB, Martin C. Molecular mechanisms of lipotoxicity-induced pancreatic β-cell dysfunction. *Int Rev Cell Mol Biol* 2021;359:357–402.
42. Pang L-Q, Liang Q-L, Wang Y-M, Ping L, Luo G-A. Simultaneous determination and quantification of seven major phospholipid classes in human blood using normal-phase liquid chromatography coupled with electrospray mass spectrometry and the application in diabetes nephropathy. *J Chromatogr B Analyt Technol Biomed Life Sci.* 2008;869(1-2):118–125.

43. Rhee SY, Jung ES, Park HM, et al. Plasma glutamine and glutamic acid are potential biomarkers for predicting diabetic retinopathy. *Metabolomics.* 2018;14(7):89.
44. Tavares G, Venturini G, Padilha K, et al. 1,5-Anhydroglucitol predicts CKD progression in macroalbuminuric diabetic kidney disease: results from non-targeted metabolomics. *Metabolomics.* 2018;14(4):39.
45. Niewczas MA, Mathew AV, Croall S, et al. Circulating modified metabolites and a risk of ESRD in patients with type 1 diabetes and chronic kidney disease. *Diabetes Care.* 2017;40(3):383–390.
46. Niewczas MA, Sirich TL, Mathew AV, et al. Uremic solutes and risk of end-stage renal disease in type 2 diabetes: metabolomic study. *Kidney Int.* 2014;85(5):1214–1224.
47. Tofte N, Suvitaival T, Trost K, et al. Metabolomic assessment reveals alteration in polyols and branched chain amino acids associated with present and future renal impairment in a discovery cohort of 637 persons with type 1 diabetes. *Front Endocrinol.* 2019;10:818.
48. Kang HM, Ahn SH, Choi P, et al. Defective fatty acid oxidation in renal tubular epithelial cells has a key role in kidney fibrosis development. *Nat Med.* 2015;21(1):37–46.
49. Afshinnia F, Nair V, Lin J, et al. Increased lipogenesis and impaired β-oxidation predict type 2 diabetic kidney disease progression in American Indians. *JCI insight* 2019;4(21):e130317.
50. Haukka JK, Sandholm N, Forsblom C, Cobb JE, Groop P-H, Ferrannini E. Metabolomic profile predicts development of microalbuminuria in individuals with type 1 diabetes. *Sci Rep.* 2018;8(1):13853.
51. Looker HC, Colombo M, Hess S, et al. Biomarkers of rapid chronic kidney disease progression in type 2 diabetes. *Kidney Int.* 2015;88(4):888–896.
52. Heerspink HJL, Stefánsson BV, Correa-Rotter R, et al. Dapagliflozin in patients with chronic kidney disease. *N Engl J Med.* 2020;383(15):1436–1446.
53. Perkovic V, Jardine MJ, Neal B, et al. Canagliflozin and renal outcomes in type 2 diabetes and nephropathy. *N Engl J Med.* 2019;380(24):2295–2306.
54. Guthrie R. Canagliflozin and cardiovascular and renal events in type 2 diabetes. *Postgrad Med.* 2018;130(2):149–153.
55. Sharma K, Karl B, Mathew AV, et al. Metabolomics reveals signature of mitochondrial dysfunction in diabetic kidney disease. *J Am Soc Nephrol*. 2013;24(11):1901–1912.
56. Wu M, Li S, Yu X, et al. Mitochondrial activity contributes to impaired renal metabolic homeostasis and renal pathology in STZ-induced diabetic mice. *Am J Physiol Renal Physiol.* 2019;317(3):F593–F605.
57. Saulnier P-J, Darshi M, Wheelock KM, et al. Urine metabolites are associated with glomerular lesions in type 2 diabetes. *Metabolomics.* 2018;14(6):84.
58. Sha Q, Lyu J, Zhao M, Li H, Guo M, Sun Q. Multi-omics analysis of diabetic nephropathy reveals potential new mechanisms and drug targets. *Front Genet.* 2020;11:616435.
59. Hoppel C. The role of carnitine in normal and altered fatty acid metabolism. *Am J Kidney Dis.* 2003;41(4 suppl 4):S4–S12.
60. You Y-H, Quach T, Saito R, Pham J, Sharma K. Metabolomics reveals a key role for fumarate in mediating the effects of NADPH oxidase 4 in diabetic kidney disease. *J Am Soc Nephrol.* 2016;27(2):466–481.
61. Wang X, He Q, Chen Q, et al. Network pharmacology combined with metabolomics to study the mechanism of Shenyan Kangfu tablets in the treatment of diabetic nephropathy. *J Ethnopharmacol.* 2021;270:113817.
62. Reddy MA, Tak Park J, Natarajan R. Epigenetic modifications in the pathogenesis of diabetic nephropathy. *Semin Nephrol.* 2013;33(4):341–353.
63. Kato M, Natarajan R. Diabetic nephropathy—emerging epigenetic mechanisms. *Nat Rev Nephrol.* 2014;10(9):517–530.
64. Villeneuve LM, Natarajan R. The role of epigenetics in the pathology of diabetic complications. *Am J Physiol Renal Physiol.* 2010;299(1):F14–F25.
65. Wang J, Wu Z, Li D, et al. Nutrition, epigenetics, and metabolic syndrome. *Antioxid Redox Signal.* 2012;17(2):282–301.
66. Chen S, Liu Y-H, Dai D-P, et al. Using circulating O-sulfotyrosine in the differential diagnosis of acute kidney injury and chronic kidney disease. *BMC Nephrol.* 2021;22(1):66.

# Chemerin Levels in Acute Coronary Syndrome: Systematic Review and Meta-Analysis

*Abdulrahman Ismaiel,[1,a] Mohammad Zeeshan Ashfaq,[2,a] Daniel-Corneliu Leucuta,[3,*] Mohamed Ismaiel,[4] Dilara Ensar Ismaiel,[5] Stefan-Lucian Popa,[1] and Dan L. Dumitrascu[1]*

[1]2nd Department of Internal Medicine, "Iuliu Hatieganu" University of Medicine and Pharmacy, Cluj-Napoca, Romania, [2]Faculty of Medicine, "Iuliu Hatieganu" University of Medicine and Pharmacy, Cluj-Napoca, Romania, [3]Department of Medical Informatics and Biostatistics, "Iuliu Hatieganu" University of Medicine and Pharmacy, Cluj-Napoca, Romania, [4]Department of Surgery, St Michael's Hospital, Dublin, Ireland, [5]Department of Medicine, Tallaght University Hospital, Dublin, Ireland. *To whom correspondence should be addressed. dleucuta@umfcluj.ro
[a]These authors contributed equally to this work.

**Keywords:** chemerin, acute coronary syndrome, stable angina pectoris, coronary artery disease, ischemic heart disease, diabetes mellitus

**Abbreviations:** ACS, acute coronary syndrome; SAP, stable angina pectoris; MD, mean difference; T2DM, type 2 diabetes mellitus; IHD, ischemic heart disease; CAD, coronary artery disease; MI, myocardial infarction; BMI, body mass index; NOS, Newcastle-Ottawa scale; ELISA, enzyme-linked immunosorbent assay.

*Laboratory Medicine* 2022;53:552–560; https://doi.org/10.1093/labmed/lmac059

## ABSTRACT

**Objective:** We evaluated the relevant published studies exploring the association between chemerin concentrations and acute coronary syndromes (ACSs).

**Methods:** A systematic search was performed in October 2021 using PubMed, Scopus, Embase, and Cochrane Library. We included full articles and assessed their quality using the Newcastle-Ottawa score.

**Results:** We found 6 studies in the systematic review and 5 of these were included in our meta-analysis. Mean difference (MD) of 41.69 ng/mL (95% CI, 10.07–73.30), 132.14 ng/mL (95% CI, −102.12–366.40), and 62.10 ng/mL (95% CI, 10.31–113.89) in chemerin levels was seen in ACS patients vs control subjects, ACS patients vs stable angina pectoris patients (SAP), and type 2 diabetes mellitus (T2DM) ACS patients vs nondiabetic ACS patients, respectively.

**Conclusion:** Chemerin levels were significantly elevated in patients with ACS compared to controls, as well as in T2DM–ACS patients compared to nondiabetic ACS patients. However, no significant MD in chemerin levels was observed between SAP and ACS patients.

Ischemic heart disease (IHD) is composed of atherosclerotic cardiovascular disease and coronary artery disease (CAD). IHD's prevalence rate is on the rise (about 1655 per 100,000 people).[1] Although the morbidity and mortality rates of IHD are decreasing worldwide, the IHD burden continues to be high, especially in areas with a low socioeconomic demographic index.[2] CAD comprises acute coronary syndrome (ACS) and chronic coronary syndrome, previously called "stable CAD".[3,4] ACS is a term representing several ischemic-related myocardial conditions such as ST-elevation myocardial infarction (MI), non-ST elevation MI, and unstable angina.[5]

Genetics and environmental factors such as hypertension, DM, and dysregulated inflammation play a role in the initiation and progression of atherosclerosis and ACS.[6,7] Obesity, classified as a global epidemic disease,[8] is another established pivotal player and risk factor in the development of cardiovascular diseases[9] and ACS.[10] Its prevalence globally is on the rise[8] and can induce cardiovascular system structural and functional alterations.[11] In addition, it can cause endothelial dysfunction and a prothrombotic and inflammatory state.[8]

Adipose tissue, a metabolically active endocrine organ[12] releasing multiple immunomodulatory (anti- and pro-inflammatory) adipokines,[13,14] is dysregulated in obesity.[15] Several adipokines, such as leptin[16] and adiponectin,[17] are associated with cardiovascular diseases and are regarded as potential biomarkers.[18] Chemerin, also called retinoic acid receptor responder 2,[19] is an adipokine initially discovered in lesions from psoriatic skin.[20] It is secreted principally by adipose tissue and skin[21] and is abundantly expressed in white adipose tissue, lung, and liver.[22] Its effect is mainly mediated by G protein-coupled receptor 1 and chemokine-like receptor 1.[19]

Chemerin is involved in multiple biological processes, including inflammation, glucose homeostasis, adipogenesis, and angiogenesis.[19] In addition, it is associated with multiple diseases including psoriasis,[23] diabetes mellitus,[24,25] rheumatoid arthritis,[26] inflammatory bowel disease,[27] cardiovascular disease,[28,29] ACS[30] and cancers (such as lung, breast,[31] gastric,[32] and hepatocellular cancers[33]). Its role as anti- or pro-inflammatory or tumorigenic is controversial and is context- and tissue-specific.[19]

A positive link between chemerin levels and severity of CAD[34] was reported; however, others have shown that it is an independent predictor of CAD.[35] Few studies have assessed the link between chemerin levels and ACS, and those reveal inconclusive findings.

Consequently, we carried out this systematic review and meta-analysis, which is, to the best of our knowledge, the first to assess the link between chemerin and ACS, as well as differences in chemerin levels in patients with and without type 2 DM (T2DM).

## Materials and Methods

This systematic review and meta-analysis was written according to the preferred reporting items for systematic reviews and meta-analyses (PRISMA) 2020 statement.[36]

### Data Sources and Search Strategy

We searched several electronic databases, including PubMed, Embase, Scopus, and Cochrane Library to identify observational studies assessing chemerin levels in ACS patients. A predefined search string was used as follows: "chemerin" OR "RARRES2 protein, human" (Supplementary Concept) AND "Acute Coronary Syndrome"(Mesh) OR "Acute Coronary Syndrome" (All Fields) OR "ST Elevation Myocardial Infarction" (Mesh) OR "ST Elevation Myocardial Infarction" (All Fields) OR "Non-ST Elevated Myocardial Infarction" (Mesh) OR "Non-ST Elevated Myocardial Infarction" (All Fields) OR "Myocardial Infarction" (Mesh) OR "Myocardial Infarction" (All Fields) for PubMed, and a similar one for Scopus, EMBASE, and Cochrane Library. Moreover, we also manually searched the references of included articles for possible relevant missed publications. The literature search was conducted from inception until October 25, 2021, by 2 investigators (A.I. and M.Z.A) independently. Discrepancies were resolved through discussion and a consensus was reached. No filters or restrictions were applied during the search regarding duration, country, or language. The titles and abstracts were screened for eligibility. Subsequently, we assessed the full text of the articles that fulfilled our inclusion and exclusion criteria. Data extraction was performed by one investigator (M.Z.A.) and verified by another (D.E.I.), and any discrepancies were resolved by mutual consensus. The extracted data included author names, publication year, country, design of the study, studied population, total sample size, ACS percentage, mean age, sex distribution, body mass index (BMI), chemerin measurement technique and source, chemerin levels, and main study outcome, which were collated and presented in the manuscript.

### Eligibility Criteria

The inclusion criteria of original articles in our systematic review and meta-analysis were as follows: (1) observational studies of cohort, cross-sectional, or case-control design assessing chemerin levels in ACS patients; (2) chemerin assessed from serum or plasma; (3) ACS diagnosis according to each study criteria; (4) human studies without restrictions to sex, race, or ethnicity; (5) studies published in English, German, French, or Romanian languages.

The exclusion criteria were as follows: (1) IHD patients without a clear ACS group; (2) stable CAD patients without ACS patients; (3) editorials, letters, commentaries, short surveys, case reports, review articles, practice guidelines, conference abstracts, and abstracts published without a full article.

### Risk of Bias Assessment in Individual Studies

The investigators (M.Z.A. and M.I.) independently used the Newcastle-Ottawa Scale (NOS), objectively evaluating the bias risk and internal validity of the included studies.[37] Discrepancies between the 2 investigators regarding the quality assessment of the included studies were handled through discussion. Separate assessment forms were used for case-control studies and cross-sectional studies. All assessed studies were scored based on how many stars were obtained. The selection, comparability, and outcome section criteria were verified, and the study was subsequently graded with scores ranging between 0 to 9 stars. The number of stars were added up in each study to compare the quality of included studies in a quantitative manner. High-quality studies were considered to have received 7 stars or more. The methodological quality assessment did not affect the eligibility of the studies.

### Summary Measures and Synthesis of Results

We used the R with Metafor package (OpenMeta [Analyst]) for the data analyses of the meta-analysis.[38,39] The principal summary outcome was the mean difference (MD) of chemerin levels. Furthermore, we assessed the inconsistencies and heterogeneities among the studies by the Q test and $I^2$ statistics. As recommended by the Cochrane Handbook[40] for identifying and measuring heterogeneity, we estimated $I^2$ values of 0% to 40% as not important, 30% to 60% as moderate heterogeneity, 50% to 90% as substantial heterogeneity, and 75% to 100% as considerable heterogeneity. To analyze the estimated total effect size, we used the random-effects model and MD. Combining groups in studies with several subgroups of ACS patients or control subjects without a total group was performed according to the Cochrane Handbook recommendations.[40] Subgroup analysis was conducted by comparing chemerin levels in ACS patients vs controls, ACS patients vs stable angina pectoris (SAP) patients, and ACS-T2DM patients vs ACS nondiabetic patients, according to the available values from the extracted data. Data from each study were reported as the estimated MD with 95% CI, lower bound, upper bound, standard error, and $P$ value. Statistical significance was considered if the $P$ value was $< .05$. The analyses were conducted if 2 or more studies reported the same outcome with available mean and SD or median (interquartile range) of chemerin levels.

## Results

### General Results

The primary search yielded 202 articles (PubMed = 11 articles, EMBASE = 36 articles, Scopus = 94 articles, and Cochrane Library = 61), as illustrated in **FIGURE 1**. A total of 16 articles were found to be duplicates and hence removed, resulting in 186 studies. The remaining studies were then evaluated according to the inclusion and exclusion criteria by the screening of titles and abstracts for eligibility. Of these, 170 articles were deemed irrelevant, and 1 article was a review, causing 171 records to be excluded and the remaining 15 reports to be sought for retrieval and assessed for eligibility. Another 10 reports were excluded for the following reasons: no clear ACS group,[41,42] Chinese language,[43] stable CAD,[44] conference abstracts (repeated in original study),[45,46] serum chemerin levels not clearly reported in different groups,[47] baseline vs postintervention study,[48] or conference abstract.[49,50] At this point, an additional study was identified through other sources (n = 1) by manually

**FIGURE 1. PRISMA flow diagram outlining the identification, screening, and inclusion phases. ACS, acute coronary syndromes, CAD, coronary artery disease.**

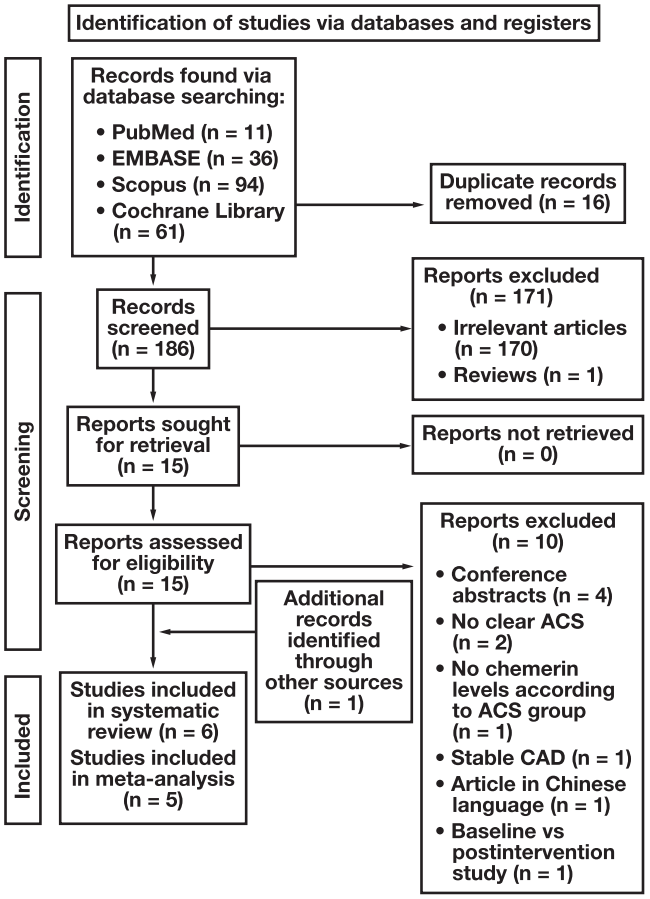


searching the reference lists of pertinent articles, leading to a final total of 6[28,51–55] studies to be included in the systematic review and only 5 studies included in the meta-analysis.

### Study Characteristics

A summary of the main characteristics of included studies is shown in **TABLE 1**. This systematic review included a total of 983 subjects. One study did not report the sex distribution among the controls,[55] hence preventing the calculation of sex distribution accurately. The meta-analysis included 731 individuals of whom 537 (73.46%) were male and 194 (26.54%) were female. All 6 studies reported the mean age of the participants. BMI of the subjects was not reported in 2 studies.[51,54] Five studies were cross-sectional by design, and 1 was a nested case-control study.[55] In terms of the region, 2 studies were conducted in Europe (1 each in Turkey and Greece), 3 in Asia (1 each in China, Saudi Arabia, and India), and 1 study was carried out in the USA.

### Chemerin Evaluation

All studies used the enzyme-linked immunosorbent assay (ELISA) method to measure chemerin, and in terms of testing samples, 4 studies used serum samples to measure chemerin, and 2 studies used plasma samples.

### Chemerin Levels in ACS Patients vs Controls

The serum and plasma chemerin levels were evaluated in three studies, comparing the levels in patients that had ACSs against the control subjects as shown in **FIGURE 2**.[28,51,52] The collective analysis of included studies showed that chemerin levels were 41.69 ng/mL (95% CI, 10.07 to 73.30) higher in ACS than controls. Considerable heterogeneity was reported with $I^2$ = 95.82% and $P$ < .001.

A subgroup analysis, including 2 studies evaluating serum chemerin levels, was conducting as outlined in **FIGURE 3**.[51,52] The pooled analysis of included studies showed serum chemerin levels were higher in ACS patients than in controls, with an MD of 53.904 ng/mL (95% CI, 15.284 to 92.524). Considerable heterogeneity was found with $I^2$ = 91.57% and $P$ < .001.

### Plasma Chemerin Levels in ACS Patients vs SAP Patients

Plasma chemerin levels were evaluated in 2 studies comparing patients with ACSs and patients with SAP; this is highlighted in **FIGURE 4**.[28,54] The pooled analysis of included studies showed plasma chemerin levels were higher in ACS than SAP patients by 132.14 ng/mL (95% CI, −102.18 to 366.40), but the results were not statistically significant. Considerable heterogeneity was reported with $I^2$ = 99.1% and $P$ < .001.

### Serum Chemerin Levels in ACS Patients with T2DM vs ACS Patients without T2DM

Chemerin levels were assessed in 2 studies comparing the serum chemerin levels in ACS patients with T2DM and ACS patients that did not have T2DM, as presented in **FIGURE 5**.[51,53] The pooled analysis of the studies assessing serum chemerin in ACS patients showed chemerin levels were higher in patients with T2DM by 62.10 ng/mL (95% CI, 10.31 to 113.89) compared to those without T2DM. Substantial heterogeneity was reported with $I^2$ = 81.89% and $P$ = .019.

### Quality Assessment

The NOS was used to evaluate the methodological quality of the included eligible studies as shown in Supplementary Tables 1 and 2. The NOS for cross-sectional studies was used in 5 studies,[28,51–54] whereas the NOS for case-control studies was used in 1 study.[55] The nested case-control study received a score of 7, rating it a good quality study, whereas the cross-sectional studies scored higher; 2 studies had a score of 8,[52,54] 2 studies received a score of 9,[51,53] and 1 cross-sectional study was rated 10.[28] By this standard, all these studies were considered "good quality." Finally, all evaluated studies had a clearly formulated research question and objective with satisfactory sample size. All studies used clearly defined measures of exposure that are considered reliable and valid. All studies assessed the ascertainment of exposure in a satisfactory fashion.[28,51–55]

## Discussion

With substantial morbidity and mortality, CAD remains a major public health concern in developed countries.[56] In the US alone, approximately 720,000 people experience a new episode of ACS every year.[57] This puts great financial stress on the health care system.[57] It is estimated that, on average, the annual cost of managing a single ACS patient in 2001–2002 was 32,000 USD.[58] The cost and utilization of resources associated with ACS would likely place an even higher level of financial burden on the healthcare system in 2021. It is therefore

**TABLE 1. Studies Evaluating Chemerin Levels in Adult ACS Patients**

| First Author/Year/Country | Study Design | Study Characteristics | Main Findings |
|---|---|---|---|
| Aronis et al/ 2014/USA[55] | Nested case-control | • Population: ACS patients and healthy controls<br>• Total subjects: 252 (cases: n = 90) (controls: n = 162)<br>• ACS: 90 (55.55%)<br>• Mean age (y): ACS: 67.25 ± 9.11; controls: 65.85 ± 9.84<br>• Sex (males): all 90 ACS cases were male (sex for controls not indicated)<br>• BMI (kg/m$^2$): ACS: 27.86 ± 3.43; controls: 26.70 ± 3.73<br>• Chemerin measurement method: ELISA (Biovendor)<br>• Chemerin level (ng/mL): ACS: 178.24 ± 116.51; controls: 183.2 ± 115.53<br>• Chemerin measurement: serum | Chemerin levels do not predict the development of ACS. |
| Ji et al/2014/China[28] | Cross-sectional | • Population: ACS (SAP, UAP, AMI) patients and healthy controls<br>• Total subjects: 220 (cases: n = 180 [SAP = 60, UAP = 60, AMI = 60]; controls: n = 40)<br>• ACS: 180 (81.8%)<br>• Mean age (y): SAP = 61.9 ± 9.9, UAP = 60.6 ± 9.9, AMI = 62.9 ± 10.3; controls: 62.6 ± 7.9<br>• Sex (males): ACS: 122 (67.7%) (SAP = 44 [73.3%], UAP = 37 [61.6%], AMI = 41 [68.3%]); controls: 29 (72.5%)<br>• BMI (kg/m$^2$): SAP = 24.8 ± 3.0, UAP = 25.8 ± 2.7, AMI = 25.9 ± 2.6); controls: 23.2 ± 3.9<br>• Chemerin measurement method: ELISA (R&D Systems)<br>• Chemerin level (ng/mL): ACS: 51.95 ± 18.13 (SAP = 42.85 ± 11.60, UAP = 53.62 ± 14.65, AMI = 59.38 ± 22.46); controls: 37.55 ± 7.42<br>• Chemerin measurement: plasma | Chemerin is a novel biomarker of ACS but not of SAP. |
| Kadoglou et al/2015/Greece[53] | Cross-sectional | • Population: ACS patients and healthy controls<br>• Total subjects:110 (cases: n = 78) (controls: n = 32)<br>• ACS: 78 (70.9%)<br>• Mean age (y): ACS: 66.2 ± 14.4; controls: 63.1 ± 9<br>• Sex (males): ACS: 63 (80.8%); controls: 25 (78.1%),<br>• BMI (kg/m$^2$): ACS: 28.86 ± 3.80; controls: 27.67 ± 3.65<br>• Chemerin measurement method: ELISA (BioVendor)<br>• Chemerin level (ng/mL): ACS: 263.37 ± 73.32; controls: not given<br>• Chemerin measurement: serum | Patients with AMI showed at admission lower omentin-1 and higher chemerin serum levels compared with healthy controls. |
| Ates et al/2018/Turkey[54] | Cross-sectional | • Population: ACS patients and SAP controls<br>• Total subjects:127 (cases: n = 97) (controls: n = 30)<br>• ACS: 97 (76.37%)<br>• Mean age (y): ACS: 59.1 ± 7.4; controls: 59.3 ± 8.3<br>• Sex (males): ACS 62 (63.3%); control 20 (66.7%),<br>• BMI (kg/m$^2$): not measured<br>• Chemerin measurement method: ELISA (BioVendor)<br>• Chemerin level (ng/mL): ACS: 451.3 ± 101.2; controls: 581.5 ± 173.7<br>• Chemerin measurement: plasma | Chemerin levels were higher in STEMI patients with greater thrombus burden and higher level of inflammation. |
| Baig et al/2020/Saudi Arabia[52] | Cross-sectional | • Population: ACS patients and healthy controls<br>• Total subjects: 174 (cases: n = 122) (controls: n = 52)<br>• ACS: 122 (70.1%)<br>• Mean age (y): ACS: 54.94 ± 9.08; controls: 53.38 ± 5.99<br>• Sex (males): ACS: 105 (86.06%); controls: 34 (65.38%),<br>• BMI (kg/m$^2$): ACS: 27.93 ± 5.22; controls: 27.68 ± 4.35<br>• Chemerin measurement method: ELISA (Mesochem Technology)<br>• Chemerin level (ng/mL): ACS: 173.80 ± 60.78; controls: 99.45 ± 57.68<br>• Chemerin measurement: serum | Serum chemerin and omentin-1 levels were independently associated with the MI. |
| Kumar et al/2020/India[51] | Cross-sectional | • Population: ACS patients (with and without diabetes) and healthy controls<br>• Total subjects: 100 (cases: n = 70, ACS-NDM: n = 37, ACS-DM: n = 33; controls: n = 30)<br>• ACS: 70 (70%); ACS-NDM: 37%, ACS-DM: 33%<br>• Mean age (y): ACS-NDM: 61.35 ± 9.49, ACS-DM: 59.06 ± 9.12; controls: 59.87 ± 5.88<br>• Sex (males): ACS: 54 (77.14%), ACS-NDM: 31 (83.78%), ACS-DM: 23 (69.69%); controls: 20 (66.66%)<br>• BMI (kg/m$^2$): not mentioned<br>• Chemerin measurement method: ELISA (Elabscience)<br>• Chemerin level (ng/mL): ACS-NDM: 0.42 ± 0.22, ACS-DM: 0.80 ± 0.61; controls: 0.25 ± 0.10<br>• Chemerin measurement: serum | Chemerin levels are markedly elevated in ACS patients, more so in those with coexisting diabetes. |

*ACS, acute coronary syndrome; AMI, acute myocardial infarction; BMI, body mass index; DM, diabetes mellitus; ELISA, enzyme-linked immunosorbent assay; MI, myocardial infarction; NDM, nondiabetic; SAP, stable angina pectoris; STEMI, ST-elevation myocardial infarction; UAP, unstable angina pectoris.*

imperative to find cost-effective ways of detecting the presence of ACS earlier. This could potentially prevent the onset of an adverse event, ensure a favorable outcome for the patient, and not stretch resources that could be used elsewhere. Hence, we have performed this systematic review and meta-analysis to examine chemerin levels in ACS patients. Chemerin levels were found to be significantly elevated in

patients with ACS in comparison to the control cases. Chemerin was also significantly elevated in patients with T2DM–ACS compared to the patients who had just ACS without T2DM.

In our systematic review and meta-analysis, we found that chemerin levels were significantly increased in ACS patients compared to controls. Chemerin is a novel adipokine that is associated with adipogenesis and inflammation, and it is known to be responsible for CAD development.[59] Chemerin is also shown to be involved in endothelial activation and the development of atherosclerosis.[60] In a cross-sectional study, chemerin was shown to be associated with peripheral arterial stiffness; the circulating chemerin level was an independent risk factor for arterial stiffness, even after adjusting for other cardiovascular risk factors.[61] Atherosclerosis and plaque disruption are known to have a principal pathological role in ACS patients.[62] Lehrke et al[63] reported that total chemerin levels do not reflect atherosclerotic plaque burden. However, the insufficient statistical power and the study's cross-sectional design could potentially explain the lack of association between total chemerin level and coronary artery atherosclerosis. In contrast, Spiroglou et al[64] showed that adiponectin, visfatin, and chemerin expressions from immunohistochemical staining were associated with both aortic and coronary atherosclerosis, indicating the possible involvement of these locally produced adipokines in the atherogenic process. Furthermore, chemerin was reported to be an independent marker for the presence of atherosclerosis in chronic kidney disease patients.[65] Chemerin may represent a novel link between metabolic signals and atherosclerosis.[34] Therefore, the elevation in chemerin levels in ACS can be explained by its role in inflammation and atherosclerosis, although further investigation is required to specifically explore chemerin's implication in coronary artery atherosclerosis. Nonetheless, chemerin appears to have extensive complicity in other cardiovascular diseases, such as heart failure, acute ischemic stroke, and dilated cardiomyopathy.[66–69]

When comparing the chemerin level in ACS patients against that of SAP patients, we found that the mean difference in chemerin levels between both groups was not significant. Chemerin was elevated in both cases; hence it is not possible to discern between ACS and SAP based on chemerin values alone. A correlation between increased serum chemerin levels and CAD was reported in 3 case-control studies.[34,35,70] Furthermore, in another study involving 131 Korean patients, the researchers were able to show a significant correlation between circulating chemerin levels and the severity of coronary artery stenosis; however, chemerin was not shown to be an independent risk factor for multiple vessel disease.[71] This was further supported by a recent investigation in which chemerin and vaspin were reported as potential biomarkers for coronary artery stenosis in Egyptian patients.[72]

The elevated chemerin levels in T2DM-ACS patients compared to nondiabetic ACS patients are in concurrence with previously reported findings. Chemerin is reported to be independently associated with the presence of CAD in patients with T2DM.[73] In 2 other case-control studies, 1 carried out in Turkey and the other in China, a similar pattern was seen where metabolic syndrome patients with CAD had higher serum chemerin levels than patients without CAD.[35,74] In patients with CAD, serum chemerin levels are correlated with other inflammation markers as well as insulin resistance and an unfavorable lipid profile.[34,50,75] Chemerin was also found to be implicated in the development of some subtypes of diabetic microangiopathy.[76] The underlying mechanism regulating chemerin secretions may be different depending on the presence or absence of diabetes/prediabetes. Chemerin was associated with metabolic syndrome in animal experiments in T2DM and obesity.[59] Moreover, in a cross-sectional study, it was seen that chemerin was found to strongly correlate with increased levels of tumor necrosis factor-α, interleukin-6, C-reactive protein, leptin, and resistin inflammation markers. Chemerin also correlated with BMI, ectopic adipose tissue, triglycerides, low high-density lipoprotein cholesterol, and hypertension, components of the metabolic syndrome trait cluster.[63] Chemerin mRNA was found to be substantially more highly expressed in adipose tissue of patients with T2DM and correlates with circulating chemerin, BMI, percentage body fat, and C-reactive protein.[77] In 2 other studies, it was shown that chemerin levels were much higher in T2DM patients compared to healthy individuals.[62,77] The cumulative increase in chemerin in ACS–T2DM patients is likely to be individually explained by the ACS and T2DM and the inflammation resulting from both of these pathologies. It seems that chemerin has the potential to be an independent biomarker for individuals that have ACS–T2DM; however, further primary research is needed with larger sample sizes to determine chemerin's feasibility in targeted therapies for cardiodiabetic patients.

There were 3 studies that used serum to measure chemerin level and the other 2 used plasma; thus, the accuracy of measurement could be different in these 2 types of specimens. At the moment, a clear recommendation regarding whether chemerin levels should be assessed from serum, plasma, or full blood in the studied pathology cannot be concluded, as the available data are very limited. Nevertheless, a study conducted by Karsten et al[78] reported a four-fold increase in the levels of 48 cytokines (interleukins, tumor necrosis factor-α, interferon-γ, proteins as chemerin) in red blood cells compared to plasma levels. They also mentioned that small hemolysis might modify the cytokine plasma levels. Chemerin might exhibit a similar behavior, but this should be confirmed in future studies. In practice, full blood analyses for chemerin levels are less common compared to serum or plasma analyses. Thus, the evaluation whether serum or plasma chemerin levels should be used in a clinical setting remains unclear until future studies clarify this issue.

In terms of limitations, the available literature on chemerin's association with ACS is very limited as it is a relatively recent topic of investigation. The number of included studies in our qualitative and quantitative synthesis is small, mainly studies of cross-sectional design, and hence causality cannot be implied. Subgroup analysis according to ACS types was not possible due to insufficient available data in the included studies. Furthermore, the patients weren't followed in the long-term. Although several studies reported that chemerin levels can differ between sexes and according to BMI,[79,80] we were not able to conduct a subgroup analysis evaluating chemerin levels in different sexes and BMI due to limited available information in the published studies. We found important heterogeneity between several included studies in our review. Concerning risk of bias assessment, the NOS scores were high. Nevertheless, 1 study suffered from comparability, and 1 in ascertainment of the exposure.

In terms of the strengths of this analysis, we conducted a comprehensive search comprising several medical databases, which allowed us to study the association in a systematic manner. The selected studies were conducted in different parts of the world, covering different ethnic regions, rendering this analysis a more representative one.

**FIGURE 2.** Chemerin levels in acute coronary syndrome patients vs controls.

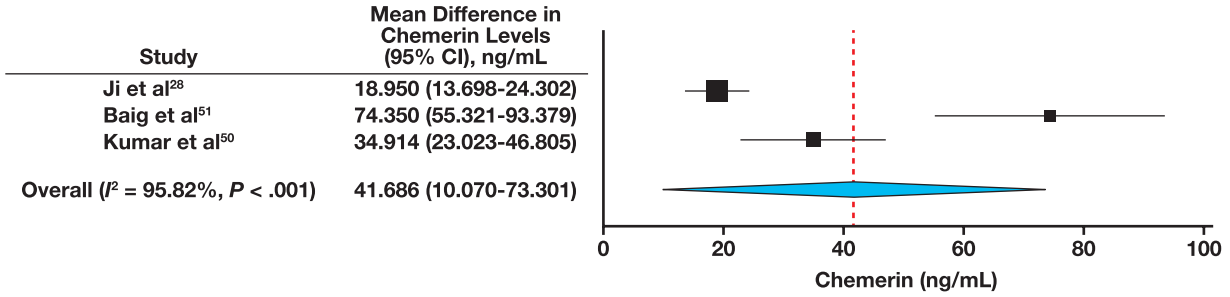


**FIGURE 3.** Serum chemerin levels in acute coronary syndrome patients vs controls.

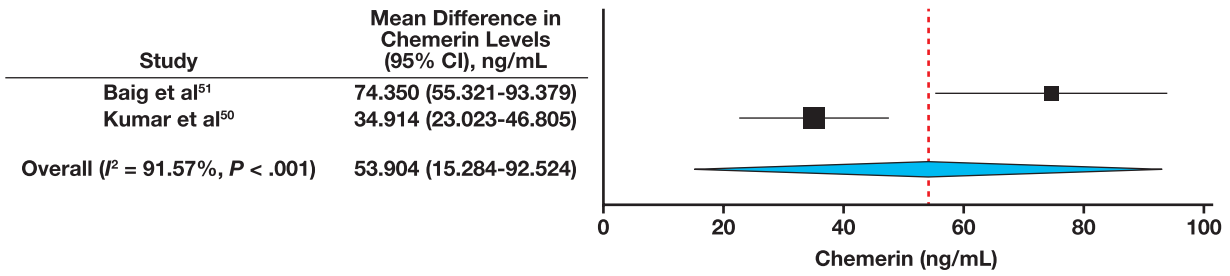


**FIGURE 4.** Plasma chemerin levels in acute coronary syndrome patients vs stable angina pectoris patients.

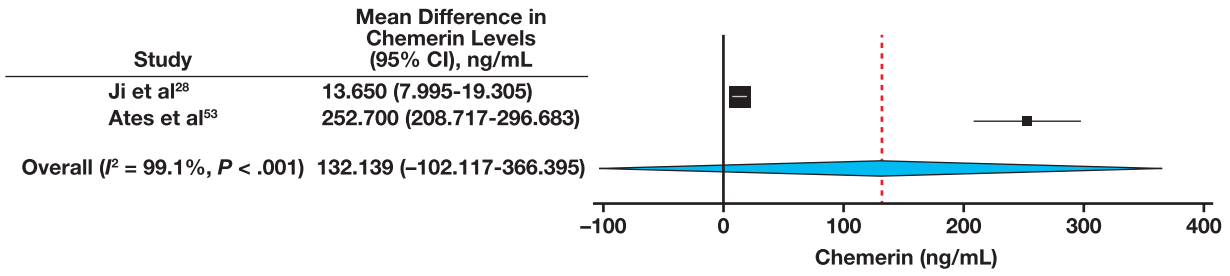


**FIGURE 5.** Serum chemerin levels in acute coronary syndrome (ACS) patients with type 2 diabetes mellitus (T2DM) vs ACS patients without T2DM.

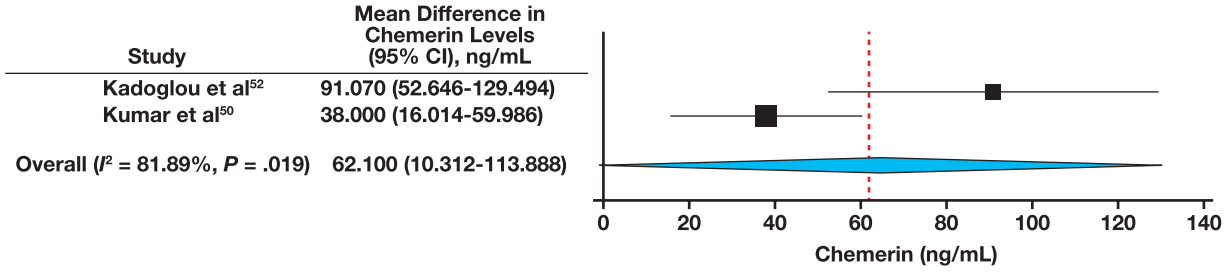


## Conclusion

Chemerin levels were considerably elevated in patients with ACS compared to controls. This pattern was not seen in SAP, where ACS and SAP patients did not present a significant mean difference in chemerin levels. Furthermore, ACS–T2DM patients presented with significantly higher chemerin levels than nondiabetic ACS patients. Thus, chemerin has the potential to become a novel biomarker for ACS and possibly play a role in developing targeted therapy, especially in patients who have concurrent T2DM.

Further research is needed to identify whether serum or plasma chemerin levels would be more practical and precise for use in a clinical setting. Moreover, chemerin levels according to sex and BMI in

ACS patients compared to controls requires further assessment. Large cohorts, a subsequent long-term follow-up, and comparison of the degree of atherosclerosis and ACS type with that of the biochemical markers are considered necessary in future studies. For chemerin to be an effective biomarker for ACS, more research is needed to establish baseline chemerin levels and cut-off limits to establish the occurrence of ACS as it is seen in the case of cardiac troponin levels. Moreover, ACS patients need to be followed up to assess the short- and long-term prognostic significance of chemerin levels.

## Supplementary Data

Supplemental figures and tables can be found in the online version of this article at www.labmedicine.com.

## REFERENCES


1. Khan MA, Hashim MJ, Mustafa H, et al. Global epidemiology of ischemic heart disease: results from the Global Burden of Disease Study. *Cureus.* 2020;12(7):e9349. doi:10.7759/cureus.9349.
2. Wang F, Yu Y, Mubarik S, et al. Global burden of ischemic heart disease and attributable risk factors, 1990-2017: a secondary analysis based on the Global Burden of Disease Study 2017. *Clin Epidemiol* 2021;13:859–870. doi:10.2147/CLEP.S317787.
3. Dekker M, Waissi F, Timmerman N, et al. Extracellular vesicles in diagnosing chronic coronary syndromes the bumpy road to clinical implementation. *Int J Mol Sci .* 2020;21(23). doi: 10.3390/ijms21239128.
4. Kurdi H. Chronic coronary syndrome—a new era for the diagnosis and management of stable coronary artery disease? British Cardiovascular Society. https://www.britishcardiovascularsociety.org/resources/editorials/articles/chronic-coronary-syndrome-a-new-era-for-the-diagnosis-and-management-of-stable-coronary-artery-disease. Accessed October 29, 2021.
5. Smith JN, Negrelli JM, Manek MB, et al. Diagnosis and management of acute coronary syndrome: an evidence-based update. *J Am Board Fam Med.* 2015;28(2):283–293. doi:10.3122/jabfm.2015.02.140189.
6. Boudoulas KD, Triposkiadis F, Geleris P, et al. Coronary atherosclerosis: pathophysiologic basis for diagnosis and management. *Prog Cardiovasc Dis.* 2016/05/01/ 2016;58(6):676–692. doi:10.1016/j.pcad.2016.04.003.
7. Wolf D, Ley K. Immunity and inflammation in atherosclerosis. *Circ Res.* 2019;124(2):315–327. doi:10.1161/CIRCRESAHA.118.313591.
8. Koliaki C, Liatis S, Kokkinos A. Obesity and cardiovascular disease: revisiting an old relationship. *Metabolism*. 2019;92:98–107. doi:10.1016/j.metabol.2018.10.011.
9. Carbone S, Canada JM, Billingsley HE, et al. Obesity paradox in cardiovascular disease: where do we stand? *Vasc Health Risk Manag.* 2019;15:89–100. doi:10.2147/VHRM.S168946.
10. Graham G. Acute coronary syndromes in women: recent treatment trends and outcomes. *Clin Med Insights Cardiol.* 2016;10:1–10. doi:10.4137/CMC.S37145.
11. Abel ED, Litwin SE, Sweeney G. Cardiac remodeling in obesity. *Physiol Rev.* 2008;88(2):389–419. doi:10.1152/physrev.00017.2007.
12. Unamuno X, Gómez-Ambrosi J, Rodríguez A, et al. Adipokine dysregulation and adipose tissue inflammation in human obesity. *Eur J Clin Invest.* 2018;48(9):e12997. doi:10.1111/eci.12997.
13. AlZaim I, Hammoud SH, Al-Koussa H, et al. Adipose tissue immunomodulation: a novel therapeutic approach in cardiovascular and metabolic diseases. *Front Cardiovasc Med.* 2020;7:602088. doi:10.3389/fcvm.2020.602088.
14. Balistreri CR, Caruso C, Candore G. The role of adipose tissue and adipokines in obesity-related inflammatory diseases. *Mediators Inflamm.* 2010;2010:802078. doi:10.1155/2010/802078.
15. Longo M, Zatterale F, Naderi J, et al. Adipose tissue dysfunction as determinant of obesity-associated metabolic complications. *Int J Mol Sci .* 2019;20(9):2358. doi:10.3390/ijms20092358.
16. Poetsch MS, Strano A, Guan K. Role of leptin in cardiovascular diseases. *Front Endocrinol.* 2020;11:354–354. doi:10.3389/fendo.2020.00354.
17. Hopkins TA, Ouchi N, Shibata R, et al. Adiponectin actions in the cardiovascular system. *Cardiovasc Res.* 2007;74(1):11–18. doi:10.1016/j.cardiores.2006.10.009.
18. Hogas S, Bilha SC, Branisteanu D, et al. Potential novel biomarkers of cardiovascular dysfunction and disease: cardiotrophin-1, adipokines and galectin-3. *Arch Med Sci* 2017 2017;13(4):897–913. doi:10.5114/aoms.2016.58664.
19. Treeck O, Buechler C, Ortmann O. Chemerin and cancer. *Int J Mol Sci .* 2019;20(15). doi: 10.3390/ijms20153750.
20. Su X, Cheng Y, Zhang G, et al. Chemerin in inflammatory diseases. *Clin Chim Acta.* 2021;517:41–47. doi:10.1016/j.cca.2021.02.010.
21. Bonomini M, Pandolfi A. Chemerin in renal dysfunction and cardiovascular disease. *Vascul Pharmacol.* 2016;77:28–34. doi:10.1016/j.vph.2015.10.007.
22. Helfer G, Wu Q-F. Chemerin: a multifaceted adipokine involved in metabolic disorders. *J Endocrinol.* 2018;238(2):R79–R94. doi:10.1530/JOE-18-0174.
23. Wang Y, Huo J, Zhang D, et al. Chemerin/ChemR23 axis triggers an inflammatory response in keratinocytes through ROS-sirt1-NF-kappaB signaling. *J Cell Biochem.* 2019;120(4):6459–6470. doi:10.1002/jcb.27936.
24. Perumalsamy S, Aqilah Mohd Zin NA, Widodo RT, et al. Chemokine like receptor-1 (CMKLR-1) receptor: a potential therapeutic target in management of chemerin induced type 2 diabetes mellitus and cancer. *Curr Pharm Des.* 2017;23(25):3689–3698. doi:10.2174/1381612823666170616081256.
25. Roman AA, Parlee SD, Sinal CJ. Chemerin: a potential endocrine link between obesity and type 2 diabetes. *Endocrine*. 2012;42(2):243–251. doi:10.1007/s12020-012-9698-8.
26. Kaneko K, Miyabe Y, Takayasu A, et al. Chemerin activates fibroblast-like synoviocytes in patients with rheumatoid arthritis. *Arthritis Res Ther.* 2011;13(5):R158. doi:10.1186/ar3475.
27. Weigert J, Obermeier F, Neumeier M, et al. Circulating levels of chemerin and adiponectin are higher in ulcerative colitis and chemerin is elevated in Crohn's disease. *Inflamm Bowel Dis.* 2010;16(4):630–637. doi:10.1002/ibd.21091.
28. Ji Q, Lin Y, Liang Z, et al. Chemerin is a novel biomarker of acute coronary syndrome but not of stable angina pectoris. *Cardiovasc Diabetol.* 2014;13:145. doi:10.1186/s12933-014-0145-4.
29. Pradyumna Agasthi SA, Chenna A, Menon V, Harris R. Abstract P013: association between serum chemerin levels and coronary heart disease: a meta analysis. *Circulation.* 2018;133(suppl 1). doi:10.1161/circ.133.suppl_1.p013.
30. Aronis KN, Sahin-Efe A, Chamberland JP, et al. Chemerin levels as predictor of acute coronary events: a case-control study nested within the Veterans Affairs Normative Aging Study. *Metabolism.* 2014;63(6):760–766. doi:10.1016/j.metabol.2014.02.013.
31. El-Sagheer G, Gayyed M, Ahmad A, et al. Expression of chemerin correlates with a poor prognosis in female breast cancer patients. *Breast Cancer (Dove Med Press).* 2018;10:169–176. doi:10.2147/BCTT.S178181.
32. Zhang J, Jin HC, Zhu AK, et al. Prognostic significance of plasma chemerin levels in patients with gastric cancer. *Peptides.* 2014;61:7–11. doi:10.1016/j.peptides.2014.08.007.

33. Lin W, Chen Y-L, Jiang L, et al. Reduced expression of chemerin is associated with a poor prognosis and a lowed infiltration of both dendritic cells and natural killer cells in human hepatocellular carcinoma. *Clin. Lab*. 2011;57(11-12):879–885.
34. Yan Q, Zhang Y, Hong J, et al. The association of serum chemerin level with risk of coronary artery disease in Chinese adults. *Endocrine.* 2012;41(2):281–288. doi:10.1007/s12020-011-9550-6.
35. Dong B, Ji W, Zhang Y. Elevated serum chemerin levels are associated with the presence of coronary artery disease in patients with metabolic syndrome. *Intern Med.* 2011;50(10):1093–1097. doi:10.2169/internalmedicine.50.5025.
36. Page MJ, McKenzie JE, Bossuyt PM, et al. The PRISMA 2020 statement: an updated guideline for reporting systematic reviews. *BMJ* 2021;372:n71. doi:10.1136/bmj.n71.
37. Wells GA, Shea B, D O'Connell, et al. The Newcastle-Ottawa Scale (NOS) for assessing the quality of nonrandomised studies in meta-analyses. http://www.ohri.ca/programs/clinical_epidemiology/oxford.asp. Accessed October 24, 2021.
38. Wallace BC, Dahabreh IJ, Trikalinos TA, et al. Closing the gap between methodologists and end-users: R as a computational backend. *J Stat Softw.* 2012;49(5):1–15. doi:10.18637/jss.v049.i05.
39. Viechtbauer W. Conducting meta-analyses in R with the metafor package. *J Stat Softw.* 2010;36(3):1–48. doi:10.18637/jss.v036.i03.
40. Higgins JPT, Thomas J, Chandler J, et al, eds. *Cochrane Handbook for Systematic Reviews of Interventions*. 2nd ed. Chichester, UK: John Wiley & Sons;. *Diabetologia.* 2019.
41. Hoellerl F, Brix JM, Schernthaner GH, et al. Increased chemerin levels are associated with peripheral arterial occlusive disease and increased urinary albumin excretion rate in type 2 diabetic patients [abstract]. *Diabetologia.* 2010;53:S501–S502. doi:10.1007/s00125-010-1872-z.
42. Chorell E, Olsson T, Jansson JH, et al. Lysophospholipids as predictive markers of ST-elevation myocardial infarction (STEMI) and non-ST-elevation myocardial infarction (NSTEMI). *Metabolites.* 2021;11(1):1–12. doi:10.3390/metabo11010025.
43. Aksakal A, Yanık A, Özdemir M, et al. The elevated levels of plasma chemerin and C-reactive protein in patients with acute coronary syndrome. *Cardiol Res Pract.* 2015;31(7):953–956. doi:10.1155/2018/5812704.
44. Leiherer A, Muendlein A, Kinz E, et al. High plasma chemerin is associated with renal dysfunction and predictive for cardiovascular events—insights from phenotype and genotype characterization. *Vascul Pharmacol.* 2016;77:60–68. doi:10.1016/j.vph.2015.08.010.
45. Ateş AH, Arslan U, Aksakal A, et al. Plasma chemerin levels are increased in ST elevation myocardial infartion patients with high thrombus burden [abstract]. *Anatol J Cardiol.* 2017;18:42.
46. Ateş AH, Arslan U. Plasma chemerin levels are increased in ST elevation myocardial infarction patients with high thrombus burden. *Cardiol Res Pract*. 2018;2018:5812704. doi:10.1155/2018/5812704.
47. Kumar M, Singh A, Misra V. Association of serum chemerin with hs-CRP in patients presenting with acute coronary syndrome with and without diabetes mellitus [abstract]. *Indian J Pathol Microbiol.* 2019;62(5):S74–S75.
48. Tunçez A, Altunkeser BB, Öztürk B, et al. Comparative effects of atorvastatin 80 mg and rosuvastatin 40 mg on the levels of serum endocan, chemerin, and galectin-3 in patients with acute myocardial infarction. *Anatol J Cardiol.* 2019;22(5):240–249. doi:10.14744/AnatolJCardiol.2019.64249.
49. Marechal P, Wéra O, Benoit A, et al. Neutrophil dynamics in acute coronary syndrome [abstract]. *Acta Clin Belg.* 2020;75:52–53. doi:10.1080/00015385.2020.1705029.
50. Szpakowicz A, Kaminski KA, Szpakowicz M, et al. Chemerin in coronary artery disease patients [abstract]. *Eur Heart J.* 2020;41(suppl 2):1263. doi:10.1093/ehjci/ehaa946.1263.
51. Kumar M, Singh A, Prajapati R, et al. Evaluation of chemerin in acute coronary syndrome and its role in cardiodiabetics. *J Clin Prevent Cardiol.* 2021;10(1):8–12. doi: 10.4103/jcpc.Jcpc_45_20.
52. Baig M, Alghalayini KW, Gazzaz ZJ, et al. Association of serum omentin-1, chemerin, and leptin with acute myocardial infarction and its risk factors. *Pak J Med Sci.* 2020;36(6):1–6. doi:10.12669/pjms.36.6.2372.
53. Kadoglou NP, Tahmatzidis DK, Giannakoulas C, et al. Serum levels of novel adipokines, omentin-1 and chemerin, in patients with acute myocardial infarction: KOZANI STUDY. *J Cardiovasc Med (Hagerstown).* 2015;16(5):341–346. doi:10.2459/JCM.0000000000000053.
54. Ateş AH, Arslan U, Aksakal A, et al. Plasma chemerin levels are increased in ST elevation myocardial infarction patients with high thrombus burden. *CardiolRes Pract*. 2018. doi:10.1155/2018/5812704.
55. Aronis KN, Sahin-Efe A, Chamberland JP, et al. Chemerin levels as predictor of acute coronary events: a case-control study nested within the Veterans Affairs Normative Aging Study. *Metab Clin Exp.* 2014;63(6):760–766. doi:10.1016/j.metabol.2014.02.013.
56. Sanchis-Gomar F, Perez-Quilis C, Leischik R, et al. Epidemiology of coronary heart disease and acute coronary syndrome. *Ann Transl Med.* 2016;4(13):256. doi:10.21037/atm.2016.06.33.
57. Virani SS, Alonso A, Benjamin EJ, et al. Heart disease and stroke statistics-2020 update: a report from the American Heart Association. *Circulation.* 2020;141(9):e139–e596. doi:10.1161/CIR.0000000000000757.
58. Menzin J, Wygant G, Hauch O, et al. One-year costs of ischemic heart disease among patients with acute coronary syndromes: findings from a multi-employer claims database. *Curr Med Res Opin.* 2008;24(2):461–468. doi:10.1185/030079908x261096.
59. Inci S, Aksan G, Dogan P. Chemerin as an independent predictor of cardiovascular event risk. *Ther Adv Endocrinol Metab.* 2016;7(2):57–68. doi:10.1177/2042018816629894.
60. Dessein PH, Tsang L, Woodiwiss AJ, et al. Circulating concentrations of the novel adipokine chemerin are associated with cardiovascular disease risk in rheumatoid arthritis. *J Rheumatol.* 2014;41(9):1746–1754. doi:10.3899/jrheum.140122.
61. Yoo HJ, Choi HY, Yang SJ, et al. Circulating chemerin level is independently correlated with arterial stiffness. *J Atheroscler Thromb.* 2012;19(1):59–66; discussion 67. doi:10.5551/jat.9647.
62. Weigert J, Neumeier M, Wanninger J, et al. Systemic chemerin is related to inflammation rather than obesity in type 2 diabetes. *Clin Endocrinol (Oxf).* 2010;72(3):342–348. doi:10.1111/j.1365-2265.2009.03664.x.
63. Lehrke M, Becker A, Greif M, et al. Chemerin is associated with markers of inflammation and components of the metabolic syndrome but does not predict coronary atherosclerosis. *Eur J Endocrinol*. 2009;161(2):339–344. doi:10.1530/EJE-09-0380
64. Spiroglou SG, Kostopoulos CG, Varakis JN, et al. Adipokines in periaortic and epicardial adipose tissue: differential expression and relation to atherosclerosis. *J Atheroscler Thromb.* 2010;17(2):115–130. doi:10.5551/jat.1735.
65. Salama FE, Anass QA, Abdelrahman AA, et al. Chemerin: a biomarker for cardiovascular disease in diabetic chronic kidney disease patients. *Saudi J Kidney Dis Transpl.* 2016;27(5):977–984. doi:10.4103/1319-2442.190867.
66. Zhou X, Tao Y, Chen Y, et al. Serum chemerin as a novel prognostic indicator in chronic heart failure. *J Am Heart Assoc.* 2019;8(15):e012091. doi:10.1161/JAHA.119.012091.
67. Menzel J, di Giuseppe R, Biemann R, et al. Association between chemerin, omentin-1 and risk of heart failure in the population-based EPIC-Potsdam study. *Sci Rep.* 2017;7(1):14171. doi:10.1038/s41598-017-14518-2.
68. Zhao D, Bi G, Feng J, et al. Association of serum chemerin levels with acute ischemic stroke and carotid artery atherosclerosis in a Chinese population. *Med Sci Monit.* 2015;21:3121–3128. doi:10.12659/msm.895866.

69. Zhang O, Ji Q, Lin Y, et al. Circulating chemerin levels elevated in dilated cardiomyopathy patients with overt heart failure. *Clin Chim Acta.* 2015;448:27–32. doi:10.1016/j.cca.2015.05.018.
70. Xiaotao L, Xiaoxia Z, Yue X, et al. Serum chemerin levels are associated with the presence and extent of coronary artery disease. *Coron Artery Dis.* 2012;23(6):412–416. doi:10.1097/MCA.0b013e3283576a60.
71. Hah YJ, Kim NK, Kim MK, et al. Relationship between chemerin levels and cardiometabolic parameters and degree of coronary stenosis in Korean patients with coronary artery disease. *Diabetes Metab J.* 2011;35(3):248–254. doi:10.4093/dmj.2011.35.3.248.
72. Motawi TMK, Mahdy SG, El-Sawalhi MM, et al. Serum levels of chemerin, apelin, vaspin, and omentin-1 in obese type 2 diabetic Egyptian patients with coronary artery stenosis. *Can J Physiol Pharmacol.* 2018;96(1):38–44. doi:10.1139/cjpp-2017-0272.
73. Lin X, Tang X, Jiang Q, et al. Elevated serum chemerin levels are associated with the presence of coronary artery disease in patients with type 2 diabetes. *Clin Lab.* 2012;58(5-6):539–544.
74. Aksan G, Inci S, Nar G, et al. Association of serum chemerin levels with the severity of coronary artery disease in patients with metabolic syndrome. *Int J Clin Exp Med.* 2014;7(12):5461–5468.
75. Szpakowicz A, Szpakowicz M, Lapinska M, et al. Serum chemerin concentration is associated with proinflammatory status in chronic coronary syndrome. *Biomolecules.* 2021;11(8):1149. doi:10.3390/biom11081149.
76. Gu P, Wang W, Yao Y, et al. Increased circulating chemerin in relation to chronic microvascular complications in patients with type 2 diabetes. *Int J Endocrinol.* 2019;2019:8693516. doi:10.1155/2019/8693516.
77. Chakaroun R, Raschpichler M, Klöting N, et al. Effects of weight loss and exercise on chemerin serum concentrations and adipose tissue expression in human obesity. *Metabolism.* 2012;61(5):706–714. doi:10.1016/j.metabol.2011.10.008.
78. Karsten E, Breen E, Herbert BR. Red blood cells are dynamic reservoirs of cytokines. *Sci Rep.* 2018;8(1):3101. doi:10.1038/s41598-018-21387-w.
79. Alfadda AA, Sallam RM, Chishti MA, et al. Differential patterns of serum concentration and adipose tissue expression of chemerin in obesity: adipose depot specificity and gender dimorphism. *Mol Cells.* 2012;33(6):591–596. doi:10.1007/s10059-012-0012-7.
80. Parlee SD, Ernst MC, Muruganandan S, et al. Serum chemerin levels vary with time of day and are modified by obesity and tumor necrosis factor-α. *Endocrinology.* 2010;151(6):2590–2602. doi:10.1210/en.2009-0794.

SCIENCE

# MicroRNA-149 rs2292832 C/T Polymorphism Predicts the Prognosis of Hepatocellular Carcinoma Patients With Bone Metastasis

*Jian Feng, MD, PhD,[1,2,a] Zhen Liu, MD, PhD,[3,a] Long Yu, MD, PhD,[4] Chaoyu Wu, MD,[5] Xiao-bo Luo, MD, PhD[4,*]*

[1]Department of Hepatopancreatobiliary Surgery, Peking University Shougang Hospital, Beijing, China, [2]Department of Hepatobiliary Surgery, The Fourth Medical Center of PLA General Hospital, Beijing, China, [3]Medical Supplies Center of PLA General Hospital, Beijing, China, [4]Senior Department of Orthopedics, The Fourth Medical Center of PLA General Hospital, Beijing, China, [5]Department of Infectious Diseases, Linyi Central Hospital, Linyi City, China. *To whom correspondence should be addressed. luoxiaobo_309@163.com [a]First authors.

**Keywords:** HCC, microRNA, polymorphism, prognosis, bone metastasis, biomarker

**Abbreviations:** HCC, hepatocellular carcinoma; OS, overall survival; RANKL, receptor activator of nuclear factor-kappaB ligand; lnc-RNA, long noncoding RNA; SNP, single-nucleotide polymorphism; TACE, transarterial chemoembolization; β-CTX, carboxy terminal peptide beta special sequence; PINP, procollagen I N-terminal propeptide; NTX, N-telopeptide of type I collagen; BAP, bone-specific alkaline phosphatase; SD, standard deviation; HBV, hepatitis B virus

*Laboratory Medicine* 2022;53:561–569; https://doi.org/10.1093/labmed/lmac036

## ABSTRACT

**Objective:** The prognostic markers of hepatocellular carcinoma (HCC) patients with bone metastasis are of great significance for the design of treatment strategy, the maintenance of life quality of the patients, and the improvement of cancer prognosis. MicroRNA-149 (miR-149) rs2292832 C/T polymorphism in HCC patients has been reported to be associated with the risk of HCC, but whether it can predict the prognosis of HCC patients with bone metastasis remains unclear. The goal of our study was to examine the prognostic impact of miR-149 rs2292832 C/T polymorphism on HCC patients with bone metastasis.

**Methods:** A total of 67 cases of HCC patients with bone metastasis (BC group) and 73 cases of HCC patients without bone metastasis (NC group) were included in this study. The miR-149 levels in blood leukocytes and tumor tissues were determined by qRT-PCR. Genotyping analysis of miR-149 rs2292832 was performed using polymerase chain reaction (PCR)-restriction fragment length polymorphism assay.

**Results:** The blood leukocyte miR-149 levels were significantly decreased in HCC patients, compared with the healthy controls, and they were significantly decreased in the BC patients, compared with the NC cases. BC patients carrying miR-149 rs2292832 CC+CT phenotype have a better overall survival (OS) rate, whereas no significant correlation was found between miR-149 rs2292832 CC+CT phenotype and the OS rate in NC group. The miR-149 rs2292832 CC+CT phenotype was correlated with certain bone turnover markers and bone metabolism markers but was not correlated with receptor activator of nuclear factor-kappaB ligand (RANKL) expression. Meanwhile, the combination of miR-149 rs2292832 CC+CT phenotype and RANKL expression could improve the prognosis assessment of HCC patients with bone metastasis.

**Conclusion:** miR-149 rs2292832 polymorphism might be a novel prognostic biomarker for HCC patients with bone metastasis. A follow-up study with a larger cohort from a multicenter should be performed to test our conclusions.

Hepatocellular carcinoma (HCC) is the fifth most common cancer worldwide and the second leading cause of cancer death in China.[1] Bone metastasis is a frequent complication of HCC, and the survival period of patients after diagnosis of bone metastasis is very short.[2] To date, it is still unclear which factors can affect prognosis in HCC patients with bone metastasis. Sporadic reports have found that the expression of some specific proteins such as receptor activator of nuclear factor-kappaB ligand (RANKL) expressions may be associated with prognosis of HCC-related bone metastasis.[3] However, due to the limitation of sensitivity and specificity, no target can be used in clinic yet. Recently, it has been reported that noncoding RNAs, like microRNAs (miRNAs) and long noncoding RNAs (lncRNAs), can predict the prognosis in HCC patients with bone metastasis, and interfering with their expression in animals can affect tumor progression. This indicates that these molecules might be both indicators and treatment targets.[4,5]

As potential therapeutic targets in tumor cells, miRNAs perform important roles in regulating gene expression.[6] Certain miRNA expression profiling has proven useful in diagnosing and understanding the development and progression of bone metastases.[7,8] As an important miRNA, miR-149 is located at 2q37.3 and has been documented to target both oncogenes and tumor suppressors, leading to dual impacts among cancers.[9,10] Further, miR-149 has been confirmed to play a key role in drug sensitivity and resistance.[11] However, the relationship between miR-149 and the occurrence and prognosis of bone metastasis in HCC is not clear yet.

Sequence variants in miRNA genes are described as mechanisms that can contribute to their deregulation.[12] A mutation or a single-nucleotide polymorphism (SNP) at a miRNA region might affect the transcription of miRNA primary transcripts, their processing to mature miRNA, or miRNA target interactions.[13] So far, many studies have investigated the association between the miR-149 rs2292832 C/T SNP and cancer risk.[14,15] However, to the best of our knowledge, the relationship between miR-149 rs2292832 C/T polymorphism and bone metastasis of HCC has not been reported. In this study, we aimed to determine the association between miR-149 expressions and miR-149 rs2292832 C/T polymorphism and bone metastasis risk in HCC and further explore their predicting functions on the prognosis of HCC patients with bone metastasis.

## Materials and Methods

### Patients

The inclusion criteria for this study were the following: (1) patients were histologically diagnosed as having HCC; (2) demographic variables, including age, race, and sex, were available; (3) tumor characteristics, including histological grade, T stage, N stage and bone metastasis status, were available. Patients diagnosed with common comorbidities, such as hepatic encephalopathy, ascites, incision infection, gastrointestinal bleeding, or with poor compliance were excluded from the present study. In total, 67 HCC patients with bone metastases (BC group) and 73 cases of age-matched HCC patients without bone metastases (NC group) were enrolled from Peking University Shougang Hospital, the Fourth Medical Center of PLA General Hospital, and Linyi Central Hospital, which are 2 academic hospitals and 1 local hospital (in Shandong), and all the included subjects were Chinese Han people. An additional 30 healthy volunteers (HV group) were included in this study as baseline analysis. The clinical assessment and grouping of all the included subjects were carried out in a double-blind way.

The diagnosis and treatment of HCC patients with or without bone metastasis were all performed according to the guidelines issued in China.[16] The treatment modalities for HCC included curative therapy (surgical resection, radiofrequency ablation, transplantation), transarterial chemoembolization (TACE), systemic chemotherapy, or symptomatic treatment, depending on the performance, extent of disease, and classification within or beyond Milan criteria at the time of presentation. Patients were considered for chemotherapy or palliative radiation based on functional status, extent of disease, presence of pain or neurologic complications, or risk for pathologic fractures. Chemotherapy that was offered to patients with bone metastases from HCC included sorafenib, doxorubicin, cisplatin, 5FU, capecitabine, gemcitabine, doxetacel, and axitinib. The putative therapeutic approaches and the corresponding outcomes were all clarified with the patients, and the therapeutic timing and approach were agreed and decided by both patients and doctors.

The presence of bone or extraskeletal metastases was determined by imaging, including bone scans, fluorodeoxyglucose-positron emission tomography, computed tomography, and magnetic resonance imaging and will be confirmed by histological examination of the disease via bone biopsy or surgical pathology. Radiologically abnormal lesions without pathological confirmation found in patients diagnosed with other types of invasive cancer within the previous 5 years were not considered as metastatic tumors.[16,17]

### Sample Preparation

Patients' blood and urine samples were collected on admission or within 24 hours. Urine was obtained as a morning second-void sample. Blood samples of all subjects were collected from cubital veins in the morning. The whole blood samples from the individuals were stored in an EDTA-coated vacutainer tube. The blood leukocytes were isolated from the whole blood of the included subjects by density-gradient centrifugation method using Ficoll medium (Amersham Pharmacy Biotechnology), according to our previous report.[18] Briefly, mix 1 mL whole blood and 1 mL PBS, and then add them to the top layer of 1 mL Ficoll solution. The mixtures were centrifuged at 2000 rpm for 20 min, and then the cell layer of blood leukocytes was gently sucked out. The serum was separated from blood samples by centrifuging at 2000*g* for 10 min at 4°C.

### Bone Turnover Markers and Bone Metabolism Markers Assay

Serum procollagen type I carboxy terminal peptide beta special sequence (β-CTX), procollagen I N-terminal propeptide (PINP), urinary N-telopeptide of type I collagen (NTX), and serum bone-specific alkaline phosphatase (BAP) were measured with electrochemiluminescence assay using kits from Roche Laboratory according to the manufacturer's instructions.

### Reverse Transcription-Quantitative Polymerase Chain Reaction Assay

TRIzol reagent (Invitrogen) was used to extract the total RNA from the blood leukocyte according to the manufacturer's protocol. Subsequently, reverse transcription-quantitative polymerase chain reaction (RT-qPCR) for miRNA and mRNA were carried out in the Eppendorf Realplex4 machine with the TaqMan MicroRNA Assay kit (Thermo Fisher) and PrimeScript RT-PCR kit (Takara), respectively. No-template cases were used as negative controls and were processed the same as the target templates. U6 small nuclear RNA and glyceraldehyde-3-phosphate dehydrogenase were used as an endogenous control for data normalization for microRNA levels and mRNA levels, respectively. Meanwhile, a fixed healthy control sample was selected as the calibration sample, and the expression of the targets in this sample were all set as "1." The normalized levels of the target genes of other samples were calculated by the $2^{-\Delta\Delta Cq}$ method, which were the ratios of them to the target gene expressions in the calibration sample.

### Genotyping of miR-149 rs2292832 C/T Polymorphism

Genomic DNA was extracted from a 200-μL whole blood sample of the patient by a commercial DNA isolation kit (BioTeke Corporation; product ID:DP2201) according to the manufacturer's instructions. The miR-149 rs2292832 genotypes for the patients were determined using a PCR-restriction fragment length polymorphism assay according to the previous report.[19]

### Statistical Analysis

Each experiment was performed no less than 3 times, and data were represented as the mean ± standard deviation (SD). All statistical analyses were performed using SPSS software version 17.0 (SPSS Company) and GraphPad (Prism 8.0, GraphPad). Descriptive data were summarized as mean (SD) or frequency (percentage) as appropriate. The differences between the 2 groups were determined using 2-tailed Student *t*-test or the Mann-Whitney U test for variables with an abnormal distribution. The $\chi^2$ test or Fisher exact test was used to analyze the relationship between miR-149 expressions or miR-149 rs2292832 C/T polymorphism and the clinicopathological features. Survival curves were calculated using the Kaplan–Meier method and compared by the log-rank test. $P < .05$ was considered to indicate a statistically significant difference.

## Results

### Patient Characteristics

The detailed information of the included HCC patients is summarized in **TABLE 1**. This study included 67 BC patients and 73 NC patients. Larger tumor size (>5 cm) patients and later T-stage (stage T3 or T4) patients were found in the BC group than in NC cases. There was no significant difference in age, histologic type, hepatitis B virus (HBV) infection between group BC and group NC. Of the 67 BC patients, bone metastasis occurred by hematogenous spread in 55 cases (82.1%). Fifty-eight patients (86.6%) had extraskeletal metastasis at the time of diagnosis of bone metastasis.

### MiR-149 Expressions in HCC Patients With or Without Bone Metastasis

The blood leukocyte miR-149 expressions were lower in total HCC patients (BC cases + NC cases) than in the HV group. Decreasing miR-149 levels were observed in BC cases, compared with the NC cases (**FIGURE 1A**). Meanwhile, the miR-149 levels in HCC tissues from BC group were significantly lower than that in NC group (**FIGURE 1B**). The miR-149 levels in HCC adjacent tissues were significantly increased, compared with that in tumor tissues, in both BC and NC group (**FIGURES 1C** and **1D**), and the miR-149 expressions in leukocytes was consistent with that in HCC tissues (**FIGURES 1E** and **1F**).

### Association of miR-149 Expressions With Prognosis of HCC Patients With or Without Bone Metastasis

Subsequently, we investigated whether miR-149 levels have clinical significance as prognostic markers in HCC patients. First, we found that there was no significant difference in the survival rate of both BC and NC patients under different curative therapy (data not shown), indicating that the therapy method had not affected overall survival rate. Subsequently, the normalized mean miR-149 level in BC group was at 0.665, and we divided the 67 BC cases into BCmiR-149$^{low}$ subgroup (36 cases) and BCmiR-149$^{high}$ subgroup (31 cases), using this mean value as cutoff. Also, the normalized mean miR-149 level in NC group was at 0.899, and we divided the 73 NC cases into NCmiR-149$^{low}$ subgroup (43 cases) and NCmiR-149$^{high}$ subgroup (30 cases) using this mean value as cutoff. Then the Kaplan-Meier survival analysis was used to determine the association of miR-149 expressions with prognosis of HCC patients with or without bone metastasis. First, we can see that the survival time of BC patients is significantly shorter than that of NC cases (**FIGURE 2A**). Meanwhile, the data indicated that the BCmiR-149$^{high}$ subgroup had significantly better overall survival (OS) prognosis than the BCmiR-149$^{low}$ subgroup (**FIGURE 2B**), while there was no significant difference in OS between NC-miR149$^{low}$ group and NC-miR-149$^{high}$ subgroup (**FIGURE 2C**). Further, as shown in **TABLE 2**, there was no significant association between any characteristics with miR-149 level in both BC and NC patients.

### Association of miR-149 rs2292832 Polymorphism With Prognosis of HCC Patients With or Without Bone Metastasis

Among 67 BC patients, a total of 37 patients carried the CT/CC genotype at miR-149 rs2292832 SNP site (BC$^{-C}$ subgroup), whereas 30 patients carried the TT genotype (BC$^{-T}$ subgroup). Meanwhile, 43 cases of NC patients carried the CT/CC genotype (NC$^{-C}$ subgroup), whereas 30 NC cases carried the TT genotype (NC$^{-T}$ subgroup). Kaplan-Meier analysis indicated that BC$^{-C}$ subgroup had a better OS prognosis, compared with the BC$^{-T}$ subgroup (**FIGURE 3A**), whereas there was no significant difference of OS prognosis between the NC$^{-C}$ and NC$^{-T}$ subgroups (**FIGURE 3B**). Furthermore, as shown in **TABLE 3**, BC$^{-C}$ subgroup exhibited less late T stage (T3 or T4) disease compared with the BC$^{-T}$

**TABLE 1. Characteristics of HCC Patients**

| Characteristics | HCC Patients (n = 140) | | *P* Value[a] |
|---|---|---|---|
| | BC Patients (n = 67) | NC Patients (n = 73) | |
| Age, y | | | |
| ≤50 | 24 | 31 | .421 |
| >50 | 43 | 42 | |
| Sex | | | |
| M | 47 | 48 | .578 |
| F | 20 | 25 | |
| Tumor size, cm | | | |
| ≤5 | 31 | 49 | .0130 |
| >5 | 36 | 24 | |
| T stage | | | |
| T1 or T2 | 32 | 50 | .0129 |
| T3 or T4 | 35 | 23 | |
| HBV infection | | | |
| Negative | 19 | 22 | .817 |
| Positive | 48 | 51 | |
| Spread pattern | | | |
| Hematogenous spread | 55 | NS | NS |
| Direct invasion from primary or metastatic tumor | 12 | NS | NS |
| Extraskeletal metastasis | | | |
| Negative | 9 | NS | NS |
| Positive | 58 | NS | NS |

*BC, HCC patients with bone metastasis; HBV, hepatitis B virus; HCC, hepatocellular carcinoma; NC, HCC patients without bone metastasis; NS, not statistically significant.*
[a]*$\chi^2$ test was used for comparison between the 2 groups.*

**FIGURE 1.** miR-149 expression is decreased in hepatocellular carcinoma (HCC) patients with (BC) or without (NC) bone metastasis. A, Quantitative polymerase chain reaction (qPCR) results comparing miR-149 levels in blood leukocyte among healthy volunteer (HV), NC, and BC groups (*$P$ < .05). B, qPCR results comparing the expression levels of miR-149 in HCC tissues between NC group and BC group (*$P$ < .05). qPCR results comparing the expression levels of miR-149 between HCC tissues and matched tumor-adjacent tissues in NC group ($P$ < .05) (C) and BC group ($P$ < .05) (D). qPCR results demonstrating the relationship between blood leukocyte miR-149 levels and HCC tissues miR-149 levels in NC group ($P$ < .05) (E) and BC group ($P$ < .05) (F). Significant differences were calculated by paired Student $t$-test.

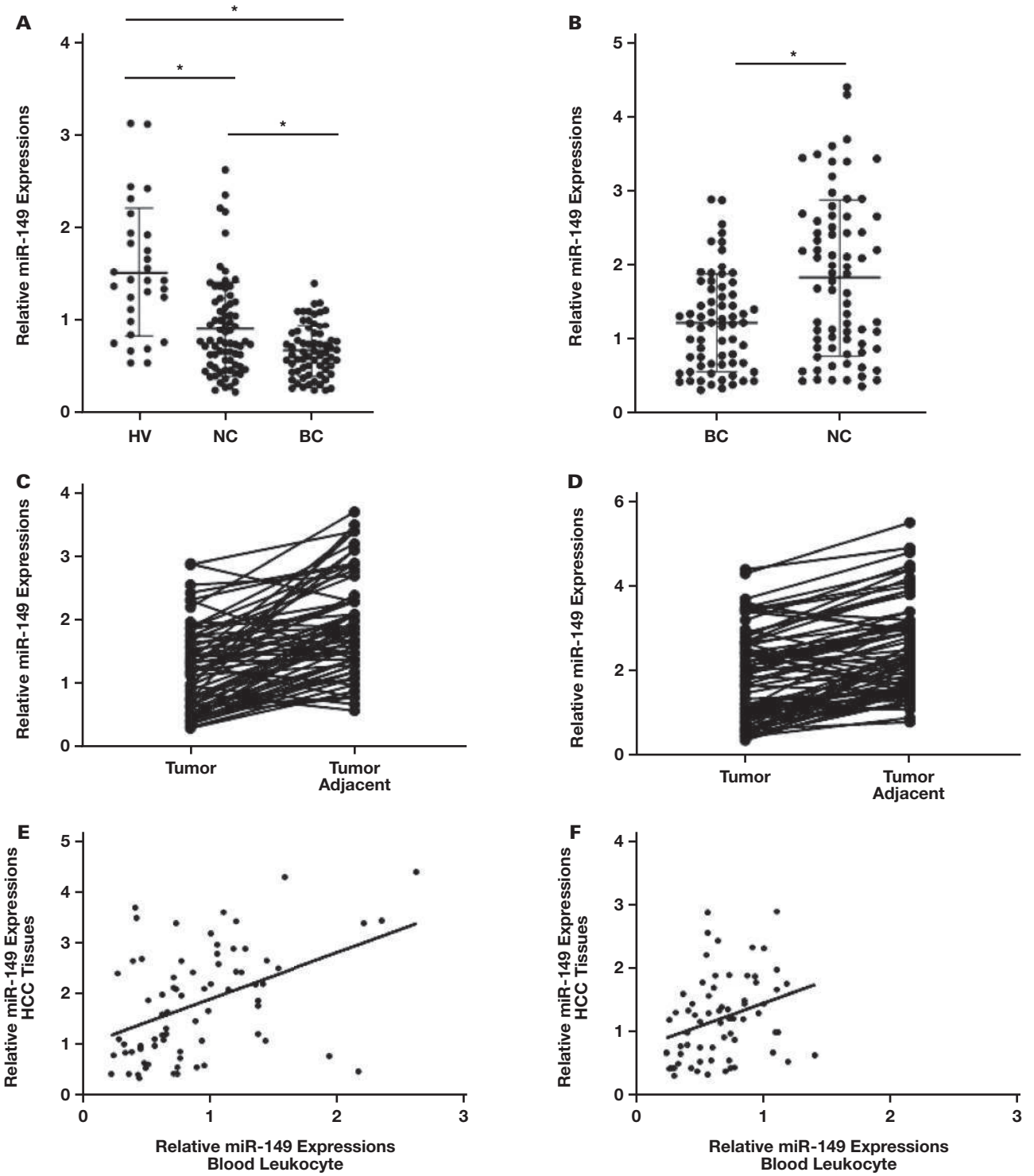






2022;53;561–569 | https://doi.org/10.1093/labmed/lmac036

**FIGURE 2.** **miR-149 expression is associated with the prognosis in hepatocellular carcinoma patients with (BC) or without (NC) bone metastasis. A, Comparing the overall survival (OS) rate between the NC patients and BC cases ($P < .05$). B, Comparing the OS rate between the BCmiR-149$^{high}$ subgroup and BCmiR-149$^{low}$ subgroup ($P < .05$). C, Comparing the OS rate between the NCmiR-149$^{high}$ subgroup and BCmiR-149$^{low}$ subgroup ($P > .05$).**

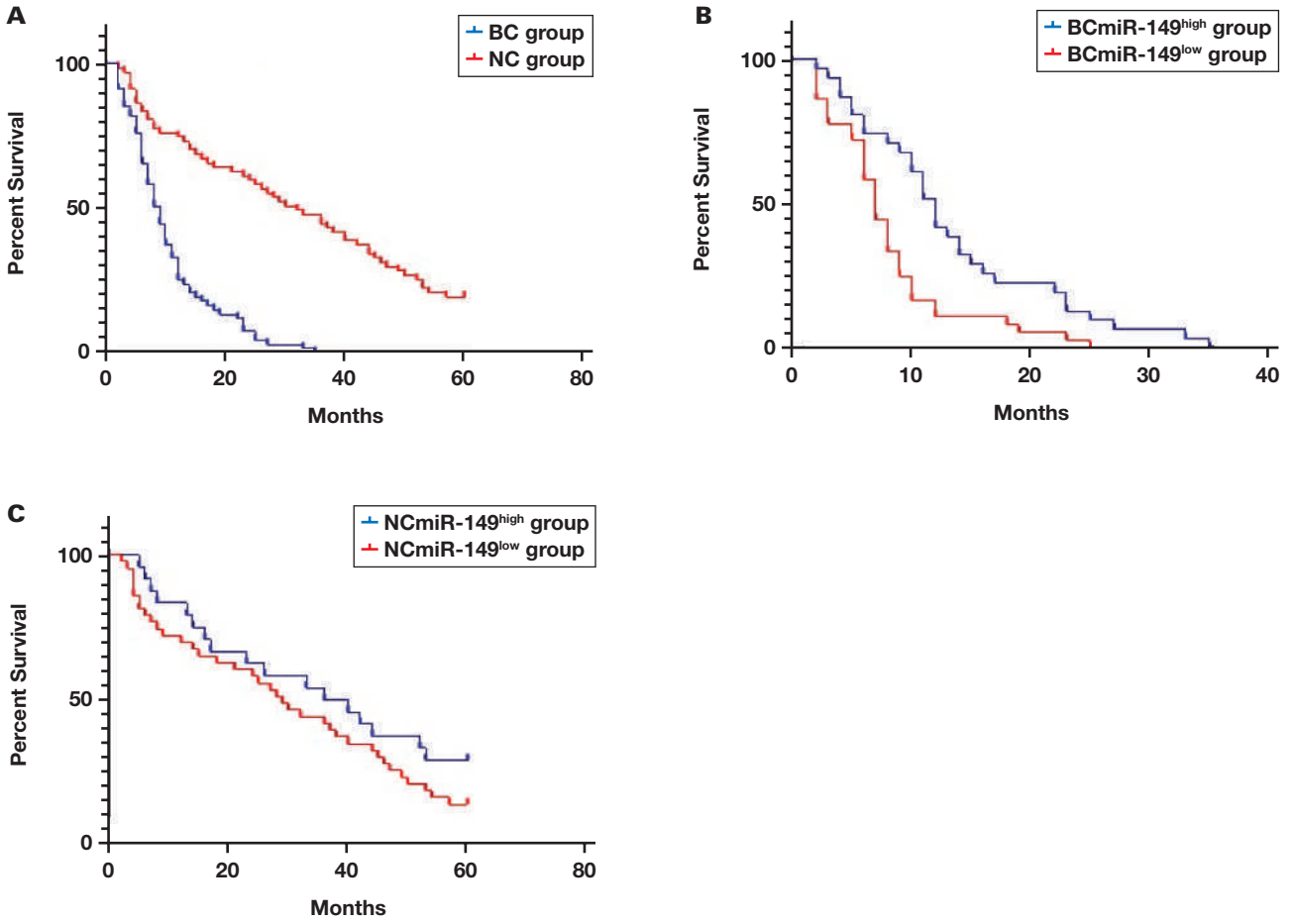


subgroup, whereas there was no significant difference of any clinical characteristics between NC$^{-C}$ and NC$^{-T}$ subgroups.

### Association of miR-149 rs2292832 Polymorphism With Bone Metastasis Markers in HCC Patients With or Without Metastasis

The above results suggest that miR-149 rs2292832 polymorphism might be closely related to the development of bone metastasis of HCC. Therefore, we next explored the relationship between miR-149 rs2292832 polymorphism and some markers of bone metastasis. The bone metabolism markers, urinary NTX, and serum BAP had been demonstrated as biomarkers for cancer bone metastasis.[20] Here, urinary NTX was significantly higher in the BC group, compared to the NC group and was correlated with miR-149 rs2292832 polymorphism in the BC group; whereas this correlation was not statistically significant in the NC group (**FIGURE 4A**). There was no significant correlation between miR-149 rs2292832 polymorphism and serum BAP levels in either the BC group or NC cases (**FIGURE 4B**). The bone turnover markers, PINP, and β-CTX, which were highly involved in bone metastasis progression,[18] were both associated with miR-149 rs2292832 polymorphism in the BC group, but not in the NC cases (**FIGURES 4C** and **4D**). However, the levels of RANKL (a key bone turnover promoter),[21] were not associated with miR-149 rs2292832 polymorphism (**FIGURE 4E**). The above results suggest that the miR-149 rs2292832 and RANKL might play important roles independently in the HCC development when it enters the bone metastasis stage.

### Combined Analysis of RANKL Level and miR-149 rs2292832 Polymorphism to Predict the Prognosis of HCC With or Without Bone Metastasis

Considering that miR-149 and RANKL are independent in predicting the prognosis of HCC bone metastases, we next explored the significance of combined analysis of RANKL level and miR-149 rs2292832 polymorphism for the prognosis of HCC bone metastasis. We divided BC patients into the following 4 subgroups: subgroup BC$^{-C}$RANKL$^{high}$, subgroup BC$^{-C}$RANKL$^{low}$, subgroup BC$^{-T}$RANKL$^{high}$, and subgroup BC$^{-T}$RANKL$^{low}$. Meanwhile, NC patients were also divided into the following 4 subgroups: subgroup NC$^{-C}$RANKL$^{high}$, subgroup NC$^{-C}$RANKL$^{low}$, subgroup NC$^{-T}$RANKL$^{high}$, and subgroup NC$^{-T}$RANKL$^{low}$. In BC patients, BC$^{-C}$ RANKL$^{low}$ subgroup had the best OS rate, whereas the 12-month OS rate for BC$^{-T}$RANKL$^{high}$ cases was the worst outcome (**FIGURE 4A**). The combined analysis of RANKL level and miR-149 rs2292832 polymorphism improved the assessment of prognosis in BC patients, compared with taking 1 (RANKL level or miR-149 rs2292832 polymorphism) as

**TABLE 2.** Relationship Between miR-149 Expressions and Clinical Features in HCC Patients

| Characteristics | BC Patients (n = 67) | | | NC Patients (n = 73) | | |
|---|---|---|---|---|---|---|
| | miR-149$^{low}$ (n = 36) | miR-149$^{high}$ (n = 31) | *P* Value | miR-149$^{low}$ (n = 43) | miR-149$^{high}$ (n = 30) | *P* Value |
| Age, y | | | | | | |
| ≤50 | 15 | 9 | .282 | 18 | 13 | .900 |
| >50 | 21 | 22 | | 25 | 17 | |
| Tumor size, cm | | | | | | |
| ≤5 | 14 | 17 | .192 | 27 | 22 | .345 |
| >5 | 22 | 14 | | 16 | 8 | |
| HBV positive | | | | | | |
| No | 8 | 11 | .230 | 11 | 11 | .310 |
| Yes | 28 | 20 | | 32 | 19 | |
| T stage | | | | | | |
| T1 or T2 | 15 | 17 | .282 | 28 | 22 | .457 |
| T3 or T4 | 21 | 14 | | 15 | 8 | |

*BC, patients with bone metastasis; HBV, hepatitis B virus; HCC, hepatocellular carcinoma; NC, patients without bone metastasis.*

**FIGURE 3.** MiR-149 rs2292832 polymorphism is associated with the prognosis in hepatocellular carcinoma patients with (BC) or without (NC) bone metastasis. A, Comparing the overall survival (OS) rate between the BC$^{-T}$ subgroup and BC$^{-C}$ subgroup (*P* < .05). B, Comparing the OS rate between the NC$^{-T}$ subgroup and NC$^{-T}$ subgroup (*P* > .05).

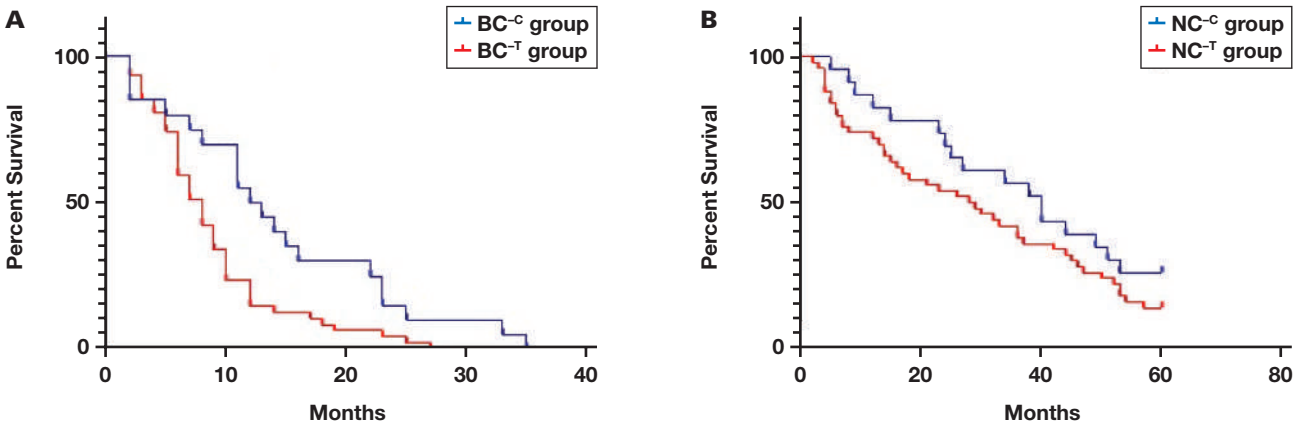


**TABLE 3.** Relationship Between miR-149 rs2292832 Polymorphisms and Clinical Features in HCC Patients

| Characteristics | BC Patients (n = 67) | | | NC Patients (n = 73) | | |
|---|---|---|---|---|---|---|
| | miR-149-T (n = 30) | miR-149-C (n = 37) | *P* Value | miR-149-T (n = 30) | miR-149-C (n = 43) | *P* Value |
| Age, y | | | | | | |
| ≤50 | 13 | 11 | .248 | 12 | 19 | .721 |
| >50 | 17 | 26 | | 18 | 24 | |
| Tumor size, cm | | | | | | |
| ≤5 | 12 | 19 | .354 | 17 | 32 | .112 |
| >5 | 18 | 18 | | 13 | 11 | |
| HBV positive | | | | | | |
| No | 7 | 12 | .411 | 6 | 16 | .115 |
| Yes | 23 | 25 | | 24 | 27 | |
| T stage | | | | | | |
| T1 or T2 | 10 | 22 | .0337 | 18 | 32 | .192 |
| T3 or T4 | 20 | 15 | | 12 | 11 | |

*BC, patients with bone metastasis; HBV, hepatitis B virus; HCC, hepatocellular carcinoma; NC, patients without bone metastasis.*

**FIGURE 4.** MiR-149 rs2292832 polymorphism is associated with bone metastasis markers in hepatocellular carcinoma patients with (BC) or without (NC) bone metastasis. A–E, Comparing the urinary NTX level (A), serum BAP level (B), serum PINP level (C), and serum β-CTX level (D) among $NC^{-T}$ subgroup, $NC^{-C}$ subgroup, $BC^{-T}$ subgroup, and $BC^{-C}$ subgroup. E, Quantitative polymerase chain reaction results comparing RANKL levels in tumor tissues among $NC^{-T}$ subgroup, $NC^{-C}$ subgroup, $BC^{-T}$ subgroup, and $BC^{-C}$ subgroup. *$P$ < .05. **$P$ > .05.

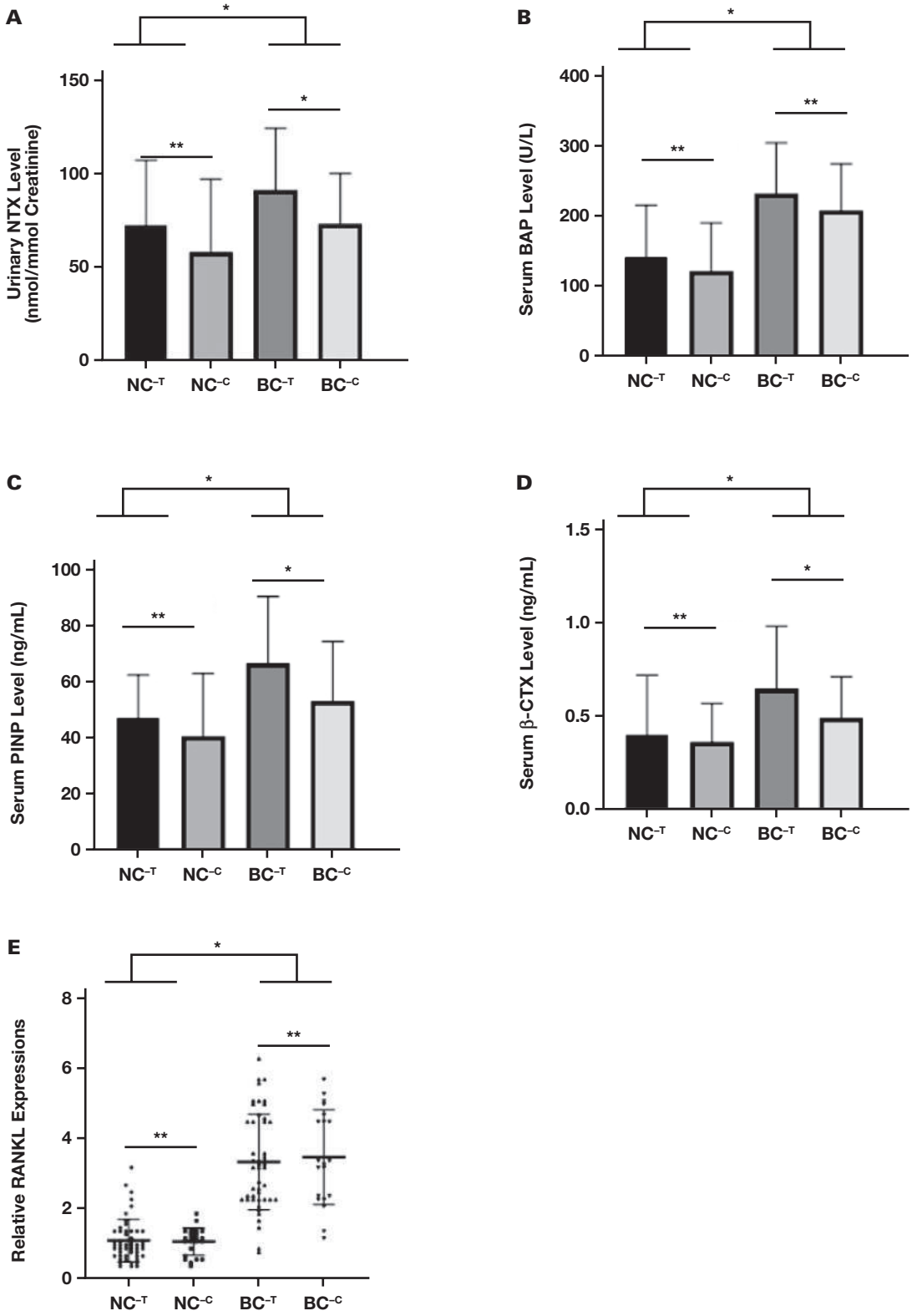

**FIGURE 5.** A, Comparing the overall survival (OS) rate among the subgroup BC$^{-C}$RANKL$^{high}$, subgroup BC$^{-C}$RANKL$^{low}$, subgroup BC$^{-T}$RANKL$^{high}$, and subgroup BC$^{-T}$RANKL$^{low}$. B, Comparing the OS rate among the subgroup NC$^{-C}$RANKL$^{high}$, subgroup NC$^{-C}$RANKL$^{low}$, subgroup NC$^{-T}$RANKL$^{high}$, and subgroup NC$^{-T}$RANKL$^{low}$. BC, hepatocellular carcinoma with bone metastasis; NC, hepatocellular carcinoma without bone metastasis.

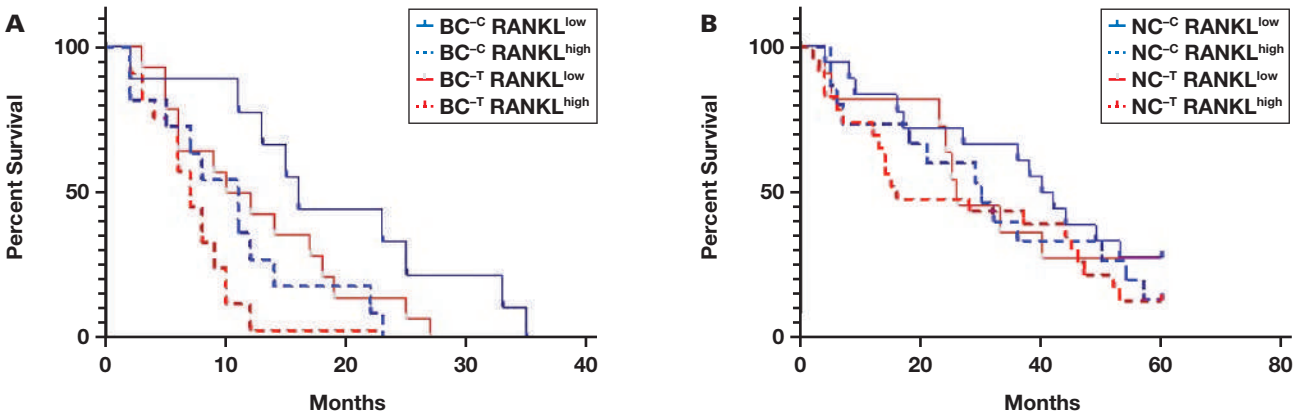


predictor ($P < .05$). As expected, there was no significant difference of the OS rate among NC$^{-C}$ RANKL$^{high}$, NC$^{-C}$ RANKL$^{low}$, NC$^{-T}$RANKL$^{high}$, and NC$^{-T}$RANKL$^{low}$ (**FIGURE 5**).

## Discussion

It is generally believed that miR-149 is an epigenetically silenced tumor-suppressive microRNA, which can inhibit the proliferation of cancer cells through directly targeting and inhibiting many key proteins, such as GIT1, AKT1, and Cyclin D1.[22–24] Our study found that lower miR-149 levels exist in blood leukocytes of HCC patients and HCC tissues than in non-HCC controls, and bone metastasis can cause downregulation of miR-149. Combined with previous evidence, these results suggest an association between miR-149 and bone metastasis-related HCC pathogenesis.

Previous work demonstrated that miR-149 rs2292832 C/T allele might impact the miR-149 level and its target-binding efficacy.[25] Based on these theories, it is not difficult to deduce that the miR-149 rs2292832 C/T genotype might be associated with tumor progressions. Many clinical studies have also proved this point. Zhang et al[25] confirmed that there was a significant association between miR-149 rs2292832 polymorphism and risk of gastric cancer. Similar results were also found in other cancer types, especially in digestive cancer.[14,15] However, whether miR-149 expression/rs2292832 polymorphism can become a universal tumor indicator remains controversial because, in some studies, the correlation between the miR-149 expressions/rs2292832 polymorphism and tumor development is not statistically significant.[26–28] Many factors can cause this controversy, including the regional differences of patients and the differences of treatment methods. Meanwhile, the miR-149 functions might vary in different tumor stages, which might also be one of the important factors that cause inconsistent clinical results. Based on these conjectures, we controlled the variables of bone metastasis or not in HCC patients and found that miR-149 expression/rs2292832 polymorphism was better as a prognostic index in HCC patients with bone metastasis. Our results confirm the correlation between miR-149 rs2292832 polymorphism and HCC risk, and this association was more prominent among bone metastasis cases. Further, our results indicated that miR-149 rs2292832 polymorphism was associated with tumor T stage and could predict the OS prognosis in bone metastasis cases but not in non–bone metastasis cases. Bone metastatic niches, in which disseminated tumor cells reside, have been defined as microdomains within the bone that support tumor cell seeding and outgrowth and are predominantly comprised of hematopoietic cells, mesenchymal stromal cells, osteoblasts, osteoclasts, and/or vascular cells.[29] It is well established that disseminated tumor cells secrete a variety of cytokines that promote osteoclast activity, which in turn causes the release of a variety of tumor-promoting growth factors from the bone, thus propagating a vicious cycle of tumor outgrowth and osteolytic bone breakdown. This is considered one of the important mechanisms of bone metastasis.[29] Considering that miR-149 has been reported to inhibit the cytokines secretion by targeting many inflammatory factors,[23] we can speculate that miR-149 might play an important regulatory role in metastatic tumor cells and thus affect the bone microenvironment.

Bone metastasis markers and bone turnover markers were reported as important indicators for bone metastasis.[20,21] Also, it was suggested that cancer patients with higher levels of RANKL carried a higher risk of bone metastasis.[21] In this study, miR-149 rs2292832 polymorphism was correlated with certain bone metastasis markers (NTX) and bone turnover markers (PINP and β-CTX) but not with RANKL expressions. This result initially puzzled us because RANKL was the bone turnover promoter and was highly associated with PINP and β-CTX. This might be because miR-149 functions on bone turnover independent of RANKL.

The sensitivity and specificity of miR-149 level and rs2292832 C/T polymorphism for HCC do not appear to be more outstanding, compared with some tumor markers that have been used in clinical trial, but they still have clinical application value. The characteristic of miR-149 is that it can be combined with some tumor markers. Here, a combined survival analysis of miR-149 rs2292832 polymorphism and the RANKL levels revealed 4 distinct subgroups with statistically significant differences in the OS prognosis in bone metastasis of HCC patients. BC$^{-c}$RANK$^{low}$ predicted the best overall survival rate, whereas BC$^{-T}$RANK$^{high}$ predicted the worst. These results demonstrate that the combined analysis of miR-149 rs2292832 polymorphism and other markers will be a potential method for future clinical prognosis evaluation of tumors.

Here, some significant study limitations also exist and need to be improved in the follow-up experiments. Further exploration based on

more patients from different regions should be performed, and the clinical variables other than bone metastasis patterns need to be controlled. Meanwhile, laboratory studies need to be held to verify the functional diversity of miR-149, in different tumor stages.

## Conclusion

In conclusion, the significance of this result is that it provides evidences that miR-149 rs2292832 polymorphism might be a novel indicator for HCC patients with bone metastasis, which was highly associated with bone metastasis markers and could predict the tumor T stage and OS prognosis.

## Ethical Statement

All the experiments were carried out according to the principles of the Helsinki Declaration. All authors confirm that they have no conflict of interest. The ethical approval was obtained from the ethics committees of all 3 included hospitals. Informed consent was obtained from all patients before participation.

## Funding

This work was financially supported by the Hygiene and Health Development Scientific Research Fostering Plan of Haidian District Beijing (HP2021-04-80501).

## REFERENCES

1. Torre LA, Bray F, Siegel RL, Ferlay J, Lortet-Tieulent J, Jemal A. Global cancer statistics, 2012. *CA Cancer J Clin*. 2015;65:87–108.
2. Guo X, Xu Y, Wang X, et al. Advanced hepatocellular carcinoma with bone metastases: prevalence, associated factors, and survival estimation. *Med Sci Monit*. 2019;25:1105–1112.
3. Sasaki A, Ishikawa K, Haraguchi N, et al. Receptor activator of nuclear factor-kappaB ligand (RANKL) expression in hepatocellular carcinoma with bone metastasis. *Ann Surg Oncol*. 2007;14:1191–1199.
4. Bharali D, Jebur HB, Baishya D, et al. Expression analysis of serum microRNA-34a and microRNA-183 in hepatocellular carcinoma. *Asian Pac J Cancer Prev*. 2018;19:2561–2568.
5. Abbastabar M, Sarfi M, Golestani A, Khalili E. lncRNA involvement in hepatocellular carcinoma metastasis and prognosis. *EXCLI J.* 2018;17:900–913.
6. Lian J, Li Y, Yu M. MicroRNA-183 and microRNA-141 are potential risk factors for poor prognosis in patients with nasopharyngeal carcinoma. *Oncol Lett*. 2019;17:1172–1176.
7. Xiang ZL, Zhao XM, Zhang L, et al. MicroRNA-34a expression levels in serum and intratumoral tissue can predict bone metastasis in patients with hepatocellular carcinoma. *Oncotarget*. 2016;7:87246–87256.
8. Fu Q, Liu X, Liu Y, Yang J, Lv G, Dong S. MicroRNA-335 and -543 suppress bone metastasis in prostate cancer via targeting endothelial nitric oxide synthase. *Int J Mol Med*. 2015;36:1417–1425.
9. Jin L, Hu WL, Jiang CC, et al. MicroRNA-149*, a p53-responsive microRNA, functions as an oncogenic regulator in human melanoma. *Proc Natl Acad Sci U S A.* 2011;108:15840–15845.
10. Xu RD, Feng F, Yu XS, Liu ZD, Lao LF. miR-149-5p inhibits cell growth by regulating TWEAK/Fn14/PI3K/AKT pathway and predicts favorable survival in human osteosarcoma. *Int J Immunopathol Pharmacol.* 2018. doi: 10.1177/2058738418786656.
11. Xiang F, Fan Y, Ni Z, et al. Ursolic acid reverses the chemoresistance of breast cancer cells to paclitaxel by targeting MiRNA-149-5p/MyD88. *Front Oncol.* 2019;9:501.
12. Diederichs S, Haber DA. Sequence variations of microRNAs in human cancer: alterations in predicted secondary structure do not affect processing. *Cancer Res.* 2006;66:6097–6104.
13. Yang W, Chendrimada TP, Wang Q, et al. Modulation of microRNA processing and expression through RNA editing by ADAR deaminases. *Nat Struct Mol Biol.* 2006;13:13–21.
14. Li L, Liu T, Li Z, Zhang L, Zhang Z. The miR-149 rs2292832 T/C polymorphism may decrease digestive cancer susceptibility: an updated meta-analysis. *Int J Clin Exp Med*. 2015;8:15351–15361.
15. Choupani J, Nariman-Saleh-Fam Z, Saadatian Z, Ouladsahebmadarek E, Masotti A, Bastami M. Association of mir-196a-2 rs11614913 and mir-149 rs2292832 polymorphisms with risk of cancer: an updated meta-analysis. *Front Genet*. 2019;10:186.
16. Zhou J, Sun HC, Wang Z, et al. Guidelines for diagnosis and treatment of primary liver cancer in China (2017 edition). *Liver Cancer*. 2018;7:235–260.
17. Matsumiya H, Todo Y, Okamoto K, et al. A prediction model of survival for patients with bone metastasis from uterine cervical cancer. *J Gynecol Oncol*. 2016;27:e55.
18. Wu C, Wang X, Zhang J, et al. MicroRNA-224 expression and polymorphism predict the prognosis of hepatitis B virus-related hepatocellular carcinoma patients after liver resection. *Clin Lab*. 2019;65:967–974.
19. Ghaffarzadeh M, Ghaedi H, Alipoor B, et al. Association of MiR-149 (RS2292832) variant with the risk of coronary artery disease. *J Med Biochem.* 2017;36:251–258.
20. Coleman RE, Major P, Lipton A, et al. Predictive value of bone resorption and formation markers in cancer patients with bone metastases receiving the bisphosphonate zoledronic acid. *J Clin Oncol.* 2005;23:4925–4935.
21. Haynes BP, Viale G, Galimberti V, et al. Differences in expression of proliferation-associated genes and RANKL across the menstrual cycle in estrogen receptor-positive primary breast cancer. *Breast Cancer Res Treat*. 2014;148:327–335.
22. Ye X, Chen X. miR-149-5p inhibits cell proliferation and invasion through targeting GIT1 in medullary thyroid carcinoma. *Oncol Lett*. 2019;17:372–378.
23. Xue L, Wang Y, Yue S, Zhang J. Low MiR-149 expression is associated with unfavorable prognosis and enhanced Akt/mTOR signaling in glioma. *Int J Clin Exp Pathol.* 2015;8:11178–11184.
24. Ghasemi A, Fallah S, Ansari M. MicroRNA-149 is epigenetically silenced tumor-suppressive microRNA, involved in cell proliferation and downregulation of AKT1 and cyclin D1 in human glioblastoma multiforme. *Biochem Cell Biol.* 2016;94:569–576.
25. Zhang L, Liu Q, Wang F. Association between miR-149 gene rs2292832 polymorphism and risk of gastric cancer. *Arch Med Res*. 2018;49:c270–277.
26. Ranjbar R, Chaleshi V, Aghdaei HA, Morovvati S. Investigating the association between miR-608 rs4919510 and miR-149 rs2292832 with colorectal cancer in Iranian population. *MicroRNA*. 2018;7:100–106.
27. Cîmpeanu RA, Popescu DM, Burada F, et al. miR-149 rs2292832 C>T polymorphism and risk of gastric cancer. *Rom J Morphol Embryol*. 2017;58:125–129.
28. Wang R, Zhang J, Ma Y, et al. Association study of miR-149 rs2292832 and miR-608 rs4919510 and the risk of hepatocellular carcinoma in a large-scale population. *Mol Med Rep*. 2014;10:2736–2744.
29. Guise T. Examining the metastatic niche: targeting the microenvironment. *Semin Oncol*. 2010;37 Suppl 2:S2–14.

# Validating the HPA-1 to -5 and -15 Detection by Homemade PCR-SSP, Real-Time PCR, and PCR-RFLP Methods

*Seyed Ghader Azizi, PhD,[1,2] Shahram Samiee, Msc,[1] Maryam Zadsar, MD,[1,*] Mojgan Shaiegan, Pharm, PhD[1]*

[1]Iranian Blood Transfusion Research Center, High Institute for Research & Education in Transfusion Medicine, Tehran, Iran, [2]Clinical Immunology Research Center, Zahedan University of Medical Sciences, Zahedan, Iran *To whom correspondence should be addressed. Maryam.zad@gmail.com

**Keywords:** human platelet antigens, HPAs, TaqMan real-time PCR, PCR-RFLP

**Abbreviations:** HPA, human platelet antigen; PCR-SSP, sequence-specific primer-polymerase chain reaction; RFLP, restriction fragment length polymorphism; SNV, single-nucleotide variant; Tm, melting temperature; MIQE, Minimum Information for Publication of Quantitative Real-Time PCR Experiments; ITBO, Iranian Blood Transfusion Organization; bp, base pairs; NIBSC, National Institute for Biological Standards and Control; ISBT, International Society of Blood Transfusion; NGS, next-generation sequencing; SBT, sequence-based typing; FAM, 6-carboxy-flourescein; VIC, Victoria.

*Laboratory Medicine* 2022;53:570–579; https://doi.org/10.1093/labmed/lmac050

## ABSTRACT

**Objective:** Human platelet antigens (HPAs) are antigenic determinants on platelet membrane glycoproteins that stimulate the host's immune system and cause platelet destruction. In this study, we share our experience with implementing sequence-specific primer-polymerase chain reaction (PCR-SSP), real-time PCR, and PCR-RFLP (restriction fragment length polymorphism) and the validation process used to evaluate the results.

**Methods:** At the Ardabil Blood Transfusion Center, 10 samples were obtained from blood donors. Validation using PCR-SSP, real-time PCR, and PCR-RFLP methods for genotyping HPAs was done by sequencing. A commercial DNA sample and a commercial kit were also used for validation.

**Results:** The results of PCR-SSP, TaqMan Real-Time PCR, melting curve analysis (HPA-15), and PCR-RFLP (HPA-3) were 100% consistent with sequencing (gold standard) and commercial kit results.

**Conclusions:** There was a 100% correlation between repeating the methods and the expected results for repeatability, and no false positives and negatives were observed.

Human platelet antigens (HPAs) are antigenic determinants on the platelet membrane glycoproteins. Single-nucleotide variants (SNVs) on corresponding coding regions generate these immunogenic antigens.[1] Twelve antigens in 6 bi-allelic groups, named HPAs-1 to -5 and -15, are considered highly abundant HPAs. When exposed to the recipient's immune system by transfusion, transplantation, or pregnancy, these antigens may stimulate the host's immune system and cause platelet-destroying immune reactions, leading to decreased platelet count.[2]

Detection of these polymorphisms is essential to diagnose and manage clinical situations like platelet refractoriness, immune thrombocytopenia, and fetal and neonatal alloimmune thrombocytopenia. Because blood services face the challenge of finding the best donors for refractory thrombocytopenic patients at risk of bleeding, we need to access validated, reliable, and cost-effective methods for HPA genotyping.[3–5]

The most applicable and conventional methods include sequence-specific primer-polymerase chain reaction (PCR-SSP) and restriction fragment length polymorphism-PCR (PCR-RFLP). In the PCR-SSP method, a mismatch at the 3' end between the primers and template DNA reduces Taq-polymerase enzyme efficiency, so the PCR process does not proceed and we have no products; on the other hand, complete matching between 3' end of primers and the target DNA leads to accumulation of PCR products.[3] The gene fragments containing the desired polymorphism region are amplified and digested by specific endonuclease enzymes at the target position in the RFLP method.

More precise methods, such as real-time PCR, sequencing, Luminex, BioArray, and Bead chip methods, are used in many laboratories worldwide.[6–8] One of the most widely used methods is the TaqMan Real-Time PCR. The release of the fluorescence from the 5' end of the SNV-specific probe by the 5'-3' exonuclease activity of the DNA-Taq polymerase enzyme is the basis of the TaqMan Real-Time PCR. When the probe stays connected to its specific sequence, the 3' end quencher on the probe suppresses the reporter's fluorescence in the 5' end; however, as the PCR process continues, the reporter dye is released by the DNA Taq-polymerase enzyme, and a fluorescence signal is emitted. During each

PCR reaction, the fluorescence intensity increases and becomes observable as a graph.[9]

The melting curve analysis is a specific method for LightCycler devices that uses hybridization probes and fluorescence resonance energy transfer. In this method, two labeled probes with fluorescent substances are used. One of these probes, called the acceptor or sensor probe, is connected to a region where the desired mutation is present. The other probe connects to an area adjacent to the sensor probe, named anchor or donor. When the two probes are close together, a laser beam with a specified wavelength is radiated to the donor, excites it, and produces a specific level of energy transmitted to the sensor probe. Finally, the sensor probe emits another light for different energy levels detected by the device and is displayed as a diagram. After annealing the probes, if the mix is heated, the sensor probe attaches to the region containing the mutant base, melts from the DNA earlier than the original base, and has a lower melting temperature (Tm); this produces a different fluorescence profile than when a single-stranded DNA and probe are matched perfectly. As a result, the mutant base and wild show different temperature patterns that are easily distinguishable.[10]

Despite these new methods, the PCR-SSP is still exploited widely because of its simplicity and low cost.[6,7,11,12] Nevertheless, the PCR-SSP has some drawbacks: interpretation errors, cross-contamination due to post-PCR manipulation of products, and unpredictable incorrect results in some samples, obligating a validation approach.[9]

Our previous study[13] determined the genotypes of blood donors with Azeri ethnicity by PCR-SSP and TaqMan Real-Time PCR methods. One of our previous significant goals was to help platelet transfusion effectively. To achieve this goal, we had to fulfill two smaller goals: finding platelet donors and establishing suitable methods for HPA genotyping. The first target can be met by establishing a platelet registry system, whereas to achieve the second goal, we must establish methods to validate previous methods (PCR-SSP and real-time PCR). Herein, we explain our experience implementing PCR-SSP by running a homemade method, real-time PCR and PCR-RFLP, and the validation process used to evaluate the results. To do this, we used the checklists used in the Minimum Information for Publication of Quantitative Real-Time PCR Experiments (MIQE) guidelines. Although these instructions apply to the real-time PCR method, we used them to validate our homemade PCR-SSP and PCR-RFLP method. MIQE includes several items such as designing, sampling, DNA extraction, target gene information, PCR protocol, and method validation. To validate the PCR-SSP, real-time PCR, and PCR-RFLP, we used sequencing analysis, a commercial kit, and a commercial DNA with a known genotype. HPA-3 and -15 have a high rate of heterozygous patterns in most populations, so we decided to use an additional method to evaluate them. For HPA-3, we used PCR-RFLP, and we used the melting curve analysis for HPA-15.

## Materials and Methods

### Sampling Process

The checklist used in the MIQE was used for the sampling process evaluation. The checklist covers the sample definition, volume, sampling procedure, conditions, freezing rate, storage conditions, and duration of storage.[14] Ten samples were obtained from blood donors after receiving informed consent in the Ardabil Blood Transfusion Center. The Ethics Committee of the High Institute for Education and Research in Transfusion Medicine (Iranian Blood Transfusion Organization [IBTO]) approved this study (approval ID: IR.TMI.REC.1397.009). Whole blood samples were collected in 5 mL tubes containing EDTA as an anticoagulant; they were then shaken gently to mix EDTA into the sample. The samples were taken from the vacuum tube accessory pouches during the donation to avoid further blood collection; this also reduces the risk of donor skin microorganisms entering the main bag. At the beginning of the phlebotomy, the first obtained samples were directed to the donor's routine test accessory pouch. The specimens were transferred to the laboratory at 2°C to 8°C.

During sampling, errors such as sample identification mistakes or wrong-blood-in-tube error, bacterial contamination, blood clots, and failure to maintain the appropriate temperature conditions may occur. Because the donor's blood collection standards were observed for our samples, the errors were minimized as much as possible. These standards included the authentication of a barcode to each donor, implementation of all instructions for disinfection of venipuncture site according to IBTO protocols, directing the first 80 mL of the sample taken at the beginning of the donation to the diversion pouch, shaking the sample tubes according to the IBTO standards, and storing the samples in the refrigerator until the samples were used.

### DNA Extraction

The considered items for DNA extraction were procedure and instrumentation, DNA extraction kit, contamination assessment, nucleic acid quantification, and purity of the DNA.[14]

The genomic DNA was extracted by the QIAamp DNA Mini kit (Qiagen) according to the manufacturer's instructions. The quality of the extracted DNAs was evaluated by a spectrophotometer (Nanodrop ND-1000, Thermo Fisher Scientific) by calculating the absorbance at a wavelength of 260 nm for DNA and absorbance in 280 nm for protein. A DNA sample with A260/A280 between 1.6 and 2.0 and a concentration of 25 ng/μL to 50 ng/μL was acceptable for our purposes.

### Design and Evaluation of Primers

The locations carrying HPAs polymorphisms were taken from the United States National Center for Biotechnology Information (NCBI). HPA-1 and -4 are encoded by ITGB3 (accession number: NG_008332.2). HPA-2, -3, -5, and -15 are encoded by GP1BA, ITGA2B, ITGA2, and CD109, respectively, with accession numbers NG_008767, NG_008331, NG_008330, and NG_033971.1, respectively. All polymorphisms were evaluated by SnapGene 3.2.1 software. Primer parameters, including the sequence size, GC content, number of annealed bases, Tm, amplified region, and product size, were evaluated by SnapGene 3.2.1 software. Also, we used the SnapGene 3.2.1 software to simulate the products' electrophoretic patterns with different agarose concentrations.

We observed our primer or product shapes (possible self-dimer, hairpin, cross-dimer, runs, and repeats) at different temperatures and concentrations of $MgCl_2$ and other salts using M-fold software. The evaluation of these structures is essential, particularly in the primer annealing temperature, where these constructions make it hard to connect primers to specific locations.

Different SNVs at the junction sites of primers, especially in their 3', prevent them from connecting to the target region and lead to false-negative results. Using SNP Masker software, the presence of different SNVs in the connection area of primers was examined. Finally, we used the Basic Local Alignment Search Tool (BLAST) program

(https://blast.ncbi.nlm.nih.gov/Blast.cgi) to compare the primer sequences with the database and evaluate statistical features.

We used sequencing as the gold standard for genotyping HPA-1 to -5 and -15. Primer Premier Software version 6.24 was used to design the sequencing primers. With this software, we could design primers for standard PCR. The parameters such as Tm, GC content, hairpin ΔG, self-dimer ΔG, GC clamp, Ta opt, and secondary structures were evaluated. **TABLE 1** shows primers for sequencing.

The primers required for PCR-SSP and TaqMan Real-Time PCR were obtained from our previous study.[13] We used Allele ID 7.85 and Primer express 3.0 software to analyze the accuracy and performance of the probes and primers. Also, the parameters such as primer and probe Tm, GC content, hairpin ΔG, self-dimer ΔG, GC clamp, Ta opt, and secondary structures were analyzed.

The primers required for PCR-RFLP were extracted from *Molecular Protocols in Transfusion Medicine*[15] 5'-TGGAAGAAAGACCTGGGAAGG-3' as forward and 5'-CTCCTTAACGTACTGGGAAGC 3' as the reverse primer. The product length was 448 base pairs (bp), and *Fok*I was used as the restriction enzyme.

The required primers and probes for melting curve analysis were obtained from Liew et al[16] and evaluated by AlleleID 7.85 software. The primer sequence consisted of ATTTTGGCTTATTTCAAAATGTATCAGT as the forward primer and GTCTTGGACTAACAACTACTACTCCAGT as the reverse primer. The sequence of probes was ACTTCAGTTCCAGGATATTACCAAA-FITC as the anchor probe and LC RED 640-AATTTGAAGTAACTGTACACG ATTCTATCACTTCTT-P as the sensor probe.

## Validation of PCR-SSP, Real-Time PCR and, PCR-RFLP

Validation of PCR-SSP, real-time PCR, and PCR-RFLP methods for genotyping of HPA-1 to -5 and -15 started from the sequencing step. Therefore, we first selected 10 samples from 100 donors with Azeri ethnicity, amplified them, and sent them for sequencing. In the next step, these samples were genotyped by PCR-SSP, real-time PCR, and PCR-RFLP methods. A commercial DNA sample (Innotrain) with a specific genotype was also genotyped along with these 10 samples and compared with the product brochure results. These samples were then genotyped again using a commercial kit, and the results were compared with the sequencing results. Finally, the samples were genotyped again in different runs and the repeatability of the methods was evaluated.

**TABLE 1. Primers Used for Sequencing**

| HPA (Sequencing) | Primer | Sequence |
|---|---|---|
| HPA-1 | Forward | 5'-TTTATGCTCCAATGTACGGGGTAAAC-3' |
| | Reverse | 5'-GATTCTGGGGCACAGTTATCCTTCAGC-3' |
| HPA-2 | Forward | 5'-GGGTGACCTCGCTGCCTCTTGGTG-3' |
| | Reverse | 5'-GGAGGAGAAGGGTGTCGAGATTCTC-3' |
| HPA-3 | Forward | 5'-CTGGGCCTGACCACTCCTTTGC-3' |
| | Reverse | 5'-TCACTACGAGAACTGGATCCTGAAG-3' |
| HPA-4 | Forward | 5'-AAGAATTTCTCCATCCAAGTGCG-3' |
| | Reverse | 5'-GGTGGGGAGATATACATGTAT-3' |
| HPA-5 | Forward | 5'-ATGAGTGACCTAAAGAAAGAGG-3' |
| | Reverse | 5'-GAAATGTAAACCATACTATCTGTGC-3' |
| HPA-15 | Forward | 5'-ATTTTGGCTTATTTCAAAATGTATCAGT-3' |
| | Reverse | 5'-ACTGGAGTAGTTGTTAGTCCAAGAC-3' |

## Sequencing

The final reaction volume for sequencing was adjusted to 20 μL, including 1 μL forward primer, 1 μL reverse primer, 10 μL 2× Mastermix (IBTO), 0.3 μL Hot start Taq polymerase, 3 μL $H_2O$, and 5 μL DNA (25–50 ng/μL). Reaction temperature conditions were 96°C for 10 min as activation, 40 cycles of 96°C for 20 s, 55°C for 30 s, 72°C for 90 s as amplification, and 72°C for 5 min as a final extension. The reaction products were sent to Royazistagene for sequencing after electrophoresis on 2% agarose. The results were analyzed by Codon code aligner software.

## Homemade PCR-SSP Method

The Metcalf procedure (https://www.nibsc.org/asset.ashx?assetid=b2dfaa8e-1148-4f73-884f-702162412507) with a slightly modified method was used for the PCR-SSP. The optimization of the PCR-SSP reaction included optimizing the concentration of $MgCl_2$, dNTP, and primers and optimizing TA. We also used the experiences of previous studies performed in IBTO. The final reaction volume was 20 μL, containing 1 μL allele-specific HPAa/b primer with 1 μL common HPA primer (1 μmol/L); 0.5 μL HGH forward primer and 0.5 μL HGH reverse primer (0.25 μmol/L) as an internal control; 7.8 μL RNase and DNase free distilled water; 0.7 μL DNTP (0.5 mmol/L); 2 μL PCR 10× Buffer (IBTO): 1.2 μL $MgCl_2$ (1.5 μmol/L): 2 μL betaine (0.5 mol/L); 0.3 μL Taq DNA-polymerase (Add Taq DNA, ADDBIO): and 3 μL DNA (25–50 ng/μL). Hot Start Taq DNA polymerase (ADDBIO) was added for HPA-3 genotyping.

A DNA sample (InnoTrain) with the known genotype for HPA-1 to -5 and -15 was used as an external control. The products were run on 2% agarose gel (Merck) for electrophoresis. The reaction temperature conditions for HPAs 1 to 5 and 15 are available in our previous study.[13]

We had many nonspecific bands for HPA-1b, -3, -4, and -5. To correct this problem with HPA-1b, we had to use the primer used in Meyer's study. For this reason, the band size for HPA-1b (196 bp) was different from HPA-1a (90 bp). We used multistep reaction temperature conditions at 95°C for 5 min as activation; 5 cycles as amplification-1 at 96°C for 25 s, 68°C for 45 s, and 72°C for 30 s; 20 cycles as amplification-2 at 96°C for 25 s, 61°C for 45 s, and 72°C for 30 s; 15 cycles as amplification-3 at 96°C for 25 s, 51°C for 60 s, and 72°C for 2 min. For HPA-3, the temperature conditions changed slightly to 95°C for 10 min as activation; 5 cycles as amplification-1 at 96°C for 25 s, 70°C for 45 s, and 72°C for 30 s; 20 cycles as amplification-2 at 96°C for 25 s, 61°C for 45 s, and 72°C for 30 s; 15 cycles as amplification-3 at 96°C for 25 s, 53°C for 60 s, and 72°C for 2 min, and the Hot Start enzyme was used. For HPA-1b and 4, temperature conditions were 95°C for 5 min as activation; 10 cycles as amplification-1 at 95°C for 30 s, 65°C for 60 s, and 72°C for 30 s; 22 cycles as amplification-2 at 95°C for 30 s, 61°C for 50 s, and 72°C for 30 s; and 72°C for 5 min as final extension. For HPA-5, the temperature conditions changed similar to HPA-3, but the regular Taq-polymerase enzyme was used.

## PCR-RFLP

The optimization of the PCR-RFLP reaction, like that of PCR-SSP, included optimizing the concentration of $MgCl_2$, dNTP, and primers and optimizing TA. Also, we used the procedures from previous studies performed in IBTO, such as PCR-SSP. The final volume for PCR-RFLP was 20 μL and included 2.5 μL forward primer (1 μmol/L), 2.5 μL reverse primer (1 μmol/L), 1 μL dNTP (0.4 mmol/L), 2.5 μL 10× buffer (IBTO), 1.5 μL $MgCl_2$ (1.5 mmol/L), 2.5 μL betaine (0.6 mol/L), 0.3 μL

Taq DNA-polymerase (Add Taq DNA), and 7.2 µL RNase and DNAse free distilled water.

Reaction temperature conditions and procedure were as follows: 95°C for 5 min as activation, 35 cycles as amplification at 94°C for 30 s, 62°C for 60 s, and 72°C for 60 s, and 72°C for 10 min as a final extension step. According to the manufacturer's protocol, the PCR products were incubated with the *Fok*I (BSe GI) (Thermo Fisher Scientific) as a restriction enzyme. The final reaction volume was 10 µL, including 1.0 µL Y + 10× buffer, 0.5 µL BSe GI Enzyme, 1.5 µL distilled water, and 7 µL PCR product. All were incubated at 55°C for 3 hours, and then the products were run on 4% agarose gel for electrophoresis.

### TaqMan Real-Time PCR

As described in our previous study,[13] the QuantiTect Probe PCR Handbook for quantitative real-time PCR and 2-step RT-PCR using sequence-specific probes (Qiagen) was used for the TaqMan Real-Time PCR assay. The reaction mix contained 0.2 µL forward primer (0.4 µmol/L), 0.2 µL reverse primer (0.4 µmol/L), 0.1 µL allele probe a (VIC) (0.2 µmol/L), 0.1 µL allele probe b (6-carboxy-fluorescein; FAM) (0.2 µmol/L), 1.9 µL RNase and DNase free distilled water, and 5 µL 2× QuantiTect Probe PCR Master Mix. A total of 2.5 µL DNA (25–50 ng/µL) was added to give a final volume of 10 µL. The PCR Program for HPA-1 to -5 and -15 consisted of 95°C for 10 minutes, 40 cycles of 95°C for 15 s, 60°C for 20 s, and 72°C for 20 s. The data were analyzed by Rotor-Gene 6 and Rotor-Gene Q series software (Qiagen) and the Corbet Research Rotor-Gene 3000 (Qiagen) was used as a thermal cycler.

### Melting Curve Profile Analysis

For the melting curve analysis of HPA-15, we used the Lightcycler 480 instrument basic real-time chemistry protocols quick reference card. The final volume of the reaction mix was 20 µL, consisting of 6.2 µL RNase and DNase free distilled water, 2.0 µL forward and 2.0 µL reverse primer (0.5 µmol/L), 0.4 µL of sensor probe (0.2 µmol/L), 0.4 µL of anchor probe (0.2 µmol/L), 4.0 µL LightCycler 480 Genotyping Master, and 5 µL DNA (25–50 ng/µL). All PCR reactions were performed in specific capillaries for LightCycler. The PCR thermal program for HPA-15 by LightCycler 2.0 as a thermal cycler was 95°C for 10 min as the initial denaturation, 45 cycles for amplification consisted of 95°C for 10 s, 55°C for 10 s, and 72°C for 10 s; 1 cycle as a melting step consisted of 95°C for 1 min, 60°C for 1 min, 50°C for 1 min, 45°C for 1 min, and 75°C for 0.0 s, and cooling step of 40°C for 30 s.

### PCR-SSP Method by Commercial Kit

A commercial kit (HPA Ready Gene Innotrain) was used to determine the HPAs genotype of 10 samples previously identified by the sequencing. The final volume of the commercial kit according to the manufacturer's instruction was 10.3 µL, consisting of 5 µL distilled water, 3 µL Innotrain Ready Mix, 0.3 µL of Taq DNA-polymerase (Add Taq DNA), and 2 µL of DNA (25–50 ng/µL). Thermal profiling of procedure was as follows: 94°C for 2 min as an activation step, 5 cycles as amplification-1 of 94°C for 20 s, 70°C for 60 s; 10 cycles as amplification-2 at 94°C for 20 s, 65°C for 1 min and 72°C for 45 s, 20 cycles as amplification-3 of 94°C for 20 s, 61°C for 50 s, 72°C for 45 s, and final extension step at 72°C for 5 min.

### Repeatability of the Methods

The genotyped samples by sequencing and commercial kit were regenotyped in different runs by PCR-SSP, real-time PCR, and PCR-RFLP, especially when problems occurred during test set-up. The results were compared to expected results (**TABLE 2**).

## Results

In the first step, we genotyped 10 samples by sequencing as a gold standard. **FIGURE 1** shows the sequencing results for homozygous samples and **FIGURE 2** for heterozygous. At the next level, these samples were genotyped by PCR-SSP (HPA-1 to -5 and -15) and TaqMan Real-Time PCR (HPA-1 to -5 and -15) (**FIGURE 3**). For PCR-SSP, if the HGH gene was amplified and an electrophoretic pattern of 429 bp was observed in the row, the negative results were considered valid. Bands related to each allele were identified using a size marker and compared with the pattern in each row, and the presence or absence of alleles was recorded as positive or negative results.

**TABLE 2. The Repeatability of the Results for PCR-SSP, Real-Time PCR, and PCR-RFLP**

| Hpa | | Repeated Sample | Number of Repeats | | | FP | FN | C |
|---|---|---|---|---|---|---|---|---|
| | | | SSP | Real-Time | RFLP | | | |
| HPA-1 | 1a/1a | 1aa, 2aa, 3ab, 4aa, 5ab, 15aa | 10 | 5 | - | 0 | 0 | 100% |
| | 1a/1b | 1ab, 2aa, 3aa, 4aa, 5aa, 15ab | 10 | 5 | - | 0 | 0 | 100% |
| HPA-2 | 2a/2a | 1aa, 2aa, 3bb, 4aa, 5aa, 15ab | 6 | 5 | - | 0 | 0 | 100% |
| | 2a/2b | 1aa, 2ab, 3ab, 4aa, 5aa, 15bb | 6 | 5 | - | 0 | 0 | 100% |
| HPA- 3 | 3a/3a | 1ab, 2aa, 3aa, 4aa, 5aa, 15ab | 12 | 5 | 5 | 0 | 0 | 100% |
| | 3a/3b | 1aa, 2ab, 3ab, 4aa, 5aa, 15bb | 12 | 5 | 5 | 0 | 0 | 100% |
| | 3b/3b | 1aa, 2aa, 3bb, 4aa, 5aa, 15ab | 12 | 5 | 5 | 0 | 0 | 100% |
| HPA- 4 | 4a/4a | 1aa, 2aa, 3aa, 4aa, 5aa, 15ab | 6 | 5 | - | 0 | 0 | 100% |
| HPA- 5 | 5a/5a | 1aa, 2aa, 3bb, 4aa, 5aa, 15ab | 10 | 5 | - | 0 | 0 | 100% |
| | 5a/5b | 1ab, 2aa, 3ab, 4aa, 5ab, 15ab | 10 | 5 | - | 0 | 0 | 100% |
| HPA- 15 | 15a/15a | 1aa, 2aa, 3ab, 4aa, 5ab, 15aa | 10 | 5 | - | 0 | 0 | 100% |
| | 15a/15b | 1aa, 2ab, 3aa, 4aa, 5aa, 15ab | 10 | 5 | - | 0 | 0 | 100% |
| | 15b/15b | 1aa, 2aa, 3ab, 4aa, 5aa, 15bb | 10 | 5 | - | 0 | 0 | 100% |

*C, consistency with expected results; FN, false negative; FP, false positive; RFLP, restriction fragment length polymorphism-polymerase chain reaction; SSP, sequence-specific primer-polymerase chain reaction.*

Also, a well containing distilled water was considered a negative result when no band was observed (**FIGURE 3A**).

The TaqMan Real-Time PCR results were illustrated in 2 ways: a product amplification analysis curve, in which the x-axis was represented for the cycles of reaction, and the y-axis for fluorescence intensity emitted from the probes (VIC for allele a and FAM for allele b). These evaluations were implemented in different channels (VIC and FAM) for alleles a and b; however, instead of using 2 separate tubes for each allele, 2 different probes were used in 1 reaction tube (**FIGURE 3B**). For the second approach, we used a scatter graph as an allelic discrimination method. A chart divided into 4 sections (negative, VIC for allele a, FAM for allele b, and a shared area for heterozygous samples) was used in this method (**FIGURE 3C**). All of these evaluations were performed by Rotor-Gene Q software.

Melting curve analysis was performed for HPA-15 genotyping. **FIGURE 4** shows the melting curve analysis in 640/530 nm for the hybridization probe. The Tm difference between alleles a and b was about 9°C. The melting curve analysis results for HPA-15 were HPA-15a/a with a Tm of approximately 62°C and a single-peak curve (**FIGURE 4A**). The HPA-15b/b also had a single-peak curve and a Tm of about 53°C (**FIGURE 4B**). The HPA-15 a/ 15b curve had both Tm and had a 2-peak curve (**FIGURE 4C**).

The PCR-RFLP method was used for genotyping of HPA-3. *Fok*I restriction enzyme yielded 3 fragments with 149, 191, and 108 bp lengths for HPA-3a and 2 fragments with 149 and 299 bp lengths for HPA-3b (**FIGURE 5**).

Finally, we genotyped these 10 samples with a commercial kit (HPA Ready Gene). **FIGURE 6** shows the results of 1 sample genotyped by commercial kit compared to the PCR-SSP method and the genotyping results of a known commercial DNA by PCR-SSP method.

The results of PCR-SSP, TaqMan Real-Time PCR, melting curve analysis (HPA-15), and PCR-RFLP (HPA-3) were 100% consistent with sequencing (gold standard) and the commercial Innotrain kit result (HPA Ready Gene) (**TABLE 3**). The PCR-SSP and TaqMan Real-Time PCR results for known DNA (Innotrain) as external control were HPA-1aa, HPA-2aa, HPA-3bb, HPA-4aa, HPA-5aa, and HPA-15aa, which was consistent with the manufacturer issue. There was a 100% correlation between repeating the methods and the expected results for repeatability, and no false positives and negatives were observed (**TABLE 2**).

**FIGURE 1.** **The sequencing results for homozygous samples. HPA, human platelet antigen.**

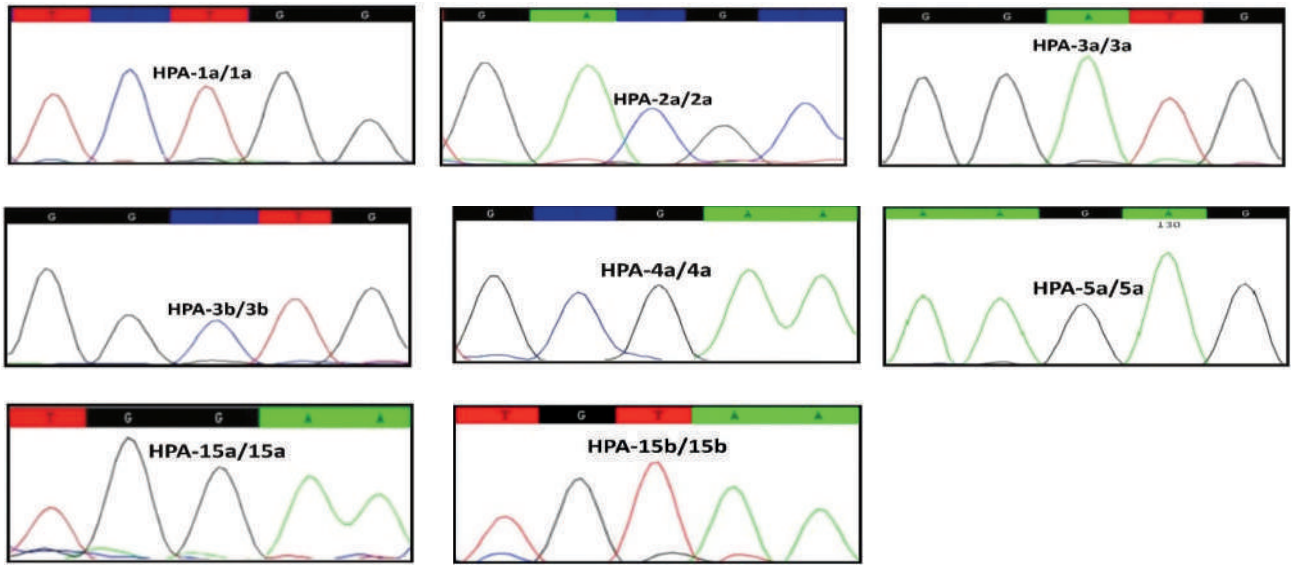


**FIGURE 2.** **The sequencing results for heterozygous samples. HPA, human platelet antigen.**

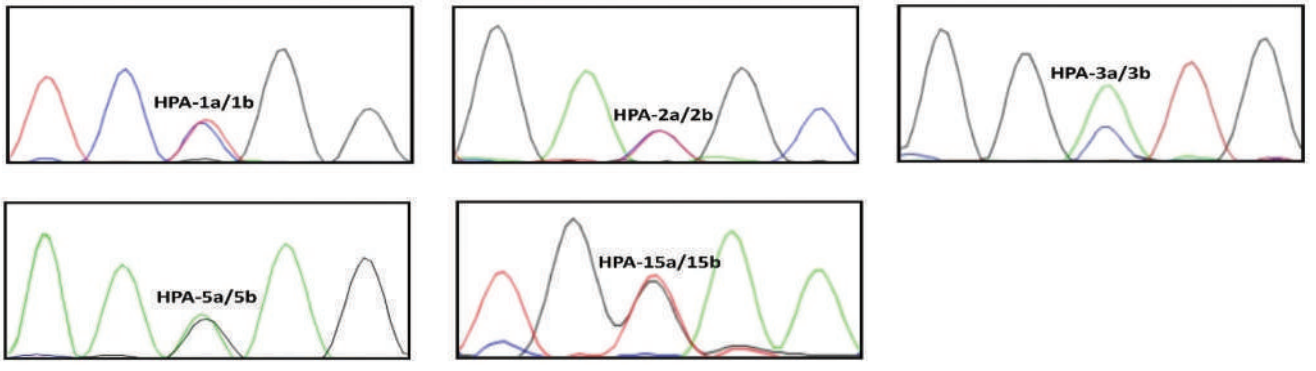

**FIGURE 3.** A, The results for HPA-1 in sample 2 (S2) and sample 6 (S6) were HPA-1ab and in samples 1, 3-5 and 7-10 were HPA-1aa. B, Quantitation analysis of 10 samples for HPA-1 genotyped by TaqMan Real-Time. C, Allelic discrimination of 10 samples by TaqMan Real-Time PCR illustrated with a scatter graph. All results were consistent with each other. FAM, 6-carboxy-fluorescein; HPA, human platelet antigen; VIC, Victoria.

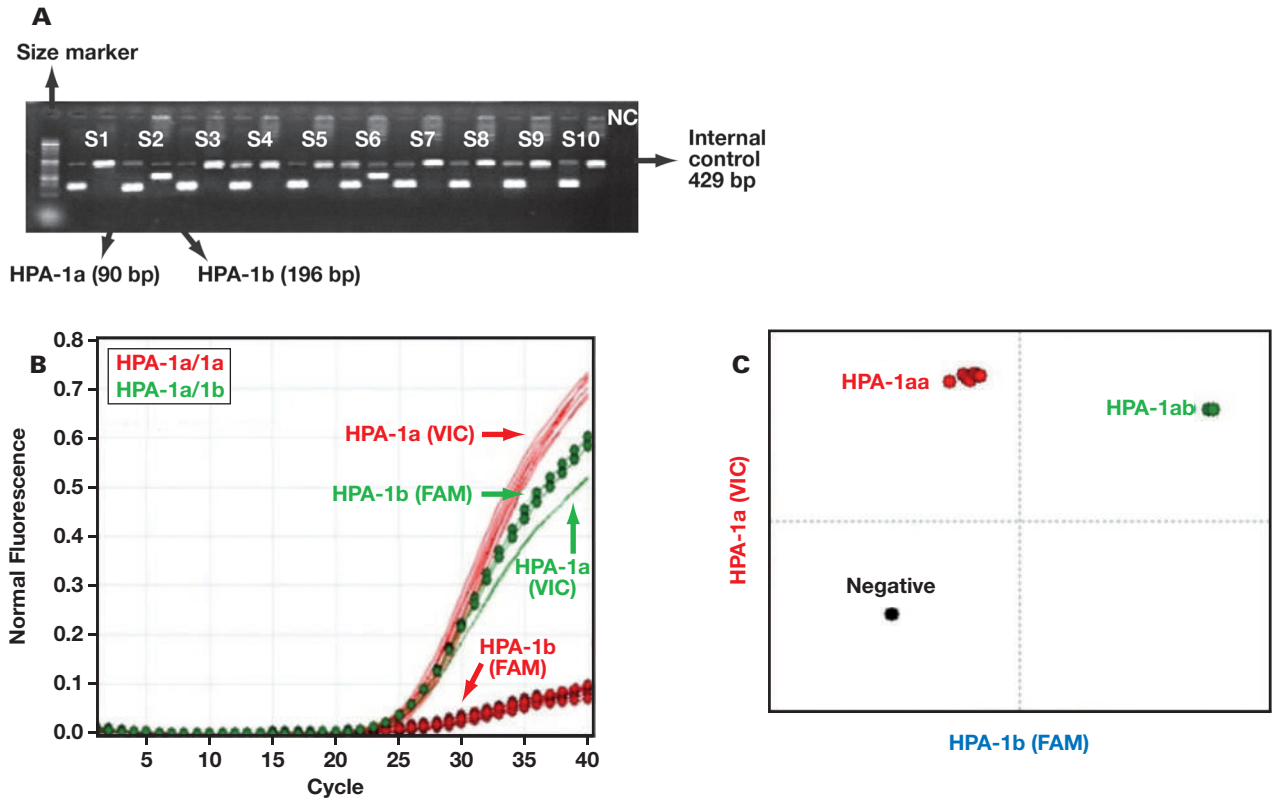


**FIGURE 4.** Melting curve analysis results for HPA-15. A, HPA-15a/15a. B, HPA-15b/15b. C, HPA-15a/15b. HPA, human platelet antigen.

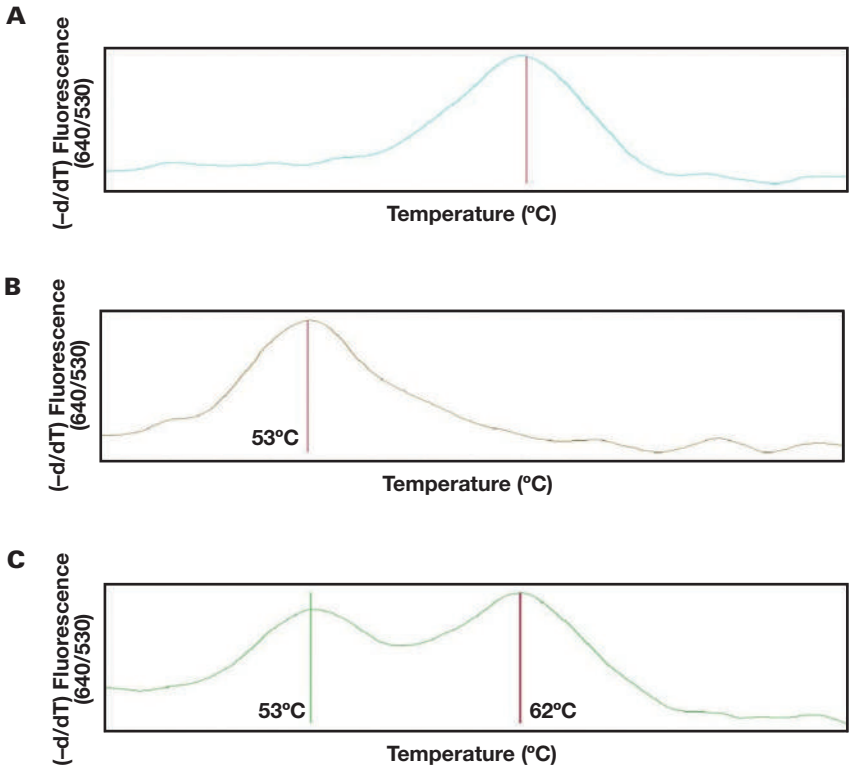

**FIGURE 5.** PCR-RFLP results for HPA-3. SM, size marker; UP, undigested product.

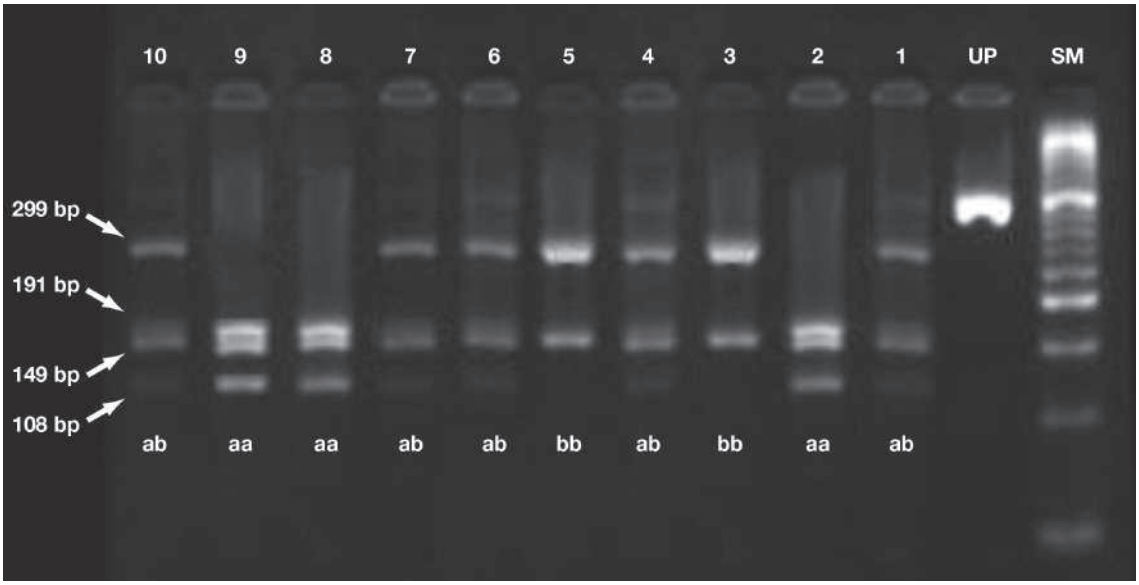


## Discussion

This study shows our approaches to an HPA-1 to -5 and -15 genotyping set-up by PCR-SSP homemade method, TaqMan Real-Time PCR, PCR-RFLP (HPA-3), and melting curve analysis (HPA-15), the steps for validating the methods, and potential sources of errors and their corrections. In our previous study, we genotyped 100 blood donors of Azeri ethnicity, but due to the complexity of the process we did not have any hint to our validation approaches. These assessments start from sampling and continue until the interpretation of the results.

HPA phenotyping was initially limited to reference laboratories with specific antisera, whereas DNA-based molecular methods can be used in every laboratory worldwide. PCR-SSP is the most widely used method for genotyping platelet antigens. This method is relatively inexpensive and simple but has disadvantages, including the difficulty of automation, the need for high proficiency in interpreting the results, and the many false-positive results.

The National Institute for Biological Standards and Control (NIBSC) established a PCR-SSP method for routine assessments of HPA-1 to -5. The NIBSC implemented some evaluations in 6 different labs where HPA-3 and -5 genotyping confronted some problems. Cavanagh et al[17] explained these problems as differences in solutions and reagents and the type of thermal cycling devices used in different laboratories. In the current study, we had some challenges, such as nonspecific bands for HPA-1b, HPA-3, HPA-4, and HPA-5, when we performed genotyping according to the NIBSC method. Therefore, we made changes in temperature profiles to fix these problems. There were many nonspecific bands for HPA-3 that any temperature protocol could not correct, but we could achieve the desired results using the Hot-Start enzyme. Also, in each run, a commercial DNA sample with known genotypes for HPAs was used and results of our homemade PCR-SSP method, real-time PCR, and PCR-RFLP were harmonized with the results in the product brochure.

In 2004, Ficko et al[9] genotyped 120 samples for HPAs -1 to -3 and -5 using real-time PCR. In the Ficko et al study, one of the samples was genotyped as HPA-1ab by PCR-SSP, but it turned out to be HPA-1aa by repeating PCR-SSP, TaqMan Real-Time PCR, and the sequencing method. For HPA-2 and -5, 1 sample was genotyped as HPA-2ab and the other as HPA-5aa by PCR-SSP. By repeating the PCR-SSP and performing the TaqMan Real-Time PCR and sequencing, they were determined to be HPA-2aa and HPA-5ab, respectively. Most of the discrepancies belonged to HPA-3; with PCR-SSP, 7 samples were typed as HPA-3ab, and 4 as HPA-3bb, whereas all of them were HPA-3aa when they were genotyped by TaqMan Real-Time PCR and sequencing. Ficko et al[9] preferred the TaqMan Real-Time method to the PCR-SSP. Simultaneous use of 2 different probes in 1 reaction tube, with no need for time-consuming post-PCR processes and the possibility of displaying results simultaneously with reaction progression by different software, makes the TaqMan Real-Time PCR a better method than PCR-SSP. Although the TaqMan Real-Time PCR is a simpler, faster, and more reliable method, one of the most critical challenges ahead, especially in Iran, is the expense of MGB probes, which reduces the possibility of using them; therefore, the PCR-SSP method still is a more widely used method in Iran's laboratories.

We used PCR-RFLP for genotyping HPA-3. However, due to the difficulty of interpreting the results and the time-consuming processes of PCR-RFLP, this method is less preferred than PCR-SSP and real-time PCR. Because of these limitations, the possibility of using this method on a large scale is low.

At the first workshop of the International Society of Blood Transfusion (ISBT) International Platelet Immunobiology Working Party, Asia Regional, in 2014, 6 DNA samples were sent to 14 laboratories, 11 of which declared their results to the ISBT. In these 11 laboratories, the most widely used method was PCR-SSP (7 labs). PCR-SSOP (commercial kit) (6 labs) was the second most widely used method in laboratories. Other methods were sequencing and real-time PCR, each used in only 1 laboratory. For HPA-2, -4, -5, and -9, there was 100% coordination between the results. The lowest coordination rate was 93% for HPA-1 and then 94%, 97%, and 97% for HPA-15, -3 and -6, respectively.[12]

At the 18th Platelet Immunology Workshop of the ISBT in 2016, 5 DNA samples were sent to 32 laboratories. The genotype of these 5 samples was known for HPA-1 to -6, -9, and -15. Also, 2 samples contained rare mutations near the SNVs related

**FIGURE 6.** **The results of PCR-SSP for one sample (S) and external control (EC) obtained by home-made PCR-SSP and commercial kit. The results of PCR-SSP for a known sample (Innotrain) as EC were HPA-1aa, HPA-2aa, HPA-3bb, HPA-4aa, HPA-5aa, and HPA-15aa (A); also, the products of amplification for HPA-1 to HPA-5 and HPA-15 for a sample were included (HPA-1aa, HPA-2aa, HPA-3ab, HPA-4aa, HPA-5aa, and HPA-15b) consistent with the results obtained by commercial kit (B).**

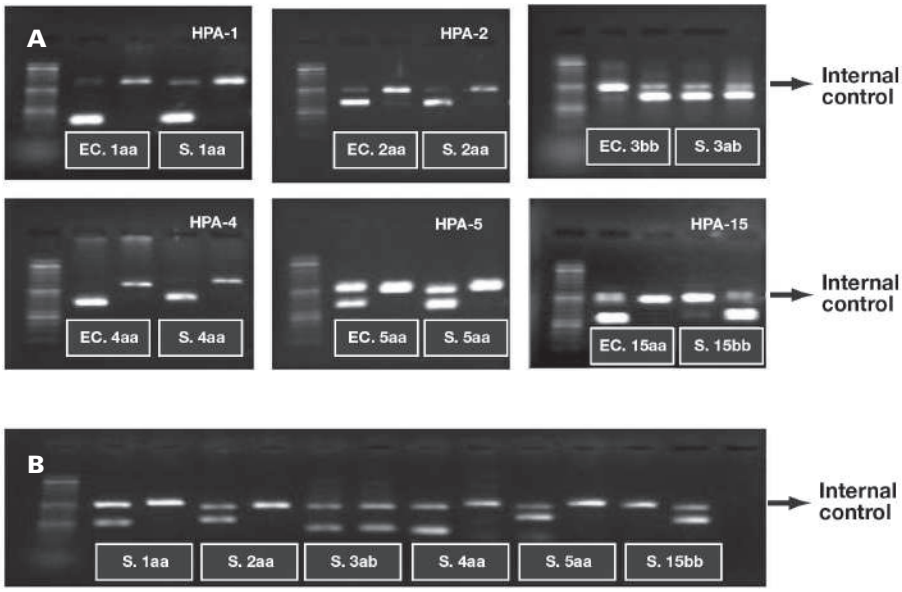


**TABLE 3.** **The Results of PCR-SSP, TaqMan Real-Time PCR, Melting Curve Analysis (HPA-15) and PCR-RFLP (HPA-3) Compared with Sequencing and Commercial Kit Results (HPA Ready Gene)**

| Sample | Sequencing | TaqMan | PCR-SSP | Commercial Kit | RFLP (HPA-3) | MCA (HPA-15) | Discrepancy |
|---|---|---|---|---|---|---|---|
| 1 | 1aa, 2aa, 3ab, 4aa, 5ab, 15aa | 1aa, 2aa, 3ab, 4aa, 5ab, 15aa | 1aa, 2aa, 3ab, 4aa, 5ab, 15aa | 1aa, 2aa, 3ab, 4aa, 5ab, 15aa | 3ab | 15aa | Not seen |
| 2 | 1ab, 2aa, 3aa, 4aa, 5aa, 15ab | 1ab, 2aa, 3aa, 4aa, 5aa, 15ab | 1ab, 2aa, 3aa, 4aa, 5aa, 15ab | 1ab, 2aa, 3aa, 4aa, 5aa, 15ab | 3aa | 15ab | Not seen |
| 3 | 1aa, 2aa, 3bb, 4aa, 5aa, 15ab | 1aa, 2aa, 3bb, 4aa, 5aa, 15ab | 1aa, 2aa, 3bb, 4aa, 5aa, 15ab | 1aa, 2aa, 3bb, 4aa, 5aa, 15ab | 3bb | 15ab | Not seen |
| 4 | 1aa, 2ab, 3ab, 4aa, 5aa, 15bb | 1aa, 2ab, 3ab, 4aa, 5aa, 15bb | 1aa, 2ab, 3ab, 4aa, 5aa, 15bb | 1aa, 2ab, 3ab, 4aa, 5aa, 15bb | 3ab | 15bb | Not seen |
| 5 | 1aa, 2aa, 3bb, 4aa, 5aa, 15ab | 1aa, 2aa, 3bb, 4aa, 5aa, 15ab | 1aa, 2aa, 3bb, 4aa, 5aa, 15ab | 1aa, 2aa, 3bb, 4aa, 5aa, 15ab | 3bb | 15ab | Not seen |
| 6 | 1ab, 2aa, 3ab, 4aa, 5ab, 15ab | 1ab, 2aa, 3ab, 4aa, 5ab, 15ab | 1ab, 2aa, 3ab, 4aa, 5ab, 15ab | 1ab, 2aa, 3ab, 4aa, 5ab, 15ab | 3ab | 15ab | Not seen |
| 7 | 1aa, 2aa, 3ab, 4aa, 5aa, 15ab | 1aa, 2aa, 3ab, 4aa, 5aa, 15ab | 1aa, 2aa, 3ab, 4aa, 5aa, 15ab | 1aa, 2aa, 3ab, 4aa, 5aa, 15ab | 3ab | 15ab | Not seen |
| 8 | 1aa, 2aa, 3aa, 4aa, 5aa, 15ab | 1aa, 2aa, 3aa, 4aa, 5aa, 15ab | 1aa, 2aa, 3aa, 4aa, 5aa, 15ab | 1aa, 2aa, 3aa, 4aa, 5aa, 15ab | 3aa | 15ab | Not seen |
| 9 | 1aa, 2ab, 3aa, 4aa, 5aa, 15ab | 1aa, 2ab, 3aa, 4aa, 5aa, 15ab | 1aa, 2ab, 3aa, 4aa, 5aa, 15ab | 1aa, 2ab, 3aa, 4aa, 5aa, 15ab | 3aa | 15ab | Not seen |
| 10 | 1aa, 2aa, 3ab, 4aa, 5aa, 15bb | 1aa, 2aa, 3ab, 4aa, 5aa, 15bb | 1aa, 2aa, 3ab, 4aa, 5aa, 15bb | 1aa, 2aa, 3ab, 4aa, 5aa, 15bb | 3ab | 15bb | Not seen |

*MCA, melting curve analysis.*

to HPA-3 and HPA-15. The most commonly used method in these laboratories was the PCR-SSP method, used in 15 laboratories, followed by the TaqMan and sequence-based typing (SBT) methods used in 5 laboratories. The other methods used included Luminex in 4 laboratories, PCR-RFLP in 3 laboratories, bead array and RT-PCR in 2 laboratories, and finally, LightCycler and the high-resolution melting analysis in 1 laboratory. The results of all laboratories for HPA-1, -2, -4, and -5 were similar. The highest inconsistencies were in the HPA-3 results, and the sample had a rare mutation in the *ITG2B* gene.[6]

At the 19th ISBT Platelet Immunology Workshop in 2018, 5 DNA samples were sent to 29 laboratories. The most commonly used methods for determining HPA genotype were PCR-SSP and real-time PCR methods used by 12 laboratories. They were followed by SBT, SSO, BioArray Beadchip, Progenika HPA XT, and RFLP, used in 6, 5, 3, 1, and 1 laboratories, respectively.[7]

From the results reported at these 3 workshops, we found that over time the number of laboratories that use the real-time method has increased compared to the PCR-SSP method, and gradually the PCR-RFLP method has become less widely used due to its time-consuming nature, problems with the use of restrictive enzymes, and problems with interpreting results.

Vorholt et al[5] used TaqMan Real-time PCR to validate the next-generation sequencing (NGS) results. In this study, there were 2 discrepancies between NGS results and TaqMan Real-Time PCR that resulted from the presence of SNVs in adjacent regions of real-time PCR primers and probes. Because of the NGS method's ability to detect HPAs and new SNVs on coding sequences simultaneously, the NGS method is preferred to TaqMan Real-Time PCR, but the Real-Time PCR can be used as a fast and precise method.[5]

Different methods have been used to validate the genotyping results of HPA-1 to -15 all over the world. Commercial DNA samples with known

genotypes are the most applicable method.[9,11,18–23] Sequencing[5,9,19] or SBT methods[24–26] are other relevant methods. Some methods are used less frequently; for example, commercial kits based on PCR-SSP,[26] blood chip,[26] the thrombotype sequence-specific method,[23] comparing the results of samples to reference laboratory results,[23] Luminex XMAP,[8] TaqMan Real-Time PCR,[5] and repeating 10% of samples with the same method.[27] In the current study, we used a combination of sequencing, commercial DNA, and a commercial kit.. Although sequencing was used as the gold standard for genotyping HPAs, this method is expensive and time-consuming and could not be done by the blood transfusion organization (IBTO), thus requiring more affordable and more rapid methods appropriate to the country's economic conditions. PCR-SSP and PCR-RFLP methods are among the main choices in low-income countries in terms of cost-effectiveness and real time in terms of speed. The main problem of real-time in Iran is the high price of probes, which makes using this method routinely problematic. It appears that different methods being used in each center can eliminate the drawbacks of other methods; for instance, in our center, the genotyping of HPA-3 using the PCR-SSP faced many challenges; as a result, real-time PCR or PCR-RFLP methods can be used for routinely genotyping of HPA-3. In general, if we do not consider the issue from a financial point of view, the TaqMan real-time PCR method using MGB probes and the melting curve analysis method using hybridization probes are preferred over PCR-SSP and PCR-RFLP.

Determination of platelet antigen genotype can help identify thrombocytopenic alloimmune syndromes, helping to treat patients with platelet refractoriness and preventing NAITP and racial studies. Appropriate methods for determining platelet antigens are crucial in platelet registry centers. Therefore, we share our validating experiences for PCR-SSP and real-time PCR in genotyping of HPA-1 to -5 and -15 and PCR-RFLP for HPA-3. These methods should be able to be harmonized across the country and tailored to the economic situation. Obtaining accurate results is a process that starts from the pre-PCR steps, such as sampling and selecting the best primers; therefore, primers must be evaluated before being ordered. Newer methods for HPA typing, including quantitative PCR and their combination with probes, are available, but the high cost of these methods limits their use, especially in Iran. Economic conditions are always an issue to consider. In this study, we tried to use somewhat simpler methods to validate our homemade PCR-SSP method and its quality control and obtain reliable results.

## Acknowledgments

This article was extracted from the project "Evaluation of immunologic complications of blood transfusion using home-made kits (first phase: laboratory assay for platelet refractoriness)," which was conducted with the financial support of the Deputy Minister of Research and Technology of the Ministry of Health and Medical Education with contract number 1700/700. Therefore, the researchers and authors of this article express their appreciation for the financial support of the Deputy Minister of Research and Technology of the Ministry of Health and Medical Education.

## REFERENCES

1. Ghoshal K, Bhattacharyya M. Overview of platelet physiology: its hemostatic and nonhemostatic role in disease pathogenesis. *Sci World J.* 2014;781857:1. doi:10.1155/2014/781857.
2. Mangerona CM, Garcia FB, Moraes-Souza H. Frequency of human platelet antigens (HPA)-1, -2, -5 and -15 in Brazilian blood donors and establishment of a panel of HPA-typed donors. *Transfus Med.* 2015;25(3):189–194. doi:10.1111/tme.12210.
3. Curtis BR. Genotyping for human platelet alloantigen polymorphisms: applications in the diagnosis of alloimmune platelet disorders. *Semin Thromb Hemost.* 2008;34(6):539–548. doi:10.1055/s-0028-1103365.
4. Wang J, Xia W, Deng J, et al. Analysis of platelet-reactive alloantibodies and evaluation of cross-match-compatible platelets for the management of patients with transfusion refractoriness. *Transfus Med.* 2018;28(1):40–46. doi:10.1111/tme.12423.
5. Vorholt SM, Hamker N, Sparka H, et al. High-throughput screening of blood donors for twelve human platelet antigen systems using next-generation sequencing reveals detection of rare polymorphisms and two novel protein-changing variants. *Transfus Med Hemother.* 2020;47(1):33–44. doi:10.1159/000504894.
6. Wikman A, Mörtberg A, Sachs U, Santoso S. Report on the 18th Platelet Immunology Workshop of the ISBT 2016. *ISBT Sci Ser.* 2017;12(1):214–222. doi:10.1111/voxs.12336.
7. Lewin A, Al Khan S, Beaudin L, Meilleur L, Clarke G, Richard L. Report on the 19th International Society of Blood Transfusion Platelet Immunology Workshop 2018. *Vox Sang.* 2020;115(8):767–782. doi:10.1111/vox.12945.
8. Londero D, Miani M, Rinaldi C, Totis V, Angelis V. Extensive human platelet specific antigens typing of blood donors of different geographical origin to manage platelet transfusion in alloimmunized patients: experience from a transfusion center in northeastern Italy. *Int J Blood Transfus Immunohematol* 2018;8:4–11. doi:10.5348/ijbti-2018-36-OA-2.
9. Ficko T, Galvani V, Rupreht R, Dovc T, Rožman P. Real-time PCR genotyping of human platelet alloantigens HPA-1, HPA-2, HPA-3 and HPA-5 is superior to the standard PCR-SSP method. *Transfus Med.* 2004;14(6):425–432. doi:10.1111/j.1365-3148.2004.00538.x.
10. Hurd C, Cavanagh G, Schuh A, Ouwehand W, Metcalfe P. Genotyping for platelet-specific antigens: techniques for the detection of single nucleotide polymorphisms. *Vox Sang.* 2002;83(1):1–12. doi:10.1046/j.1423-0410.2002.00187.x.
11. Kengkate M, Butthep P, Kupatawintu P, Srisuddee A, Chantratita W, Nathalang O. Comparison of a simple-probe real-time PCR and multiplex PCR techniques for HPA-1 to HPA-6 and HPA-15 genotyping. *J Clin Lab Anal.* 2015;29(2):94–99. doi:10.1002/jcla.21734.
12. Matsuhashi M, Tsuno N, Takahashi K, et al. Report of the first workshop of the ISBT International Platelet Immunobiology Working Party, Asia Regional. *ISBT Sci Ser* 2014;9(2):304–308. doi:10.1111/voxs.12101.
13. Seyed Ghader A, Shahram S, Mojgan S, Maryam Z. Genotyping of human platelet antigen-1 to -5 and -15 by polymerase chain reaction with sequence-specific primers (PCR-SSP) and real-time PCR in Azeri blood donors. *Iran J Allergy Asthma Immunol.* 2021;20(3):350–363. doi:10.18502/ijaai.v20i3.6333.
14. Bustin SA, Benes V, Garson JA, et al. The MIQE guidelines: minimum information for publication of quantitative real-time PCR experiments. *Clin Chem.* 2009;55(4):611–622. doi:10.1373/clinchem.2008.112797.
15. Denomme GA, Rios M, Reid ME. Platelet blood groups. In: *Molecular Protocols in Transfusion Medicine*, London, England: Academic Press; 2000:141–146. doi: 10.1016/B978-012209370-8/50006-4.
16. Liew M, Nelson L, Margraf R, et al. Genotyping of human platelet antigens 1 to 6 and 15 by high-resolution amplicon melting and conventional hybridization probes. *J Mol Diagn.* 2006;8(1):97–104. doi:10.2353/jmoldx.2006.050053.
17. Cavanagh G, Dunn AN, Chapman CE, Metcalfe P. HPA genotyping by PCR sequence-specific priming (PCR–SSP): a streamlined method for rapid routine investigations. *Transfus Med.* 1997;7(1):41–45. doi:10.1046/j.1365-3148.1997.d01-72.x.
18. De La Vega EC, Nogues N, Fernandez Montoya A, et al. Human platelet-specific antigens frequencies in the Argentinean population. *Transfus Med.* 2008;18(2):83–90. doi:10.1111/j.1365-3148.2007.00819.x.

19. Lyou JY, Chen YJ, Hu HY, Lin JS, Tzeng CH. PCR with sequence-specific primer-based simultaneous genotyping of human platelet antigen-1 to-13w. *Transfusion* 2002;42(8):1089–1095. doi:10.1046/j.1537-2995.2002.00172.x.

20. Rozˇman P, Drabbels J, Schipper R, Doxiadis I, Stein S, Claas F. Genotyping for human platelet-specific antigens HPA-1,-2,-3,-4 and-5 in the Slovenian population reveals a slightly increased frequency of HPA-1b and HPA-2b as compared to other European populations. *Eur J Immunogenet*. 1999;26(4):265–9. doi:10.1046/j.1365-2370.1999.00142.x.

21. Ruan L, Pei B, Li Q. Multicolor real-time polymerase chain reaction genotyping of six human platelet antigens using displacing probes. *Transfusion.* 2007;47(9):1637–1642. doi:10.1111/j.1537-2995.2007.01335.x.

22. Bhatti F, Uddin M, Ahmed A, Bugert P. Human platelet antigen polymorphisms (HPA-1,-2,-3,-4,-5 and-15) in major ethnic groups of Pakistan. *Transfus Med*. 2010;20(2):78–87. doi:10.1111/j.1365-3148.2009.00982.x

23. Merzoni J, Fagundes I, Lunardi L, et al. Human platelet antigen genotyping of platelet donors in southern Brazil. *Int J Immunogenet.* 2015;42(5):329–335. doi:10.1111/iji.12220.

24. Xu X, Zhu F, Ying Y, et al. Simultaneous genotyping of human platelet antigen-1 to 17w by polymerase chain reaction sequence-based typing. *Vox Sang.* 2009;97(4):330–337. doi:10.1111/j.1423-0410.2009.001213.x.

25. An QX, Li CY, Xu LJ, et al. High-throughput simultaneous genotyping of human platelet antigen-1 to-16 by using suspension array. *Transfusion.* 2013;53(11):2722–2728. doi:10.1111/trf.12164.

26. Edinur H, Dunn P, Lea R, Chambers G. Human platelet antigens frequencies in Maori and Polynesian populations. *Transfus Med.* 2013;23(5):330–337. doi:10.1111/tme.12061.

27. Eyada TK, Amin DG, Samih I, Khedr SM. Human platelet antigen 1, 2 and 5 gene polymorphisms in Egyptians and their potential association with susceptibility to immune thrombocytopenic purpura in Egyptian patients. *Hematology* 2018;23(2):111–116. doi:10.1080/10245332.2017.1365435.

# Use of Self-Collected Saliva Samples for the Detection of SARS-CoV-2

*Kehinde Sogbesan, Taiwo Sogbesan,[1] D. Jane Hata, PhD,[1] Edward L. White,[1] Wyeth Daniel,[1] Samuel L. Gasson,[1] Dylan S. Jones,[1] Brittany R. Vicari,[1] Carleen P. Van Siclen,[1] Carla Palmucci,[1] Christopher P. Marquez, MD,[1] Mark A. Parkulo, MD,[2] Kent R. Thielen, MD,[3] Aziza Nassar, MD, MPH[1,*]*

[1]Department of Laboratory Medicine and Pathology, Mayo Clinic, Jacksonville, FL, USA, [2]Division of Community, Internal Medicine, Mayo Clinic, Jacksonville, FL, USA, [3]Department of Radiology, Mayo Clinic, Jacksonville, FL, USA *To whom correspondence should be addressed. Nassar.aziza@mayo.edu

**Keywords:** saliva, SARS-CoV-2, self-collection, nasopharyngeal swab, sensitivity, cycle threshold

**Abbreviations:** SARS-CoV-2, SARS coronavirus-2; FDA, US Food and Drug Administration; EUA, emergency use authorization; RT-PCR, reverse transcription polymerase chain reaction; NP, nasopharyngeal; CDC, Centers for Disease Control and Prevention; Ct, cycle threshold; E, envelope; NUC, nucleocapsid; ORF, open reading frame; E, envelope.

*Laboratory Medicine* 2022;53:580–584; https://doi.org/10.1093/labmed/lmac051

## ABSTRACT

**Objective:** Using a US Food and Drug Administration (FDA) emergency use authorization (EUA) reverse transcription polymerase chain reaction (RT-PCR) method, we examined the analytic performance accuracy of saliva specimens as compared to nasopharyngeal (NP) specimens in symptomatic patients. Correlation between test results and symptoms was also evaluated.

**Methods:** Over a 5-week period in 2020, 89 matched saliva and nasopharyngeal swabs were collected from individuals exhibiting symptoms consistent with SARS-CoV-2. Specimens were tested with an FDA EUA-approved RT-PCR method, and performance characteristics were compared.

**Results:** The concordance rate between saliva and nasopharyngeal testing was 93.26%. The mean cycle threshold value of saliva when compared to the NP specimen was 3.56 cycles higher. As compared to NP swab, saliva testing demonstrates acceptable agreement but lower sensitivity.

**Conclusion:** When compared to a reference method using NP swabs, the use of saliva testing proved to be a reliable method. Self-collected saliva testing for SARS-CoV-2 allows for a viable option when trained staff or collection materials are in short supply.

As part of the management of the COVID-19 pandemic, accurate detection of infected individuals lies at the forefront of health care. The current criterion standard specimen type, nasopharyngeal (NP) swabs, must be collected by health care professionals and later analyzed via reverse transcription polymerase chain reaction (RT-PCR). The lack of sufficient supplies (collection swabs, viral transport medias, collection tubes) and availability of health care professionals to facilitate viral collection poses a persistent challenge in the detection of SARS coronavirus-2 (SARS-CoV-2). Discomfort reported by patients along with possible transmission associated with the NP collection method highlights the importance of pursuing alternative sampling methods for SARS-CoV-2.[1] Self-collected saliva is a noninvasive sample type that may improve detection of SARS-CoV-2 as compared to NP swabs.[1,2]

The consideration of saliva as a sample type centers around differences in sensitivities to NP swabs and the potential of increasing access to COVID-19 diagnostic tests. As new strains of SARS-CoV-2 continue to emerge and spread, the urgent need for efficient collection and testing methods remains pivotal.[3] Utilization of self-collected saliva may diminish the possibility of SARS-CoV-2 transmission as compared to assisted NP swab testing.[4] Other studies note test results from self-collected saliva specimens demonstrate similar analytical performance to NP samples collected by trained health care professionals.[5] In the summer of 2020, the pandemic greatly affected minorities and disenfranchised communities due to preexisting conditions, crowded living spaces, and lack of access to COVID-19 testing.[6] Newer variants of the virus may affect such communities yet again, further highlighting the importance of providing access to reliable testing with readily collectable specimens. Self-collected saliva samples for detection of the virus could potentially increase access to testing, thus reducing the negative effects on underserved communities.

Our study objective was to assess the viability of saliva as a sample type in detection of SARS-CoV-2, as compared to the standard NP swab, using a high-throughput US Food and Drug Administration (FDA) emergency use authorization (EUA) method. We analyzed cycle threshold (Ct) values to discern sensitivity differences between NP swabs and saliva samples to illustrate the potential utility of saliva as a sample type.

## Materials and Methods

The study was approved by the Mayo Clinic Florida institutional review board (IRB# 20-004895). In recruiting study participants,

clinical researchers invited individuals via telephone to participate in the study. Informed consent was digitally obtained via remote technology (iPad) by an email containing a link to the study consent form. In addition to completing the digital consent form, written consent was received from each participant on the date of specimen collection.

In the study, 89 participants between the ages of 20 and 83 were sampled from August 25, 2020, to October 2, 2020. Participants were identified as symptomatic through self-reporting the following symptoms or occurrences through the nurse triage call line: loss of sense of taste and/or smell, fever greater than 37°C, cough, shortness of breath, headache, sore throat, nasal congestion, diarrhea, vomiting, or nausea. The collection from study participants was held in conjunction with community testing at a COVID drive-through facility.

### NP Swab Collection

Trained health care professionals collected NP swab specimens from all study participants while abiding by standard precautionary techniques. Swabs placed in viral transport media (Remel) were then sent to the testing laboratory every 60 minutes (+20 minutes transport; total time range, 20–80 minutes) on wet ice after collection to reduce potential degradation of the patient samples. NP swabs were tested in the laboratory within 24 hours of receipt.

### Saliva Collection

Supervised by a health care provider, participants were provided a self-collection kit for collection of saliva, which featured kit instructions in the form of a video tutorial and paper handout. Using an FDA EUA-approved self-collection device (Spectrum DNA), participants were to spit approximately 2.0 mL into the device. The instructions then required participants to add 1.50 mL of an RNA stabilization/lysing agent to their sample. Once completed, the samples were placed on wet ice and sent every 60 minutes (+20 minutes transport; total time range, 20–80 minutes) to the laboratory for testing.

### Nucleic Acid Extraction and SARS-CoV-2 Detection

The two matched sample specimens (saliva and NP) were transported to the testing laboratory and tested with the cobas SARS-CoV-2 test using the cobas 6800 system (Roche Molecular Diagnostics). NP specimens were processed according to the manufacturer's recommendations under the FDA EUA. Saliva specimens were considered an alternative specimen type and processed as a laboratory-developed test. Saliva specimens were checked to meet the 2.0 mL collection volume by visual inspection before testing. NP specimens were stored at 4°C–8°C and tested within 24 hours of collection at the clinical laboratory, and saliva specimens were stored at 4°C–8°C and tested within 1 to 20 days of collection.

The targets detected in the cobas assay consisted of the *ORF1ab* and SARS-CoV-2 envelope (E) genes. In the interpretation of results from the instrument's software, specimens positive for *ORF1ab* and E targets or *ORF1ab* alone were classified as presumptive positive. When positive for E alone, results were reported as indeterminate, and both targets resulting as negative were reported as SARS-CoV-2 undetected. Ct values for each target were collected and later analyzed to assess sensitivity.

### Statistical Analyses

The study compared qualitative results between NP specimens and the participant's matched self-collected saliva samples. Diagnostic accuracy was analyzed with a 2-by-2 table in detecting SARS-CoV-2 between the two sample types, and a Cohen's coefficient agreement was analyzed. The symptoms were tabulated in an agreement table to view the most prevalent symptoms among the participants. Pearson coefficient was generated through a regression analysis equation.

## Results

The 89 participants consisted of 38 men (42.7%) and 51 women (57.3%); the participant mean age was 48 years old (range, 21–84 years). Among the participants, the self-reported onset of infection had a median of 3 days with an upper limit of 7 days. The most common symptoms from all symptomatic participants consisted of muscle or body aches (34.8%), headache (33.7%), cough (32.6%), and fever or chills (30.3%). The remaining symptoms included difficulty breathing, fatigue, loss of taste or smell, sore throat, congestion or runny nose, nausea, and diarrhea (**TABLE 1**). Among symptomatic participants with a positive SARS-CoV-2 result in NP, the most common symptom consisted of loss of smell or taste (50%), nasal congestion (31.2%), diarrhea (25.0%), and difficulty breathing (25.0%) (**FIGURE 1**).

Eighty-nine matched specimens for both NP and saliva were found to be of sufficient volume and acceptable for testing. Saliva samples tested positive for SARS-CoV-2 among 17 participants (19.1%), and NP specimens tested positive among 19 participants (21.3%) demonstrating a statistically significant difference ($P < .0001$). Both specimen types demonstrated positive agreement for detection of SARS-CoV-2 in 15 patients. Saliva samples detected 2 positive specimens that remained undetected (negative) in the matched NP specimen. Conversely, NP specimens detected 4 positive samples that were undetected in the paired saliva samples. Sensitivity and specificity of saliva samples was calculated at 78.95% (15/19), and 97.14% (68/70), respectively. The overall agreement between the 2 tests was 93.26%, positive agreement was 89.5% (17/19), with a substantial kappa agreement of 79.1% (**TABLE 2**).

To analyze the correlation between paired PCR Ct values among NP specimens vs saliva samples, 2 Pearson correlation coefficients were generated for the 2 targets, *ORF1ab* and E. The correlation (*R* value) was 0.739 for ORF; the saliva deviation remained above the line of equivalence (**FIGURE 2**). In addition, the correlation (*R* value) was 0.729 for E and illustrated a saliva deviation above the line of equivalence (**FIGURE 3**).

The Ct values between the saliva samples and NP specimen demonstrated different values for both *ORF1ab* and E. Positive saliva samples targeting *ORF1ab* had a mean of 27.17 cycles (SD, ±4.28; range, 17.87–33.40). The positive NP specimens targeting ORF demonstrated a mean of 24.85 cycles (SD, ±5.95; range, 16.68–34.24) A statistically significant difference between the means were noted (95% CI, 0.33–4.41; $P = .026$) (**FIGURE 4**). In targeting the E region amongst positive saliva samples, the mean was 28.32 cycles (SD, ±4.77; range, 18.52–35.63). NP specimens targeting E had a mean of 24.76 cycles (SD, ±6.46; range, 16.56–36.85) A statistically significant difference between the means was noted (95% CI, 0.06–7.03; $P = .046$) (**FIGURE 5**). The paired saliva samples demonstrated a narrower

**TABLE 1. Clinical Symptoms Detected in all Participants (n = 89)**

| Characteristic | Overall (%) |
|---|---|
| Muscle or body aches | 31/89 (34.8) |
| Headache | 30/89 (33.7) |
| Cough | 29/89 (32.6) |
| Fever or chills | 27/89 (30.3) |
| Sore throat | 27/89 (30.3) |
| Fatigue | 26/89 (29.2) |
| Congestion or runny nose | 16/89 (18.0) |
| Diarrhea | 8/89 (9.0) |
| Nausea or vomiting | 6/89 (6.7) |
| Loss of smell/taste | 6/89 (6.7) |
| Difficulty breathing | 4/89 (4.5) |

**FIGURE 1. Symptoms noted in participants testing positive for SARS-CoV-2 in nasopharyngeal swab (n = 19). DOB, difficulty of breathing.**

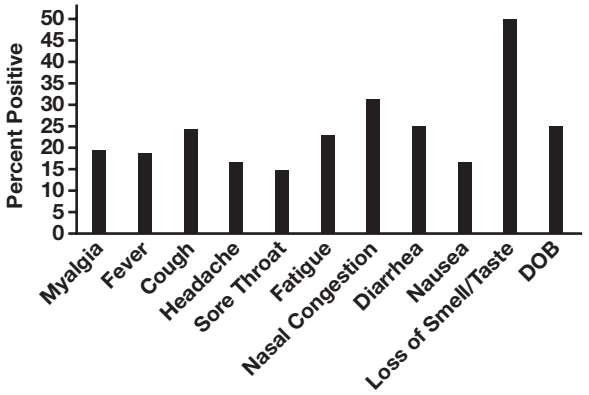


**TABLE 2. Comparison of Cobas Testing Results: Nasopharyngeal vs Saliva[a]**

| | Nasopharyngeal Specimen | | |
|---|---|---|---|
| Saliva Specimen | Detected | Not Detected | Total |
| Detected | 15 | 2 | 17 |
| Not detected | 4 | 68 | 72 |
| Total | 19 | 70 | 89 |

*[a]Sensitivity: 78.95%. Specificity: 97.14%. Overall percent agreement: 93.26%. Cohen's κ coefficient: 0.791. P < .0001.*

range and higher mean for the Ct values, inferring a lower viral load of SARS-CoV-2. In contrast, the NP specimens showed a narrower range and lower mean, indicating higher viral load of SARS-CoV-2 among the samples (**FIGURE 6**).

In assessing test sensitivity between the 2 sample types, Ct values among positive SARS-CoV-2 cases were used. For the purposes of this work, low sensitivity was arbitrarily classified as Ct values 31 to 40, whereas high sensitivity was arbitrarily classified as Ct values 15 to 25. Saliva samples demonstrated higher Ct values for each of the target genes, indicating SARS-CoV-2 detection in saliva is slightly less sensitive as compared to NP specimens (**FIGURES 4** and **5**).

**FIGURE 2. Correlation of ORF cycle thresholds (Ct) between saliva and nasopharyngeal (NP) swabs. y = 0.6577x + 12.351; $R^2$ = 0.5462; $R$ = 0.7391.**

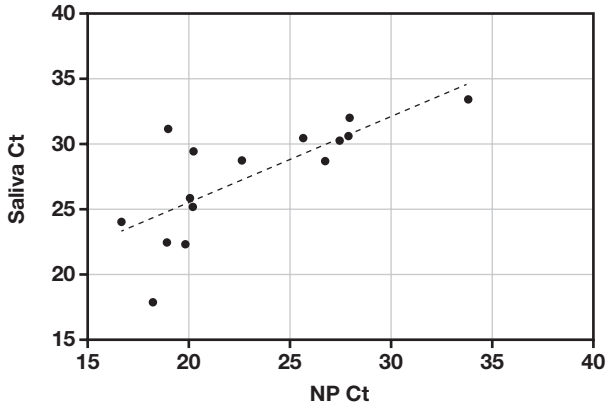


## Discussion

The study assessed the differences in test accuracy between NP specimens and self-collected saliva samples in symptomatic individuals using an FDA EUA method for detection of SARS-CoV-2. The majority of participants demonstrated symptoms, with the most commonly reported being muscle/body aches, headache, cough, and fever/chills. Saliva is shown to be an acceptable collection specimen, as patients reported no dissatisfaction or adverse events from use of the self-collection device. Overall, detection of SARS-CoV-2 in saliva was 19.1% and 21.3% in NP specimens, with overall 93.26% concordance of positive/negative results between the NP and saliva specimens. The saliva test sensitivity was calculated at 78.95%; thus, the potential for false-negative results compared to NP swabs does exist. This observation may be less relevant when the actual prevalence of SARS-CoV-2 is low; however, it does not lessen the potential adverse downstream effects of false-negative results for patient misdiagnosis, need for additional testing, and possible delays in infection control. No PCR inhibition was noted in either specimen type; PCR inhibitors present in saliva were most likely inactivated when SpectrumDNA lysis buffer was added to the sample specimen.

In this study, we sought to identify the differences in SARS-CoV-2 detection between NP swabs and saliva to prove the viability of saliva as a comparable specimen. As a rule, use of Ct values for quantitative comparison of different PCR assays has been strongly discouraged due to myriad factors other than viral load that affect Ct values. However, as true SARS-CoV-2 quantitation was not available, Ct values were considered a reasonable surrogate metric for comparison as the same tests, test platforms, and testing laboratory were used in this study. The Ct values were used to compare and assess test sensitivities, based on results from positive SARS-CoV-2 RT-PCR (**FIGURES 4** and **5**). The higher the Ct value, the less sensitive the test, due to low viral load in saliva. Among the positive samples, saliva samples generally demonstrated a higher Ct value, indicating lower levels of SARS-CoV-2 detection in saliva specimens than NP specimens. In agreement with previous studies, we note that saliva specimens tended to have higher Ct values, whereas NP specimens demonstrated lower Ct values.[2,7] A study by Hitzenbichler et al[4] suggests that close resemblances in Ct values reflect slight analogous sensitivities. In their study, these authors were able to draw such conclusions through confirming similar median viral loads in different specimen types.

**FIGURE 3.** Correlation of envelope cycle thresholds (Ct) between saliva and nasopharyngeal (NP) swabs. y = 0.6661x + 13.184; $R^2$ = 0.5309; $R$ = 0.7286.

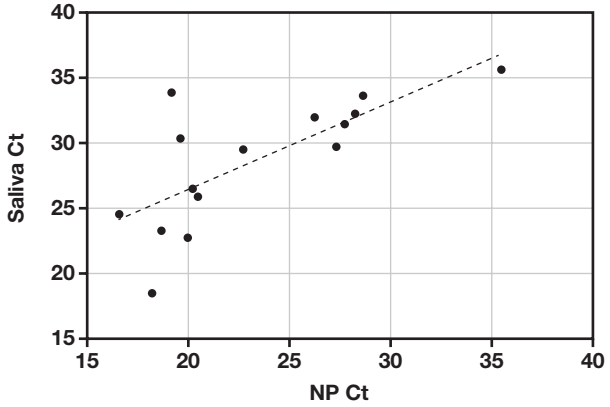


**FIGURE 4.** Cycle thresholds for *ORF1ab* in saliva samples (mean = 27.17) and nasopharyngeal (NP) swabs (mean = 24.85) (95% CI, 0.33–4.41; $P$ = .026).

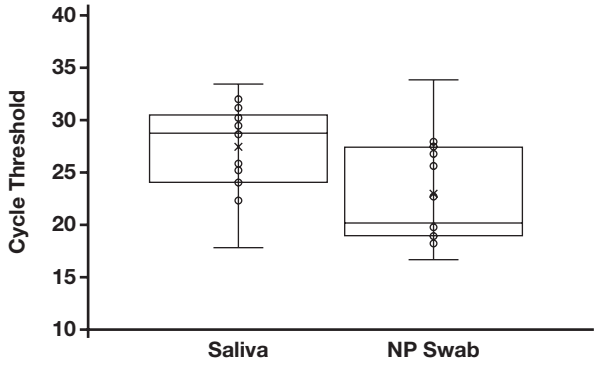


**FIGURE 5.** Cycle thresholds for envelope gene in saliva samples (mean = 28.32) and nasopharyngeal (NP) swabs (mean = 24.76) (95% CI, 0.06–7.03; $P$ = .046).

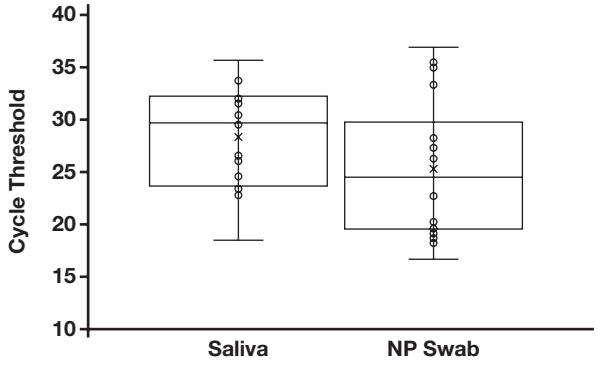


In our study, the discordant rate was 6.7% (6/89), highlighting the differences in detection based on sample type. Due to inadequate sample volumes and severe constraints on reagent availability, additional testing of discrepant saliva specimens could not be performed. Results of 4 positive NP swab specimens were considered true (standard of care testing). In 2 saliva specimens that were SARS-CoV-2 positive but had negative matched NP specimens, 1 patient was SARS-CoV-2 nucleocapsid antibody positive 13 days after PCR collection, indicating exposure had occurred at some point. In the other case, the patient was negative for influenza A/B but no other viral testing was performed, and the true cause of respiratory disease was not determined. The discordant results are likely a consequence of the medium to low viral load demonstrated in saliva specimens in this study. Our study had an overall concordance of 93.26%, thus supporting saliva as a viable specimen type for SARS-CoV-2 detection.

An advantage of our study lies in the use of the automated high-throughput cobas 6800 instrument for testing both the saliva sample and the NP specimen. Previous studies highlight the accurate detection of SARS-CoV-2 in NP swabs using the cobas method.[8] It should be noted that saliva is not a specimen type approved under EUA for the cobas SARS-CoV-2 test, and that NP swabs are considered the specimen source for the most accurate results. Early and accurate detection of COVID-19 serves to disrupt the transmission of the virus and better aid in contact tracing.[4] Importantly, supply chain challenges resulting in the lack of reagents and NP swabs may enhance consideration of saliva collection as a viable specimen alternative for SARS-CoV-2 detection. The noninvasive nature of saliva testing coupled with patient self-collection increases access to SARS-CoV-2 testing and limits potential SARS-CoV-2 exposure to health care workers.[4–6]

This study suggests increased access and availability to reliable SARS-CoV-2 detection with diminished patient discomfort by using self-collected saliva samples. The ongoing pandemic has disproportionately affected underserved Black and Hispanic communities due to some preexisting conditions, such as crowded housing conditions and inconsistent access to health care.[9] In the peak of the pandemic, supply shortages and limited access to COVID-19 testing contributed to inadequate testing coverage overall among minority communities.[6,9] Our study demonstrates that the application of saliva testing can provide efficient and reliable results using an easily collected specimen type. Implementation of saliva testing in minority communities could potentially increase detection and contribute to contact tracing efforts and decrease the disproportionate rate of testing.[10] This study does not assess the exact applicability of such innovation; rather, it serves to show how our findings could be beneficial to disenfranchised and minority groups. Previous studies have shown adoption of mobile testing units for HIV in underserved communities increased the access to testing and early detection for minorities and disenfranchised individuals.[11] Therefore, mobile testing units for detecting SARS-CoV-2 by collecting saliva samples may serve to further diminish the disparate rate.

Our study has several limitations. The sample size (n = 89) was limited by the availability of viral transport media, saliva collection devices, and reagents for molecular testing in mid-2020. This affected our ability to perform testing on known SARS-CoV-2 negative individuals and additional testing on discrepant specimens. The symptoms reported, disease severity, and date of symptom onset relied on self-reporting bias, which may have affected accuracy in detection of SARS-CoV-2 symptoms. Participants in this study were limited to symptomatic individuals presenting to a drive-through COVID testing site. Although participants were instructed not to eat or drink for 30 minutes prior to saliva collection, they were not directly observed by collection staff.

## Conclusion

In this proof-of-concept study the utility and diagnostic accuracy of self-collected saliva specimens for detection of SARS-CoV-2 among symptomatic patients compared favorably to NP specimens. Self-collection of saliva for SARS-CoV-2 testing is a viable option when

**FIGURE 6.** **Saliva samples paired with nasopharyngeal (NP) specimens and their demonstrated cycle threshold values for *ORF1ab* (A) and E (B) targets. Single NP points did not have a matched saliva result (result was undetected).**

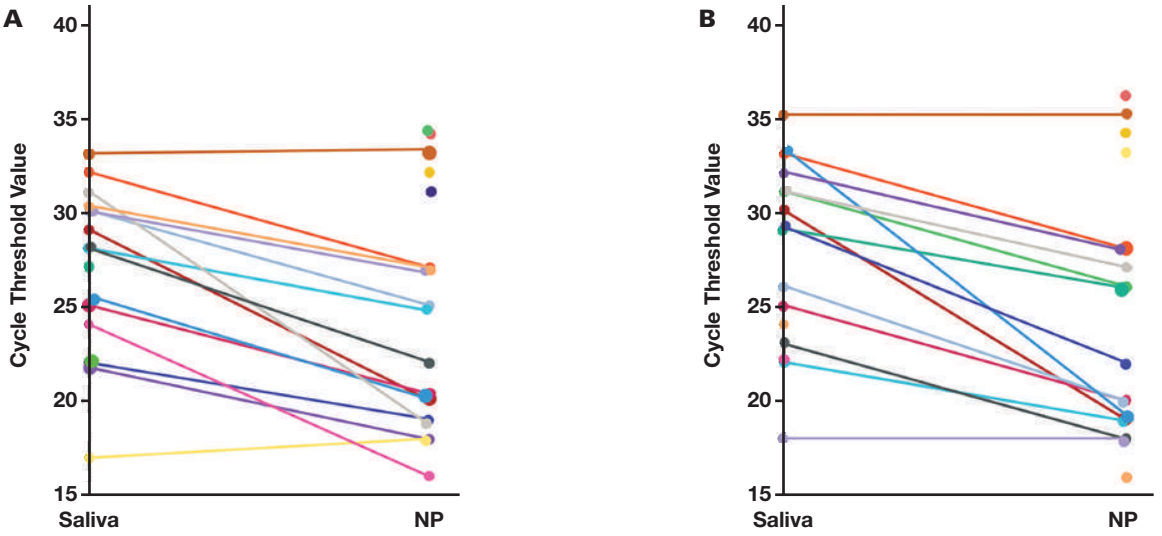


trained health care providers are unavailable or when a lack of NP swabs exists. Furthermore, Ct values in saliva specimens are comparable to NP specimens for detection of SARS-CoV-2. Clearly, additional studies are needed to fully characterize and validate assay analytical performance with a saliva sample matrix. Future studies should aim to explore the preferred quantity of saliva needed to detect viral SARS-CoV-2 particles, which could contribute to greater concordance in crossing point thresholds between NP specimens and saliva samples. In addition, given the rapid emergence of multiple genetic variants of SARS-CoV-2, saliva testing may allow for further expansion of testing options. Adoption of saliva sampling may alleviate challenges associated with increased need for testing due to supply chain challenges noted during the ongoing COVID-19 pandemic.

## Funding

This work was supported by Mayo Clinic COVID-19 Innovation funds.

## REFERENCES

1. Azzi L, Carcano G, Gianfagna F, et al. Saliva is a reliable tool to detect SARS-CoV-2. *J Infect.* 2020;81(1):e45–e50. doi:10.1016/j.jinf.2020.04.005.
2. Sakanashi D, Asai N, Nakamura A, et al. Comparative evaluation of nasopharyngeal swab and saliva specimens for the molecular detection of SARS-CoV-2 RNA in Japanese patients with COVID-19. *J Infect Chemother.* 2021;27(1):126–129. doi:10.1016/j.jiac.2020.09.027.
3. Planas D, Veyer D, Baidaliuk A, et al. Reduced sensitivity of SARS-CoV-2 variant Delta to antibody neutralization. *Nature.* 2021. doi:10.1038/s41586-021-03777-9.
4. Hitzenbichler F, Bauernfeind S, Salzberger B, Schmidt B, Wenzel JJ. Comparison of throat washings, nasopharyngeal swabs and oropharyngeal swabs for detection of SARS-CoV-2. *Viruses*. 2021;13(4):653. doi:10.3390/v13040653
5. Lee RA, Herigon JC, Benedetti A, Pollock NR, Denkinger CM. Performance of saliva, oropharyngeal swabs, and nasal swabs for SARS-CoV-2 molecular detection: a systematic review and meta-analysis. *J Clin Microbiol.* 2021;59(5):e02881–e02820. doi:10.1128/JCM.02881-20.
6. Golden SH. Coronavirus in African Americans and other people of color. Johns Hopkins Medicine. https://www.hopkinsmedicine.org/health/conditions-and-diseases/coronavirus/covid19-racial-disparities. Published April 20, 2020. Accessed July 13, 2021.
7. Centers for Disease Control and Prevention. Overview of testing for SARS-CoV-2 (COVID-19). https://www.cdc.gov/coronavirus/2019-ncov/hcp/testing-overview.html. Accessed July 13, 2021.
8. Poljak M, Korva M, Knap Gašper N, et al. Clinical evaluation of the cobas SARS-CoV-2 test and a diagnostic platform switch during 48 hours in the midst of the COVID-19 pandemic. *J Clin Microbiol*. 2020;58(6):e00599–20. doi:10.1128/JCM.00599-20.
9. Vasquez Reyes M. The disproportional impact of COVID-19 on African Americans. *Health Hum Rights.* 2020;22(2):299–307.
10. Centers for Disease Control and Prevention. COVID-19 racial and ethnic disparities. https://www.cdc.gov/coronavirus/2019-ncov/community/health-equity/racial-ethnic-disparities/index.html. Published December 10, 2020. Accessed July 13, 2021.
11. Bowles KE, Clark HA, Tai E, et al. Implementing rapid HIV testing in outreach and community settings: results from an advancing HIV prevention demonstration project conducted in seven U.S. cities. *Public Health Rep.* 2008;123(suppl 3):78–85. doi:10.1177/00333549081230S310.

# Anti-*Saccharomyces cerevisiae* Antibodies in Rheumatoid Arthritis

*Sarra Melayah,[1,2] Mariem Ghozzi,[1,2] Malek Jemni,[1,2] Nabil Sakly,[2,3] Ibtissem Ghedira,[1,2] Amani Mankai[1,4]*

[1]Laboratory of Immunology, Farhat Hached Hospital, Sousse, Tunisia, [2]Department of Immunology, Faculty of Pharmacy, Monastir University, Monastir, Tunisia, [3]Laboratory of Immunology, Fattouma Bourguiba Hospital, Monastir, Tunisia, [4]High School of Sciences and Techniques of Health, Tunis El Manar University, Tunis, Tunisia *To whom correspondence should be addressed. sarra.125@hotmail.fr

**Keywords:** anti-*Saccharomyces cerevisiae* antibodies, phosphopeptidomannan, rheumatoid arthritis, anti-CCP antibodies, rheumatoid factors, autoimmune disease

**Abbreviations:** ASCA, anti-*Saccharomyces cerevisiae* antibodies; RA, rheumatoid arthritis; PPM, phosphopeptidomannan; β2GPI, β2 glycoprotein I; aβ2GPI, anti-β2GPI; AID, autoimmune diseases; anti-CCP, anti-cyclic citrullinated antibodies; HBD, healthy blood donors; RF, rheumatoid factors; MBL, mannose binding lectine.

*Laboratory Medicine* 2022;53:585–589; https://doi.org/10.1093/labmed/lmac054

## ABSTRACT

**Objective:** This study was conducted to evaluate the frequency of anti-*Saccharomyces cerevisiae* antibodies (ASCA) in patients with rheumatoid arthritis (RA).

**Methods:** Eighty-three RA patients with positive anti-cyclic citrullinated antibodies (anti-CCP) and 160 healthy blood donors were included in this study. ASCA IgG and IgA were assessed with enzyme-linked immunosorbent assay.

**Results:** The frequency of ASCA was significantly higher in RA patients than in healthy subjects (22.9% vs 3.7%, $P < 10^{-3}$). Both ASCA IgG and ASCA IgA were significantly more frequent in RA patients than in the control group (20.5% vs 3.1%, $P < 10^{-3}$ and 9.6% vs 0.6%, $P = .002$, respectively). ASCA IgG and ASCA IgA levels were significantly higher in RA patients than in healthy subjects (7.8 ± 8.4 U/mL vs 2.3 ± 2.8 U/mL, $P < 10^{-6}$ and 6.2 ± 10.9 U/mL vs 3.4 ± 1.7 U/mL, $P = .002$, respectively).

**Conclusion:** A high frequency of ASCA IgG and ASCA IgA has been found in RA patients.

Rheumatoid arthritis (RA) is an autoimmune disease characterized by persistent synovial inflammation leading potentially to cartilage and bone damage and disability.[1] The etiology of RA is unknown; however, genetic, epigenetic, and environmental factors including gut dysbiosis might be involved in RA.[2,3] In fact, a gut-joint axis has been incriminated in RA and suggested to contribute to arthritis.[4] In this context, 2 pathways have been described: intestinal inflammation, which could be responsible for the generation of autoantibodies, and the migration of proinflammatory immune cells, present in the intestine, to the joints.[4]

Anti-*Saccharomyces cerevisiae* (ASCA) are directed against the phosphopeptidomannan (PPM), part of the cell wall of *S cerevisiae*. ASCA have been previously considered as a serological marker of Crohn's disease.[5] Interestingly, ASCA also have been described in rheumatic diseases such as Behçet's disease,[6] ankylosing spondylitis,[7] psoriatic arthritis,[8] and spondyloarthritis.[9] Furthermore, ASCA have been described as a valuable test in evaluating patients with RA.[10] Additionally, the frequency of ASCA IgA but not of ASCA IgG was found to be significantly higher in RA patients than in a healthy population in one study,[11] whereas other studies failed to show an association between ASCA and RA.[8,12]

The pathogenic role of ASCA remains unknown, and one of the hypotheses of their synthesis is molecular mimicry with self-antigens.[13] The β2 glycoprotein I (β2GPI), a phospholipid-binding glycoprotein, is normally present in plasma at the concentration of 50 μg/mL to 500 μg/mL and is a member of the complement control family.[14] Interestingly, a structural similarity between the PPM of the yeast and β2GPI has been reported.[15] Anti-β2GPI (aβ2GPI) antibodies have been found in antiphospholipid syndrome but also in other autoimmune diseases (AID).[16] We have previously described aβ2GPI in patients with RA[17]; in the present study, our aim was to determine whether ASCA are also frequent in RA.

## Materials and Methods

### Study Population

We included 83 RA patients (51 females and 32 males). The mean age of our study population was 52 ± 15 years (range, 17–84 years). Sera samples were collected between 2017 and 2018 from 4 hospitals in the center of Tunisia. All patients fulfilled the American College of Rheumatology/European League Against Rheumatism[18] criteria for RA. Patients

with RA and Crohn's disease were excluded from our study. The inclusion criterion of our study was anti-cyclic citrullinated peptide antibodies (anti-CCP) positive.

Sera from 160 healthy blood donors (HBD) (128 females and 32 males) were included as control group (mean age, 21 ± 4 years; range, 17–45 years). Samples of 4 mL venous blood were received in our laboratory for anti-CCP and rheumatoid factors (RF) assay. Sera were collected by centrifugation at 3000 rpm for 15 minutes and an enzyme-linked immunosorbent assay (ELISA) was carried out for anti-CCP and RF. A total of 400 µL positive anti-CCP sera was aliquoted and stored at −80°C until use for analysis. The ethics committee of Farhat Hached Hospital gave approval for this study.

### ASCA Assays

ASCA IgG and IgA were assessed by ELISA (Orgentec Diagnostika). Highly purified mannan from *S cerevisiae* was bound to microwells and served as an antigen. Sera of patients were diluted at 1:100 before the assay and 100 µL was added to the reaction wells. Specific antibodies in the patient sample bound to the antigen. After incubation, a washing step was performed and subsequently added enzyme conjugate bound to the immobilized antibody-antigen complexes. After incubation, a second washing step removed unbound enzyme conjugate. After the addition of substrate solution, the bound enzyme conjugate hydrolyzed the substrate, forming a blue product. Addition of an acid stopped the reaction, generating a yellow end product. The intensity of the yellow color correlates with the concentration of the antibody-antigen complex and can be measured photometrically at 450 nm. Results were expressed as arbitrary units with a cutoff for positivity of 10 U/mL.

**TABLE 1. Characteristics of RA Patients and the Control Group**

| | RA Patients (n = 83) | Control Group (n = 160) | *P* |
|---|---|---|---|
| Sex ratio (F/M) | 1.6 (51/32) | 4 (128/32) | .002 |
| Mean age (y) ± SD | 52 ± 15 | 21 ± 4 | $<10^{-6}$ |
| Age range (y) | 17-84 | 17-45 | — |
| Positive anti-CCP, No. (%) | 83 (100) | — | — |
| Positive IgG-RF, No. (%) | 65 (78.3) | — | — |
| Positive IgA-RF, No. (%) | 64 (77.1) | — | — |
| Positive IgM-RF, No. (%) | 71 (85.5) | — | — |

*anti-CCP, cyclic citrullinated peptide antibodies; RA, rheumatoid arthritis; RF, rheumatoid factors.*

### RF and Anti-CCP Assays

Serum samples were evaluated for IgG, IgA, and IgM RF by using an ELISA (Orgentec Diagnostika) according to the manufacturer's instructions. Anti-CCP were detected by using an available second generation ELISA (Euroimmun). Optimal cutoff values were determined by plotting sensitivity against 1 – specificity to receiver operating characteristic curve as we have described in our previous studies.[19,20]

### Statistical Analysis

The comparison of frequencies of ASCA was performed using $\chi^2$ or Fisher exact test. The variables were tested for normality using the Kolmogorov-Smirnov test with Lilliefors adjustment. To compare mean levels of ASCA, we used the parametric Student *t*-test. Correlation was assessed using the Spearman test. A *P* value less than .05 was considered statistically significant. SPSS software, version 22, was used for statistical analysis.

## Results

**TABLE 1** shows patients and HBD characteristics.

### Frequency of ASCA in RA Patients and the Control Group

Out of 83 RA patients, 19 (22.9%) had ASCA (IgG or IgA). The frequency of ASCA was significantly higher in RA patients than in healthy subjects (22.9% vs 3.7%, $P < 10^{-3}$). Both ASCA IgG and ASCA IgA were significantly more frequent in RA patients than in the control group (20.5% vs 3.1%, $P < 10^{-3}$; 9.6% vs 0.6%, $P = .002$, respectively) (**TABLE 2**).

### Frequency of ASCA According to Gender

Among the 19 patients who had ASCA (IgG or IgA), 15 were females. ASCA (IgG or IgA) was more frequent in females (15/51, 29.4%) than in males (4/32, 12.5%), but the difference was not statistically significant. In RA patients, the frequencies of ASCA IgG and ASCA IgA were not statistically different between males and females (**TABLE 2**).

### Comparison between ASCA IgG and ASCA IgA

The frequency of ASCA IgG was higher than that of ASCA IgA in RA patients but the difference was of borderline significance (20.5% vs 9.6%, $P = .05$) (**TABLE 2**).

ASCA IgG and ASCA IgA levels were significantly higher in RA patients than in healthy subjects (7.8 ± 8.4U/mL vs 2.3 ± 2.8 U/mL, $P < 10^{-6}$ and 6.2 ± 10.9 U/mL vs 3.4 ± 1.7 U/mL, $P = .002$, respectively) (**FIGURE 1**). In RA patients, no difference was detected between the mean levels of ASCA IgG and ASCA IgA.

**TABLE 2. Comparison of the Frequency of ASCA between Female and Male Patients and between RA Patients and the Control Group[a]**

| | RA Females (n = 51) | RA Males (n = 32) | *P* Value | RA Patients (n = 83) | Control Group (n = 160) | *P* Value |
|---|---|---|---|---|---|---|
| ASCA IgG or IgA | 15 (29.4) | 4 (12.5) | .07 | 19 (22.9) | 6 (3.7) | $<10^{-3}$ |
| ASCA IgG and IgA | 3 (5.9) | 3 (9.4) | .85 | 6 (7.2) | 0 | .003 |
| ASCA IgG | 3 (25.5) | 4 (12.5) | .51 | 17 (20.5)[b] | 5 (3.1) | $<10^{-3}$ |
| ASCA IgA | 5 (9.8) | 3 (9.4) | .99 | 8 (9.6)[b] | 1 (0.6) | .002 |

*ASCA, anti-*Saccharomyces cerevisiae *antibodies; RA, rheumatoid arthritis.*
[a]*Data are given as No. (%).*
[b]*Comparison between ASCA IgG and ASCA IgA (P = .05).*

**FIGURE 1. Comparison of ASCA IgG (A) and ASCA IgA (B) levels in RA patients and control group. ASCA, anti-*Saccharomyces cerevisiae* antibodies; RA, rheumatoid arthritis.**

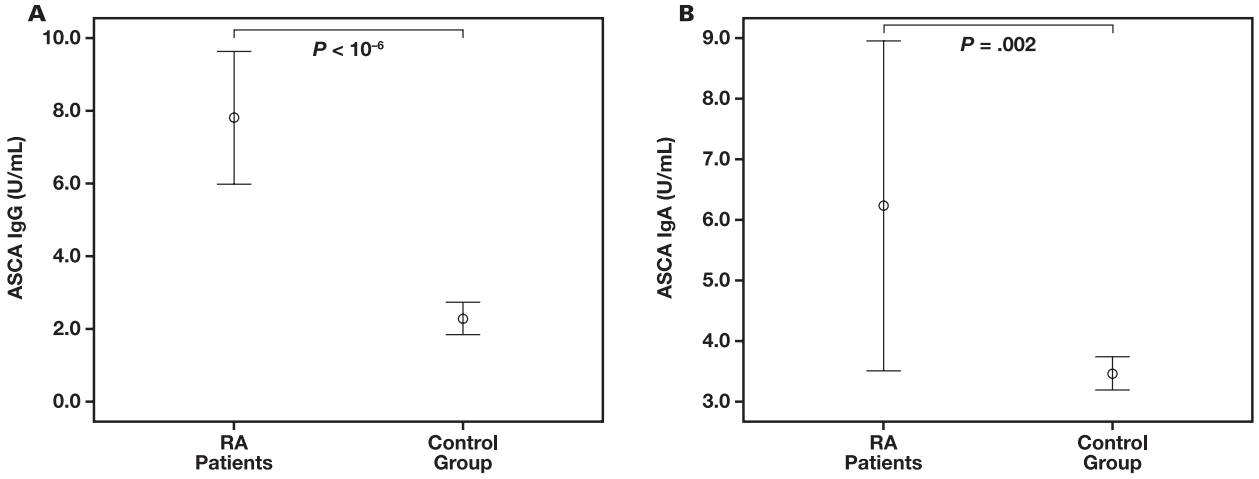


**TABLE 3. Titers of ASCA in Patients with Positive Results**

| Patients | ASCA IgG Titer (U/mL) | ASCA IgA Titer (U/mL) |
|---|---|---|
| 1 | 24.1 | 3.5 |
| 2 | 25.8 | 4.2 |
| 3 | 19 | 4 |
| 4 | 13.6 | 13.2 |
| 5 | 31.4 | 19.1 |
| 6 | 13.3 | 3.2 |
| 7 | 11.5 | 3.1 |
| 8 | 29.9 | 11.3 |
| 9 | 15.5 | 11.1 |
| 10 | 9.8 | 11 |
| 11 | 36.1 | 100 |
| 12 | 11 | 3.6 |
| 13 | 19.8 | 4.7 |
| 14 | 20.3 | 3.1 |
| 15 | 13.6 | 4.9 |
| 16 | 11.2 | 1.6 |
| 17 | 14.8 | 1.6 |
| 18 | 47.8 | 12 |
| 19 | 7.3 | 59.2 |

*ASCA, anti-*Saccharomyces cerevisiae *antibodies.*

Geometric mean titer of ASCA IgG was 5.5 U/mL in RA patients and 1.5 U/mL in the control group. Geometric mean titer of ASCA IgA was 4.1 U/mL and 3.2 U/mL in patients and controls, respectively. **TABLE 3** shows titers of ASCA in patients with positive results.

### Association between ASCA and anti-CCP

There was no correlation between ASCA IgG or ASCA IgA levels and anti-CCP levels in patients with RA ($r$ = 0.212, = 0.055; $r$ = 0.082, $P$ = .465 respectively) (**FIGURE 2**).

### Contribution of ASCA in Patients without RF

In 19 RA patients with ASCA, 2 (10.5%), 4 (21%), and 3 (15.8%) did not have RF-IgG, RF-IgA and RF-IgM, respectively. Two patients among these 19 (10.5%) did not have any of the 3 isotypes of RF.

## Discussion

In this study, we assessed the frequency of ASCA IgG and IgA in a series of 83 patients with RA. We found a significantly higher frequency of both ASCA IgG and ASCA IgA in RA patients than in the control group (20.5% vs 3.1%, $P$ = .001; 9.6% vs 0.6%, $P$ = .002, respectively). In studies by Hoffman et al[12] and Riente et al,[8] the frequency of ASCA IgG and ASCA IgA was not significantly different between RA patients and healthy subjects. Another study showed a significant difference for ASCA IgA and not IgG in RA patients compared to controls.[11] The frequency of ASCA IgG that we found in this study was similar to that of Dai et al[11] (20.5% and 20%, respectively); however, the frequency of ASCA IgA is lower than that found in Dai et al[11] (9.6% and 40%, respectively). In the Dai et al[11] study, IgA was the predominant isotype of ASCA but in our study, IgG was predominant. In fact, in all our previous studies on ASCA in AID,[21–26] ASCA IgA frequencies were significantly lower than those of ASCA IgG. The frequency of ASCA (IgG or IgA) in our series was lower than that of Lichtenstein et al (22.9% vs 65.6%, respectively).[10] This difference seems to be due to the inclusion criteria selected for the 2 studies. We included only patients who were positive for anti-CCP, whereas 52% of patients in the study of Lichtenstein et al were negative for anti-CCP. Moreover, in their series, 29% of patients with ASCA had neither anti-CCP nor RF.[10] Consequently, it is possible that if we included seronegative patients for anti-CCP, the ASCA frequency could be higher. Interestingly, 10.5% of patients with ASCA in our series had no RF. Thus, when we combine ASCA with the known serological markers of RA (anti-CCP and RF), we increase RA diagnostic sensitivity.

Why are ASCA produced during RA? In RA, an altered intestinal barrier function seems to be secondary to the upregulation of zonulin, an intestinal peptide responsible for the regulation of the integrity of tight junctions.[4] The increased production of zonulin has been associated with gluten consumption[27] and gut microbiota dysbiosis.[4] Furthermore, it has been demonstrated that treatment with a zonulin antagonist specifically increases intestinal barrier integrity and reduces arthritis

**FIGURE 2. Correlation between ASCA IgG (A) and ASCA IgA (B) levels and anti-CCP titers in RA patients. ASCA, anti-*Saccharomyces cerevisiae* antibodies; anti-CCP, anti-cyclic citrullinated peptide antibodies.**

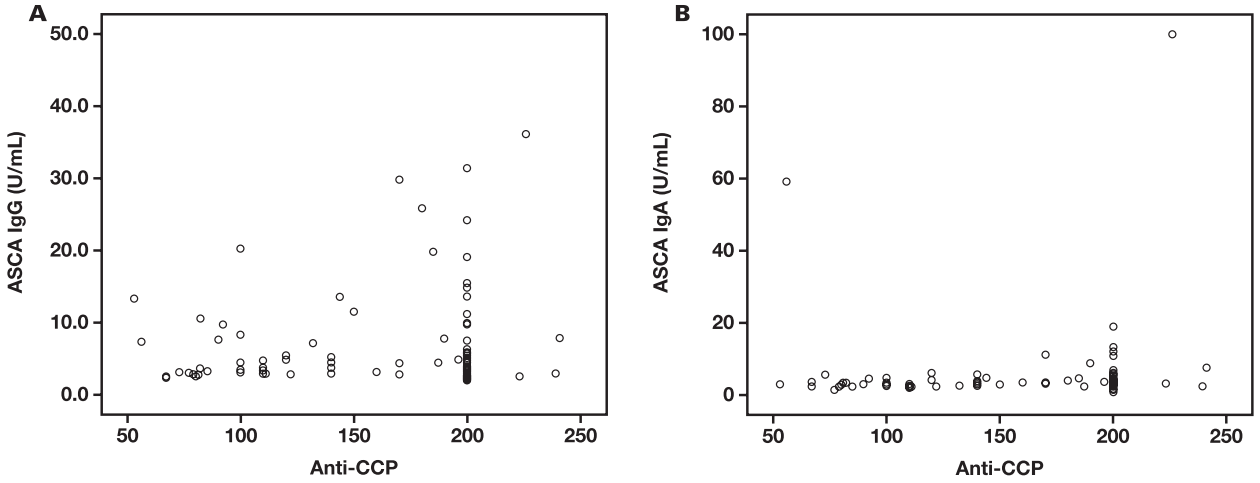


onset.[28] In RA, the resulting leaky intestinal wall allows passage of environmental antigens and exposes further *S cerevisiae* to the mucosal immune system, explaining the high frequency of ASCA. Moreover, we have previously found a significantly higher frequency of ASCA in patients with other AID in comparison to healthy subjects[21–26] and in all these AID, gut microbiota dysbiosis and altered intestinal permeability have been described.[29,30]

The high frequency of ASCA in our RA patients could also be explained by a possible cross-reactivity between the mannan of *S cerevisiae* and the mannan of mannose binding lectine (MBL). Interestingly, increased MBL levels have been reported in RA, suggesting that MBL could play a differential role in the pathogenesis of RA.[31,32] In addition, the innate immune complement protein MBLs and their MBL2 genetic variants have been shown to be associated with many AID such as RA.[33,34] Remarkably, plasma levels of MBL are also elevated in AID in which we have previously detected ASCA and in particular type 1 diabetes, celiac disease, primary biliary cholangitis and Graves disease.[25]

Could ASCA be implicated in the pathogenesis of RA? We have previously demonstrated a high frequency of aβ2GPI in RA patients.[17] Interestingly, Krause et al[15] demonstrated that a subpopulation of aβ2GPI is specific to the glycosylated site of the β2GPI molecule that cross-reacts with the PPM, part of the cell wall of *S cerevisiae*. In fact, a similarity in molecular structures (39%) was found between the mannan of the yeast *S cerevisiae* and the β2GPI.[13] Therefore, could we hypothesize that ASCA detected in our RA patients are aβ2GPI cross-reactive antibodies? Interestingly, the frequency of ASCA IgG (20.5%) in the present study is similar to that of aβ2GPI-IgA (26.7%) in our previous study on RA.[17] Moreover, because β2GPI is a ubiquitous glycoprotein and is present even in the joint,[35] ASCA could bind to β2GPI in the joint and induce complement activation and inflammation. On the other hand, Rinaldi et al[13] found that some autoantigens of RA share sequences with mannan expressed by the cell wall of *S cerevisiae*. So, could we imagine that ASCA synthesized during RA could bind to citrullinated peptides in the joint? The binding of those antibodies to citrullinated peptides will result in immune complex formation, complement activation, and a release of proinflammatory cytokines promoting chronic joint inflammation that is typical for RA.[36] Moreover, because *S cerevisiae* could migrate from the gut to the joint because of a leaky gut, so ASCA could bind to *S cerevisiae* in the joint and induce the inflammatory process described above.

In conclusion, in this retrospective study, we found a high frequency of ASCA in patients with RA. This suggests that PPM, a component of the *S cerevisiae* cell wall, might induce chronic arthritis, and ASCA could improve the immunological diagnosis of RA.

## Author Contributions

The authors contributed equally to study concept and design. All authors contributed to acquisition of data, analysis and interpretation, drafting of the manuscript and critical revision for important intellectual content. All authors approved the final version of this paper, including the authorship statement.

## Funding

This study is supported by Unité de recherche, Auto-immunité et Allergie (03/UR/07-02), Faculté de Pharmacie de Monastir, Université de Monastir, Monastir, Tunisia.

## REFERENCES

1. Smolen JS, Aletaha D, McInnes IB. Rheumatoid arthritis. *Lancet.* 2016;388:2023–2038. doi:10.1016/S0140-6736(16)30173-8.
2. Aletaha D, Smolen JS. Diagnosis and management of rheumatoid arthritis: a review. *JAMA.* 2018;320:1360–1372. doi:10.1001/jama.2018.13103.
3. Picchianti-Diamanti A, Panebianco C, Salemi S, et al. Analysis of gut microbiota in rheumatoid arthritis patients: disease-related dysbiosis and modifications induced by etanercept. *Int J Mol Sci .* 2018;19:2938. doi:10.1016/j.jbspin.2015.10.011.
4. Zaiss MM, Joyce Wu HJ, Mauro D, Schett G, Ciccia F. The gut-joint axis in rheumatoid arthritis. *Nat Rev Rheumatol.* 2021;17:224–237. doi:10.1038/s41584-021-00585-3.
5. Peeters M, Joossens S, Vermeire S, Vlietinck R, Bossuyt X, Rutgeerts P. Diagnostic value of anti-*Saccharomyces cerevisiae* and

antineutrophil cytoplasmic autoantibodies in inflammatory bowel disease. *Am J Gastroenterol.* 2001;96:730–734. doi:10.1111/j.1572-0241.2001.03613.x.

6. Krause I, Monselise Y, Milo G, Weinberger A. Anti-*Saccharomyces cerevisiae* antibodies—a novel serologic marker for Behçet's disease. *Clin Exp Rheumatol.* 2002;20(4 suppl 26):S21–S24.
7. Aydin SZ, Atagunduz P, Temel M, Bicakcigil M, Tasan D, Direskeneli H. Anti-*Saccharomyces cerevisiae* antibodies (ASCA) in spondyloarthropathies: a reassessment. *Rheumatology (Oxford)* 2008;47:142–144. doi:10.1093/rheumatology/kem324.
8. Riente L, Chimenti D, Pratesi F, et al. Antibodies to tissue transglutaminase and *Saccharomyces cerevisiae* in ankylosing spondylitis and psoriatic arthritis. *J Rheumatol.* 2004;31(5):920–924.
9. Maillet J, Ottaviani S, Tubach F, et al. Anti-*Saccharomyces cerevisiae* antibodies (ASCA) in spondyloarthritis: prevalence and associated phenotype. *Joint Bone Spine.* 2016;83(6):665–668.
10. Lichtenstein JR, Epstein AL. Antibodies to brewer's yeast in rheumatoid arthritis. *Cureus.* 2019;11:e4691. doi:10.7759/cureus.4691.
11. Dai H, Li Z, Zhang Y, Lv P, Gao XM. Elevated levels of serum IgA against *Saccharomyces cerevisiae* mannan in patients with rheumatoid arthritis. *Cell Mol Immunol.* 2009;6:361–366. doi:10.1038/cmi.2009.47.
12. Hoffman IE, Demetter P, Peeters M, et al. Anti-*Saccharomyces cerevisiae* IgA antibodies are raised in ankylosing spondylitis and undifferentiated spondyloarthropathy. *Ann Rheum Dis.* 2003;62:455–459. doi:10.1136/ard.62.5.455.
13. Rinaldi M, Perricone R, Blank M, Perricone C, Shoenfeld Y. Anti-*Saccharomyces cerevisiae* autoantibodies in autoimmune diseases: from bread baking to autoimmunity. *Clin Rev Allergy Immunol.* 2013;45:152–161. doi:10.1007/s12016-012-8344-9.
14. de Groot PG, Meijers JC. β(2) -Glycoprotein I: evolution, structure and function. *J Thromb Haemost.* 2011;9:1275–1284. doi:10.1111/j.1538-7836.2011.04327.x.
15. Krause I, Blank M, Cervera R, et al. Cross-reactive epitopes on beta2-glycoprotein-I and *Saccharomyces cerevisiae* in patients with the antiphospholipid syndrome. *Ann N Y Acad Sci.* 2007;1108:481–488. doi:10.1196/annals.1422.051.
16. Gómez-Puerta JA, Cervera R. Diagnosis and classification of the antiphospholipid syndrome. *J Autoimmun*. 2014;48–49:20–25.
17. Melayah S, Changuel M, Mankaï A, Ghedira I. IgA is the predominant isotype of anti-β2 glycoprotein I antibodies in rheumatoid arthritis. *J Clin Lab Anal.* 2020;34:e23217. doi:10.1002/jcla.23217.
18. Aletaha D, Neogi T, Silman AJ, et al. 2010 Rheumatoid arthritis classification criteria: an American College of Rheumatology/European League Against Rheumatism collaborative initiative. *Arthritis Rheum.* 2010;62:2569–2581. doi:10.1002/art.27584.
19. Sghiri R, Bouajina E, Bargaoui D, et al. Value of anti-mutated citrullinated vimentin antibodies in diagnosing rheumatoid arthritis. *Rheumatol Int.* 2008;29:59–62. doi:10.1007/s00296-008-0614-8.
20. Sghiri R, Bouagina E, Zaglaoui H, et al. Diagnostic performances of anti-cyclic citrullinated peptide antibodies in rheumatoid arthritis. *Rheumatol Int.* 2007;27:1125–1130. doi:10.1007/s00296-007-0351-4.
21. Toumi D, Mankaï A, Belhadj R, Ghedira-Besbes L, Jeddi M, Ghedira I. Anti-*Saccharomyces cerevisiae* antibodies in coeliac disease. *Scand J Gastroenterol.* 2007;42:821–826. doi:10.1080/00365520601154996.
22. Sakly W, Jeddi M, Ghedira I. Anti-*Saccharomyces cerevisiae* antibodies in primary biliary cirrhosis. *Dig Dis Sci.* 2008;53:1983–1987. doi:10.1007/s10620-007-0092-y.
23. Sakly W, Mankaï A, Sakly N, et al. Anti-*Saccharomyces cerevisiae* antibodies are frequent in type 1 diabetes. *Endocr Pathol.* 2010;21:108–114. doi:10.1007/s12022-010-9118-7.
24. Mankaï A, Sakly W, Thabet Y, Achour A, Manoubi W, Ghedira I. Anti-*Saccharomyces cerevisiae* antibodies in patients with systemic lupus erythematosus. *Rheumatol Int.* 2013;33:665–669. doi:10.1007/s00296-012-2431-3.
25. Mankaï A, Thabet Y, Manoubi W, Achour A, Sakly W, Ghedira I. Anti-*Saccharomyces cerevisiae* antibodies are elevated in Graves' disease but not in Hashimoto's thyroiditis. *Endocr Res.* 2013;38:98–104.
26. Mankaï A, Layouni S, Ghedira I. Anti *Saccharomyces cerevisiae* antibodies in patients with anti-β2 glycoprotein I antibodies. *J Clin Lab Anal.* 2016;30:818–822. doi:10.1002/jcla.21942.
27. Bruzzese V, Scolieri P, Pepe J. Efficacy of gluten-free diet in patients with rheumatoid arthritis. *Reumatismo.* 2021;72:213–217. doi:10.4081/reumatismo.2020.1296.
28. Tajik N, Frech M, Schulz O, et al. Targeting zonulin and intestinal epithelial barrier function to prevent onset of arthritis. *Nat Commun*. 2020;24;11:1995.
29. Levy M, Kolodziejczyk AA, Thaiss CA, Elinav E. Dysbiosis and the immune system. *Nat Rev Immunol.* 2017;17:219–232. doi:10.1038/nri.2017.7.
30. Chen B, Sun L, Zhang X. Integration of microbiome and epigenome to decipher the pathogenesis of autoimmune diseases. *J Autoimmun.* 2017;83:31–42. doi:10.1016/j.jaut.2017.03.009.
31. Saevarsdottir S, Steinsson K, Grondal G, Valdimarsson H. Patients with rheumatoid arthritis have higher levels of mannan-binding lectin than their first-degree relatives and unrelated controls. *J Rheumatol.* 2007;34(8):1692–1695.
32. Ammitzboll CG, Thiel S, Ellingsen T, et al. Levels of lectin pathway proteins in plasma and synovial fluid of rheumatoid arthritis and osteoarthritis. *Rheumatol Int.* 2012;32:1457–1463. doi:10.1007/s00296-011-1879-x.
33. Turner MW, Hamvas RM. Mannose-binding lectin: structure, function, genetics and disease associations. *Rev Immunogenet.* 2000;2(3):305–322.
34. Goeldner I, Skare TL, Utiyama SR, et al. Mannose binding lectin and susceptibility to rheumatoid arthritis in Brazilian patients and their relatives. *PLoS One.* 2014;9:e95519. doi:10.1371/journal.pone.0095519.
35. Pawlak Z, Mrela A, Kaczmarek M, Cieszko M, Urbaniak W. Natural joints: boundary lubrication and antiphospholipid syndrome (APS). *Biosystems.* 2019;177:44–47. doi:10.1016/j.biosystems.2018.10.018.
36. De Brito Rocha S, Baldo DC, Andrade LEC. Clinical and pathophysiologic relevance of autoantibodies in rheumatoid arthritis. *Adv Rheumatol.* 2019;59:2. doi:10.1186/s42358-018-0042-8.

# IgG-RBD Response Due to Inactivated SARS-CoV-2 Vaccine: Alteration in D-Dimer and Fibrinogen Concentrations, Association with Comorbidities and Adverse Effects

*Murat Kaytaz, MD,[1] Emre Akkaya, MD,[1] Sefika Nur Gumus, MD,[1] Sema Genc,[2,*] Halim Issever,[3] and Beyhan Omer[1]*

[1]Department of Biochemistry Istanbul Faculty of Medicine Istanbul University, Capa, Istanbul, Turkey, [2]Department of Biochemistry, Acibadem Maslak Hospital, Istanbul, Turkey, [3]Department of Medical Sciences and Public Health, Istanbul Faculty of Medicine, Istanbul University, Capa, Istanbul, Turkey, *To whom correspondence should be addressed: nsgenc@hotmail.com.

**Keywords:** COVID-19 infection, vaccination, D-dimer, fibrinogen, side effects

**Abbreviations:** IgG-RBD, immunoglobulin G-receptor-binding domain; SARS-CoV-2, severe acute respiratory syndrome coronavirus 2; WHO, World Health Organization; COVID-19, coronavirus disease 2019; IHME, Institute for Health Metrics and Evaluation; S, spike; ACE2, angiotensin-converting enzyme 2; RBD, receptor-binding domain; RT-PCR, reverse transcription-polymerase chain reaction; COPD, chronic obstructive pulmonary disease; AU/mL, arbitrary units per milliliter; CLSI, Clinical and Laboratory Standards Institute.

*Laboratory Medicine* 2022;53:590–595; https://doi.org/10.1093/labmed/lmac047

## ABSTRACT

**Objective:** To examine the immunoglobulin G-receptor-binding domain (IgG-RBD) response and changes in fibrinogen and D-dimer concentrations in individuals with a past coronavirus infection and followed by CoronaVac.

**Methods:** The study consisted of a total of 116 participants. Blood samples were drawn from subjects 21–25 days after they received first and second doses of CoronaVac as well as from individuals with a past infection. Fibrinogen, D-dimer, and IgG-RBD concentrations were measured.

**Results:** The IgG concentrations of the vaccinated subjects were significantly higher ($P < .001$), fibrinogen levels were lower ($P < .001$), and D-dimer levels increased following the second vaccination compared with the first vaccination ($P = .083$). No difference was obtained in IgG-RBD between vaccinated and previously infected individuals ($P = .063$). The differences in fibrinogen and D-dimer were statistically nonsignificant between both groups.

**Conclusion:** The CoronaVac vaccine appears to be safe and effective. It is essential for individuals to take personal protective measures, such as using masks and distancing.

Severe acute respiratory syndrome coronavirus 2 (SARS-CoV-2) was accepted as a pandemic by the World Health Organization (WHO) on March 11, 2020, and has spread globally, presenting high morbidity and mortality. The clinical findings and severity of coronavirus disease 2019 (COVID-19) show variations from asymptomatic cases to mild-to-moderate and severe cases, and studies have demonstrated the relationship of disease severity with advanced age and underlying comorbidities.[1] However, severe infections may not be limited to risk groups: severe cases have also been seen in young people.[2]

According to the reports of the Institute for Health Metrics and Evaluation (IHME), the cumulative total COVID-19 death rate was reported as approximately 91.7 per 100,000 by May 2021, and an increased disparity has been reported in terms of mortality and morbidity rates among countries, and even subcommunities within countries, depending on the testing strategies, capacities, and healthcare policies of the countries.[3]

To date, no specific therapeutic approaches have emerged for COVID-19 infections beyond the preventive strategies, including widespread testing, distancing, and isolation; and thus, SARS-CoV-2 vaccination became the priority of global health services. With preventive strategies and vaccination of a sufficient number of people, individual protection is ensured, and consequently, herd immunity prevents the global spread of the virus and reduces morbidity and mortality.[4] Most vaccine studies were developed primarily against the SARS-CoV-2 spike (S) protein because of the increased T cell responses targeting the SARS-CoV-2 S protein on the viral membrane in patients with past SARS-CoV-2 infection.[5] The S protein consists of S1 and S2 subunits. The S1 region binds to angiotensin-converting enzyme 2 (ACE2) receptors on the host membrane by its receptor-binding domain (RBD); and the S2 region is responsible for virus-membrane fusion and facilitates viral entry.[6,7] The RBD of the S protein has been shown to be a primary target of neutralizing antibodies. In an experimental study, it was shown that the

RBD has a role in stimulating the neutralizing antibody response and protecting against SARS-CoV-2.[8]

Vaccines against SARS-CoV-2 are classified according to the different technologies in which they are developed: live attenuated vaccines, inactivated vaccines, soluble protein vaccines, viral vectors, nanoparticles, and DNA or RNA vaccines.[9,10] CoronaVac (Sinovac Life Sciences), is an inactivated vaccine that has been used in China, Brazil, and Turkey against SARS-CoV-2 during the pandemic. It is produced in African green monkey kidney cells (Vero E6), then chemically inactivated using β-propiolactone and formulated with a specific adjuvant, CpG oligonucleotide, and aluminum hydroxide.

mRNA vaccines BNT162b2 and mRNA-1273—Pfizer, BioNTech, and Moderna—were the first approved vaccines in the world that were developed by modifying RNA to code the SARS-CoV-2 S protein. Inversely, DNA vaccines were produced by cloning the S protein gene into bacterial plasmids.[11] Live-attenuated vaccines (SARS-CoV-2-VAC) (trial numbers NCT04619628 and MV-014–212) are developed by either using an avirulent strain of the virus or by creating a genetically weakened form of the virus and stimulating mucosal and cellular immunity without adjuvants.[12] However, different antibody kinetics have been demonstrated due to the variability in assay type—qualitative or quantitative manner—or target antigen.[13] In all these vaccines, neutralizing antibodies and Th1-driven CD4+T cell responses are essential for protective immunity against SARS-CoV-2.[14] However, an immunologic cutoff for the vaccines for protection against SARS-CoV-2 infection has not yet been clarified.[15]

SARS-CoV-2 infection activates the coagulation system together with immune responses associated with the severity of the disease.[16,17] Several studies have revealed similar or altered results for coagulation parameters during SARS-CoV-2 infection.[18] Therefore, we aimed to examine the IgG-RBD response and changes in fibrinogen and D-dimer concentrations in individuals who were previously infected with coronavirus or vaccinated following the first and second doses of inactivated CoronaVac vaccine. We also aimed to evaluate the relationship of the IgG response in terms of age, sex, comorbidities, and local or systemic adverse effects.

## Materials and Methods

### Subjects

This cross-sectional study was carried out between December 2020 and April 2021 by medical biochemists, laboratory technicians, phlebotomists, and administrative staff working in the central laboratory of Istanbul Medical Faculty who were vaccinated with CoronaVac vaccine in 2 doses, 5 μL per injection, 28 days apart, intramuscularly in the deltoid muscle. Blood samples were drawn from the subjects on days 21–25 after the first and second doses of vaccination (n = 91) and from individuals who had a previous coronavirus infection 14–21 days after the beginning of the symptoms, as a comparison group (n = 25). The diagnosis of COVID-19 infection was made using real-time reverse transcription polymerase chain reaction (RT-PCR) with nasopharyngeal and throat swabs using a SARS-CoV-2 Double Gene RT-qPCR kit (Bio-Speedy R&D Technologies).

For the evaluation of age and comorbidities related to the antibody response, all groups were classified according to their age groups: group 1, 20–40 years; group 2, 40–60 years; and group 3, ≥60 years. The comorbidities of the subjects were evaluated in 5 groups: hypertension and cardiovascular disease, diabetes mellitus, asthma/chronic obstructive pulmonary disease (COPD), hypo/hyperthyroidism, and other autoimmune diseases (eg, rheumatoid arthritis, Sjögren's disease). While immunocompetent individuals of both sexes were included in the study, the exclusion criteria included pregnancy, organ failures such as liver or kidney failure, and immune system deficiency. Written informed consent was obtained from each participant, and the clinical trial protocol was approved by the Ethical Committee of Istanbul University (#2021-26).

### Methods

Blood samples were drawn into 3.2% sodium citrate tubes for fibrinogen, D-dimer, and serum separator tubes (BD Vacutainer) for IgG-RBD measurements. Tubes were centrifuged at 2000*g* for 15 minutes. Supernatant serum samples were aliquoted and stored frozen at −80°C until measuring of IgG-RBD concentrations. But, fibrinogen and D-dimer were measured in the separated plasma samples on days 21–25, after first and second dose of vaccination, or 14–21 days after a past infection within 2 hours on the same day.

IgG antibodies against the RBD of the S protein (SARS-CoV-2 RBD IgG) were quantitatively assessed by chemiluminescence immunoassay using Maglumi SARS-CoV-2-S-RBD-IgG kit (LOT#:270210111) on a Maglumi 2000 analyzer (SNIBE, Shenzhen New Industries Biomedical Engineering). In this assay, IgG test results of ≥1.10 arbitrary units per milliliter (AU/mL) are considered reactive. The reproducibility was between 5.5% and 6.2%.

Fibrinogen and D-dimer measurements were performed in accordance with the manufacturer's recommendations using a Sysmex CN 6000 coagulation analyzer with original reagents from Siemens (Sysmex). D-dimer measurements were made using the immunoturbidimetric method with the INNOVANCE D-dimer assay (LOT#:561598), and fibrinogen was measured using the Clauss clotting method with the Dade Thrombin reagent (LOT#:565102). Precision results were between 2.3% and 5.2% for fibrinogen and 2.5% and 6% for D-dimer. All precision studies for IgG-RBD, fibrinogen, and D-dimer were performed in our laboratory according to Clinical and Laboratory Standards Institute (CLSI) document EP5-A2.[19] Within-run precision was performed by repeatedly (n = 20) analyzing the manufacturer's 2-level controls, while the between-day precision was analyzed using the 2-level controls on 20 consecutive days.

The participants were asked about any adverse events during their visit for blood sampling, and they also filled out a questionnaire 7 days after vaccination, which questioned whether they experienced adverse effects, including both systemic and local effects, along with all relevant factors related to the participants. Systemic adverse effects were headache, fatigue, fever, diarrhea, arthralgia, myalgia, and nausea; and local adverse effects were local pain, swelling, tenderness, redness, warmth, and swollen lymph glands on the same side.

### Statistical Evaluation

The data were analyzed using the SPSS 21 software package (SPSS). The results are expressed as median (Q1–Q3). The normality of the data distribution was evaluated using the Kolmogorov–Smirnov test. A $\chi^2$ or Fisher's exact test were used to assess the differences in the categorical variables between the groups. Kruskal–Wallis test and Mann–Whitney *U* test were performed to compare the unpaired samples. Correlation

analyses were performed using Spearman's test. Statistical significance was defined as $P < .05$.

## Results

The characteristics of the study population are presented in **TABLE 1**. The study consisted of a total of 116 participants, 63.8% female and 36.2% male. The average age was 44 (range, 21–83) years for women and 44 (range, 24–70) years for men. Twenty-five of 116 subjects had a previous infection (21.6%). The percentage of age groups was presented in **TABLE 2**. In terms of age, 39.7% of the participants were aged 20–40 years, 47.4% were aged 40–60 years, and 12.9% were aged ≥60 years.

The antibody concentrations of the vaccinated subjects were significantly higher after the second vaccination compared with that of the first vaccination (0.42 [0.18–3.11] vs 29.99 [9.43–95.50] AU/mL, [$P < .001$]). The fibrinogen concentrations were significantly lower (307 [264.3–356] vs 334 [279.6–375.4] mg/dL, [$P < .001$]); however, D-dimer levels were increased following the second vaccination compared with the first vaccination (250 [190–240] and 310 [200–430] μg/L, [$P = .083$]), respectively (**TABLE 1**).

Of the participants, 21.6% had a previous coronavirus infection. When the IgG concentrations of vaccinated individuals were compared with those of previously infected individuals, no statistically significant difference was obtained ($P = .063$). Also, the differences in fibrinogen and D-dimer concentrations were statistically nonsignificant between both groups.

When we evaluated IgG-RBD concentrations across the age groups (**TABLE 2**), the first and second IgG concentrations were the highest in the 20–40 year age group and were the lowest in the ≥60 year age group. The second IgG concentrations were higher in the 20–40 year age group compared with those of 40–60 year and ≥60 year age groups. The second IgG concentration of the 40–60 year age group was also higher than that of the ≥60 year age group, but the differences were statistically not significant. Within the age groups, antibody concentrations on the 25th day following the second dose were also higher compared with the first antibody concentration ($P = .001$ for the 20–40 year age group; $P < .001$ for 40–60 year age group; and $P = .028$ for the ≥60 year age group). Across the age groups, the fibrinogen levels also showed statistically significant alterations for all age groups (40–60 years $P = .009$ and $P = .011$ for ≥60 years).

The local and general adverse effects are presented in **FIGURE 1**. Fifteen percent of the subjects had systemic adverse effects, and 15% had local adverse effects after the second dose. After the first vaccination, no statistically significant differences were obtained in the IgG, D-dimer, and fibrinogen concentrations. However, after the second vaccination, statistically significant changes were obtained only in D-dimer levels in subjects with local and general adverse effects compared with the subjects with no adverse effects ($P = .017$, for both), but the IgG and fibrinogen concentrations were higher in subjects with no adverse effects.

We also evaluated the relationship of comorbidities in individuals with IgG-RBD levels. Of the entire group, 12.1% had hypertension/cardiovascular disease, 4.4% had diabetes mellitus, 5.5% had hypo/hyperthyroidism, and 3.3% had asthma/COPD. Only D-dimer concentrations were significantly higher in the subjects with any of the chronic diseases, (290 μg/L vs 375 μg/L; $P = .020$) compared with the healthy subjects. Also, in the subjects with hypertension/cardiovascular diseases, the median IgG concentrations were lower than those of healthy subjects

**TABLE 1. Anti S-RBD IgG Antibody, D-Dimer, and Fibrinogen Concentrations at 21–25 Days Following First and Second Dose of SARS-CoV-2 Vaccination (CoronaVac)**

| Status | Age, y (Median [Q1-Q3]) | Anti S-IgG-RBD (AU/mL) | | | Fibrinogen (mg/dL) | | | D-Dimer (μg/L) | | |
|---|---|---|---|---|---|---|---|---|---|---|
| | | After First Dose of Vaccination | After Second Dose of Vaccination | *P* | After First Dose of Vaccination | After Second Dose of Vaccination | *P* | After First Dose of Vaccination | After Second Dose of Vaccination | *P* |
| Vaccinated (n = 91) | 44 (34–56) | 0.42 (0.18–3.11) | 29.99 (9.43–95.50) | <.001[a] | 334.4 (279.6–375.4) | 307 (264.3–356) | <.001[a] | 250 (190–420) | 310 (200–430) | .083 |
| COVID-19 inf (n = 25) | 40 (36–46) | - | 13.26 (6.857–50.38) | | - | 260 (238.9–278) | | - | 190 (190–270) | |
| All groups (n = 116) | 44 (35–52) | 1.02 (0.24–7.67) | 31.46 (10.2–99.63) | | 327.9 (279.6–375.4) | 302.8 (264–353.3) | | 245 (190–405) | 310 (200–430) | |
| Women (n = 61) | 44 (34–51) | 0.54 (0.21–4.75) | 37.35 (10.28–111.3) | <.001[a] | 335.1 (298.6–390) | 312.4 (279–364.6) | .003[a]<br>.029[b] | 270 (190–440) | 330 (250–440) | .169<br>.016[b] |
| Men (n = 30) | 44 (36–55) | 0.39 (0.17–1.01) | 21.8 (8.66–58.83) | <.001[a] | 312 (253.7–370.5) | 279.5 (249.1–334.2) | .015[a] | 195 (190–325) | 220 (190–355) | .408 |

[a]*In comparison with vaccination doses;* P < *.05.*
[b]*In comparison with men after second dose of vaccination;* P < *.05.*




2022;53;590–595 | https://doi.org/10.1093/labmed/lmac047

**TABLE 2. Anti S-RBD IgG Antibody, Fibrinogen, and D-Dimer Levels Across the Age Groups and Following SARS-CoV-2 First and Second Vaccinations**

| Age Groups (y) | Anti S-RBD IgG (AU/mL) | | | Fibrinogen (mg/dL) | | | D-Dimer (µg/L) | | |
|---|---|---|---|---|---|---|---|---|---|
| | After First Dose of Vaccination | After Second Dose of Vaccination | *P* | After First Dose of Vaccination | After Second Dose of Vaccination | *P* | After First Dose of Vaccination | After Second Dose of Vaccination | *P* |
| 20–40 (n = 33) | 0.39 (0.17–4.46) | 46.11 (16.05–186) | <.001[a] | 290.5 (260.0–381.2) | 302.8 (264.0–372.0) | .109 | 195 (190–340) | 280 (190–360) | .570 |
| 40–60 (n = 43) | 0.53 (0.20–5.16) | 32.02 (10.45–92.24) | <.001[a] | 335.2 (310.0–375.4) | 309.9 (278–353.3) | .011[a] | 275 (190–430) | 310 (200–400) | .290 |
| >60 (n = 15) | 0.33 (0.11–0.66) | 13.15 (7.21–25.85) | .005[a] | 364.7 (290.4–394.1) | 293.3 (251.8–353.3) | .022[a] | 310 (200–440) | 435 (270–690) | .046[a] |

[a]*In comparison with vaccination doses;* P < *.05.*

**FIGURE 1. The percentages of local and systemic adverse effects following the first and second administration of CoronaVac vaccine in 91 subjects.**

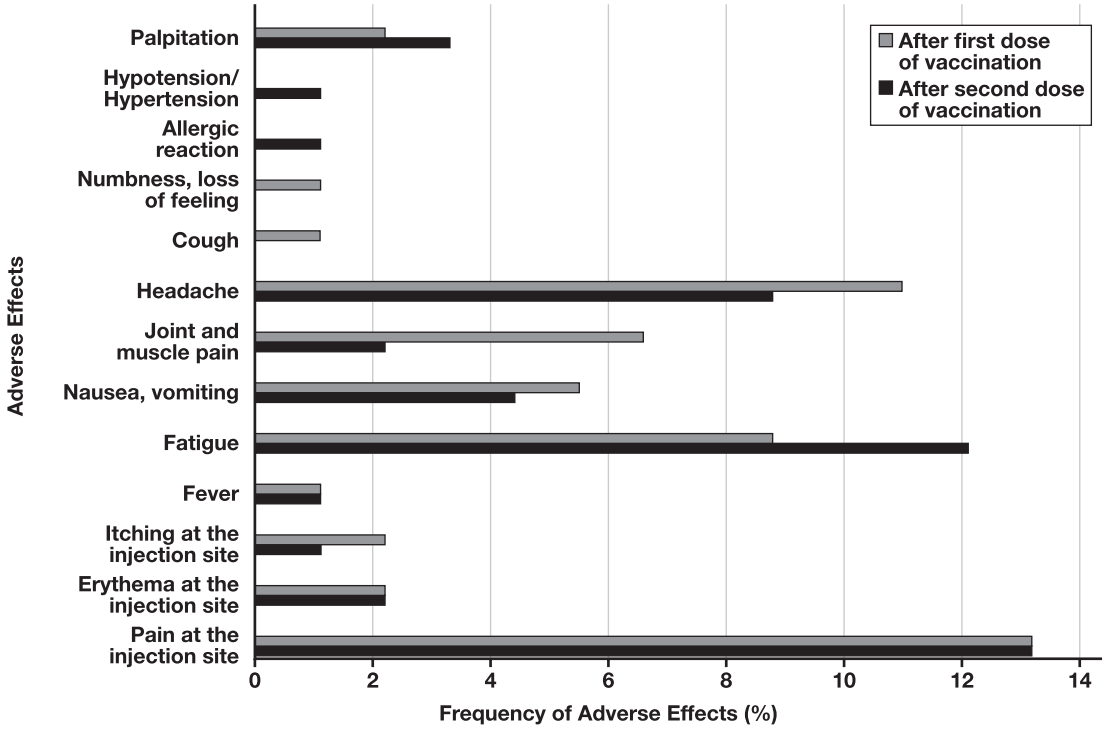


following the second dose of vaccine (34.9 AU/mL vs 12.1 AU/mL, *P* = .006); and a 58.1% increase was detected in D-dimer concentrations after the second dose. The percentage of participants with IgG concentrations higher than 1 AU/mL and 5 AU/mL after the first vaccination was almost the same as the normotensive patients. After the second vaccination, these percentages were significantly different compared with those with no hypertension (63.6% vs 90.4%; *P* = .034 and *P* = .031, respectively). In patients with diabetes mellitus, hypo/hyperthyroidism, or asthma, no statistically significant changes were obtained in IgG, fibrinogen, and D-dimer concentrations compared with healthy subjects.

Also, weak association was found between age and IgG (*P* = .021, *r* = −0.252), with D-dimer (*P* = .020, *r* = 0.255) following the second vaccination using Spearman's test.

## Discussion

In this study, we evaluated the IgG antibody concentrations against the RBD of SARS-CoV-2 S protein using chemiluminescence assays following the first and second dose of CoronaVac. IgG-RBD concentrations on the 25th day of the second vaccination were significantly higher than the first vaccination. IgG responses against SARS-CoV-2 after vaccination may vary significantly depending on age, sex, previous COVID-19 infection, and the health conditions of the individual.[20,21] The IgG concentrations of vaccinated individuals did not differ significantly when compared with previously infected individuals. However, there are studies revealing stronger T cell responses and higher antibody concentrations in subjects with known past SARS-CoV-2 infections compared with vaccinated subjects using SARS-CoV-2 IgG and IgG Quant II, contrary to our findings.[22] While IgG-RBD concentrations did not increase in 13% of the subjects in our study group after 2 doses of CoronaVac vaccine, this rate was 5% in the study of Muena et al.[23] In another randomized, placebo-controlled, phase 3 clinical trial study conducted in Turkey, it was reported that the percentage of seronegativity increased from 5% to 14% over the age of 50, and seropositive cases decreased with age.[24]

We also found the highest IgG-RBD concentrations in the 20–40 year age group and the lowest in the ≥60 year age group, in accordance with

other studies.[20,23,24] The IgG levels of the younger group were significantly higher compared with the 40–60 and ≥60 year age groups. Despite the pathogenesis, immunosenescence is multifactorial; the decreased ability to respond to antigens due to reduced plasmablasts and lower memory T cell function are the main reasons for the low antibody levels, decreased response to vaccines, and increased susceptibility to infectious diseases.[25] In another study performed with 2 doses of CoronaVac vaccine, the association between neutralizing antibody levels and antireceptor binding of IgG has been shown in subjects aged 18–59 years; however, there is insufficient evidence for immunosenescence in subjects aged ≥60 years.[26]

Several studies have demonstrated the role of T cells in the stimulation of the immune system and the association of CD4+CD25+T cells with the IgG concentration against SARS-CoV-2.[27,28] Supporting these results, Goel et al[29] showed stimulation of preexisting memory cells specific to the SARS-CoV-2 antigen after the first dose of vaccine, in subjects who recovered from the coronavirus infection, and an increase in antibody and memory cells in vaccinated subjects after 2 doses of vaccine. They also showed diminished memory cell responses with age, similar to our findings. Consequently, Muena et al[23] also indicated similar findings for neutralizing antibodies, showing that neutralizing antibody levels in naive subjects who received 2 doses of CoronaVac or 1 dose of BNT162b2 vaccine were similar to those of individuals with past coronavirus infection who were boosted with either CoronaVac or BNT162b2 vaccine.

In our study, we also investigated the fibrinogen and D-dimer concentrations following the first and second doses of the vaccine. In all groups, the fibrinogen concentrations decreased whereas D-dimer levels remained unchanged after the second vaccination in the 40–60 and ≥60 year age groups. Additionally, no statistically significant differences in fibrinogen and D-dimer concentrations were found across the age groups or between the subjects vaccinated and individuals with known past SARS-CoV-2 infections. Peyvandi et al[18] also detected no statistically significant changes in D-dimer concentration or other coagulation parameters other than mild thrombocytopenia after administration of the first and second doses of BioNTech.

When we evaluated the general and local adverse effects together with antibody responses, no differences in the IgG-RBD concentrations were obtained between the groups. Twelve subjects in the entire group had local reactions, including pain and swelling, whereas 15 subjects had systemic reactions after the second-dose vaccination. However, systemic reactions were observed in 20 of 91 subjects, and local adverse effects were seen in 12 of 91 subjects after the first dose. The most common adverse effects were pain at the injection site, making up 13% of local effects, and headache and vertigo, accounting for 10% of systemic effects. Systemic adverse effects were approximately 2 times more common than local effects for the 2 doses of vaccine. Zhang et al[26] reported that the most common adverse effect was local pain at injection site with a rate of 17% with CoronaVac, and the most severe adverse effect was observed as an acute hypersensitivity with urticaria with a rate of 4%. On the other hand, Tanriover et al[24] also reported that 0.1% of their study group had serious adverse effect including allergy and seizures. However, in our study no serious complications, including anaphylaxis or severe allergic reactions, were detected—except hypertensive attack, which was seen in 1 subject out of 91. Therefore, increased D-dimer concentrations were observed in subjects with systemic adverse effects compared with the noncomplicated subjects, while higher IgG and fibrinogen concentrations were obtained in noncomplicated subjects. In another study investigating the prevalence of side effects following CoronaVac, it was reported that the risk of experiencing side effects was higher in women than in men, in individuals younger than 30 years of age compared to older people, and that subjects with chronic diseases have a higher risk than those without chronic diseases.[30] Nevertheless, more severe complications, such as the development of immune thrombocytopenia, bleeding with no thrombosis, or thrombosis, were reported following the administration of mRNA vaccines.[31]

When we evaluated the variables affecting the IgG-RBD concentrations after the second dose of CoronaVac, age and hypertension in comorbidities were found associated with the IgG-RBD responses. Twelve percent of the entire study population had hypertension, and the IgG-RBD concentrations of the participants with hypertension were significantly lower compared with the normotensive subjects following the second vaccination. IgG concentration of 1.0 AU/mL and above was found in 63% of people with hypertension, while this rate was found to be 90.4% in normotensive individuals. However, no statistically significant associations were obtained among IgG responses with diabetes mellitus, asthma/COPD, or hypo/hyperthyroidism.

According to the recommendations of the Advisory Committee on Immunization Practices and WHO, the benefits of the COVID-19 vaccine are greater than the risk of progression to serious conditions or death when comparing healthy individuals with those with comorbidities.

In this study, we did not measure neutralizing antibody levels, which determines the ability to bind and inhibit the entrance of the host cells. Therefore, the limitations of the study are the lack of evaluation of neutralizing antibody levels and T cell responses following vaccines, the limited study group, and the lack of other validation studies such as carry-over and linearity but not precision.

## Conclusion

Based on our results, the CoronaVac vaccine was safe and showed good efficacy against SARS-CoV-2 infection. However, the protective efficacy and duration of efficacy remain controversial for CoronaVac. Accordingly, it is essential for individuals to take personal protective measures, such as using masks and distancing, despite undergoing vaccination.

## Acknowledgments

We thank Snibe Company for their technical support and reagent support.

## REFERENCES

1. Rothe C, Schunk M, Sothmann P, et al. Transmission of 2019-nCoV infection from an asymptomatic contact in Germany. *N Engl J Med.* 2020;382(10):970–971.
2. Badawi A, Ryoo SG. Prevalence of comorbidities in the Middle East respiratory syndrome coronavirus (MERS-CoV): a systematic review and meta-analysis. *Int J Infect Dis.* 2016;49:129–133.
3. Institute for Health Metrics and Evaluation. COVID-19 has caused 6.9 million deaths globally, more than double what official reports show. http://www.healthdata.org/news-release/covid-19-has-caused-69-million-deaths-globally-more-double-what-official-reports-show. Accessed May 6, 2021.
4. DeRoo SS, Pudalov NJ, Fu LY. Planning for a SARS-COVID-19 vaccination program. *JAMA.* 2020;323(24):2458–2459.

5. Du L, He Y, Zhou Y, et al. The spike protein of SARS-CoV-2: a target for vaccine and therapeutic development. *Nat Rev Microbiol.* 2009;7(3):226–236.
6. Barnes CO, West AP, Huey-Tubman KE, et al. Structures of human antibodies bound to SARS-CoV-2 spike reveal common epitopes and recurrent features of antibodies. *Cell.* 2020;182(4):828–842 e16.
7. Walls AC, Park YJ, Tortorici MA, et al. Structure, function, and antigenicity of the SARS-CoV-2 spike glycoprotein. *Cell.* 2020;181(2):281–292.e6.
8. Routhu NK, Cheedarla N, Bollimpelli VS, et al. SARS-CoV-2 RBD trimer protein adjuvanted with Alum-3M-052 protects from SARS-CoV-2 infection and immune pathology in the lung. *Nat Commun.* 2021;12(1):3587.
9. Enjuanes L, Zuniga S, Castano-Rodriguez C, et al. Molecular basis of coronavirus virulence and vaccine development. *Adv Virus Res.* 2016;96:245–286.
10. Roper RL, Rehm KE. SARS vaccines: where are we? *Expert Rev Vaccines.* 2009;8(7):887–898.
11. Walsh EE, Frenck RW, Falsey AR, et al. Safety and immunogenicity of two RNA-based Covid-19 vaccine candidates. *N Engl J Med.* 2020;383(25):2439–2450.
12. World Health Organization. Covid-19 vaccine tracker and landscape. https://www.who.int/publications/m/item/draft-landscape-of-covid-19-candidate-vaccines. Accessed August 17, 2021.
13. Dittadi R, Afshar H, Carraro P. Two SARS-CoV-2 IgG immunoassays comparison and time-course profile of antibodies response. *Diagn Microbiol Infect Dis.* 2021;98(4):115297.
14. Jeyanathan M, Afkhami S, Smaill F, et al. Immunological considerations for COVID-19 vaccine strategies. *Nat Rev Immunol.* 2020;20(10):615–632.
15. Vabret N, Britton GJ, Gruber C, et al; Sinai Immunology Review Project. Immunology of COVID-19: current state of the science. *Immunity.* 2020;52(6):910–941.
16. Cao X. COVID-19: immunopathology and its implications for therapy. *Nat Rev Immunol.* 2020;20(5):269–270.
17. Xiong M, Liang X, Wei Y-D. Changes in blood coagulation in patients with severe coronavirus disease 2019(COVID-19): a meta-analysis. *Br J Hematol.* 2020;189(6):1050–1052.
18. Peyvandi F, Artoni A, Novembrino C, et al. Hemostatic alterations in COVID-19. *Haematologica.* 2021;106(5):1472–1475.
19. Clinical and Laboratory Standard Institute (CLSI). *Evaluation of Precision Performance of Quantitative Measurement Methods: Approved Guideline-Second Edition. CLSI document EP5-A2.* Wayne, PA: Clinical and Laboratory Standards Institute; 2004.
20. Müller L, Andrée M, Moskorz W, et al. Age-dependent immune response to the Biontech/Pfizer BNT162b2 COVID-19 vaccination. *Clin Infect Dis.* 2021;73(11):2065–2072.
21. Ebinger JE, Fert-Bober J, Printsev I, et al. Antibody responses to the BNT162b2 mRNA vaccine in individuals previously infected with SARS-CoV-2. *Nat Med.* 2021;27(6):981–984.
22. Wei J, Stoesser N, Matthews PC, et al. Antibody responses to SARS-CoV-2 vaccines in 45,965 adults from the general population of the United Kingdom. *Nat Microbiol.* 2021;6(9):1140–1149.
23. Muena NA, Garcia-Salum T, Pardo-Roa C, et al. Long-lasting neutralizing antibody responses in SARS-CoV-2 seropositive individuals are 2 robustly boosted by immunization with the CoronaVac and BNT162b2 vaccines. *medRxiv.* 2021;18. https://www.medrxiv.org/content/10.1101/2021.05.17.21257197v1
24. Tanriover MD, Doğanay HL, Akova M, et al. Efficacy and safety of an inactivated whole-virion SARS-CoV-2 vaccine (CoronaVac): interim results of a double-blind, randomised, placebo-controlled, phase 3 trial in Turkey. *Lancet.* 2021;398(10296):213–222.
25. Crooke SN, Ovsyannikova IG, Poland GA, et al. Immunosenescence and human vaccine immune responses. *Immun Ageing.* 2019;16:25.
26. Zhang Y, Zeng G, Pan H, et al. Safety, tolerability, and immunogenicity of an inactivated SARS-CoV-2 vaccine in healthy adults aged 18–59 years: a randomised, double-blind, placebo-controlled, phase 1/2 clinical trial. *Lancet Infect Dis.* 2021;21(2):181–192.
27. Yang Z, Kong W, Huang Y, et al. A DNA vaccine induces SARS coronavirus neutralization and protective immunity in mice. *Nature* 2004;428:561–564.
28. Sahin U, Muik A, Derhovanessian E, et al. COVID-19 vaccine BNT162b1 elicits human antibody and TH 1 T cell responses. *Nature* 2020;586:594–599.
29. Goel RR, Apostolidis SA, Painter MM, et al. Distinct antibody and memory B cell responses in SARS-CoV-2 naïve and recovered individuals following mRNA vaccination. *Sci Immunol.* 2021;6(58):eabi6950.
30. Riad A, Sağıroğlu D, Üstün B, et al. Prevalence and risk factors of CoronaVac side effects: an independent cross-sectional study among healthcare workers in Turkey. *J Clin Med.* 2021;10(12):2629.
31. Lee EJ, Cines DB, Gernsheimer T, et al. Thrombocytopenia following Pfizer and Moderna SARS-CoV-2 vaccination. *Am J Hematol.* 2021;96(5):534–537.

# Pathogenic Homozygous Mutations in the *DBT* Gene (c.1174A>C) Result in Maple Syrup Urine Disease in a rs12021720 Carrier

*Morteza Alijanpour, MD,*[1,a] *Omid Jazayeri, PhD,*[2,*,a] *Shima Soleimani Amiri, MD,*[3] *and Erwin Brosens, PhD*[4]

[1]Non-Communicable Pediatric Disease Research Center, Health Research Institute, Babol University of Medical Science, Babol, Iran, [2]Department of Molecular and Cell Biology, Faculty of Science, University of Mazandaran, Babolsar, Iran, [3]Razi Pathobiology and Genetic Diagnostic Laboratory, Babol, Iran, [4]Department of Clinical Genetics, Erasmus MC – Sophia Children's Hospital, Rotterdam, Netherlands *To whom correspondence should be addressed. o.jazayeri@umz.ac.ir. [a]Morteza Alijanpour and Omid Jazayeri are shared first authors.

**Keywords:** *DBT* gene, MSUD, mutation, rs12021720, *BCKDHA* gene, *BCKDHB* gene

**Abbreviations:** MSUD, maple syrup urine disease; BCKD, branched-chain α-ketoacid dehydrogenase; BCKA, branched-chain α-ketoacid; BCAA, branched-chained amino acid; BCKDC, branched-chain α-ketoacid dehydrogenase complex; DLD, dihydrolipoamide dehydrogenase; PCR, polymerase chain reaction; LD, linkage disequilibrium; HPLC, high-performance liquid chromatography; GCMS, gas chromatography mass spectrometry.

*Laboratory Medicine* 2022;53:596–601; https://doi.org/10.1093/labmed/lmac034

## ABSTRACT

**Objective:** Maple syrup urine disease (MSUD; OMIM #248600) is an autosomal recessive metabolic disorder in the catabolism of branched-chain amino acids (leucine, isoleucine, and valine) and may be lethal if untreated in affected newborns.

**Methods:** Single-nucleotide polymorphism haplotyping and Sanger sequencing of *BCKDHA*, *BCKDHB*, and *DBT* genes were performed in a cohort of 10 MSUD patients.

**Results:** We identified a 16.6 Mb homozygous region harboring the *DBT* gene in an Iranian girl presenting with MSUD. Sanger sequencing revealed a pathogenic homozygous variant (NM_001918.3: c.1174A > C) in the *DBT* gene. We further found a controversial variant (rs12021720: c.1150 A > G) in the *DBT* gene. This substitution (p.Ser384Gly) is highly debated in literature. Bioinformatics and cosegregation analysis, along with identifying the real pathogenic variants (c.1174 A > C), lead to terminate these various interpretations of c.1150 A > G variant.

**Conclusion:** Our study introduced c.1150 A > G as a polymorphic variant, which is informative for variant databases and also helpful in molecular diagnosis.

Maple syrup urine disease (MSUD; OMIM #248,600) is an autosomal recessive inherited metabolic disorder caused by deficiency of the branched-chain α-ketoacid dehydrogenase complex (BCKDC). BCKDC is a mitochondrial complex that is encoded by 4 nuclear genes (*BCKDHA*, *BCKDHB*, *DBT*, and *DLD*), and MSUD can be caused by mutation within any of these 4 genes.[1] Based on the Human Gene Mutation Database (HGMD professional 2021.2; http://www.hgmd.cf.ac.uk), 129 pathogenic variants in *BCKDHA*, 160 pathogenic variants in *BCKDHB*, 95 pathogenic variants in *DBT*, and 30 pathogenic variants in *DLD* have been currently reported. The molecular pathomechanism of this disease is the failure of metabolizing branched-chain α-ketoacids (BCKA) derived from the essential branched-chained amino acids (BCAA; leucine, isoleucine, and valine). Increases in BCAA and BCKA levels result in serious clinical outcomes, including ketoacidosis, neurological damage, and intellectual disability in affected newborns.

Clinical manifestations of MSUD are classified into 5 MSUD types: classic, intermediate, intermittent, thiamine-responsive, and E3-deficient forms.[1,2] The classic form, which comprises from 75% to 80% of MSUD patients, is presented within 2 weeks after birth by seizures, coma, poor feeding, lethargy, and death if they do not receive medical care. Intermediate MSUD is associated with increased BCAAs and BCKAs, progressive intellectual disability, and developmental delay without a history of catastrophic illness. These individuals can experience severe metabolic intoxication and encephalopathy in the face of sufficient catabolic stress.[1] The intermittent form of MSUD shows normal levels of BCAAs, whereas it presents clinical phenotypes during episodes of stress, including concurrent illness, fasting, or surgery. Thiamine-responsive MSUD is similar to the intermediate or intermittent phenotype; however, treatment with thiamine leads to the normal levels of BCAAs. The E3-deficient form is caused by impairment in the dihydrolipoyl dehydrogenase (E3) component of the BCKD complex that is common to the pyruvate and α-ketoglutarate dehydrogenase complexes. Mutation in the third component (E3) causes an overlapping, but more severe, phenotype known as dihydrolipoamide dehydrogenase

(DLD) deficiency (OMIM #246,900). DLD deficiency is sometimes referred to as MSUD3. Patients with E3 defects manifest dysfunction of all 3 enzyme complexes and die often in infancy with serious lactic acidosis.[2–4]

In this study, we investigated a 15-day-old girl with clinical MSUD from Babol city (in the north of Iran) to find causative variants. MSUD incidence is higher (≈1:5700) than the worldwide (1:185,000) live births in this population.[5] We identified the pathogenic changes in this patient. Additionally, we were faced with a controversial homozygous variant in the *DBT* gene with different ideas about its pathogenicity in literature.[6–12] Having the real pathogenic culprits in our patient, we could terminate these various interpretations and introduced it as a polymorphic variant that would be beneficent in molecular diagnostics.

## Materials and Methods

A cohort of 10 MSUD patients from unrelated families who had been referred to our center were chosen for this study. Inclusion criteria included clinical presentations of the disease, tandem mass spectrometry (mass-mass) results, and biochemical data. The Ethics Committee of Babol University of Medical Sciences approved the study protocol (IR.MUBABOL.REC.1397.038). Among this cohort, the clinical and biochemical data in the patient (R-96-33) in whom the pathogenic variant was recognized were described in the results section.

### Molecular Analysis of the *BCKDHA*, *BCKDHB,* and *DBT* Genes

For molecular evaluations, peripheral blood samples were collected after obtaining an informed consent from the patient's parents. The coding regions and the exon/intron boundaries of the 3 aforementioned genes were amplified and sequenced by the Sanger sequencing method using standard protocols. All primer sequences and amplification conditions are available on request from the corresponding author. Polymerase chain reaction (PCR) products were sequenced using BigDye Terminator kit (Thermo Fisher Scientific) according to the manufacturer's protocol, and the samples were run on an ABI3500 Genetic Analyzer.

### Genotyping

Using 200 ng dsDNA input, we genotyped the samples with the Infinium Global Screening Array v1.0 (Illumina), according to the manufacturer's standard protocol. Genotype output was generated with Illumina Genomestudio v2.0. Using Nexus Biodiscovery CN8.0 (Biodiscovery), we determined if deleterious copy number variations were present and visualized the runs of homozygosity (**TABLE 1**; see Supplemental Table 1). Genotyping was carried out for all samples except sample R-98-23, as we received that sample after genotyping the others.

### Mutation Analysis

The sequence data were compared with the reference genomic (GRCh38/hg38) and cDNA sequences of MSUD genes (with the accession number; *BCKDHB* gene (NM_000056.5), *BCKDHA* (NM_000709.4), *DBT* (NM_001918.5). Furthermore, familial segregation was investigated to determine whether the found homozygous or compound heterozygous variants were consistent with the expected mode of inheritance.

### In Silico Analysis of *DBT* c.1150 A > G Substitution

To interpret the causality of substitution c.1150 A > G, we utilized the Iranian national genetic database (Iranome) to check allele frequency in the Iranian population. Iranome was launched by performing whole-exome sequencing on 800 individuals. The groups included 100 healthy individuals from each of 8 major ethnic groups in Iran (https://www.iranome.ir).[13] Additionally, the Genome Aggregation Database (gnomAD; https://gnomad.broadinstitute.org) was investigated to study allele frequency in the other populations. This database has aggregated 15,708 whole genomes and 125,748 exomes and provides a reference map for diagnostic screening. We also used Combined Annotation Dependent Depletion (CADD; https://cadd.gs.washington.edu) to score the deleteriousness impact of found variants. CADD is a tool for scoring the deleteriousness of single nucleotide variants as well as insertion/deletion variants in the human genome. That is a framework that integrates multiple annotations into 1 metric, by contrasting variants that survived natural selection with simulated mutations, and prioritizes causal variants in genetic analyses.[14] Linkage disequilibrium (LD), a measure of the nonrandom association of alleles at 2 or more loci that descend from a single and ancestral chromosome, was estimated by the LD calculator tool through Ensembl (https://grch37.ensembl.org/Homo_sapiens/Tools/LD). All impeded subpopulations in the aforementioned tool were selected.

## Results

### Case Presentation (R-96-33)

The proband was a 15-day-old girl (at the time of the study) and the result of a consanguineous marriage. She was hospitalized due to poor feeding and vomiting. From the fifth day of birth, she showed a reduced tendency to breastfeeding and gradually vomiting after feeding also appeared. The patient was the second child of this family. She was born by cesarean section with a birth weight of 3200 grams and good condition, but she had lost 500 grams of weight since birth. The patient's parents had a distant family relationship. The first child of the family was healthy and there was no positive family history of a specific disease.

The patient was lethargic and hypotonic, with decrease of neonatal reflexes and poor feeding with vomiting at the time of admission. The vital signs were as follows: pulse rate = 125/min, respiratory rate = 38/min, temperature = 36.5°C. She had a normal examination of her heart, lungs, abdomen, and genitalia. The patient showed hypoglycemia at the time of hospitalization (blood glucose level with the glucometer was 31 mg/dL); therefore, serum dextrose water 10% began immediately. Due to hypotonia and poor feeding, she was initially examined for sepsis; so, after taking samples and cultures, antibiotic therapy was started with ampicillin and amikacin. The initial tests results were as follows: WBC = 5800, Hb = 11.9, PLT = 557.000, CRP = 0.1, ESR = 1, Na = 131 mEq/L, K = 5 mEq/L, BUN = 10.4 mg/dL, Cr = 0.59 mg/dL, $T_4$ = 10.9 μg/dL, TSH = 2.3 U/L, SGOT = 37 IU/L, SGPT = 31 IU/L, ALP = 574 IU/L, U/A & U/C = normal. Arterial blood gases were: pH = 7.27, $pCO_2$ = 34.5, $HCO_3$ = 14.1, ammonia = 88.5 μg/dL. Lumbar puncture was normal.

According to normal levels of liver enzymes and electrolytes (except blood glucose), normal assessment of sepsis, and due to a history of hypoglycemia–metabolic acidosis and persistence of lethargy, the patient underwent a metabolic assay. High-performance liquid chromatography (HPLC) results showed a reduction of

**TABLE 1.** Summarized Clinical Characteristic of Patients and Their Runs of Homozygosity[a]

| Patient | Age of Onset (d) | Clinical Presentation | Blood Amino Acid Levels (μmol/L) | f | F | ROH Mb | *BCKDHA* | *BCKDHB* | *DBT* |
|---|---|---|---|---|---|---|---|---|---|
| R-96-27 | 7 | Poor feeding, decreased urination | Leucine = 1615.7<br>Valine = 297.1<br>Isoleucine = 234.6<br>Alloisoleucine = —<br>Alanine = 90.5 | 3/16 | 3/32 | 261 | NP | NP | chr1:86,311,209–104,366,435 |
| R-97-6 | 7 | Poor feeding, seizure | Leucine = 2443.4<br>Valine = 389.7<br>Isoleucine = 329<br>Alloisoleucine = —<br>Alanine = 69.4 | 5/16 | 5/32 | 436 | NP | NP | chr1:98,157,356–108,023,098 |
| R-96-39 | 10 | Poor feeding, fever, lethargy | Leucine = 3440.7<br>Valine = 413.8<br>Isoleucine = 278.7<br>Alloisoleucine = —<br>Alanine = 104.2 | 5/16 | 5/32 | 465 | NP | NP | chr1:97,659,759–102,193,054 |
| R-97-15 | 7 | Poor feeding, lethargy | Leucine = 1550<br>Valine = 428.84<br>Isoleucine = 280<br>Alloisoleucine = —<br>Alanine = 72 | 3/16 | 3/32 | 256 | NP | NP | chr1:94,528,721–107,692,211 |
| R-97-29 | 10 | Poor feeding, lethargy, decreased urination, and defecation | Leucine = 2519<br>Valine = 672<br>Isoleucine = 375<br>Alloisoleucine = —<br>Alanine = 112 | 1/8 | 1/16 | 174 | NP | chr6:79,818,663–80,984,230 | chr1:98,723,985–111,745,582 |
| R-96-33 | 15 | Vomiting, poor feeding | Leucine = 2392<br>Valine = 240.3<br>Isoleucine = 32.87<br>Alloisoleucine = —<br>Alanine = 47 | 5/32 | 5/64 | 245 | NP | NP | chr1:94,510,250–111,120,518 |
| R-97-25 | 6 | Poor feeding, grunting | Leucine = 2836.66<br>Valine = 494.21<br>Isoleucine = 338.66<br>Alloisoleucine = 349<br>Alanine = 54.97 | 1/8 | 1/16 | 199 | NP | chr6:74,505,909–85,897,978 | NP |
| R-97-12 | 60 | Staring, seizure | Leucine = 1118<br>Valine = 549<br>Isoleucine = —<br>Alloisoleucine = —<br>Alanine = — | 3/32 | 3/64 | 138 | NP | NP | NP |
| R-96-28 | 7 | Poor feeding | Leucine = 2823<br>Valine = 782.9<br>Isoleucine = 447<br>Alloisoleucine = —<br>Alanine = 48.8 | 3/32 | 3/64 | 155 | NP | chr6:80,740,681–81,953,637 | chr1:94,539,913–101,941,097 |
| R-98-23 | 5 | Poor feeding, lethargy | Leucine = 2141.61<br>Valine = 464.97<br>Isoleucine = 43.86<br>Alloisoleucine = 65.29<br>Alanine = 42.26 | NA | NA | NA | NA | NA | NA |

*f, coefficient of consanguinity; F, coefficient of inbreeding; NA, not available; NP, not present.*
*[a]Depicted are the runs of homozygosity (ROH) > 1 Mb in size over the 3 disease genes. ROH Mb, amount of ROH in regions > 1 Mb. We profiled 9 patients with maple syrup urine disease (MSUD) of which 7 had a large ROH over the DBT gene and 3 for the BCKDHB gene. None of the patients were homozygous (>1 Mb) for BCKDHA gene. All patients represent a variable degree of consanguinity.*

alanine (47 μmol/L) and an increase in leucine (2392 μmol/L) and valine (240.3 μmol/L) (**FIGURE 1**). In urine gas chromatography mass spectrometry (GCMS), high excretion of α-ketoacids was observed: 2-ketoisovaleric acid (97.13% > 0.50%), 2-keto-3-methylvaleric acid (296.65% > 0.50%), and 2-ketoisocaproic acid (400.69% > 0.73%). These findings were collectively diagnostic for MSUD. Therefore, treatment with carnitine 10% (100 mg/kg/d) and vitamin B1 (100 mg/d) were started. Gradually, her condition improved after a few days. Then after consulting a nutritionist, feeding with breast milk and MSUD formula was started, and gradually their volume increased. Finally, the patient was discharged on the 16th day of hospitalization (at the age of 31 days) in good general condition.

## Genotyping

We identified 245 Mb copy-neutral regions of homozygosity, including 16.6 Mb run of homozygosity on chromosome 1 located between

**FIGURE 1. Blood amino acid profile of case R-96-33 by high-performance liquid chromatography. The arrows indicate the amino acids that change significantly in patients with maple syrup urine disease.**

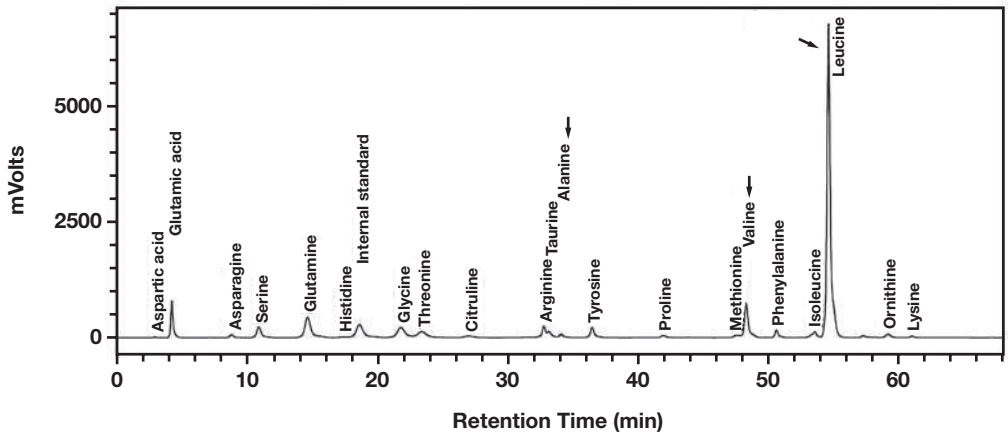


94,510,253–94,510,248 and 111,119,214–111,121,822 (GRCh19/hg37) (**TABLE 1**), and harboring the *DBT* gene (**FIGURE 2B**). Sanger sequencing revealed homozygous variants in *DBT* (NM_001918.5: c.1174 A > G). Cosegregation analysis confirmed that the homozygous variants in the patient were inherited from her heterozygous carrier parents. The mutation was undetected in her healthy brother (**FIGURE 2C**). The variant is located in exon 9 and creates a missense change (p.Thr392Pro) (**TABLE 2**). This substitution has previously been reported in another Iranian MSUD patient from a central area of Iran.[15] We also found an extra homozygous variant in this patient (DBT: c.1150 A > G; p. Ser384Gly) with different interpretations about its effect in MSUD patients. As it was shown in **TABLE 2**, this substitution with CADD score 14.3 has previously been reported 8 times in the literature (3 times pathogenic and 5 times polymorphic). Two authors with uncertain explanations[10,12] mentioned their ambiguity about the pathogenicity of c.1150 A > G substitution. We identified a homozygous variant of *DBT*: c.1150 A > G in our patient's unaffected mother. Additionally, cosegregation analysis of c.1150 A > G substitution in our cohort revealed that this substitution is homozygous in all patients along with at least 1 of their healthy parents. In 6 families, both parents were homozygous for c.1150 A > G substitution (see Supplemental Table 2). Therefore, our finding is concordant with the current understanding that the c.1150 variant is benign.

## Discussion

We identified the pathogenic variant (*DBT*: c.1174 A > C) in a patient from the north of Iran. The mutated residue (p.Thr392Pro) is located in the 2-oxoacid dehydrogenase acyltransferase catalytic domain and in contact with the E2 domain. Abiri and her colleagues[15] found this pathogenic mutation (c.1174 A > C) in another Iranian patient from a central region of Iran with the age of diagnosis of 15 days. Despite that, this mutation was detected twice in Iran in 2 separate geographical regions; nevertheless, there is no evidence for c.1174 A > C mutation in the other countries.

Additionally, we were faced with a variant of uncertain significance (rs12021720; c.1150 A > G; p.Ser384Gly), with a borderline CADD score of 14.3, and different ideas about its pathogenicity in the literature (**TABLE 3**).[6-12,16] Finally, cosegregation analysis, along with identifying the real pathogenic mutation in our patient (c.1174 A > C), resulted in terminating the various interpretations of c.1150 A > G mutation and certain decisions about this polymorphic variant. Indeed, the patient's mother had a homozygous variant of c.1150 A > G mutation; therefore, we considered it as a polymorphic variant. The allele frequency of rs12021720 (G > 0.9) in populations further supports this idea. Furthermore, the UniProtKB annotation database (ID: P11182) introduces p.Ser384Gly as a natural variant. To identify possible associations between rs12021720 and c.1174 A > C (chr1:100672036 in hg19), we performed LD analysis using Ensembl LD calculator tool. The result revealed that these 2 alleles are independent and therefore not coinherited in the 1000 genome subpopulations. Altogether, the variant c.1150 A > G is classified as benign according to American College of Medical Genetics and Genomics (ACMG) standards and guidelines.[17] Excluding this polymorphic variant is informative for the regional mutation database and also helpful in molecular diagnosis.

Although we identified a pathogenic variant in our case report, the other patients in our cohort remained unsolved. Finding a common homozygous region covering the *DBT* gene and confirming consanguinity (**TABLE 1**) highlight it as the most possible candidate gene in unsolved patients. Indeed, it is possible that the pathogenic variant(s) are located in noncoding regions of the *DBT* gene. Therefore, sequencing of these noncoding regions would be an essential next step.

In conclusion, we identified a pathogenic mutation in *DBT* gene in an MSUD patient, explained her phenotypic features in detail, and terminated the arguments about the pathogenicity of *DBT*: c.1150 A > G mutation and introduced it as a polymorphic variant, which is beneficial for mutation interpretation and genetic diagnosis. This finding will facilitate prenatal diagnosis of affected families and also effective carrier detection in the future.

## Supplementary Data

Supplemental figures and tables can be found in the online version of this article at www.labmedicine.com.

**FIGURE 2.** **A, The pedigree of the proband (arrow) with maple syrup urine disease, demonstrating his consanguineous parents. B, Sanger sequencing revealed a homozygous mutation in *DBT* (NM_001918.5: c.1174 A > G). Both parents were found to be heterozygous carriers in this mutation, and her healthy brother has the wild-type genotype. The mutation is located in exon 9 and creates a missense mutation at codon Thr392 leading to p.Thr392Pro. C, Single-nucleotide polymorphism array data showing a 16.6 Mb run of homozygosity on chromosome 1 located between 94,510,253–94,510,248 and 111,119,214–111,121,822 (GRCh19/hg37).**

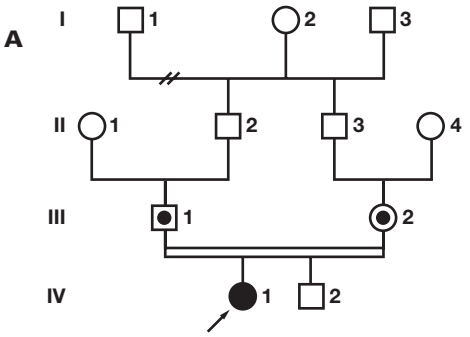


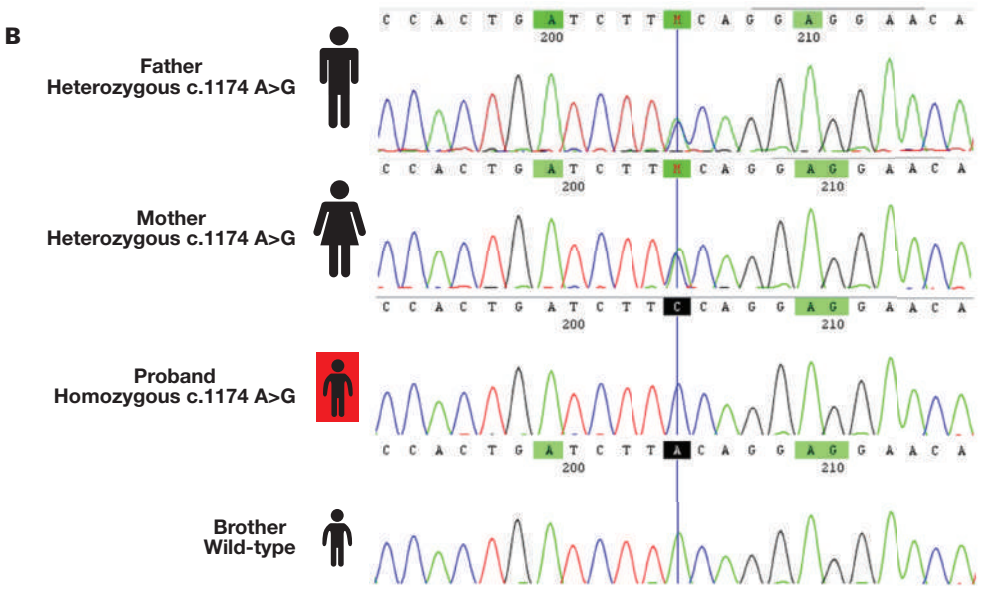


**TABLE 2. In Silico Analysis of Pathogenic and c.1150 A>G Mutations in This Study**

| Gene | Mutation | Protein | SIFT Version 5.2.2 | Mutation Taster | PolyPhen-2 | CADD Score V1.6 | Allele Frequency in Iranome | Allele Frequency in gnomAD |
|---|---|---|---|---|---|---|---|---|
| *DBT* | c.1174 A > C | p.Thr392Pro | Deleterious | Disease causing | Damaging | 23.3 | 0 | 0 |
| *DBT* | c.1150 A > G rs12021720 | p. Ser384Gly | Tolerated | Polymorphism | Benign | 14.3 | 0.916 | 0.912 |

*CADD, Combined Annotation Dependent Depletion; SIFT, Sorting Intolerant From Tolerant.*

**TABLE 3. *DBT*: c.1150 A > G (rs12021720) Various Interpretations in the Literature[a]**

| Publication | Ethnicity | Interpretation |
|---|---|---|
| Sedaghat et al[12] | Iranian | Might be neutral variation |
| Jaradat et al[10] | Jordanian | Polymorphism rather than a mutation |
| Margutti et al[11] | Brazilian | Nondamaging |
| Zeynalzadeh et al[16] | Iranian | Pathogenic |
| Couce et al[6] | Spanish | Pathogenic |
| Gorzelany et al[8] | Turkish | Polymorphism |
| Flaschker et al[7] | German/Turkish | Polymorphism |
| Henneke et al[9] | Spanish/German | Pathogenic |

[a]*The variant was homozygous in all listed publications.*


## Acknowledgments

The authors appreciate the staff of Babol Razi Pathobiology and Genetic Center and also the families of MSUD patients for their cooperation. The authors also would like to acknowledge Professor Robert M.W. Hofstra, who died during this scientific collaboration.

## Funding

This work was a joint project and supported by the Babol University of Medical Science, University of Mazandaran, and Babol Razi Pathobiology and Genetic Center Diagnostic Laboratory.


## REFERENCES


1. Gorjizadeh N, Jazayeri O, Najavand S, Alijanpour M. The genes responsible for maple syrup urine disease, molecular pathomechanisms, and causative mutations in Iranian population. *J Babol Univ Med Sci.* 2018;20:39–48.
2. Chuang JL, Cox RP, Chuang DT. E2 transacylase-deficient (type II) maple syrup urine disease. Aberrant splicing of E2 mRNA caused by internal intronic deletions and association with thiamine-responsive phenotype. *J Clin Invest.* 1997;100:736–744. doi:10.1172/JCI119586.
3. Sun W-H, Wu B-B, Wang Y-Q, et al. Identification of eight novel mutations in 11 Chinese patients with maple syrup urine disease. *World J Pediatr.* 2020;16:401–410.
4. Quental S, Macedo-Ribeiro S, Matos R, et al. Molecular and structural analyses of maple syrup urine disease and identification of a founder mutation in a Portuguese Gypsy community. *Mol Genet Metab.* 2008;94:148–156.
5. Gorgizadeh N, Alijanpour M, Jazayeri O. Incidence of maple syrup urine disease in infants 2007–2017, Babol, Mazandaran. Do we have founder effect? Paper presented at: 3rd International and 15th Iranian Genetics Congress; May 2018; Tehran, Iran. https://en.civilica.com/doc/983917/.
6. Couce M, Ramos F, Bueno M, et al. Evolution of maple syrup urine disease in patients diagnosed by newborn screening versus late diagnosis. *Eur J Paediatr Neurol.* 2015;19:652–659. doi:10.1016/j.ejpn.2015.07.009.
7. Flaschker N, Feyen O, Fend S, Simon E, Schadewaldt P, Wendel U. Description of the mutations in 15 subjects with variant forms of maple syrup urine disease. *J Inherit Metab Dis.* 2007;30:903–909.
8. Gorzelany K, Dursun A, Coskun T, et al. Molecular genetics of maple syrup urine disease in the Turkish population. *Turk J Pediatr.* 2009;51:97.
9. Henneke M, Flaschker N, Helbling C, et al. Identification of twelve novel mutations in patients with classic and variant forms of maple syrup urine disease. *Hum Mutat.* 2003;22:417. doi:10.1002/humu.9187.
10. Jaradat SA, Al-Qa'qa K, Amayreh W, et al. Molecular analysis of maple syrup urine disease in Jordanian families. *Meta Gene* 2016;10:81–85.
11. Margutti AVB, Silva WA, Garcia DF, et al. Maple syrup urine disease in Brazilian patients: variants and clinical phenotype heterogeneity. *Orphanet J Rare Dis.* 2020;15:1–11.
12. Sedaghat A, Zamani M, Jahanshahi A, et al. Frequent novel mutations are causative for maple syrup urine disease from Southwest Iran. *Meta Gene.* 2018;16:96–104. doi:10.1016/j.mgene.2018.01.010.
13. Behnam B, Zakeri M. Genetics and genomic medicine in Iran. *Mol Genet Genomic Med.* 2019;7:e00606. doi:10.1002/mgg3.606.
14. Rentzsch P, Witten D, Cooper GM, Shendure J, Kircher M. CADD: predicting the deleteriousness of variants throughout the human genome. *Nucleic Acids Res.* 2019;47:D886–D894. doi:10.1093/nar/gky1016.
15. Abiri M, Saei H, Eghbali M, et al. Maple syrup urine disease mutation spectrum in a cohort of 40 consanguineous patients and insilico analysis of novel mutations. *Metab Brain Dis.* 2019;34:1145–1156. doi:10.1007/s11011-019-00435-y.
16. Zeynalzadeh M, Tafazoli A, Aarabi A, et al. Four novel mutations of the BCKDHA, BCKDHB and DBT genes in Iranian patients with maple syrup urine disease. *J Pediatr Endocrinol Metab.* 2018;31:205–212. doi:10.1515/jpem-2017-0305.
17. Richards S, Aziz N, Bale S, et al. Standards and guidelines for the interpretation of sequence variants: a joint consensus recommendation of the American College of Medical Genetics and Genomics and the Association for Molecular Pathology. *Genet Med.* 2015;17:405.

# Influenza Vaccine Booster Stimulates Antibody Response in Beta Thalassemia Major Patients

*Maryam Sheikh, MS,[1,a] Abbas Ahmadi-Vasmehjani, PhD,[2,a] Mohammad Reza Atashzar, PhD,[3] Mohammad Hadi Karbalaie Niya, PhD,[4] Arefeh Ebrahimian, MS,[5] and Rasoul Baharlou, PhD[1,6,*]*

[1]Cancer Research Center, Semnan University of Medical Sciences, Semnan, Iran, [2]Department of Immunology and Microbiology, School of Medicine, Jahrom University of Medical Sciences, Jahrom, Iran, [3]Department of Immunology, School of Medicine, Fasa University of Medical Sciences, Fasa, Iran, [4]Gastrointestinal and Liver Disease Research Center, Iran University of Medical Sciences, Tehran, Iran, [5]Department of Microbiology, School of Medicine, Golestan University of Medical Sciences, Gorgan, Iran, [6]Department of Immunology, School of Medicine, Semnan University of Medical Sciences, Semnan, Iran. *To whom correspondence should be addressed: baharlour@gmail.com. [a]These two authors contributed equally to this work as co-first authors.

**Keywords:** influenza vaccine, trivalent, beta thalassemia major, immunogenicity, hemagglutination inhibition, seroconversion, seroprotection, geometric mean titers

**Abbreviations:** GMT, geometric mean titer; HI, hemagglutination inhibition; TIVs, trivalent influenza vaccines; QIV, quadrivalent influenza vaccine; AEs, adverse events; SAEs, serious AEs.

*Laboratory Medicine* 2022;53:602–608; https://doi.org/10.1093/labmed/lmac035

## ABSTRACT

The aim of this study was to evaluate antibody response against influenza vaccine in beta thalassemia major patients from Iran. Thirty beta thalassemia major patients were enrolled and divided into three groups: single dose (group 1), double dose (group 2), and control (group 3). Seroconversion, seroprotection, and geometric mean titer (GMT) assays were performed through hemagglutination inhibition (HI) on days 0, 14, and 60. Based on the results, the level of antibody titer was increased in group 2. Two weeks after vaccination, seroconversion rate was about 20% and 30% in groups 1 and 2. Sixty days after vaccination, the seroconversion rate was around 70% and GMT showed a more than 2-fold increase in group 2. Based on the results, the immunogenicity of double dose vaccination against influenza infection appears to be higher than the single dose vaccine in beta thalassemia major patients, and thus it is recommended to use two doses of vaccine, especially in splenectomized patients who are more sensitive than others.

Beta thalassemia syndromes are the most common hereditary disorders characterized when bone marrow does not make enough hemoglobin in red blood cells and, consequently, these cells fail to deliver sufficient oxygen to all parts of the body. The alpha- and beta-globin chains are the main proteins in red blood cells that form hemoglobin. A genetic deficiency in the synthesis of beta-globin chains leads to severe anemia, increased erythrocyte buildup, and excess iron absorption.[1,2]

The annual incidence of beta thalassemia is estimated to be 1 in 100,000 around the world.[3] Due to high consanguinity among the population, it is estimated that there are between two and three million beta thalassemia carriers and 25,000 patients in Iran.[4] In beta thalassemia, infections and immune abnormalities decrease the quality of life of the affected individuals. The main treatment of these patients involves blood transfusion, which can cause iron overload followed by reduced host defense and increased susceptibility to bacterial and viral infections. Therefore, it is desirable to remove the excess iron using iron chelation therapy.[5] Alidoost et al[6] have reported a wide range of immune abnormalities that are seen in patients receiving blood. These abnormalities are both quantitative and functional, being related to the components of immune response. Most patients with beta thalassemia may require splenectomy that can cause a further increase in the risk of infections such as *Streptococcus pneumoniae*, *Neisseria meningitidis*, *Haemophilus influenzae*, and influenza-related complications, as thalassemia is associated with a reduced specific antibody response.[6,7]

Annually, seasonal influenza is associated with 250,000–500,000 deaths worldwide. Influenza vaccine administration, which can prevent and reduce the risk of infections,[8] is especially recommended for immunocompromised individuals and also patients with chronic blood disorders such as beta thalassemia major. Injection of viral vaccines boosts Th1 cellular immunity in individuals with thalassemia major (who have iron overload) and protects them from intracellular pathogens.[8]

Several clinical trials have revealed that the split-virus vaccine (produced based on disrupted virus) against the 2009 A/H1N1 virus, both with or without adjuvant, is very effective and can establish sufficient protection against this infection in the general population.[9,10] Sun et al[11] have reported that 14 or 21 days after vaccine administration the recipients generally developed protection against the 2009 A/H1N1 influenza virus. A study on immunogenicity and safety of trivalent influenza vaccines (TIVs) and inactivated quadrivalent influenza vaccine (QIV) demonstrated antibody responses to the QIV were noninferior

to the response to the TIV for the matched strains.[12] Meanwhile, it is reported that TIVs can reduce the hospitalization rate in vaccinated individuals compared to unvaccinated children.[13]

Although a number of specific vaccines against this virus can generate adequate antibody responses in healthy subjects, their efficacy in splenectomized and nonsplenectomized patients with beta thalassemia has not yet been specified. The humoral and cell-mediated immune responses in immunodeficient and immunocompromised patients following influenza vaccination are inefficient, and probably a single dose of vaccine is not enough to elucidate immune response.[14] It seems necessary that each different patient group have its own vaccination program.

Therefore, the aim of this study was to evaluate the immunogenicity and tolerability of the influenza vaccine in patients with beta thalassemia major and compare the efficacy of influenza vaccine in single-dose and double-dose regimens in patients with beta thalassemia.

## Materials and Methods

### Population

In this study, beta thalassemia major patients were enrolled and referred to Motahari Hospital, which is affiliated with Jahrom University of Medical Sciences (Iran). Informed consent was obtained from each participant. This research was approved by the Ethical Committee of Jahrom University of Medical Sciences. To conduct this study, 30 patients who come to Motahari Hospital twice a week for blood transfusion were selected for sample collection according to the study inclusion criteria. All patients had received transfusions of filtered red blood cell concentrates at regular intervals. Patients were divided into 3 groups of 10 individuals using blocked randomization. In the first group (group 1), participants with mean age 15 ± 2 years (4 males and 6 females) received 1 dose (0.5 mL) of the trivalent vaccine consisting of A (H1N1), A (H3N2), and B viruses (Novartis) on day 0, and the second group (group 2) with mean age 17 ± 4.5 years (2 males and 8 females) received 2 doses of the same vaccine on days 0 and 14. In the third group (group 3), patients with mean age 18 ± 3.5 years (3 males and 7 females) received no influenza vaccine (unvaccinated control group). All patients were referred to the hospital for monitoring on a weekly basis. A clinical follow-up questionnaire was used for at least 2 months. All patients were monitored for influenza and other infectious diseases during the study period. Details of the demographic characteristics of the participants at the beginning of the study are presented in **TABLE 1**.

### Study Setting and Sampling

Three separated blood samplings were performed for each participant on days 0, 14 and 60. Briefly, at the beginning (on day 0), a 5 mL blood sample collection for serum separation and subsequent laboratory tests was performed for all groups and then patients in groups 1 and 2 were vaccinated. On day 14, blood samples were obtained for the second measurements and then the second dose of vaccine was administered to group 2. Six weeks later (on day 60), all sample collections and measurements were repeated for three groups.

### Laboratory Assays and Data Analysis

The sera were treated with receptor-destroying enzyme from *Vibrio cholera* at 37°C overnight to remove nonspecific inhibitors of influenza virus hemagglutinin. An 8% sodium citrate solution was then added to the sera and incubated at 56°C for 1 hour before testing. An initial serum dilution of 1:10 was followed by 2-fold serial dilutions to 1:2560. Four hemagglutinin units of each antigen were added and incubated for 1 hour at room temperature. Thereafter, chicken red blood cells were added and incubated for 1 hour at room temperature and scored for hemagglutination. All sera were titrated simultaneously and in duplicate. The hemagglutination inhibition (HI) titers were expressed as the reciprocal of the highest dilution of serum that completely inhibited hemoagglutination.[15] A titer of 1:40 was considered to be protective. All subjects were tested for influenza virus antibodies before transfusion. The parameters used as indications of a humoral immune response were the seroconversion rates, defined as the percentage of subjects experiencing at least a 4-fold increase in the HI titer, the geometric mean titer (GMT), which is the difference between the HI titer means before and after vaccination, and the seroprotection rate, which is the percentage of subjects reaching an HI titer equal to or higher than 40.

### Safety

Safety endpoints included the frequency of solicited injection site and systemic reactions occurring within 7 days after vaccination. Unsolicited adverse events (AEs), including serious AEs (SAEs), were collected during 28 days after vaccination.

### Statistical Analysis

The data were analyzed using two-way ANOVA. Categorical data were analyzed using contingency table analysis and the $\chi^2$ or Fisher's test, as required. The variable levels were evaluated by means of Prism 8 software. $P < .05$ was regarded as significant in all statistical analyses.

## Results

### A Double Dose of Influenza Vaccine Induces More Humoral Immune Responses in Patients with Beta Thalassemia

Following vaccination, it was attempted to determine whether different numbers of influenza vaccine doses induce different effective humoral immune responses. To this end, group 1 received a single dose of vaccine on day 0, group 2 received two doses of vaccine on days 0 and 14, and group 3 received no vaccine. Blood samples were collected from all groups on days 0, 14, and 60 (**FIGURE 1**).

About 83% of the subjects in all groups had baseline specific antibody titers of 40 or more upon HI assay and a measurable level of GMT, and their seroprotectivity level was similar. Two weeks after vaccine administration, groups 1, 2, and 3 were associated with seroconversion rates of 20%, 30%, and 0%, respectively (**FIGURE 2A**). However, seroprotection rates were 100%, 100%, and 90%, respectively (**FIGURE 2B**). Surprisingly, groups 1 and 2 showed about 2.5-fold increases in GMT level compared to group 3 (**FIGURE 2C**). Two months after vaccination, 70% of the subjects in group 2 were seroconverted compared to group 1 and 3, whereas 100% of the patients in groups 1 and 2 and 80% in group 3 were still seroprotected. Meanwhile, participants receiving no vaccine showed a reduced antibody titer after 6 weeks. GMT levels and their increases from the baselines showed about 5-fold titers. Remarkably, GMT in group 1 was reduced during 8 weeks of follow up.

**TABLE 1.** Descriptive Statistics of General Characteristics and Hematological Findings for Three Groups of Beta Thalassemia Major Patients in the Beginning of the Study (Day 0)[a]

| Variables | Group 1 (n = 10) | Group 2 (n = 10) | Group 3 (n = 10) |
|---|---|---|---|
| Age (y) | 15 ± 2 | 17 ± 4.5 | 18 ± 3.5 |
| Male (%) | 4 (40%) | 2 (20%) | 3 (30%) |
| Female (%) | 6 (60%) | 8 (80%) | 7 (70%) |
| White blood cell count ($\times 10^9$/L) | 9.1 ± 5.3 | 10.1 ± 4.9 | 9.5 ± 6.3 |
| Red blood cell count ($\times 10^{12}$/L) | 3.2 ± 0.7 | 4.1 ± 0.2 | 3.6 ± 0.5 |
| Hemoglobin (g/L) | 10 ± 1.0 | 9.4 ± 1.4 | 9.8 ± 1.0 |
| Hematocrit (L/L) | 27.3 ± 3.2 | 30.3 ± 5.8 | 29.3 ± 5.2 |
| Splenectomy (%) | 4 (40%) | 2 (20%) | 3 (30%) |
| Deferoxamine treatment/night | 3 ± 1 | 3 ± 1 | 3 ± 1 |
| Flu during vaccination | 0 | 0 | 0 |

[a]*Group 1 received one dose of the trivalent vaccine at day 0. Group 2 obtained two doses of vaccine, at day 0 and 14. Group 3 included patients without vaccine administration (control group).*

**FIGURE 1.** Flow chart of the study design.

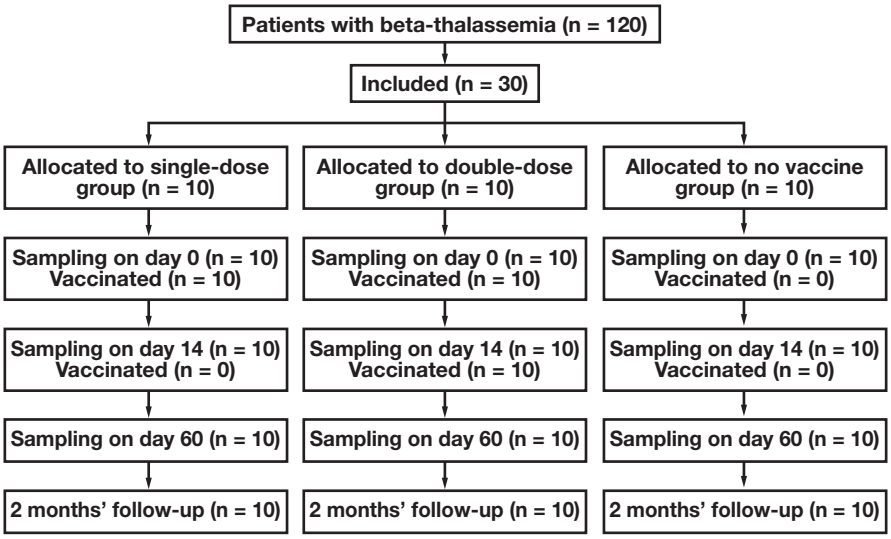


### A Double Dose of Influenza Vaccine Can Stimulate Better Humoral Immune Responses in Nonsplenectomized Patients with Beta Thalassemia

After verifying the protective effect of double doses of influenza vaccine, we assessed the protective immunity response in splenectomized and nonsplenectomized patients after 2 doses of vaccine. There was no significant difference in seroconversion and seroprotection rates between the splenectomized and nonsplenectomized patients (**FIGURES 3A** and **3B**). However, nonsplenectomized patients showed higher GMT levels on day 60 than splenectomized patients (**FIGURE 3C**).

### Single- and Double-Dose Influenza Vaccination Present Similar Incidence of Solicited and Unsolicited Local and Systemic Reactions

The proportions of subjects exhibiting solicited injection-site or systemic reactions in groups 1 (single-dose vaccination) and group 2 (double-dose vaccination) were similar (**TABLE 2**). In subjects receiving the first dose of vaccine, the most commonly reported injection site reaction was pain. The majority of subjects that received the second dose exhibited grade 1 (mild) or 2 (moderate) solicited reactions, and most reactions occurred and were resolved within 3 days of vaccination. These were mostly cases of nasopharyngitis, cough, and injection site pruritus in the first and second injection. No AEs led to discontinuation within 28 days after vaccination. No SAE was reported during the study and no case of death after 2 months postvaccination was considered vaccine-related.

## Discussion

The immunogenicity of inactivated influenza vaccines can be evaluated using the HI test and the HI titer that serologically show HA-specific antibody level.[17] Vaccination is regarded as the most important strategy to prevent influenza virus mortality and morbidity in individuals who are at high risk, such as pregnant women, young children, people with underlying diseases, and health care personnel.[18] The aim of the present study was to evaluate the protective immunity against

**FIGURE 2.** **Immune responses by hemagglutination inhibition (HI) test in three groups: single dose, double dose, and no influenza vaccine administration. At the baseline, groups had specific antibody titers of 40 or more upon HI assay. Two and 8 weeks after vaccine administration, the group had received two doses of vaccine that were associated with an increased seroconversion rate (A). The seroprotection rates were 100% in groups that had received vaccines after 8 weeks (B). The geometric mean titer (GMT) level in the group that had received two doses of vaccine was increased during 60 days compared to single dose and no vaccine groups (C). Results were analyzed with the two-way ANOVA and $\chi^2$ or Fisher's test. Values are the mean ± SEM and percentage; *$P$ < .05 and **$P$ < .01.**

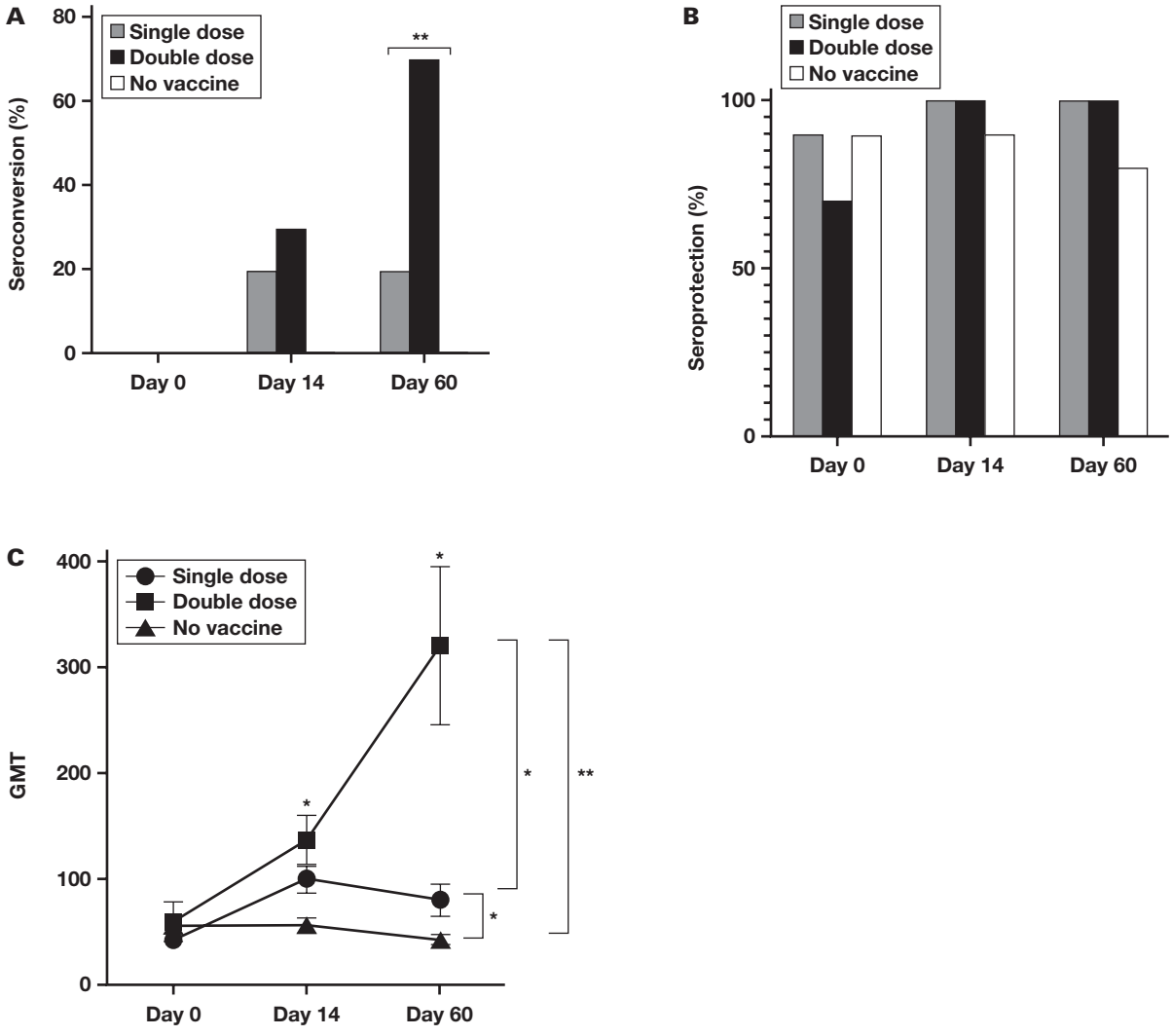


influenza virus by the trivalent vaccine consisting of A (H1N1), A (H3N2), and B virus (Novartis) in two groups of single- and double-dose vaccination in patients with beta thalassemia. The HI test was used to evaluate seroprotection and seroconversion. Our findings indicate that the antibody response-related seroconversion after administration of 2 doses of the trivalent vaccine in patients with beta thalassemia major was statistically higher than that after single dose vaccination. In addition, the group receiving no vaccine showed a reduced antibody titer after 6 weeks. This means that seroconversion and GMT can be reduced over time in individuals that had no exposure to natural infection or vaccine.

Moreover, immunogenicity level was compared between the splenectomized and nonsplenectomized patients, which indicated an increased GMT among the two groups and showed the necessity of double dose of vaccination in nonsplenectomized patients.

Although Esposito et al[19] previously observed that seroprotective antibody titers of influenza A/H1N1 MF59-adjuvanted vaccine were more than 90% 3 months after vaccination, we detected no difference in terms of seroprotective antibody induction among the single-dose vaccinated thalassemia patients. In our study, seroprotective antibody rates were sufficiently high to suggest that factors such as history of previous influenza infection can influence antibody response rate.

We found that antibody levels and GMT in group 2 were significantly higher than those in group 1. Although seroprotection in both groups were similar, the single-dose vaccine seems to usually have insufficient GMT and may not result in the expected immunity for long periods.[19] In agreement with the our study results, it has been reported that two-dose injection of avian and human influenza vaccines could elevate HI antibody titer in individuals without the preexisting antibody (as in the case of the 2009 pandemic).[20] A study by Hu et al[21] on a trivalent inactivated

**FIGURE 3.** **Immune response in splenectomized and nonsplenectomized beta thalassemia patients who received a double dose of influenza vaccine during 60 days. At the baseline, groups had specific antibody titers of 40 or more on hemagglutination inhibition assay. Two and 8 weeks after vaccine administration, the nonsplenectomized group was associated with an increased seroconversion rate (A). The seroprotection rates were 100% after 8 weeks in both groups (B). The geometric mean titer (GMT) level in the nonsplenectomized group was increased during 60 days compared to the splenectomized group (C). Results were analyzed with the two-way ANOVA and $\chi^2$ or Fisher's test. Values are the mean ± SEM and percentage; *$P < .05$ and **$P < .01$.**

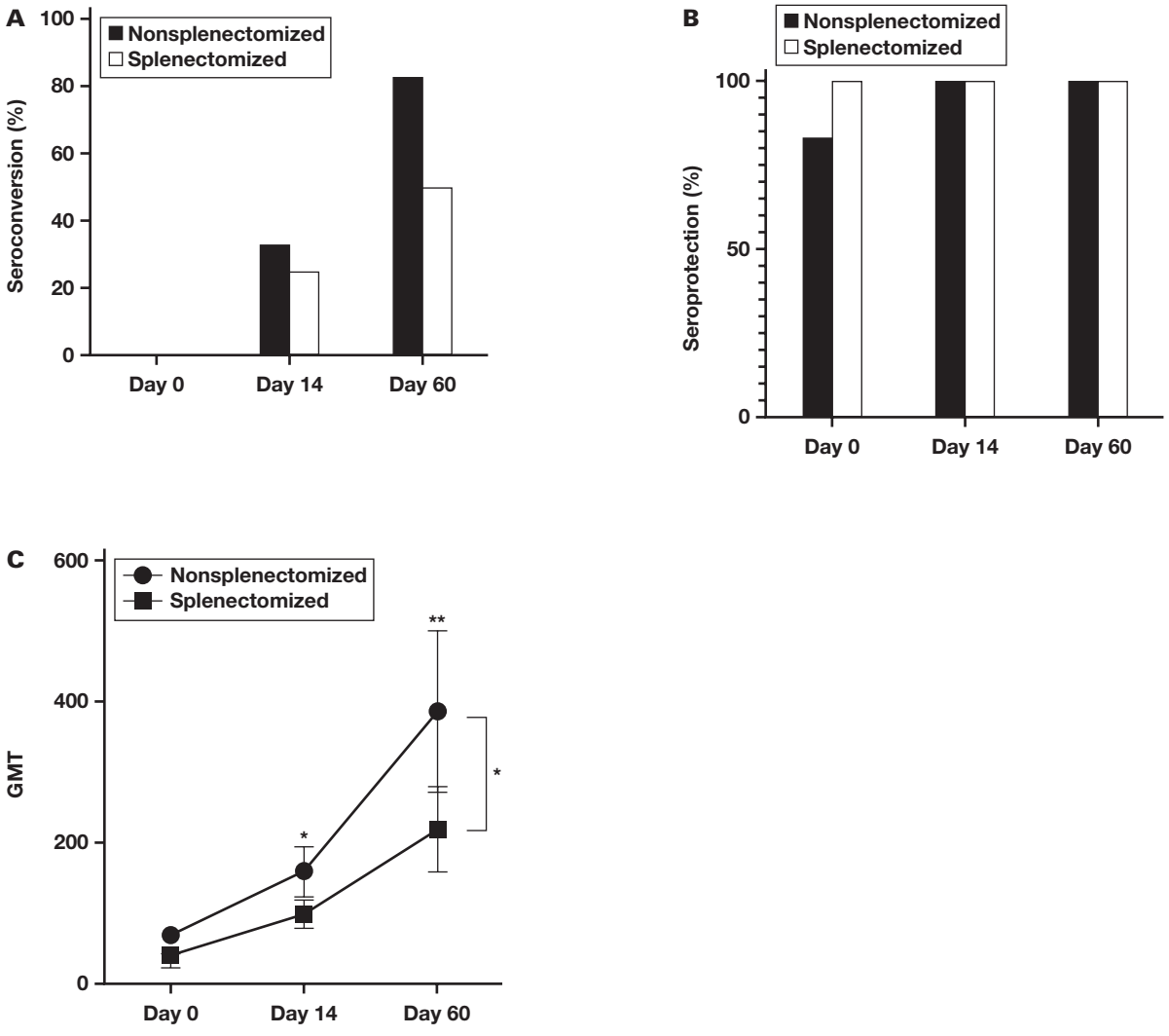


influenza vaccine produced in Shenzhen compared with the comparator IIV3 vaccine showed that the immunogenicity and safety of a marketed influenza vaccine, Shz-IIV3, were similar to the comparator Chinese IIV3 in individuals aged 18 to 59 years. Although the study did not include individuals aged <5 years or ≥60 years who are considered at greater risk, the vaccine was recently shown to be immunogenic and well tolerated in these age groups. Greenberg et al[22] compared safety and immunogenicity of quadrivalent inactivated influenza vaccine with licensed trivalent inactivated influenza vaccine. The QIV formulation tested induced antibody responses that were noninferior to those of the 2009–2010 TIV and the 2008–2009 TIV with respect to each A strain and each included B strain. Antibody responses to B/Brisbane/60/2008 (Victoria lineage) and B/Florida/04/2006 (Yamagata lineage) were markedly greater among study participants who received QIV than the responses to these strains among persons given the TIV not containing these strains (2008–2009 TIV and 2009–2010 TIV, respectively). Their findings support the clinical observations and the use of QIV would be expected to adequately protect against B strains from either lineage.[22] In addition, Cowling et al[23] showed that postvaccination HAI titers mediated 57% of the effect of vaccination on protection against disease caused by influenza B virus infection in the spring of 2010. This indicates that other immune mechanisms may also play a role in the protection conferred by IIV. A meta-analysis study demonstrated that the higher-dose strategy had significantly superior seroconversion and seroprotection for A/H1N1 strains than the standard dose.[24] That means alternative higher-dose vaccination strategies appear to be associated with superior immunogenicity responses for A/H1N1 strains.

Odongo et al[25] compared the immunogenicity of a standard-dose trivalent inactivated influenza vaccination, double-dose trivalent inactivated influenza vaccination (DDTIIV), and booster-dose

**TABLE 2. Adverse Events After Vaccination[a]**

| Adverse Events | First Dose (n = 20) | Second Dose (n = 10) |
|---|---|---|
| | No. (%) | No. (%) |
| Immediate unsolicited AE | 0 (0) | 0 (0) |
| Solicited reaction | | |
| Solicited injection site reaction | 12 (60) | 4 (40) |
| Solicited systemic reaction | 0 (0) | 0 (0) |
| Unsolicited AE | | |
| Nonserious | 6 (30) | 4 (40) |
| Nonserious vaccine-related | 2 (10) | 1 (10) |
| Injection site nonserious vaccine-related | 7 (35) | 3 (30) |
| Systemic nonserious vaccine-related | 0 (0) | 0 (0) |
| AE leading to study discontinuation | 0 (0) | 0 (0) |
| SAE within 3 months | 0 (0) | 0 (0) |

[a]*Safety was analyzed in all subjects who received a study vaccine, per the Guideline for Clinical Safety Data Management: Definitions and Standards for Expedited Reporting.[16] Subjects recorded information about solicited reactions in a diary card for up to 7 days after vaccination and about unsolicited adverse events (AEs) up to 28 days after vaccination. Any serious AEs (SAEs) were reported to investigators throughout a 2-month safety follow-up. Investigators assessed unsolicited AEs and SAEs as unrelated or possibly related to the vaccination. Immediate unsolicited AEs were defined as those occurring within 30 minutes following vaccination.*

trivalent inactivated influenza vaccination of trivalent inactivated influenza vaccine in kidney transplant recipients. They showed that DDTIIV and booster dose trivalent inactivated influenza vaccination regimens are more immunogenic than a standard-dose trivalent inactivated influenza vaccination. In agreement with this study, we also demonstrated that a two-dose vaccine can induce more antibody against virus antigens to protect immunocompromised individuals that are at risk.

Many patients with thalassemia major need to be splenectomized, and the incidence of postsplenectomy infections is higher in these patients. Given the role of red and white pulp of spleen in producing antibodies, trapping antigens by the macrophages of the marginal zone, this organ can act against infections by making a link between innate and adaptive immunities.[26] Moreover, the age at the time of splenectomy seems to play a critical role in the risk of infection, as the incidence of postsplenectomy infections is higher in younger patients.[26] It has been shown that the MF59-adjuvant vaccine in the splenectomized and nonsplenectomized subjects results in similar immunogenicities.[19] However, the risk of infection is higher in the first 2 to 3 years after splenectomy, and the negative impacts of splenectomy are reduced after 3 years postsurgery, especially in young patients.[27] Because some of patients in our study had undergone splenectomy at least 3 years before enrollment, we were able to analyze splenectomy impact on antibody responses. Although our splenectomized and nonsplenectomized patients showed no statistically significant difference in seroconversion and seroprotection, the nonsplenectomized patients had higher GMT levels than the splenectomized patients. This finding shows the important role of the spleen in the induction of antibody response. Moreover, it has been reported that influenza immunization in asplenic patients can reduce the risk of death by up to 54% compared to unimmunized asplenic patients.[26]

In our study, solicited reactions, unsolicited AEs, and SAEs were comparable between the first and second dose of vaccine. This indicates that regardless of each vaccination, TIV safety is acceptable between the different vaccination strategies. According to a meta-analysis study that compared the safety of alternative higher-dose and standard-dose trivalent vaccines in immunocompromised individuals, no differences in safety were observed.[24] It seems that different programs of administration have no effect on the safety of influenza vaccines.

This study had several limitations. First, our sample size was low and a definitive diagnosis of influenza requires a PCR-based method. Finally, it cannot be excluded that a previous vaccination with the traditional seasonal A/H1N1 strain may play a role. Although the strains are antigenically somewhat different from each other in different years, previous vaccinations may have led to the development of a certain degree of immune memory.

Further prospective long-term studies need to be performed to clarify survival rate, as we were not able to determine the mortality rate in the studied groups.

## Conclusion

Although protection can be induced by a single vaccine dose, double dose can ensure seroconversion and seroprotection in immunocompromised individuals, especially thalassemia patients. On the other hand, safety and tolerability of vaccine in immunocompromised patients are a key concerns, and patients who participated in our vaccination study had no critical complaints. Although these data need to be confirmed using larger study populations, they could be extrapolated when considering influenza vaccine in subjects with hemoglobinopathy (ie, sickle cell disease) or other types of splenectomized patients. The current study suggests that optimization in the vaccination program of immunocompromised individuals can help to provide long-lasting protection for seasonal influenza, especially in patients with thalassemia.

## Statement of Ethics

The investigation was carried out in accordance with the rules of the Declaration of Helsinki. The Institutional Review Board (human subject committee), Jahrom University of Medical Sciences approved the protocol (IR.JUMS.REC.1391.58). All subjects gave written consent.


## Funding Sources

This work was supported by a grant from the Jahrom University of Medical Sciences.


## Data Availability

All data generated or analyzed during this study are included in this article. Further enquiries can be directed to the corresponding author.

## REFERENCES


1. Bajwa H, Basit H. Thalassemia. In: *StatPearls*. Treasure Island, FL: StatPearls Publishing; 2019.
2. Olivieri NF, Brittenham GM. Iron-chelating therapy and the treatment of thalassemia. *Blood*. 1997;89(3):739–761.

3. Galanello R, Origa R. Beta-thalassemia. *Orphanet J Rare Dis*. 2010;5:11.
4. Khodaei GH, Farbod N, Zarif B, Nateghi S, Saeidi M. Frequency of thalassemia in Iran and Khorasan Razavi. *Int J Pediatr.* 2013;1(1):45–50.
5. Yavarian M, Karimi M, Bakker E, Harteveld CL, Giordano PC. Response to hydroxyurea treatment in Iranian transfusion-dependent beta-thalassemia patients. *Haematologica*. 2004;89(10):1172–1178.
6. Alidoost F, Gharagozloo M, Bagherpour B, et al. Effects of silymarin on the proliferation and glutathione levels of peripheral blood mononuclear cells from beta thalassemia major patients. *Int Immunopharmacol*. 2006;6(8):1305–1310.
7. Chen J, Deng Y-M. Influenza virus antigenic variation, host antibody production and new approach to control epidemics. *Virol J.* 2009;6(1):30.
8. Sasaki S, He X-S, Holmes TH, et al. Influence of prior influenza vaccination on antibody and B-cell responses. *PLoS One*. 2008;3(8):e2975.
9. Greenberg ME, Lai MH, Hartel GF, et al. Response to a monovalent 2009 influenza A (H1N1) vaccine. *N Engl J Med.* 2009;361(25):2405–2413.
10. Zhu F-C, Wang H, Fang H-H, et al. A novel influenza A (H1N1) vaccine in various age groups. *N Engl J Med.* 2009;361(25):2414–2423.
11. Sun Y, Bian C, Xu K, et al. Immune protection induced on day 10 following administration of the 2009 A/H1N1 pandemic influenza vaccine. *PLoS One*. 2010;5(12):e14270.
12. Pépin S, Donazzolo Y, Jambrecina A, Salamand C, Saville M. Safety and immunogenicity of a quadrivalent inactivated influenza vaccine in adults. *Vaccine*. 2013;31(47):5572–5578.
13. Uchida M, Takeuchi S, Saito M-M, Koyama H. Effects of influenza vaccination on seasonal influenza symptoms: a prospective observational study in elementary schoolchildren in Japan. *Heliyon*. 2020;6(2):e03385.
14. Resende MR, Husain S, Gubbay J, et al. Low seroconversion after one dose of AS03-adjuvanted H1N1 pandemic influenza vaccine in solid-organ transplant recipients. *Can J Infect Dis Med Microbiol.* 2013;24(1):e7–e10.
15. Menegon T, Baldo V, Bonello C, Dalla Costa D, Di Tommaso A, Trivello R. Influenza vaccines: antibody responses to split virus and MF59-adjuvanted subunit virus in an adult population. *Eur J Epidemiol.* 1999;15(6):573–576.
16. Guideline IHT. Clinical safety data management: definitions and standards for expedited reporting E2A. Paper presented at International Conference on Harmonisation of Technical Requirements for Registration of Pharmaceuticals for Human Use; 1994.
17. Huang K-YA, Chang S-C, Huang Y-C, Chiu C-H, Lin T-Y. Antibody responses to trivalent inactivated influenza vaccine in health care personnel previously vaccinated and vaccinated for the first time. *Sci Rep*. 2017;7:40027.
18. Uyeki TM. Preventing and controlling influenza with available interventions. *N Engl J Med.* 2014;370(9):789–791.
19. Esposito S, D'Angelo E, Daleno C, et al. Immunogenicity, safety and tolerability of monovalent 2009 pandemic influenza A/H1N1 MF59-adjuvanted vaccine in patients with beta-thalassemia major. *Vaccine*. 2010;28(50):7825–7828.
20. Nelson JC, Bittner RC, Bounds L, et al. Compliance with multiple-dose vaccine schedules among older children, adolescents, and adults: results from a vaccine safety datalink study. *Am J Public Health*. 2009;99(suppl 2):S389–S397.
21. Hu Y, Chu K, Lavis N, et al. Immunogenicity and safety of a trivalent inactivated influenza vaccine produced in Shenzhen, China versus a comparator influenza vaccine: a phase IV randomized study. *Hum Vaccin Immunother*. 2019;15(5):1066–1069.
22. Greenberg DP, Robertson CA, Noss MJ, Blatter MM, Biedenbender R, Decker MD. Safety and immunogenicity of a quadrivalent inactivated influenza vaccine compared to licensed trivalent inactivated influenza vaccines in adults. *Vaccine*. 2013;31(5):770–776.
23. Cowling BJ, Lim WW, Perera RA, et al. Influenza hemagglutination-inhibition antibody titer as a mediator of vaccine-induced protection for influenza B. *Clin Infect Dis*. 2019;68(10):1713–1717.
24. Lai J-J, Lin C, Ho C-L, Chen P-H, Lee C-H. Alternative-dose versus standard-dose trivalent influenza vaccines for immunocompromised patients: a meta-analysis of randomised control trials. *J Clin Med*. 2019;8(5):590.
25. Odongo FCA, Braga PE, Palacios R, et al. An open-label randomized controlled parallel-group pilot study comparing the immunogenicity of a standard-, double-, and booster-dose regimens of the 2014 seasonal trivalent inactivated influenza vaccine in kidney transplant recipients. *Transplantation*. 2022;106(1):210–220.
26. Bonanni P, Grazzini M, Niccolai G, et al. Recommended vaccinations for asplenic and hyposplenic adult patients. *Hum Vaccin Immunother*. 2017;13(2):359–368.
27. Castagnola E, Fioredda F. Prevention of life-threatening infections due to encapsulated bacteria in children with hyposplenia or asplenia: a brief review of current recommendations for practical purposes. *Eur J Haematol*. 2003;71(5):319–326.

# T Cell Senescence by Extensive Phenotyping: An Emerging Feature of COVID-19 Severity

*Jenny Zuin, MD,[1] Paola Fogar, MD, PhD,[1] Giulia Musso, MD, PhD,[1,2*] Andrea Padoan, PhD,[1,2] Elisa Piva, MD,[1] Michela Pelloso, MD,[1] Francesca Tosato, MD,[1] Annamaria Cattelan, MD,[3] Daniela Basso, MD,[1,2] Mario Plebani, MD[1,2]*

[1]Department of Laboratory Medicine, Padova University-Hospital, Padova, Italy, [2]Department of Medicine-DIMED, University of Padova, Padova, Italy, [3]Unit of Infectious and Tropical Diseases, Padova University-Hospital, Padova, Italy *To whom correspondence should be addressed. giulia.musso.1@phd.unipd.it

**Keywords:** T cell subsets, COVID-19, extensive immunophenotyping, senescence, exhaustion, prognostic biomarker

**Abbreviations:** ARDS, acute respiratory distress syndrome; HCV, hepatitis C virus; HBV, hepatitis B virus; HIV-1, human immunodeficiency virus; NLR, neutrophil-to-lymphocyte ratio; AUC, area under the curve; LYM, total lymphocytes; ROC, receiver operating characteristic; N, naïve; CM, central memory; EM, effector memory; TEMRA, terminal effector memory.

*Laboratory Medicine* 2022;53:609–613; https://doi.org/10.1093/labmed/lmac048

## ABSTRACT

**Objective:** To identify the potential prognostic value of lymphocyte subsets in COVID-19 patients, where lymphopenia is a common finding.

**Methods:** In 353 COVID-19 inpatients and 40 controls T cell subsets with markers of senescence and exhaustion were studied by flow cytometry.

**Results:** In severe illness, total lymphocytes B, NK, and all T subsets were dampened. Senescent CD4+, but mainly CD8+ T cells, increased in patients with respect to controls. The most significant index predicting fatal outcome was neutrophils/CD3+ T ratio.

**Conclusion:** In conclusion, an altered T cell pattern underlies COVID-19 severity and is involved in predicting the outcome.

Since late December 2019, the COVID-19 pandemic caused by SARS-CoV-2 registered more than 244.3 million of cases and more than 4.9 million deaths as of October 27, 2021, according to the WHO Coronavirus (COVID-19) Dashboard. A wide range of clinical manifestations is associated with SARS-CoV-2 infection, which causes few and mild symptoms in the vast majority of cases but potentially results in severe pneumonia and acute respiratory distress syndrome (ARDS), mainly in frail and/or aged patients.[1]

Advanced age and comorbidities concur in enhancing disease severity: elderly patients are more likely to have severe disease with a higher death rate compared to younger individuals.[2] This age-related outcome might depend in part to age-related differences in the immune response: while children express more naïve T cells, elders are characterized by increased levels of memory cells.[3]

A reduction of lymphocytes was demonstrated in the most severe COVID-19 cases,[1] and several studies reported a significant, although not univocal, specific reduction of T cell subsets,[4] which are pivotal in the immune response against viral infections.[5]

The aim of this study was to identify the potential prognostic value of lymphocyte subsets in COVID-19 patients by extensive phenotyping of differentiation, senescence, and exhaustion markers on the surface of CD4+ and CD8+ T cells.

## Materials and Methods

In this retrospective study, approved by the local ethic committee (number 27444), a total of 353 COVID-19 patients consecutively admitted at the University Hospital of Padova were studied. Included patients from March to October 2020 had a maximum of 10 days' disease history and were comprised of 221 males (mean age, 57 ± 16.47 years; range, 21–95 years) and 132 females (mean age, 60 ± 19.06 years; range, 19–98 years) with no difference in age (Student *t*-test, $P = .0882$). Peripheral blood immune cell data were analyzed the same day or the day after hospital admission. For comparison, 40 unselected healthy blood donors (HDs) were included as a control group. In accordance with Italian law, HD are screened at each donation with NAAT for hepatitis C virus (HCV), hepatitis B virus (HBV), and human immunodeficiency virus (HIV-1); moreover, they must be free from any symptoms, including COVID-19–related symptoms, for at least 14 days.

The studied inpatients were referred to a semi-intensive and intensive care unit (ICU, n = 74) or to the Tropical and Infectious diseases care unit (NOT-ICU, n = 279). A total of 24 patients (7%) died within 3 months from hospital admission due to COVID-19–related causes.

Full blood cell count with differential were obtained from K2-EDTA tubes (Sysmex XE-series, Sysmex). Lymphopenia was defined as lymphocytes <1.10 × $10^9$/L. Neutrophil count was used to obtain the neutrophil-to-lymphocyte ratio (NLR) and neutrophil-to-T cell indexes.

Lymphocyte subsets were analyzed within 2 days from sample collection. Samples were loaded on AQUIOS CL Flow Cytometer (Beckman Coulter), stained with AQUIOS TETRA-1 panel (CD45-FITC/CD4-RD1/CD8-ECD/CD3-PC5) and AQUIOS TETRA-2 panel (CD45-FITC/(CD56+ CD16)-RD1/CD19-ECD/CD3-PC5), and analyzed using the Tetra Combo analytical mode for the detection of CD3+/CD4+/CD8+ T cells, CD19+ B cells, and CD16+ 56+ NK cells.

Duraclone IMT cell panel (CD45RA-FITC/CCR7-PE/CD28-ECD/PD1-PC5.5/CD27-PC7/CD4-APC/CD8-A700/CD3-APC-A750/CD57-PB/CD45-KO) was used for the detailed analysis of T cell phenotype on a 10-color NAVIOS EX Flow Cytometer (Beckman Coulter).

Kaluza Analysis Software (Beckman Coulter) was used to set a gate for identification of T lymphocytes (CD45+ CD3+ cells) and then to identify CD4+ (helper) or CD8+ (suppressor) lymphocytes. Within the CD4+ or CD8+ population we analyzed markers of differentiation (CD45RA, CCR7, CD28, CD27), senescence, and exhaustion (CD57 and PD1).

Procedures for calibration, internal quality controls, and external quality assessment schemes were performed in accordance with ISO 15189 accreditation requirements for clinical laboratories, being the laboratory accredited since 2006.

Statistical analyses were performed using Stata v13.1 (StataCorp) and GraphPad Prism version 9.2.0 (GraphPad Software). Student *t*-test and 1-way ANOVA or multivariate ANOVA were used to assess differences between 2 or more groups, using Bonferroni's adjustment for multiple testing. Nonparametric test for trend was used to evaluate increasing or decreasing trends. Nonparametric receiver operating characteristic (ROC) analyses were used for assessing predictive performances of studied variables and estimating the area under the curve (AUC), with the Benjamini–Hochberg procedure for adjusting *P* value. Multivariate analyses were performed including age and sex as covariates.

## Results

### Total Lymphocytes and Lymphocyte Subsets Decline as Age and Disease Severity Increases

Lymphopenia occurred in 64% (225/353) of all patients and in 75% (117/157) of those >60 years. Total lymphocytes (LYM), CD4+ and CD8+ T cells, B cells, and NK cells were significantly lower in patients (F = 45.38 $P < .0001$ for LYM; F = 42.44, $P < .0001$ for CD4+; F = 28.27 $P < .0001$ for CD8+; F = 29.11, $P < .0001$ for CD19+ B cells; F = 21.83, $P < .0001$ for NK cells) than in controls. A decreasing trend in CD3+ T cells was observed, although the variation was not significant (F = 0.87, $P$ = ns).

The following age-related categories were defined for further statistical analysis: <40 years (52 patients and 13 HDs), 40–60 years (144 patients and 23 HD), and >60 years (157 patients and 4 HDs).

As shown in **FIGURE 1A**, among COVID-19 patients a significant age-related decrease was found in LYM, CD3+ T cells, and their subsets and B cells; whereas no difference was seen in healthy controls (F = 14.23, $P < .0001$ vs F = 0.99, $P$ = ns for LYM; F = 8.22, $P = .0003$ vs F = 1.21, $P$ = ns for CD3+ T cells; F = 18.98, $P < .0001$ vs F = 0.65, $P$ = ns for CD4+; F = 17.86, $P < .0001$ vs F = 0.37, $P$ = ns for CD8+; F = 4.83, $P = .0086$ vs F = 0.96, $P$ = ns for B cells). No age-related change was found for NK cells (F = 0.64, $P$ = ns vs F = 1.14, $P$ = ns). For any age class, the decrease in LYM and subsets that was observed was more pronounced in ICU than NOT-ICU, except for CD3+ and B cells (F = 11.92, $P = .0006$ for LYM; F = 0.93, $P$ = ns for CD3+; F = 13.68, $P = .0003$ for CD4+; F = 8.41, $P = .004$ for CD8+; F = 1.62, $P$ = ns for B cells; F = 4.73, $P < .05$ for NK).

In healthy controls NLR, neutrophil-to-CD3+ cells ratio (N3R), neutrophil-to-CD4+ cells ratio (N4R), and neutrophil-to-CD8+ cells ratio (N8R) did not differ significantly between age classes (**FIGURE 1B**). Conversely, ICU care for >60 year-old patients showed a sustained increase of NLR, N3R, N4R, and N8R; F = 13.43, $P = .0003$ for NLR; F = 8.28, $P = .0043$ for N3R; F = 10.76, $P = .0011$ for N4R; F = 4.90, $P = .0275$ for N8R).

ROC curve analyses examining whether the lymphocyte count and subsets were associated with the referring hospitalization unit (NOT-ICU vs ICU) based on patients age classes are shown in **TABLE 1**.

Pairwise comparisons of ROC showed that, although NLR presented the higher AUC value, the difference was not significant with respect to other AUC values.

It is worth noting that in our studied population the patient deaths (n = 24) occurred in the >60 year age class, therefore the prognostic role of laboratory findings on survival, estimated with ROC curve analysis, was made in patients belonging to this age class only. The most discriminant index was N3R with an AUC of 0.877.

### Disease Severity Is Associated with T Cell Senescence and Exhaustion

Markers of T cell differentiation, senescence, and exhaustion were further analyzed in 68 COVID-19 patients (61 NOT-ICU and 7 ICU) and 20 HD. The following CD4+ and CD8+ subsets were identified: naïve (N) (CCR7+ CD45RA+), central memory (CM) (CD45RA– CCR7+), effector memory (EM) (CD45RA– CCR7–), and terminal effector memory (TEMRA) (CD45RA+ CCR7–).

None of CD4+ T cell subsets varied between HD, NON-ICU, and ICU. On the contrary, CD8+ CM ($P < .001$) and EM ($P = .012$) subsets significantly decreased in ICU patients (Supplemental Figure 1A). No significant age-related differences were found for any of the studied subsets (data not shown).

Both CD4+ and CD8+ senescent cells, that is CD57+ PD1– and CD57+ PD1+, showed a trend toward increasing values in NON-ICU and ICU patients with respect to HD ($P < .05$) (Supplemental Figure 1B). Among these, the variations of CD8+ senescent and exhausted CD57+ PD1+ cells were independent from age ($P = .089$), while increasing age was correlated with CD4+ CD57+ cells ($P = .015$), CD4+ CD57+ PD1+ cells ($P = .025$) and CD8+ CD57+ cells ($P = .04$).

When analyzing both markers in each subset (N, CM, EM, and TEMRA) among HD, NOT-ICU and ICU groups, naïve CD4+ CD57–PD1+ and CD4+ CD57+ PD1+ cells tended to progressively increase among NON-ICU and ICU patients ($P = .011$ and $P = .005$, respectively). A similar and age-independent pattern was found for EM CD4+ CD57+ PD1+, CM, and EM CD8+ CD57+ PD1+ cells ($P = .006$, $P = .044$, and $P = .014$, respectively) (Supplemental Figures 2 and 3). On the contrary, the increase of naïve CD8+ CD57+ PD1+ cells observed in more severe cases ($P = .048$), was in part correlated with age ($P = .010$). No significant trend was identified for CM, TEMRA CD4+, and TEMRA CD8+.

## Discussion

During viral infection, T cells are crucial to viral clearance; CD8+ cytotoxic T cells directly attack and kill virus-infected cells, whereas CD4+ helper T cells assist cytotoxic T cells and B cells and enhance their ability to eliminate pathogens. In contrast to HIV-1, cytomegalovirus, and Epstein-Barr virus infections, which lead to proliferative lymphocyte response, one prominent feature of SARS-CoV-2 is lymphopenia due to pulmonary recruitment from the blood and direct virus killing.[6]

Previous studies in COVID-19 patients reported lymphopenia to affect all subsets (T, B, and NK cells), with the lowest lymphocyte counts found in severe disease that needed ICU care being reversed in almost all convalescents.[7]

In our study, lymphopenia was confirmed to be a common finding in COVID-19 patients, being more severe among those >60 years old; however, we should mention as a limitation of our study that only 4 HDs aged >60 were enrolled. This pattern was also found when considering the absolute number of CD4+ and CD8+ T cells and B cells, being the lowest levels detected in older patients of the ICU group. Furthermore, in COVID-19 patients, lymphopenia associated with normal/increased neutrophils explained the observed increase in NLR, a marker of systemic inflammation and infection; again, the highest NLR was found in the >60 year olds in ICU care. Interestingly, other hematologic features were noted in the COVID-19 cohort, such as an average eosinophilic count lower in COVID-19 patients than in HD ($0.02 \pm 0.04 \times 10^9$/L vs $0.17 \pm 0.09 \times 10^9$). This finding is in agreement with recent data reported by Outh et al.[8]

Qin et al[9] proposed some parameters derived from lymphocyte subsets to predict disease severity and survival. To confirm these findings, we performed ROC curve analysis to evaluate the role of total lymphocyte (CD3+, CD4+, and CD8+) counts and NLR/N3R/N4R/N8R for association with hospitalization unit and survival prediction—the last one estimated only for patients >60 years, since no death occurred among those younger. The most significant index of disease severity was NLR, while N3R was the best in predicting survival.

**FIGURE 1. A, Age-related decrease of total lymphocytes and lymphocyte subsets in COVID-19 patients compared to healthy donors (F = 14.23, *P* < .0001 vs F = 0.99, *P* = ns for total lymphocytes; F = 8.22, *P* = .0003 vs F = 1.21, *P* = ns for total T cells; F = 18.98, *P* < .0001 vs F = 0.65, *P* = ns for CD4+; F = 17.86, *P* < .0001 vs F = 0.37, *P* = ns for CD8+; F = 4.83, *P* = .0086 vs F = 0.96 *P* = ns for B cells; not significant for NK cells F = 0.64, *P* = ns vs F = 1.14, *P* = ns); age-related decrease both in NOT-ICU and ICU for total lymphocytes, CD4+ and CD8+ subsets only (F = 11.92, *P* = .0006 total lymphocytes; F = 0.93, *P* = ns total T cells; F = 13.68, *P* = .0003 CD4+; F = 8.41, *P* = .004 CD8+; F = 1.62, *P* = ns B cells; F = 4.73, *P* < .05 for NK).**

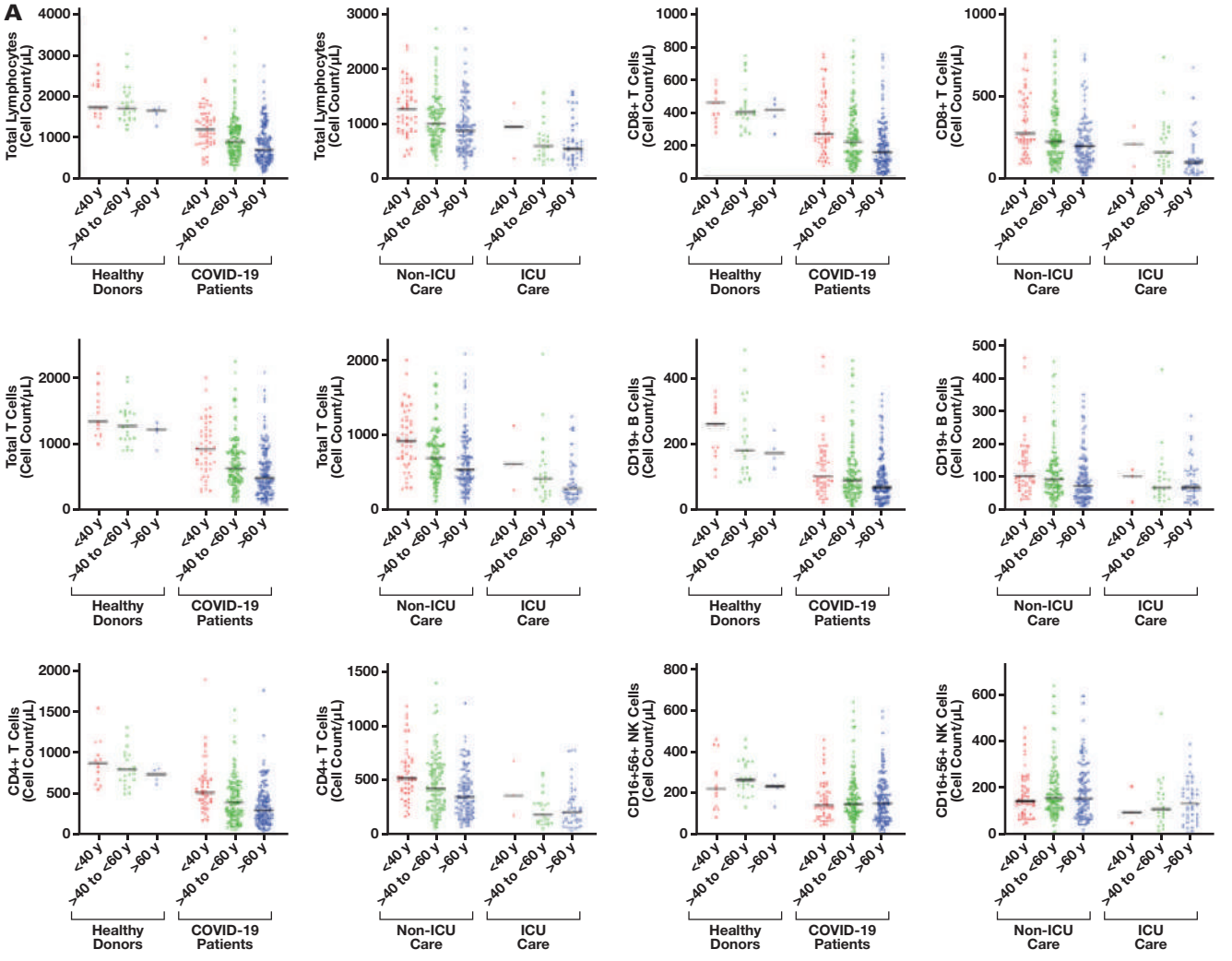

**FIGURE 1.** (cont) B, Neutrophil-to-lymphocyte ratio (NLR), neutrophil-to-CD3+ cells ratio (N3R), neutrophil-to-CD4+ cells ratio (N4R), and neutrophil-to-CD8+ cells ratio (N8R) between age classes in healthy donors (*P* = ns) vs COVID-19 patients (highest ratios in >60-year-old patients. F = 14.95, *P* < .0001 for NLR, F = 11.97, *P* < .0001 for N3R, F = 11.97, *P* < .0001 for N4R, F = 11.20, *P* < .0001 for N8R) and NOT-ICU vs ICU care (highest ratios in >60 years ICU F = 13.43, *P* = .0003 for NLR; F = 8.28, *P* = .0043 for N3R; F = 10.76, *P* = .0011 for N4R; F = 4.90, *P* = .0275 for N8R).

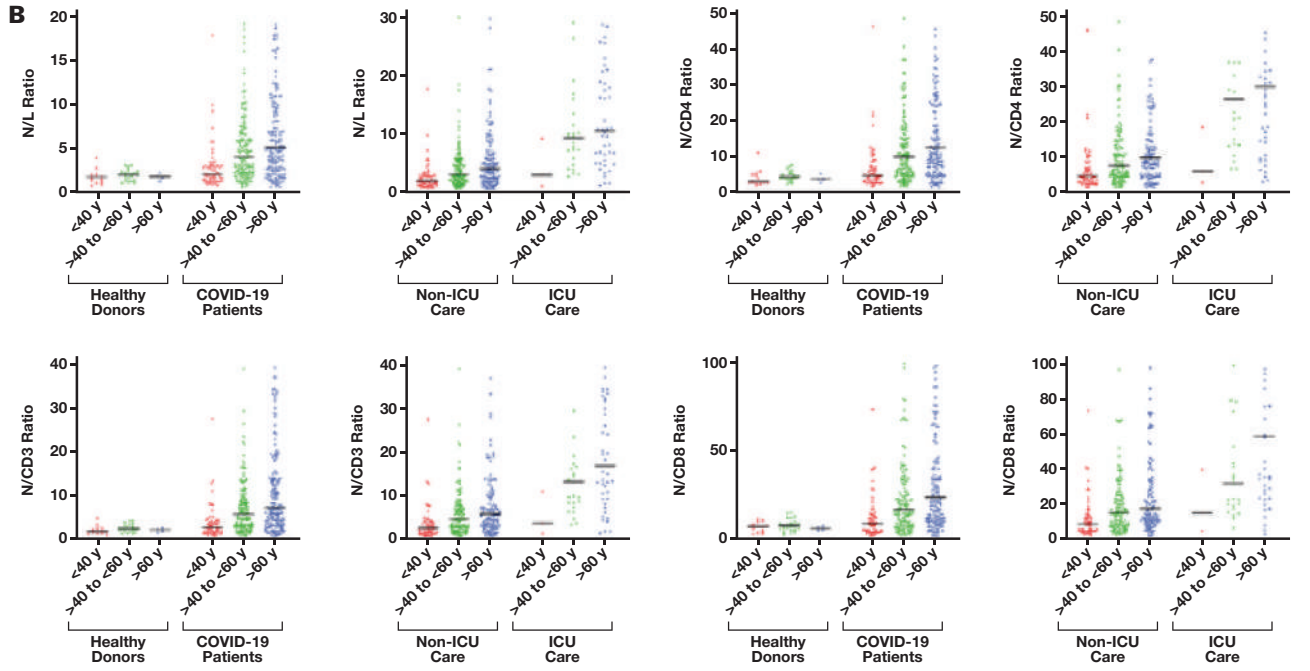


**TABLE 1.** ROC Curve Analyses for Lymphocyte Count and Subsets Associated with Referring Hospitalization Unit (NOT-ICU vs ICU) and in Survival Prediction Based on Patients Age Classes

| Variable | AUC (95% Confidence Interval) | | | |
|---|---|---|---|---|
| **Hospitalization Unit** | **Age < 40 y** | **40 y < Age < 60 y** | **Age > 60 y** | **Overall** |
| LYM | 0.7143 (0.31485–1.0000) | 0.7339 (0.61017–0.85760) | 0.7007 (060979–0.79153) | 0.7358 (0.67041–0.80126) |
| CD3+ T cells | 0.6871 (0.25313–1.0000) | 0.7189 (0.59572–0.84206) | 0.7425 (0.65739–0.82762) | 0.7666 (0.70496–0.82822) |
| CD4+ T cells | 0.6803 (0.23878–1.0000) | 0.7556 (0.64209–0.86916) | 0.7098 (0.62083–0.79876) | 0.7637 (0.70385–0.82352) |
| CD8+ T cells | 0.7279 (0.36817–1.0000) | 0.6034 (0.46939–0.73751) | 0.7379 (0.65531–0.82056) | 0.7363 (0.67081–0.80183) |
| NLR | 0.7958 (0.73857–0.85296) | 0.8467 (0.75735–0.93606) | 0.7466 (0.66600–0.82727) | 0.8050 (0.74953–0.86038) |
| N3R | 0.6939 (0.39524–0.99251) | 0.8325 (0.74269–0.92222) | 0.7597 (0.67991–0.83952) | 0.7950 (0.73676–0.85317) |
| N4R | 0.7007 (0.42987–0.97149) | 0.8349 (0.73976–0.93003) | 0.7443 (0.66337–0.82528) | 0.8047 (0.74708–0.86239) |
| N8R | 0.7483 (0.47900–1.0000) | 0.7365 (0.62245–0.85057) | 0.7349 (0.65215–0.81764) | 0.7581 (0.69561–0.82058) |
| **Survival** | | | | |
| LYM | | | 0.734 (0.628–0.840) | |
| CD3+ T cells | | | 0.866 (0.784–0.947) | |
| CD4+ T cells | | | 0.831 (0.747–0.915) | |
| CD8+ T cells | | | 0.821 (0.735–0.907) | |
| NLR | | | 0.849 (0.754–0.943) | |
| N3R | | | 0.877 (0.793–0.961) | |
| N4R | | | 0.858 (0.765–0.950) | |
| N8R | | | 0.826 (0.726–0.926) | |

*AUC, area under the curve; LYM, total lymphocytes; NLR, neutrophil-to-lymphocyte ratio.*

In our patients, a decreasing, not age-related, trend of CM and EM CD8+ from HD to NON-ICU and ICU care patients was found. Although we could not determine whether lower percentages of CM and EM CD8+ might be a preexisting condition or a direct effect of COVID-19 infection, these results indicate that patients with lower percentages at admission might need ICU care and confirm reports

that T cell compartment displays several alterations.[10] Indeed, known conditions of decreased numbers of CD8+ memory T cells include solid cancer[11] and autoimmune diseases[12] that affected our extended immunophenotyped patients in 7% and 15%, respectively. Given the not-so-infrequent occurrence of these disorders in the general population, a planned phenotyping at selected time points during clinical follow-up might enhance infection-related risk stratification in chronic diseases.

We observed that the same populations, CM and EM CD8+ T cells, along with naïve and EM CD4+, express markers of senescence and exhaustion (CD57 and PD1) in higher percentages than in HD, as already noted[13]; this exhausted phenotype, peculiar to T cells that are chronically stimulated by antigens from viral infection and malignancies, might worsen the already impaired response capability of those cell populations. The prognostic impact of T cell exhaustion in chronic viral illnesses is debated: as PD-1 expression on T cells seems to correlate with disease progression in HIV-1 infection, its role as a target of specific therapy is considered in different animal models of HCV and HBV.[14]

## Conclusion

T cell subsets along with lymphocyte and neutrophil counts at the time of admission of COVID-19 patients might allow an early identification of individuals at risk of developing critical illness. Extensive phenotyping of T cell subsets ensures a deeper insight of SARS-CoV-2 pathological mechanisms, highlighting that an exhausted phenotype associated with a severe disease could lead to a state of low-cell responsiveness impairing immune response.

## Supplementary Data

Supplemental figures and tables can be found in the online version of this article at www.labmedicine.com.

## Acknowledgments

We thank Barbara Barbin, Enzo Cortini, Graziana Marangi, and Laura Zambonin for their technical support.

## REFERENCES

1. Huang C, Wang Y, Li X, et al Clinical features of patients infected with 2019 novel coronavirus in Wuhan, China. *Lancet.* 2020;395:497–506. doi:10.1016/S0140-6736(20)30183-5.
2. Chen N, Zhou M, Dong X, et al. Epidemiological and clinical characteristics of 99 cases of 2019 novel coronavirus pneumonia in Wuhan, China: a descriptive study. *Lancet.* 2020;395:507–513. doi:10.1016/S0140-6736(20)30211-7.
3. Cossarizza A, Ortolani C, Paganelli R, et al. CD45 isoforms expression on CD4+ and CD8+ T cells throughout life, from newborns to centenarians: implications for T cell memory. *Mech Ageing Dev.* 1996;86:173–195. doi:10.1016/0047-6374(95)01691-0.
4. Chen Z, John Wherry E. T cell responses in patients with COVID-19. *Nat Rev Immunol.* 2020;20(9):529–536. doi:10.1038/s41577-020-0402-6.
5. Li C, Wu H, Yan H, et al. T cell responses to whole SARS coronavirus in humans. *J Immunol.* 2008;181:5490–5500.
6. Tay M, Poh C, Rénia L, MacAry P, Ng L. The trinity of COVID-19: immunity, inflammation, and intervention. *Nat Rev Immunol.* 2020;20(6):363–374.
7. Liu J, Li H, Luo M, et al Lymphopenia predicted illness severity and recovery in patients with COVID-19: a single-center, retrospective study. *PLoS One.* 2020;15:e0241659. doi:10.1371/journal.pone.0241659.
8. Outh R, Boutin C, Gueudet P, Suzuki M, Saada M, Aumaître H. Eosinopenia <100/µL as a marker of active COVID-19: an observational prospective study. *J Microbiol Immunol Infect.* 2021;54(1):61–68. doi:10.1016/j.jmii.2020.12.005.
9. Qin C, Zhou L, Hu Z, et al. Dysregulation of immune response in patients with coronavirus 2019 (COVID-19) in Wuhan, China. *Clin Infect Dis.* 2020;71(15):762–768. doi:10.1093/cid/ciaa248.
10. De Biasi S, Meschiari M, Gibellini L, et al Marked T cell activation, senescence, exhaustion, and skewing towards TH17 in patients with COVID-19 pneumonia. *Nat Commun.* 2020;11(1):3434. doi:10.1038/s41467-020-17292-4.
11. Han J, Khatwani N, Searles TG, Turk MJ, Angeles CV. Memory CD8+ T cell responses to cancer. *Semin Immunol.* 2020;49:101435. doi:10.1016/j.smim.2020.101435.
12. Pender MP. CD8+ T-cell deficiency, Epstein-Barr virus infection, vitamin D deficiency, and steps to autoimmunity: a unifying hypothesis. *Autoimmune Dis.* 2012;2012:189096. doi:10.1155/2012/189096.
13. Diao B, Wang C, Tan Y, et al Reduction and functional exhaustion of T cells in patients with coronavirus disease 2019 (COVID-19). *Front Immunol.* 2020;11:827. doi:10.3389/fimmu.2020.00827.
14. Fenwick C, Joo V, Jacquier P, et al. T-cell exhaustion in HIV infection. *Immunol Rev.* 2019;292(1):149–163. doi:10.1111/imr.12823.

# Retrospective Assessment of a National Reflex Cryptococcal Antigen Screening Program in South Africa Through Interlaboratory Comparison of Lateral Flow Assay Results

*Nozuko P. Blasich, MTech,[1] Lindi M. Coetzee, PhD,[2,3] Charlotte Sriruttan, FCPath,[1,2] Daniel DeSanto, MSc,[1] Gregory S. Greene, MSPH,[1] Deborah K. Glencross, MMed,[2,3] Nelesh P. Govender, MMed, FRCPath,[1,2,4,*]*

[1]Centre for Healthcare-Associated Infections, Antimicrobial Resistance and Mycoses, National Institute for Communicable Diseases, a Division of the National Health Laboratory Service, Johannesburg, South Africa, [2]School of Pathology, Faculty of Health Sciences, University of the Witwatersrand, Johannesburg, South Africa, [3]National Priority Programmes CD4 Unit, National Health Laboratory Service, Johannesburg, South Africa, [4]Division of Medical Microbiology, Faculty of Health Sciences, University of Cape Town, Cape Town, South Africa. *To whom correspondence should be addressed. neleshg@nicd.ac.za

**Keywords:** cryptococcal antigen, interlaboratory comparison, discordant results, cryptococcal meningitis, lateral flow assay, advanced HIV disease

**Abbreviations:** CrAg, cryptococcal antigen; LFA, lateral flow assay; WHO, World Health Organization; HIV, human immunodeficiency virus; NHLS, National Health Laboratory Service; CSF, cerebrospinal fluid; LP, lumbar puncture; PTS, proficiency testing scheme; LIS, laboratory information system; EDTA, ethylene diamine tetra acetic acid; NICD, National Institute for Communicable Diseases; EIA, enzyme immunoassay.

*Laboratory Medicine* 2022;53:614–618; https://doi.org/10.1093/labmed/lmac037

## ABSTRACT

**Objective:** Reflex cryptococcal antigen (CrAg) screening of blood specimens with a CD4 count of <100 cells/μL was performed at 45 South African CD4 laboratories using a lateral flow assay (LFA). Our objective was to evaluate the reliability of routine LFA results through comparative interlaboratory testing.

**Methods:** All CrAg-positive and a selected number of CrAg-negative samples from the CD4 laboratories were retested at paired microbiology laboratories using the same LFA. Samples with discordant results were tested at a reference laboratory, using the LFA (with CrAg titers).

**Results:** During interlaboratory testing, 12,502 samples were retested, with 93 (0.7%) discordant results and a between-laboratory agreement of 99.3% (Cohen's kappa, 0.98). The proportion of retested samples with discordant results ranged from 0.17% to 5.31% per laboratory pair (median 0.28%), with 3 reporting >3% of results as discordant.

**Conclusion:** Routine CrAg screening results were reliable, with <1% of samples having discordant results, mainly due to interpretation and transcription errors.

Cryptococcal antigen (CrAg) screening followed by preemptive antifungal treatment of CrAg-positive persons with advanced HIV disease is recommended by the World Health Organization (WHO) to reduce mortality associated with cryptococcal meningitis.[1,2] In October 2016, South Africa's National Health Laboratory Service (NHLS) initiated reflex CrAg screening of remnant blood specimens with a CD4+ T-cell (CD4) count of <100 cells/μL.[3–6] Screening was performed using a CrAg lateral flow assay (LFA) (IMMY) across a national network of 45 CD4 laboratories.[5,6] These laboratories are equipped with flow cytometry instruments to perform routine CD4+ T-cell enumeration for the national HIV program. From February 1, 2017, through September 30, 2021, 99% (n = 1,012,493) of eligible patients in the public health sector were screened, with a national prevalence of 6.0%[7] (unpublished data, National Institute for Communicable Diseases). Clinician-requested CrAg tests on blood and cerebrospinal fluid (CSF) were performed at NHLS microbiology laboratories using the same LFA method. Patients with a new positive blood CrAg result were recommended to have a lumbar puncture (LP) to exclude cryptococcal meningitis.[1] Asymptomatic patients with antigenemia who were CSF CrAg-negative or who declined an LP were recommended to be treated preemptively with fluconazole until antiretroviral treatment-mediated immune reconstitution occurs.

To ensure accurate result reporting through the screening program, all NHLS CD4 laboratories performed verification procedures before patient testing commenced in 2016. This included testing of a verification panel of random CrAg-negative and -positive samples, using the IMMY LFA kit. In addition, an in-house proficiency testing scheme (PTS) was developed in 2017 for CrAg testing of simulated blood samples; NHLS CD4 and microbiology laboratories participated in this PTS.[5] However, commonly encountered analytical and postanalytical issues are

seldom detected by these quality assurance methods. Most CrAg-positive samples included in the PTS are strongly CrAg-positive or -negative, making assessment of reading faint bands on the test strip a challenge (personal communication, NHLS Quality Assurance Department). This is the most common error noted, where faint results may be interpreted differently by individuals as the results are manually read and verified. Due to manual recording of CrAg test results on a paper worksheet before being transferred manually to the electronic laboratory information system (LIS), transcription errors can also occur.

Routine samples are tested once and authorized results are immediately reported, making it difficult to gauge the reliability of CrAg results in the routine national program. We thus assessed the reliability of routine CrAg LFA results through national interlaboratory comparison, testing during a 7-month period in 2018, with retesting at secondary laboratories and confirmatory testing of samples with discordant results at a reference laboratory. We also conducted a root cause analysis to identify the underlying reasons for discordant results, with recommendations on how these could be rectified in practice.

## Methods

### Primary CrAg Testing

Remnant-settled ethylenediaminetetraacetic acid (EDTA)-plasma samples with a confirmed CD4 count of <100 cells/μL were routinely tested by 45 CD4 laboratories using the IMMY CrAg LFA, as per the manufacturer's instructions and an internal standard operating procedure, available through a Q-Pulse quality management system portal. CrAg LFA results were routinely entered by laboratory personnel into the NHLS TrakCare electronic LIS, and authorized results were then immediately accessible to health care providers.

### Interlaboratory CrAg Testing

Interlaboratory testing was set up between paired CD4 and microbiology laboratories, most based at the same health care facility, over a 6-month period from April to October 2018. Staff training at each site was provided by the reference laboratory through on-site visits and telephone or video conference calls. The purpose of training was to explain and/or arrange CrAg retesting procedures and logistics at each laboratory pair. Participating laboratory pairs were provided with a supplementary SOP guiding additional requirements. For a period ranging from 3 to 6 months (depending on availability of reagents), each of the 45 CD4 laboratories sent a 2 mL aliquot of settled plasma from all CrAg-positive samples and a minimum of 5 CrAg-negative samples daily to their partner microbiology laboratory. The CrAg LFA results obtained by the CD4 laboratory for the selected samples, CrAg LFA lot numbers, and kit expiry dates were transcribed onto study worksheets and also sent to the microbiology laboratory, where samples were retested using the IMMY CrAg LFA method. The results of these tests, the LFA lot number, and kit expiry date were also recorded.

### Confirmation CrAg Testing at the Reference Laboratory

Concordant result lists were sent to the Mycology Reference Laboratory at the National Institute for Communicable Diseases (NICD), Johannesburg, for data capture. For discordant results, plasma samples were shipped on ice to the reference laboratory for testing within 48 hours, that included: (1) IMMY LFA strips from 2 or more lot numbers to test samples (to exclude lot-to-lot variation), with results being independently and manually read by 2 investigators; and (2) serial dilutions were performed in samples with sufficient volumes to determine CrAg titers and to exclude a high-dose hook effect.[8]

### Root Cause Analysis of Discordant Results

Possible reasons for discordant results were investigated according to the confirmatory results. A validity check was performed for quality controls and kit lot number expiry dates recorded on worksheets. For each sample with discordant results, a detailed laboratory report with recommended corrective actions was compiled. Recommendations were based on the type of preanalytical, analytical, and postanalytical errors that frequently occurred (see Supplemental Table 1). The identified issues were resolved through on-site training on CrAg testing, interpretation, and results capture followed by competency recertification. In addition, we delivered a dedicated session on CrAg test troubleshooting within an online series of training seminars to all NHLS end users. Consolidated reports were compiled and shared with each testing laboratory pair at the end of the 6-month test period. Data were captured using REDCap electronic data capture tools hosted at the University of the Witwatersrand[9] and Microsoft Excel and analyzed using Stata version 15.0 software (StataCorp). The agreement between CrAg results obtained by the primary and secondary testing laboratories was assessed using the Cohen's kappa statistic. Ethics approval was obtained from the Human Research Ethics Committee (Medical), University of the Witwatersrand (M140111 of 2014, for 5 years).

## Results

During the interlaboratory comparison period (April through October 2018), 202,345 blood specimens with a CD4 count of <100 cells/μL were eligible for CrAg screening at the 45 CD4 laboratories, of which 200,387 (99%) specimens were tested. The remaining 1958 (1%) samples were either of insufficient volume or otherwise unsuitable for CrAg testing due to hemolysis, an abnormally high viscosity, or high concentration of lipids, with the plasma appearing white or milky in color. Of the 200,387 specimens, 11,576 (5.7%) were CrAg-positive. A total of 12,502 blood samples were included in the retesting program. Of these samples, 2936 CrAg-positive (23.6%) and 9473 CrAg-negative results (76.4%) were concordant between the paired testing laboratories (**FIGURE 1**). The overall agreement between paired laboratory CrAg test results was 99.3% (Cohen's kappa statistic, 0.98). Ninety-three (0.7% of total) samples with discordant results between paired testing laboratories were sent for confirmatory testing to the reference laboratory (see Supplemental Table 2).

### Reference Laboratory Results

Of the 93 discordant samples referred to the reference laboratory, 76 (82%) were reported as LFA-positive by the primary testing CD4 laboratory but LFA-negative by the secondary testing microbiology laboratory. Of these 76 samples, the reference laboratory confirmed that 46 (61%) were indeed LFA-negative and thus discordant with the primary testing laboratory's routine results; 41/46 were also LFA-negative on serial dilutions (5 had insufficient volume for dilutions) (**TABLE 1**). Of the remaining 30/76 (39%), 1 had an insufficient volume for confirmatory testing; the other 29 were confirmed as LFA-positive at the reference laboratory (and thus concordant with the primary testing laboratory),

**FIGURE 1.** **Algorithm to test plasma samples for cryptococcal antigenemia, with primary IMMY lateral flow assay (LFA) testing at CD4 laboratories, retesting of selected samples at secondary microbiology laboratories, and confirmatory testing (IMMY LFA plus titers) of samples with discordant results at a reference laboratory.**

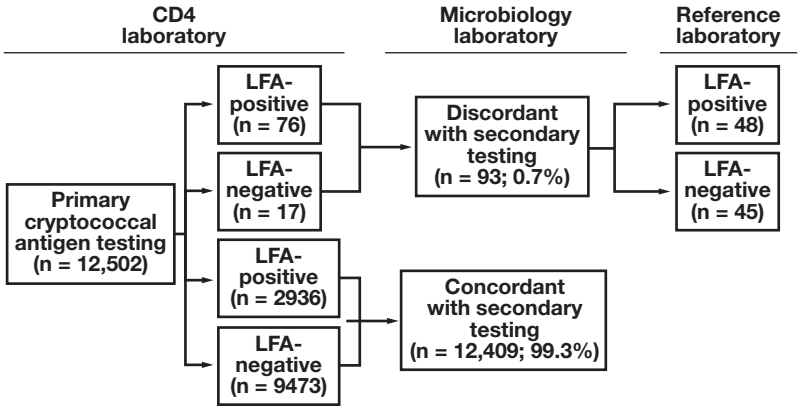


**TABLE 1.** **Samples with Discordant Results Between Paired Testing Laboratories Sent for Confirmatory Testing to the Reference Laboratory (n = 93)**

| | Reference Laboratory Results | | | Total |
|---|---|---|---|---|
| | LFA-Positive | LFA-Negative | Insufficient Sample | |
| **Primary laboratory results** | | | | |
| **LFA-positive**[a] | 29 | 46 | 1 | 76 |
| **LFA-negative**[a] | 15 | 2 | 0 | 17 |
| **Total** | 44 | 48 | 1 | 93 |

*LFA, lateral flow assay.*
[a]*Secondary laboratory results were discordant with those of the primary laboratory.*

and all (except 4 with insufficient volumes for dilutions) had a low CrAg titer of ≤80 (median titer of 5). The remaining 17/93 (18%) samples were originally reported as LFA-negative by the primary testing CD4 laboratory and were LFA-positive on retesting. Fifteen of these 17 samples were confirmed to be LFA-positive at the reference laboratory; 2 had very high LFA titers of ≥2560, 11 had low LFA titers of ≤40, and 2 had insufficient volumes for titer determination. The other 2/17 samples were LFA-negative (on serial dilutions) at the reference laboratory, confirming the result of the primary testing laboratory.

### Discordant Samples Per Testing Laboratory

The total number of samples earmarked for retesting ranged from 46 to 653 per laboratory pair (median of 246), with a range of 0 to 315 positive samples (median of 38) and 46 to 482 negative samples (median of 183) tested per laboratory pair. Twenty-two of the 45 laboratory pairs (49%) reported discordant results, ranging from 0 to 22 per laboratory pair for the 6-month period. Thus 23 of 45 (51%) laboratory pairs reported no discordant results at all during the testing period. The proportion of retested samples with discordant results ranged from 0.17% to 5.31% per laboratory pair (median 0.28%), with 42/45 laboratories reporting a proportion of <1%. Only 3 laboratory pairs, all in the same province, exceeded 3% (laboratory pair A: 22/414 [5.3%], laboratory pair B: 8/243 [3.3%], and laboratory pair C: 10/307 [3.3%]). On closer investigation of the individual data for these 3 laboratory pairs, 14/22 of the primary LFA results from laboratory pair A were confirmed as discordant at the reference laboratory, with 3/14 samples tested on 1 day. Six of 8 primary LFA results for laboratory pair B were confirmed as discordant at the reference laboratory and of these, 5/6 samples were tested at the primary laboratory on the same day. For laboratory pair C, all 10 samples with discordant results were confirmed as such at the reference laboratory and tested separately on nonconsecutive dates.

## Discussion

On average, 280,000 patients were screened per annum in the South African national reflex CrAg screening program since it was initiated in 2016.[5,10,11] This laboratory screening directly supports South Africa's large public sector HIV program and, at the time of this study, was aligned to recommendations from both the South African Department of Health and Southern African HIV Clinicians Society to screen HIV-seropositive individuals with a CD4 count of <100 cells/μL.[1,2] Clinicians can also request diagnostic CSF CrAg tests from NHLS microbiology laboratories for patients with symptomatic cryptococcal meningitis or order blood screening CrAg tests for asymptomatic patients with CD4 counts of 100 to 200 cells/μL (ie, above the current reflex CrAg testing threshold). The current study was logistically feasible because plasma samples initially tested by a CD4 laboratory could be retested by a paired microbiology laboratory on the same premises using the same standardized method of testing (ie, IMMY LFA). These conditions provided a unique opportunity to evaluate routine laboratory results reported by the national CrAg screening program through interlaboratory analysis.

Accurate result reporting in pathology laboratories is a high priority, and several systems are in place to ensure continuous excellent performance. This includes laboratory accreditation with a national

body such as the South African National Accreditation System to ISO 15189:2012, participation in external quality assessment (or proficiency testing) schemes for CD4 and CrAg testing; internal quality control per batch tested (as per manufacturer instructions); and verification of a test method upon implementation using panels of control material.[12,13] More than 98% of NHLS laboratories participated in an external quality assessment scheme for CrAg testing (personal communication, NHLS Quality Assurance Department). The limitation of this, and similar PTSs, is that each distributed survey includes a panel of strong-positive and -negative samples with fewer samples with a low antigen concentration to mimic the faint CrAg positivity often seen on LFA strips in the laboratory. The point-of-care nature of the CrAg LFA test may also pose challenges for an external quality assessment scheme, as interpretation and reporting of results are manual. Regular interlaboratory comparison would be an ideal way to assess the true number of samples with discordant results, but is not always feasible in a resource-limited country with staffing shortages and additional reagent and distribution costs.

In this study, we report interlaboratory comparative testing, for a period of 3 to 6 months at each laboratory pair, using both CrAg-negative and -positive samples for parallel testing at CD4 and microbiology laboratories, with confirmatory testing at a reference laboratory, using LFA and LFA-titer methods as standards. *Cryptococcus* cannot be cultured directly from serum or EDTA-plasma samples. However, published data has confirmed the excellent accuracy of the LFA in serum and plasma to the reference standard of CSF fungal culture among patients with cryptococcal meningitis, with superior performance compared to the older CrAg latex agglutination test.[14] In serum, there is good agreement between the enzyme immunoassay (EIA) and LFA for diagnosis of antigenemia.[15,16] The manufacturer states in the package insert that the limit of detection for the IMMY EIA is 5.3 ng/mL of antigen, while the IMMY LFA has a lower limit (ie, 1.5 to 3 ng/mL of antigen) and would thus be expected to be more sensitive than the EIA.[17,18] There is no equivalent comparison for EDTA-plasma samples since the EIA is not validated for use on this specimen matrix and thus was not used as a reference in this study. This study is not a report on method comparison under ideal laboratory conditions but instead is a reflection of daily CrAg testing results and operational challenges in routine laboratories. In this study, we also did not aim to describe national or local CrAg prevalence or test positivity rates; this information has been reported in earlier publications using a more representative study sample.[10,19,20]

Overall, only 0.7% of all samples tested in this interlaboratory comparison had discordant results across 45 paired laboratories. The median proportion of tested samples with discordant results across the 45 laboratory pairs was very low (0.28%). Twenty-three laboratory pairs did not report any samples with discordant results, while the 3 laboratories with >3% discordant results tested low daily volumes and routinely reported few CrAg-positive results; the actual number of samples with discordant results equated to <2 per month of testing. Two laboratories had several samples with discordant results reported on the same day. This could indicate a new staff member reporting or verifying results. Additional training was done at the identified 3 laboratories with recertification of staff competency through test witnessing. All other discordant results reported for the 22 testing laboratory pairs were single samples on non-consecutive days.

The discordant test results noted in this study could be in part caused by very low antigen concentrations, near the limit of detection for the LFA. This is supported by 36 samples with low antigen titers (of 81 total with sufficient volumes for serial dilutions). In addition, 2 of 81 had very high LFA titers of ≥2560, suggesting false-negative results caused by a possible high-dose hook effect. This latter issue is likely to be a far less common problem unless a patient with antigenemia has concurrent symptomatic meningitis or fungemia and thus very high plasma antigen concentrations. On root cause analysis, approximately 95% of discordant samples tested at the reference laboratory were attributed to misinterpretation of LFA bands or transcriptional errors onto the worksheet and/or LIS. Because the LFA results are manually read and interpreted, the visual acuity of the observer or poor ambient lighting could contribute to misclassification of faint-positive bands, for example. The impact of transport to the reference laboratory on sample stability was minimized by shipping samples in cold boxes, with retesting performed within 48 hours. This does not rule out the impact of sample age on retesting, as most samples tested at the primary CD4 laboratories are older than 48 hours (post venesection). Local studies have, however, indicated that CrAg results are stable over time (up to 72 hours post venesection) under controlled laboratory conditions (data not shown) when performed on settled plasma. This is also within the stipulation of the package insert of the IMMY LFA, where storage of specimens is allowed at 2°C to 8°C for up to 72 hours.

Our study highlights the importance of assessing not only strong-positive and -negative samples in PTSs but also samples with concentrations of CrAg close to the limit of detection in a panel to test the ability of laboratories to accurately identify and report on tests with faint lines. A challenge of the CrAg LFA is the manual reading and reporting of results, since this was designed for use at the point of care. The NHLS has conducted a validation of commercially available strip readers (data not shown) in an effort to reduce human error. These readers were either not suitable for multiple strip verification and/or had no LIS connectivity for direct upload of results (most use an Excel-based program for data capture). New-generation readers may address these issues and be validated for introduction into high-volume CrAg testing laboratories. Fully automated CrAg EIA systems as a possible solution to eradicate human error have also been investigated, with high sensitivity and specificity compared to the LFA (>95%). These are, however, expensive and not ideal for low- to medium-volume testing. A limitation of this study was that microbiology laboratories were not blinded to CrAg results from the CD4 laboratory for practical reasons (routinely reported authorized results from the CD4 laboratory were available on the LIS). Samples were collected over a long period to ensure adequate test numbers, yet some laboratories had either low daily test volumes and/or CrAg positivity that may have led to an overestimation of the proportion with discordant results. Not all CrAg-negative samples were retested to save costs. These data are not a reflection of CrAg prevalence because we retested selected CrAg-negative and all CrAg-positive samples at each laboratory pair for a defined period.

## Conclusion

CrAg screening results are critically important for clinical decision-making in people with advanced HIV disease, and a positive CrAg test result will prompt invasive investigations and or potentially toxic treatment regimens. Reliable and accurate results are thus essential in a screening program. This is the first study to report the operational discordant results for CrAg testing in a national screening program rather

than in the context of method validation or duplicate sample testing. Routine reflex CrAg test results were confirmed to be very reliable. Interlaboratory comparisons are useful to identify errors not detected by PTSs and internal quality control measures and should be conducted more frequently to ensure ongoing excellent performance.

## Supplementary Data

Supplemental figures and tables can be found in the online version of this article at www.labmedicine.com.

## Acknowledgments

We thank Adeboye Adelekan from US Centers for Disease Control and Prevention, South Africa; Ivy Rukasha, Molebogeng Kolojane, Phelly Matlapeng, Nikiwe Valashiya, and Siphiwe Kutta from the National Institute for Communicable Diseases; and participating staff at all National Health Laboratory Service CD4 and microbiology laboratories.

## Disclosures

CrAg LFA kits for retesting at microbiology laboratories were sourced at no cost to the National Health Laboratory Service from Immuno-Mycologics for the purpose of this project. IMMY was not involved in the design and implementation of the study or analysis of data.

## Funding

This work was supported by a Cooperative Agreement between the National Health Laboratory Service and US Centers for Disease Control and Prevention (CDC-RFA-GH15-1575), and a grant from the National Institute of Allergy and Infectious Diseases of the National Institutes of Health (www.niaid.nih.gov) under Award Number R01AI118511. The content is solely the responsibility of the authors and does not necessarily represent the official views of the National Institutes of Health or US Centers for Disease Control and Prevention.

## REFERENCES

1. Govender NP, Meintjes G, Mangena P, et al. Southern African HIV Clinicians Society guideline for the prevention, diagnosis, and management of cryptococcal disease among HIV-infected persons: 2019 update. *South Afr J HIV Med*. 2019;20(1):1–16.
2. World Health Organization. Guidelines for the diagnosis, prevention, and management of cryptococcal disease in HIV-infected adults, adolescents, and children; 2018. https://www.who.int/publications/i/item/9789241550277. Accessed May 19, 2022.
3. Coetzee L, Cassim N, Moodley K, et al. Roadmap for implementing a national early detection programme for reflexed CrAg screening in national health CD4 laboratories in South Africa. Presented at 7th South African AIDS Conference; Durban, South Africa; June 9–12, 2014.
4. Coetzee LM, Cassim N, Glencross DK. Rapid scale up of reflexed cryptococcal antigen screening across a CD4 laboratory network in South Africa. Presented at International AIDS Society Conference; Paris, France; July 23-26, 2017.
5. Govender NP, Glencross DK. National coverage of reflex cryptococcal antigen screening: a milestone achievement in the care of persons with advanced HIV disease. *South Afr Med J.* 2018;108(7):534–535.
6. Larson BA, Rockers PC, Bonawitz R, et al. Screening HIV-infected patients with low CD4 counts for cryptococcal antigenemia prior to initiation of antiretroviral therapy: cost effectiveness of alternative screening strategies in South Africa. *PLoS One*. 2016;11(7):e0158986.
7. Greene G, Desanto D, Matlapeng P, Govender N. Cryptococcal antigen screening surveillance report, South Africa, February 2017–July 2019. NICD Public Health Surveillance Bulletin, 2019. https://www.nicd.ac.za/wp-content/uploads/2019/12/CRYPTOCOCCAL-ANTIGEN-SCREENING-SURVEILLANCE-NICD-Bulletin-Vol17-Iss3-December2019.pdf. Updated December 1, 2019. Accessed May 19, 2022.
8. Lourens A, Jarvis JN, Meintjes G, Samuel CM. Rapid diagnosis of cryptococcal meningitis by use of lateral flow assay on cerebrospinal fluid samples: influence of the high-dose "hook" effect. *J Clin Microbiol*. 2014;52(12):4172–4175.
9. Harris PA, Taylor R, Minor BL, et al. The REDCap consortium: building an international community of software platform partners. *J Biomed Inform*. 2019;95:103208.
10. Cassim N, Coetzee LM, Govender NP, et al. District and sub-district analysis of cryptococcal antigenaemia prevalence and specimen positivity in KwaZulu-Natal, South Africa. *Afr J Lab Med*. 2018;7(1):1–8.
11. Coetzee LM, Cassim N, Glencross DK. Cryptococcal antigen (CrAg) positivity rates reported from a national CD4-reflexed screening programme identify high-risk regions of co-existent HIV/Cryptococcal disease, requiring urgent programmatic focus into care. Presented at 11th Interest Workshop; Lilongwe, Malawi; May 16–19, 2017.
12. Glencross DK, Aggett HM, Stevens WS, et al. African regional external quality assessment for CD4 T-cell enumeration: development, outcomes, and performance of laboratories. *Cytometry*. 2008;74(S1):S69–S79.
13. Glencross DK, Janossy G, Coetzee LM, et al. Large-scale affordable PanLeucogated CD4+ testing with proactive internal and external quality assessment: in support of the South African national comprehensive care, treatment and management programme for HIV and AIDS. *Cytometry*. 2008;74(S1):S40–S51.
14. Jarvis JN, Percival A, Bauman S, et al. Evaluation of a novel point-of-care cryptococcal antigen test on serum, plasma, and urine from patients with HIV-associated cryptococcal meningitis. *Clin Infect Dis*. 2011;53(10):1019–1023.
15. Hansen J, Slechta ES, Gates-Hollingsworth MA, et al. Large-scale evaluation of the immuno-mycologics lateral flow and enzyme-linked immunoassays for detection of cryptococcal antigen in serum and cerebrospinal fluid. *Clin Vaccine Immunol*. 2013;20(1):52–55.
16. Lindsley MD, Mekha N, Baggett HC, et al. Evaluation of a newly developed lateral flow immunoassay for the diagnosis of cryptococcosis. *Clin Infect Dis*. 2011;53(4):321–325.
17. Immy Mycologics. ALPHA cryptococcal antigen EIA. https://immy.com/package_inserts/cry101/CRY101%20IFU%20-%20English.pdf. Accessed May 19, 2022.
18. Immy Mycologics. Cryptococcal antigen lateral flow assay. 2016. https://www.immy.com/package_inserts/cr2003/CR2003%20IFU%20(Int'l)%20-%20English.pdf. Accessed May 19, 2022.
19. Coetzee L-M, Cassim N, Glencross DK. Using laboratory data to categorise CD4 laboratory turn-around-time performance across a national programme. *Afr J Lab Med*. 2018;7(1):1–7.
20. Coetzee L-M, Cassim N, Sriruttan C, et al. Cryptococcal antigen positivity combined with the percentage of HIV-seropositive samples with CD4 counts <100 cells/μl identifies districts in South Africa with advanced burden of disease. *PLoS One*. 2018;13(6):e0198993.

# Clinical Value of Early-Pregnancy Glycated Hemoglobin, Fasting Plasma Glucose, and Body Mass Index in Screening Gestational Diabetes Mellitus

*Yanqin Lou, MM,[1,a] Li Xiang, MM,[1,a] Xuemei Gao, MM,[1] and Huijun Jiang, MM[1,*]*

[1]Department of Obstetrics, The No. 1 Hospital of Wuhan, Wuhan, Hubei Province, China. *To whom correspondence should be addressed. jianghj_060821@163.com
[a]Yanqin Lou and Li Xiang are first authors.

**Keywords:** fasting plasma glucose, glycated hemoglobin, body mass index, gestational diabetes mellitus, pregnancy, receiver operator characteristic

**Abbreviations:** HbA1c, glycated hemoglobin; FPG, fasting plasma glucose; BMI, body mass index; GDM, gestational diabetes mellitus; OGTT, oral glucose tolerance test; ROC, receiver operating characteristic; OR, odds ratio; AUC, area under the curve.

*Laboratory Medicine* 2022;53:619–622; https://doi.org/10.1093/labmed/lmac058

## ABSTRACT

**Objective:** To investigate clinical values of early-pregnancy (8–13 weeks) glycated hemoglobin (HbA1c), fasting plasma glucose (FPG), and body mass index (BMI) in screening gestational diabetes mellitus (GDM).

**Methods:** A total of 1120 cases underwent a 75 g oral glucose tolerance test (OGTT), of which 216 cases with GDM were selected as the study group, and 278 cases without GDM were selected as the control group. FPG, HbA1c, and BMI in early pregnancy were measured. The correlation between FPG, HbA1c and BMI in early pregnancy and the incidence of GDM was analyzed by binary logistic regression, and the value of each index in predicting GDM alone or in combination was evaluated.

**Results:** FPG, HbA1c, and BMI in early pregnancy in the GDM group were higher than those in the control group, and the differences were statistically significant ($P < .05$). Binary logistic regression analysis showed that FPG, HbA1c, and BMI were risk factors for GDM in early pregnancy (odds ratio [OR] values were 3.374 [$P < .05$], 4.644 [$P < .001$], and 1.077 [$P < .001$], respectively). The area under the receiver operating characteristic (ROC) curve of FPG, glycated hemoglobin, and BMI in screening GDM for early pregnancy were 0.647, 0.661, and 0.608, respectively, while the area under the ROC curve of the combination of these 3 indicators was 0.736.

**Conclusion:** We found that FPG, HbA1c, and BMI in early pregnancy might be the potential risk factors for the occurrence of GDM, and the combination of them had certain clinical predictive value for GDM. However, it is still necessary for more studies, especially prospective studies, to validate our findings in the future.

Gestational diabetes mellitus (GDM), defined as a metabolic disease in which abnormal blood glucose is first detected during, but not before, the pregnancy, can lead to adverse pregnancy outcomes, such as ketoacidosis, gestational hypertension, fetal macrosomia, intrauterine growth restriction, fetal distress, etc, and is associated with the increased risk of developing type 2 diabetes after delivery.[1,2] Due to the high incidence and multiple adverse effects of GDM, early screening and diagnosis allows timely intervention and reduction of the occurrence of adverse pregnancy outcomes. At present, the oral glucose tolerance test (OGTT) has been recommended for the diagnosis of GDM at 24–28 weeks of gestation, but OGTT requires complicated operations and more time, resulting in poor acceptance and compliance of pregnant women.[3,4] It is also susceptible to other factors, the details of which are as follows: (1) dietary control and living habits around the OGTT affect the outcome; (2) a small number of pregnant women experience nausea and vomiting after taking the glucose solution, which also affects blood sugar; (3) a small number of pregnant women do not draw blood on time after drinking the glucose solution, which leads to an inaccurate outcome. If there were more convenient and simpler methods for screening GDM at an earlier stage, it will become possible to perform earlier clinical intervention, thereby reducing the risk of adverse perinatal outcomes. The purpose of this study was to determine the clinical value of early-pregnancy (8–13 weeks) glycated hemoglobin (HbA1c), fasting plasma glucose (FPG), and body mass index (BMI) in screening for GDM.

## Materials and Methods

This study was conducted in accordance with the declaration of Helsinki. This study was conducted with approval from the Ethics Committee of The No. 1 Hospital. Written informed consent to publish the clinical details and images of the patients was obtained.

### Participants

We selected 1120 cases of women with singleton pregnancy who had their records and regular maternity checkups in our hospital from May 2017 to May 2019. All of the 1120 cases underwent 75 g OGTT, of which 216 cases were diagnosed with GDM, with an incidence of 19%, and the other 994 cases did not suffer GDM. The 216 cases with GDM were selected as the study group. Of the 994 cases without GDM, 278 cases were randomly selected as the control group.

Exclusion criteria were as follows: multiple pregnancies; patients with prepregnancy diabetes, hypertensive diseases, thyroid dysfunction, and combined disease of the liver and kidney or tumor; and patients with gestational hypertensive disease during pregnancy.

### Methods

All pregnant women had fasting blood glucose and glycated hemoglobin tests as well as their BMI measured at the phase of early pregnancy (8–13 weeks) and took a 1-step 75 g 2-hour OGTT to diagnose GDM at 24–28 weeks. All pregnant women fasted for 12 hours before blood sampling, and 5 mL of brachial venous blood was collected on the following morning to determine FPG, HbA1c, and BMI. BMI formula = weight/height squared (kg/m$^2$).

### Diagnosis

A 1-step 75 g OGTT was performed following overnight fasting (for 12 hours). A diagnosis of GDM is made if 1 plasma glucose value is abnormal (fasting ≥5.1 mmol/L, 1 hour ≥10.0 mmol/L, 2 hours ≥8.5 mmol/L).[5]

### Statistical Methods

The data of the 2 groups were analyzed using SPSS 20. The mean ± standard deviation was used to express the measurement data. Independent sample t-test was used for comparison between groups if the variance was equal. $\chi^2$ test was used to count the data. $P < .05$ indicated that the difference was statistically significant. The influencing factors were analyzed by binary logistic regression, and ROC curves were drawn to analyze the clinical value of BMI, FPG, HbA1c, and the combination of them all in predicting GDM.

## Results

### Comparison of General Data of Pregnant Women Between Two Groups

There was no statistically significant difference ($P > .05$) between the 2 groups in terms of maternal age, gravidity, and parity. The BMI of the study group was higher than that of the control group with a statistically significant difference ($P < .05$). See **TABLE 1**.

### Comparison of FPG and HbA1c of Pregnant Women Between Two Groups

The FPG and HbA1c levels in the study group were higher than those in the control group, with a statistically significant difference ($P < .05$). See **TABLE 2**.

### The Correlation Between GDM and Serum FPG, HbA1c, and BMI in Pregnant Women

Logistic regression analysis showed that FPG, HbA1c, and BMI in early pregnancy had significant correlations with the occurrence of GDM ($P < .05$), with OR values of 3.374, 4.644, and 1.077, respectively, which suggested FPG, HbA1c, and BMI might be the potential risk factors for the occurrence of GDM. See **TABLE 3**.

### Predictive Value of the Combination of the Three Indicators for GDM

FPG, HbA1c, and BMI individually predicted GDM with sensitivities of 0.588, 0.505, and 0.634, and specificities of 0.633, 0.745, and 0.554, while the combination of the 3 had the sensitivity of 0.689 and the specificity of 0.640. The area under the curve (AUC) of the combination curve was 0.736, significantly higher than that of the individual test (FPG, 0.647; HbA1c, 0.661; BMI, 0.608), as shown in **FIGURE 1** and **TABLE 4**.

## Discussion

The prevalence of GDM has gradually increased,[6] accompanied by the improved living standard and constantly revised diagnostic criteria for GDM in recent years, threatening the mental and physical health of pregnant women and the safety of the fetus. Despite this, the cause of GDM remains unclear. The generally accepted explanation at the moment is insulin resistance and islet cell damage from various causes,[7] although the exact mechanism is still uncertain.[1] The internationally recognized diagnostic criterion of GDM is OGTT at 24–28 weeks of gestation, but there are no approaches to do the diagnosis in early pregnancy, so that it is impossible to perform the early intervention. Therefore, in recent years, many investigators have committed to exploring the reliable screening indicators of GDM in early pregnancy.

Some studies have revealed a certain correlation between early-pregnancy FPG, HbA1c, BMI, and GDM.[8] FPG in early pregnancy is the initial screening of blood glucose during pregnancy. Han[9] found that fasting blood glucose in early pregnancy has predictive value for GDM, which is consistent with this study. HbA1c is originally used to measure the level of glycemic control in recent months.[10] At present, there has been a fierce debate on whether HbA1c can be used for GDM screening in early pregnancy. It is generally accepted that HbA1c is a reflection of blood glucose over the past 3 months. It allows blood sampling at

**TABLE 1. Comparison of General Data of Pregnant Women Between Two Groups (Mean ± SD)**

| Groups | Age (y) | Gravidity (No.) | Parity (No.) | BMI (kg/m2) |
|---|---|---|---|---|
| Study (GDM) group (n = 216) | 29.39 ± 4.70 | 1.95 ± 0.86 | 0.48 ± 0.54 | 26.08 ± 5.21 |
| Control group (n = 278) | 29.05 ± 4.74 | 2.04 ± 0.79 | 0.43 ± 0.53 | 24.09 ± 4.55 |
| *t* | 0.810 | 1.170 | 1.009 | 4.435 |
| *P* | .418 | .243 | .314 | <.001 |

*BMI, body mass index; GDM, gestational diabetes mellitus.*

**TABLE 2. Comparison of FPG and HbA1c Levels in Early Pregnancy Between Two Groups (Mean ± SD)**

| Groups | FPG (mmol/L) | HbA1c (%) |
|---|---|---|
| Study (GDM) group (n = 216) | 4.02 ± 0.44 | 4.81 ± 0.37 |
| Control group (n = 278) | 3.79 ± 0.44 | 4.60 ± 0.35 |
| *t* | 5.905 | 6.441 |
| *P* | <.001 | <.001 |

*FPG, fasting plasma glucose; GDM, gestational diabetes mellitus; HbA1c, glycated hemoglobin.*

**TABLE 3. The Correlation Between Serum FPG, HbA1c Levels, BMI, and GDM**

| Items | β | SD | Wals $\chi^2$ | *P* | OR (95% CI) |
|---|---|---|---|---|---|
| BMI | 0.074 | 0.021 | 12.983 | <.001 | 1.077 (1.035–1.122) |
| FPG | 1.216 | 0.235 | 26.667 | .010 | 3.374 (2.127–5.353) |
| HbA1c | 1.536 | 0.284 | 29.148 | <.001 | 4.644 (2.659–8.109) |

*BMI, body mass index; CI, confidence interval; FPG, fasting plasma glucose; GDM, gestational diabetes mellitus; HbA1c, glycated hemoglobin; OR, odds ratio.*

**FIGURE 1. Receiver operator characteristic (ROC) curves of glycated hemoglobin (HbA1c), fasting plasma glucose (FPG), and body mass index (BMI) individually predicting gestational diabetes mellitus (GDM), and the ROC curve of the 3 combined predicting GDM.**

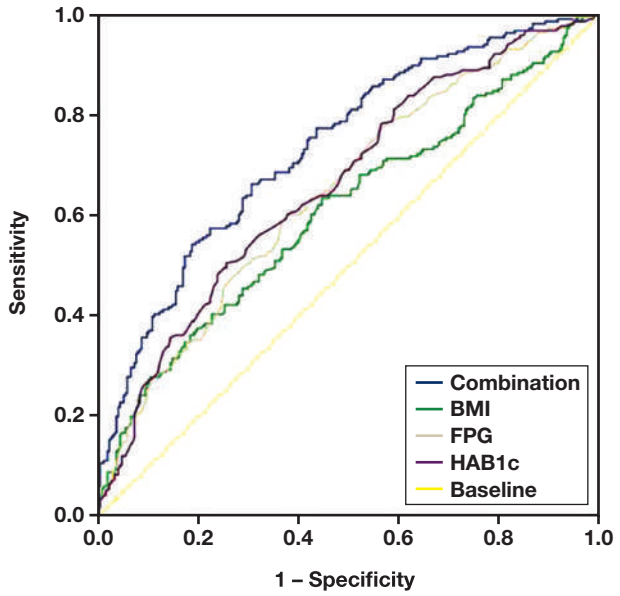


any time without fasting, which is easier to perform and more acceptable to patients, with better compliance from pregnant women, thereby benefiting clinical work. In this study, early-pregnancy HbA1c and FPG of pregnant women with GDM were found to be higher than those in the control group, which is consistent with an earlier study.[11] Regression analysis showed that HbA1c and FPG were high-risk factors for GDM, and high levels of early-pregnancy HbA1c and FPG could predict the occurrence of GDM.

Studies have shown that obese patients have more severe insulin resistance and impaired pancreatic β-cell function. A meta-analysis[12] showed that overweight and obese pregnant women were 2.01 times more likely to develop GDM than those with a normal BMI. Therefore, diet, lifestyle intervention, and weight control are important parts of GDM therapy.[13] Studies by Harper et al[14] and Li et al[15] suggest that early detection of GDM in obese women can prevent fetal overgrowth and reduce perinatal outcomes such as macrosomia. This study found that pregnant women who developed GDM also had a higher body mass index in early pregnancy than those in the control group. Logistic regression analysis suggests that pregnant women with a high BMI are 1.077 (95% CI, 1.035–1.122) times more likely to develop GDM than those with a low BMI, indicating that BMI in early pregnancy might be a risk factor for GDM. However, there are still some limitations in our study, such as a small sample size and the use of a single center.

In this study, we found that early-pregnancy FPG, HbA1c, and BMI of pregnant women with GDM were higher than those of the control group. The ROC curve analysis showed that the AUC values of FPG, HbA1c, and BMI in predicting GDM were 0.647, 0.661, and 0.608, respectively; the sensitivity was 0.588, 0.505, and 0.634, respectively; and the specificity was 0.633, 0.745, and 0.554, respectively. The AUC value of the combination of FPG, HbA1c, and BMI was 0.736, with a sensitivity of 0.689 and a specificity of 0.640. These implied that the combination of the 3 indicators in early pregnancy was more accurate in clinically predicting GDM than using each indicator alone. Currently, 75 g OGTT at 24–28 weeks of gestation is used to diagnose GDM. This test requires waiting for 2 hours and blood draws 3 times, which increases the burden on patients. What's more, it cannot be used to identify GDM in the first trimester, so that early intervention on GDM cannot be performed. The actual situation in clinical practice is that some high-risk pregnant women have high blood sugar in the first trimester, and high blood sugar affects both the fetus and mother. If high blood sugar is detected early, it can be treated by diet, exercise, weight control, and oral medication, accompanied by monitoring blood sugar, to reduce the impact of hyperglycemia on the fetus and mother. Our present study examined glycated hemoglobin and fasting plasma glucose in the first trimester and prepregnancy body mass index to identify women who will develop GDM in the future for which interventions can be employed to reduce the incidence of GDM-associated complications. The combination of

**TABLE 4. Comparison of the Efficacy of Individual and Combined Tests for GDM Diagnosis**

| Items | AUC | 95% CI | *P* | Sensitivity | Specificity | Maximum Younden index |
|---|---|---|---|---|---|---|
| BMI | 0.608 | 0.558–0.659 | <.001 | 0.634 | 0.554 | 0.188 |
| FPG | 0.647 | 0.598–0.695 | <.001 | 0.588 | 0.633 | 0.221 |
| HbA1c | 0.661 | 0.613–0.709 | <.001 | 0.505 | 0.745 | 0.249 |
| Combination | 0.736 | 0.692–0.779 | <.001 | 0.689 | 0.640 | 0.356 |

*AUC, area under the curve; BMI, body mass index; CI, confidence interval; FPG, fasting plasma glucose; HbA1c, glycated hemoglobin.*

the 3 indicators were more effective in identifying GDM patients than each one alone. This method may be simpler than the conventional 75 g OGTT. At present, a unified standard for early prediction of GDM has not yet come into being in clinical practice, and multicenter prospective randomized controlled trials with large sampling are necessary to provide a solid theoretical basis for early prediction of GDM, early intervention, and less incidence of adverse perinatal outcomes.

## Conclusion

Our present study found that FPG, HbA1c, and BMI in early pregnancy might be the potential risk factors for the occurrence of GDM, and the combination of them had certain clinical predictive value for GDM. However, it is still necessary for more studies, especially prospective studies, to validate our findings.

## Data Availability

The datasets used and/or analyzed during the current study are available from the corresponding author on reasonable request.

## REFERENCES


1. Peng HY, Li HP, Li MQ. Downregulated ABHD5 aggravates insulin resistance of trophoblast cells during gestational diabetes mellitus. *Reprod Sci*. 2020;27:233–245. doi: 10.1007/s43032-019-00010-x.
2. Zhou P, Cong L, Yuan J, et al. Nuclear transcription factor-κ B and the relationship between the pathogenesis of gestational diabetes [in Chinese]. *J Pract Obstet Gynecol.* 2017;33:189–193.
3. Koivusalo SB, Rönö K, Klemetti MM, et al. Gestational diabetes mellitus can be prevented by lifestyle intervention: the Finnish Gestational Diabetes Prevention Study (RADIEL): a randomized controlled trial. *Diabetes Care*. 2016;39:24–30. doi: 10.2337/dc15-0511.
4. Artzi NS, Shilo S, Hadar E, et al. Prediction of gestational diabetes based on nationwide electronic health records. *Nat Med*. 2020;26:71–76. doi: 10.1038/s41591-019-0724-8.
5. American Diabetes Association. Classification and diagnosis of diabetes. *Diabetes Care*. 2015;38:S8–S16. doi: 10.2337/dc15-S005.
6. Guan H, Shang LX. Prevalence of gestational diabetes mellitus [in Chinese]. *Chin J Pract Gynecol Obstet.* 2015;31:91–94. doi: 10.7504/fk2014120120.
7. Lal KK, Jarwar R, Farhat S, Fatima SS. Association of Vaspin levels and its SNP rs2236242 with gestational diabetes at a tertiary care setting. *J Pak Med Assoc*. 2018;68:1736–1740.
8. Kansu-Celik H, Ozgu-Erdinc AS, Kisa B, Eldem S, Hancerliogullari N, Engin-Ustun Y. Maternal serum glycosylated hemoglobin and fasting plasma glucose predicts gestational diabetes at the first trimester in Turkish women with a low-risk pregnancy and its relationship with fetal birth weight: a retrospective cohort study. *J Matern Fetal Neonatal Med*. 2021;34:1970–1977. doi: 10.1080/14767058.2019.1651837.
9. Han WL. Predictive value of fasting blood glucose in early pregnancy for gestational diabetes mellitus [in Chinese]. *J Pract Obstet Gynecol.* 2020;36:200–203.
10. Braga FO, Negrato CA, Matta MFBD, Carneiro JRI, Gomes MB. Relationship between inflammatory markers, glycated hemoglobin and placental weight on fetal outcomes in women with gestational diabetes. *Arch Endocrinol Metab*. 2019;63:22–29. doi: 10.20945/2359-3997000000099.
11. Zhao M, Li GH. The value of fasting plasma glucose and lipid profiles between 7 and 15 gestational weeks in the prediction of gestational diabetes mellitus [in Chinese]. *Chin J Obstet Gynecol.* 2016;51:835–839. doi: 10.3760/cma.j.issn.0529-567x.2016.11.007.
12. Najafi F, Hasani J, Izadi N, et al. The effect of prepregnancy body mass index on the risk of gestational diabetes mellitus: a systematic review and dose-response meta-analysis. *Obes Rev*. 2019;20:472–486. doi: 10.1111/obr.12803.
13. Wang WJ. Effects of individualized dietary therapy on pregnancy outcomes in patients with gestational diabetes mellitus [in Chinese]. *Diabetes New World.* 2017;20:15–16. doi: 10.16658/j.cnki.1672-4062.2017.13.015.
14. Harper LM, Jauk V, Longo S, Biggio JR, Szychowski JM, Tita AT. Early gestational diabetes screening in obese women: a randomized controlled trial. *Am J Obstet Gynecol*. 2020;222:495.e1–495.e8. doi: 10.1016/j.ajog.2019.12.021.
15. Li M, Hinkle SN, Grantz KL, Kim S, et al. Glycaemic status during pregnancy and longitudinal measures of fetal growth in a multiracial US population: a prospective cohort study. *Lancet Diabetes Endocrinol*. 2020;8:292–300. doi: 10.1016/S2213-8587(20)30024-3.

# Treatment of COVID-19 Patients with Two Units of Convalescent Plasma in a Resource-Constrained State

*Tina S. Ipe, MD, MPH,[1,2,*] Blessing Ugwumba, BMLS,[1] Horace J. Spencer, MS,[3] Tuan Le, MD,[2] Terry Ridenour,[2] John Armitage, MD,[2] Stefanie Ryan, APRN,[4] Shanna Pearson, APRN,[4] Atul Kothari, MD,[4] Naveen Patil, MD,[4] Ryan Dare, MD,[5] Juan C. R. Crescencio, MD,[5] Anand Venkata, MD,[6] Jennifer Laudadio, MD,[1] Khalid Mohammad, MD,[7] Naznin Jamal, MD,[8] John Thompson, MD,[9] Hailey McNew, MHSA,[10] McKenzie Gibbs,[11] Steve Hennigan, MD,[12] Stan Kellar, MD,[13] Keith Reitzel, MD,[14] Brandon E. Walser, MD,[15] Amanda Novak, MD,[16] Brian Quinn, MD[17]*

[1]Department of Pathology and Laboratory Medicine, University of Arkansas for Medical Sciences, Little Rock, AR, USA, [2]Oklahoma/Texas/and Arkansas Blood Institute, Oklahoma City, OK, USA, [3]Department of Biostatistics, University of Arkansas for Medical Sciences, Little Rock, AR, USA, [4]Arkansas Department of Health, Little Rock, AR, USA, [5]Department of Internal Medicine, Division of Infectious Diseases, University of Arkansas for Medical Sciences, Little Rock, AR, USA, [6]Division of Pulmonary and Critical Care Medicine, Department of Internal Medicine, University of Arkansas for Medical Sciences, Little Rock, AR, USA, [7]Division of Pulmonary and Critical Care Medicine, Department of Internal Medicine, Jefferson Regional Medical Center, Pine Bluff, AR, USA, [8]Department of Internal Medicine, Jefferson Regional Medical Center, Pine Bluff, AR, USA, [9]Division of Pulmonary and Critical Care Medicine, Department of Internal Medicine, St Bernards Healthcare, Jonesboro, AR, USA, [10]Research Center, St Bernards Healthcare, Jonesboro, AR, USA, [11]Department of Laboratory Medicine, Northwest Medical Center, Springdale, AR, USA, [12]Department of Internal Medicine, Washington Regional Medical Center, Fayetteville, AR, USA, [13]Department of Pulmonary Medicine, Baptist Health, Little Rock, AR, USA, [14]Baptist Health, Fort Smith, AR, USA, [15]Department of Infectious Diseases, Baptist Health, Little Rock, AR, USA, [16]Department of Infectious Diseases, Baptist Health, North Little Rock, AR, USA, [17]Department of Pathology, Baptist Health, Little Rock, AR, USA.
*To whom correspondence should be addressed. tina.ipe@obi.org

**Keywords:** CCP, SARS-CoV-2, plasma, clinical study, outcome analysis, low-resource

**Abbreviations:** CCP, COVID-19 convalescent plasma; FDA, (US) Food and Drug Administration; eIND, emergency Investigational New Drug; COVID-19, coronavirus disease 2019; SARS-CoV-2, severe acute respiratory syndrome coronavirus 2; AICP, Arkansas Initiative for Convalescent Plasma; S/Co, signal to cutoff; UAMS, University of Arkansas for Medical Sciences; CPH, Cox proportional hazards; ICU, intensive care unit; RCT, randomized controlled study; WHO, World Health Organization; EUA, Emergency Use Authorization.

*Laboratory Medicine* 2022;53:623–628; https://doi.org/10.1093/labmed/lmac055

## ABSTRACT

**Objective:** Many therapies are used to treat COVID-19, the disease caused by the virus SARS-CoV-2, including convalescent plasma. The clinical utility of using 2 units of convalescent plasma for COVID-19 hospitalized patients is not fully understood. Our study aims to determine the safety and efficacy of treating hospitalized COVID-19 patients with 2 units of COVID-19 convalescent plasma (CCP).

**Method:** This was a retrospective study of Arkansas patients treated with CCP using the (US) Food and Drug Administration (FDA) emergency Investigational New Drug (eIND) mechanism from April 9, 2020, through August 9, 2020. It was a multicenter, statewide study in a low-resource setting, which are areas that lack funding for healthcare cost coverage on various levels including individual, family, or social. Adult patients (n = 165, volunteer sample) in Arkansas who were hospitalized with severe or life-threatening acute COVID-19 disease as defined by the FDA criteria were transfused with 2 units of CCP (250 mL/unit) using the FDA eIND mechanism. The primary outcome was 7- and 30-day mortality after the second unit of CCP.

**Results:** Unadjusted mortality was 12.1% at 7 days and 23.0% at 30 days. The unadjusted mortality was reduced to 7.7% if the first CCP unit was transfused on the date of diagnosis, 8.7% if transfused within 3 days of diagnosis, and 32.0% if transfused at or after 4 or more days of diagnosis. The risk of death was higher in patients that received low, negative, or missing titer CCP units in comparison to those that received higher titer units.

**Conclusion:** The provision of 2 units of CCP was associated with a reduction in mortality in patients treated with high titer units within 3 days of COVID-19 diagnosis. Given the results, CCP is a viable, low-cost therapy in resource-constrained states and countries.

Coronavirus disease 2019 (COVID-19), which is caused by the severe acute respiratory syndrome coronavirus 2 (SARS-CoV-2), was first reported in Arkansas on March 11, 2020.[1] The Arkansas Initiative for Convalescent Plasma (AICP) was a statewide effort to provide COVID-19 convalescent plasma (CCP) to every patient in Arkansas diagnosed with

COVID-19 disease. This collaborative effort by several hospitals in the state and the Arkansas Department of Health was initiated because Arkansans experience many barriers to accessing healthcare, including potentially life-saving therapies.

Convalescent plasma is a passive antibody therapy that has been used successfully to treat respiratory illnesses during previous epidemics.[2,3] Given early reports of mortality secondary to COVID-19 in the United States during the early phases of the pandemic and the lack of effective treatment to combat the disease, patients in Arkansas were treated with CCP via the Food and Drug Administration (FDA) emergency Investigational New Drug (eIND) mechanism. Patients began receiving 2 units of CCP starting in April 2020. The AICP provided oversight and coordination for providing 2 units of CCP for adult patients with severe or life-threatening COVID-19 in many hospitals in the state. We performed exploratory analyses on the efficacy and safety of CCP and present here the first large multicenter study on this treatment for this patient population in the United States.

## Methods

### Population

A retrospective medical chart review was conducted of 165 patients treated for COVID-19 with 2 units of CCP at 5 hospitals in Arkansas utilizing the FDA eIND mechanism. Two units of CCP were provided in accordance with an interinstitutional protocol established by the participating hospitals in Arkansas. We previously described the process for providing CCP in Arkansas through the AICP program.[1] Eligible patients were adults 18 years or older meeting the following FDA criteria: laboratory-confirmed COVID-19 and severe or immediately life-threatening COVID-19 disease.[4] Severe disease was defined as having 1 or more of the following: shortness of breath (dyspnea), respiratory frequency >30/min, blood oxygen saturation <93%, partial pressure of arterial oxygen to fraction of inspired oxygen ratio <300, and lung infiltrates >50% determined radiographically by computed tomography within 24 to 48 hours.[5] Immediately life-threatening disease was defined as having 1 or more of the following: respiratory failure, septic shock, and multiple organ dysfunction or failure.[5] Informed consent was obtained from either the patient or a healthcare proxy before CCP was transfused.

Compatible or low-titer isohemagglutinin, anti-A and/or anti-B, CCP was administered according to the transfusion policies and practices at the 5 participating institutions. Some of these institutions had satellite facilities that participated in this study. Two units of CCP (approximately 250 mL each) were transfused to each patient. The second unit was transfused approximately 24 hours after the first unit, according to an interinstitutional protocol.

### Convalescent Plasma

CCP was obtained from a registered and licensed blood collector. It was donated by individuals who had recovered from COVID-19 and met the following FDA criteria: (1) evidence of COVID-19 documented by a diagnostic test (eg, nasopharyngeal swab) at the time of illness; (2) complete resolution of symptoms at least 14 days before the donation; (3) male donors, female donors who had never been pregnant, or female donors who had tested negative for HLA antibodies since their most recent pregnancy; and (4) negative diagnostic results for COVID-19 if donating after 14 days or before 28 days postsymptom resolution.[4] Antibody titer and neutralizing antibody testing were not performed at the time of CCP donation. However, the blood center collected retention serum samples from each convalescent plasma donation in Arkansas. A total of 500 of these serum samples were randomly tested for antibody titers. Antibody titer testing was performed using an immunometric/sandwich ELISA-based assay which detects IgG antibodies to the spike protein of SARS-CoV-2 (Ortho Vitros anti-SARS-CoV-2 IgG; Ortho Clinical Diagnostics). The signal to cutoff (S/Co) ratio of the SARS-CoV-2 IgG immunoassay was defined as follows in the study: >12 (high titer), <11.99 to 1 (low titer), and <0.99 (negative).

### Data Collection

The University of Arkansas for Medical Sciences (UAMS) served as the academic research institution coordinating the collection of this exploratory data. After an institutional review board protocol was issued, a data use agreement was obtained from the 5 hospitals included in this study. A form was provided to the hospitals for the collection of laboratory and clinical parameters, including CCP administration and transfusion reaction reporting. Patient information was collected concurrently with their hospital admission and treatment with CCP. The clinical data were abstracted retrospectively from 165 patients' charts using a standardized data collection form by healthcare providers at each institution and then reviewed by a second physician at UAMS. The data were transferred for analysis into an Excel file.

### Statistical Analysis

Patients who were transfused with 2 units of CCP between April 9, 2020, and August 9, 2020, were included in our analyses. This allowed for a 7- and 30-day follow-up after the transfusions. Demographic and baseline medical characteristics were summarized using counts and percentages. Our primary outcome was 7- and 30-day mortality after transfusion with the second unit of CCP. Unadjusted mortality estimates and corresponding 95% confidence intervals were calculated. Crude mortality for various demographic and treatment categories was also estimated. A Cox proportional hazards (CPH) model was used to compare the survival distributions between the titer groups. Titer results were available for 54 (33%) patients in the study. For the CPH model, patients for whom titer testing was not performed were classified as "missing."

## Results

### Patient Demographics and Characteristics

A total of 165 patients who were transfused with 2 units of CCP using the FDA eIND between April 9 and August 9, 2020, were included in the analyses. Five hospitals provided the data. These hospitals were representative of the 5 metropolitan regions in the state. Demographic and medical characteristics are presented in **TABLE 1**. The male to female ratio was 1.7:1. White (n = 77, 46.67%) and Black (n = 62, 37.58%) patients made up the majority of COVID-19 cases in our sample, and most patients (n = 127, 76.97%) received CCP within the first 3 days of diagnosis. A large percentage of patients were in the intensive care unit (ICU) and progressing to respiratory failure but were not on a ventilator at the time of CCP transfusion (n = 124, 75.15%). The majority of patients had at least 1 or more comorbidities (n = 149, 90.30%), with 29.70% (n = 82) having 1 to 2, and 40.61% (n = 67) having 3 or more comorbidities. The

**TABLE 1. Summary of Demographic, Medical, and Outcome Characteristics of the Patients (n = 165) Included in This Study**

| Variable | No. (%) |
|---|---|
| Age, y | |
| 18–39 | 9 (5.45) |
| 40–59 | 58 (35.15) |
| 60–69 | 46 (27.88) |
| 70–79 | 38 (23.03) |
| 80+ | 14 (8.48) |
| Sex | |
| Female | 62 (37.58) |
| Male | 103 (62.42) |
| Race | |
| White | 77 (46.67) |
| Black | 62 (37.58) |
| Hispanic | 15 (9.09) |
| Other | 11 (6.67) |
| Time to first CCP transfusion, d | |
| 0 | 13 (7.88) |
| 1–3 | 127 (76.97) |
| 4+ | 25 (15.15) |
| On ventilator prior to CCP transfusion? | |
| Yes | 41 (24.85) |
| No | 124 (75.15) |
| In ICU prior to CCP transfusion? | |
| Yes | 89 (53.94) |
| No | 76 (46.06) |
| No. of comorbidities | |
| 0 | 16 (9.70) |
| 1–2 | 82 (49.70) |
| 3+ | 67 (40.61) |
| Medications | |
| Remdesivir | 105 (63.64) |
| Hydroxychloroquine | 8 (4.85) |
| Mortality | |
| 7-day | 20 (12.12) |
| 30-day | 38 (23.03) |

*CCP, COVID-19 convalescent plasma; ICU, intensive care unit.*

most common comorbidities were hypertension (n = 114, 69.1%), diabetes mellitus (n = 76, 46.1%), obesity (n = 59, 35.8%), hypercholesterolemia (n = 49, 29.7%), pulmonary disease (n = 29, 17.6%), and renal disease (n = 26, 15.8%). Many patients (n = 105, 63.64%) received remdesivir before receiving the 2 units of CCP.

### Efficacy of CCP in COVID-19

The unadjusted mortality was 12.1% (n = 20; 95% CI, 7.6%-18.1%) at 7 days and 23.0% (n = 38; 95% CI, 16.8%-30.2%) at 30 days for the patients who received 2 units of CCP. The unadjusted mortality was reduced to 7.7% (n = 13; 95% CI, 0.2%-36.0%) if the first unit of CCP was transfused on the day of diagnosis. It was 8.7% (n = 127; 95% CI, 4.4%-15.0%) if CCP was transfused within 3 days of diagnosis and 32.0% (n = 25; 95% CI, 14.9%-53.5%) if CCP was transfused 4 or more days after diagnosis. The 30-day unadjusted mortality was 23.1%, 17.3%, and 52.0%, respectively, for the 3 CCP specified intervals. Additional risk modifiers such as age, sex, and race were analyzed (**TABLE 2**). The mortality rate at 7 days after CCP transfusion was 35.7% for patients who were >80 years, 14.5% for females, 10.7% for men, 14.3% for Whites, and 12.9% for Blacks. Patients on a ventilator had a 7-day mortality rate of 26.8% compared to 7.3% for patients not on a ventilator. Similarly, the mortality rate for patients in the ICU was 3.4 times higher than that of patients not in the ICU (18.0% for ICU patients vs 5.3% for non-ICU patients).

The competing risk analysis graph (**FIGURE 1**) shows the proportion of patients in various categories over time. The categories or states include in-hospital, discharged, and death. The time-to-event outcomes of death and discharge are competing risks in the context of this CCP analysis. This means that when estimating the time-to-death distribution, we must also account for patients who are discharged and vice versa. Initially, during multistate modeling, all patients are "in-hospital" immediately after receiving their first CCP treatment. And patients transition to either the discharged or the death state. The death state is a terminal, absorbing state.

Over time, most patients were discharged from hospitals within 30 days of follow-up. On average, the patient spent 11.7 days in the initial in-hospital state, 13.5 in the discharged state, and 4.9 days in the death state. Patients who received CCP treatment 4 or more days after diagnosis experienced more deaths and fewer discharges compared to the other 2 strata, that is, those who received CCP on the date of diagnosis or within 2–3 days of diagnosis. The strata, that is, in-hospital and discharged, were significantly different with respect to death distribution ($P$ = .0029). However, the differences between in-hospital strata to discharge distribution were not significant.

The CPH model indicated that the overall effect of titer level (low, high, negative) on survival was not statistically significant ($P$ = .1625) (**TABLE 3**). However, the model suggests that the risk of death may be higher in the low, negative, and missing categories as compared to the high titer category since the risk ratio is greater than 1 in all cases.

### Safety of CCP in COVID-19

There were no reports of transfusion reactions among the 165 patients who received 2 units of CCP in this study.

## Discussion

Analysis of the data from the 165 adult patients in Arkansas who were treated with 2 units of CCP demonstrated that CCP was safe and associated with lower rates of 7-day and 30-day mortality. Mortality was lower in patients treated within 3 days of diagnosis compared to patients treated 4 or more days after diagnosis (8.7% [95% CI, 5.7%-23.9%] vs 32% [95% CI, 14.9%-53.5%], respectively). This effect was also shown using a competing risk analysis graph, in which patients that received CCP on the day or within 2 to 3 days of diagnosis experienced less death and more discharges than patients who received their CCP treatment 4 or more days after diagnosis. Our mortality data were similar to data reported for the Mayo Clinic Expanded Access program (8.7% [95% CI, 8.3%-9.2%]).[6] Patients in Arkansas had reduced unadjusted 7-day and 30-day mortality rates, similar to their study. In terms of age groups, our study also shared similarities with the

**TABLE 2. Mortality Estimates for Various Demographic and Treatment Categories**

| Variable | No. | 7-Day Mortality | | 30-Day Mortality | |
|---|---|---|---|---|---|
| | | No. (%) | 95% CI | No. (%) | 95% CI |
| Unadjusted | 165 | 20 (12.1) | 7.6–18.1 | 38 (23.0) | 16.8–30.2 |
| Age, y | | | | | |
| 18–39 | 9 | 0 (0.0) | 0.0–33.6 | 1 (11.1) | 0.3–48.2 |
| 40–59 | 58 | 5 (8.6) | 2.9–19.0 | 10 (17.2) | 8.6–29.4 |
| 60–69 | 46 | 7 (15.2) | 6.3–28.9 | 14 (30.4) | 17.7–45.8 |
| 70–79 | 38 | 3 (7.9) | 1.7–21.4 | 8 (21.1) | 9.6–37.3 |
| 80+ | 14 | 5 (35.7) | 12.8–64.9 | 5 (35.7) | 12.8–64.9 |
| Sex | | | | | |
| Female | 62 | 9 (14.5) | 6.9–25.8 | 15 (24.2) | 14.2–36.7 |
| Male | 103 | 11 (10.7) | 5.5–18.3 | 23 (22.3) | 14.7–31.6 |
| Race | | | | | |
| White | 77 | 11 (14.3) | 7.4–24.1 | 21 (27.3) | 17.7–38.6 |
| Black | 62 | 8 (12.9) | 5.7–23.9 | 13 (21.0) | 11.7–33.2 |
| Hispanic | 15 | 0 (0.0) | 0.0–21.8 | 2 (13.3) | 1.7–40.5 |
| Other | 11 | 1 (9.1) | 0.2–41.3 | 2 (18.2) | 2.3–51.8 |
| Time to first CCP, d | | | | | |
| 0 | 13 | 1 (7.7) | 0.2–36.0 | 3 (23.1) | 5.0–53.8 |
| 1–3 | 127 | 11 (8.7) | 4.4–15.0 | 22 (17.3) | 11.2–25.0 |
| 4+ | 25 | 8 (32.0) | 14.9–53.5 | 13 (52.0) | 31.3–72.2 |
| On ventilator prior to first CCP transfusion? | | | | | |
| Yes | 41 | 11 (26.8) | 14.2–42.9 | 21 (51.2) | 35.1–67.1 |
| No | 124 | 9 (7.3) | 3.4–13.3 | 17 (13.7) | 8.2–21.0 |
| ICU prior to first CCP transfusion? | | | | | |
| Yes | 89 | 16 (18.0) | 10.6–27.5 | 31 (34.8) | 25.0–45.7 |
| No | 76 | 4 (5.3) | 1.5–12.9 | 7 (9.2) | 3.8–18.1 |
| No. of comorbidities | | | | | |
| 0 | 16 | 1 (6.2) | 0.2–30.2 | 3 (18.8) | 4.0–45.6 |
| 1–2 | 82 | 13 (15.9) | 8.7–25.6 | 18 (22.0) | 13.6–32.5 |
| 3+ | 67 | 6 (9.0) | 3.4–18.5 | 17 (25.4) | 15.5–37.5 |

*CCP, COVID-19 convalescent plasma; CI, confidence interval; ICU, intensive care unit.*

largest expanded access program in that patients between 40 and 59 years of age in our study were most affected.[6] Similarly, men were predominantly affected by COVID-19, but we found that women were more likely than men to die from COVID-19. Whites were most likely to die after contracting COVID-19 (14.3% [95% CI, 7.4%-24.1%]) at 7 days after receiving CCP. Blacks were the predominant minority group affected (37.58%), and these patients had a 12.9% (95% CI, 5.7%-23.9%) mortality rate at 7 days. The mortality rate increased if the patient was on a ventilator in the ICU before receiving CCP, and patients with more comorbidities were more likely to die from COVID-19.

There are 3 studies that reviewed the clinical benefit of 2 units of CCP: the PLACID study, the REMAP-CAP study, and the Stony Brook Medicine COVID Plasma Trial Group study.[7–9] The PLACID study, which was a randomized controlled study (RCT) conducted in India, did not demonstrate a significant benefit with 2 units of CCP transfusion. The limitations of this study included low participant enrollment and low titers of the administered CCP units.[7] REMAP-CAP, an open-label RCT, enrolled patients from 4 countries including the United States.[8] This study also did not find significant benefits in primary or secondary outcomes, such as hospital survival and organ support-free days. However, in immunodeficient subjects, a trend toward benefit was observed. The limitations included the study design in which the physicians and patients knew the treatment administered and the lack of patient recruitment from the United States. The study conducted at Stony Brook hospital randomized 74 patients in a 4:1 ratio to either 2 units of CCP or standard plasma. A total of 59 patients were randomized to receive CCP units. This study found that while CCP increased antibodies to SARS-CoV-2, it did not show significant differences in ventilator-free days, death, or World Health Organization (WHO) ordinal scale.[9] Our large, multicenter observational study demonstrated that the risk of death was higher in patients who received low or negative titer CCP units. While the overall effect was not statistically significant, given the number of missing titer results, there was a trend toward reduced mortality in patients who were administered high titer CCP. This is in contrast to the PLACID and the Stony Brook Medicine COVID Plasma Trial Group study, which did not observe a difference between patients who received 2 units of CCP compared to standard of care.[7]

Although there were several limitations to this study, no studies in the United States have investigated the safety and efficacy of

**FIGURE 1.** **Cumulative discharge and death rates stratified by time from diagnosis to COVID-19 convalescent plasma (CCP) treatment.**

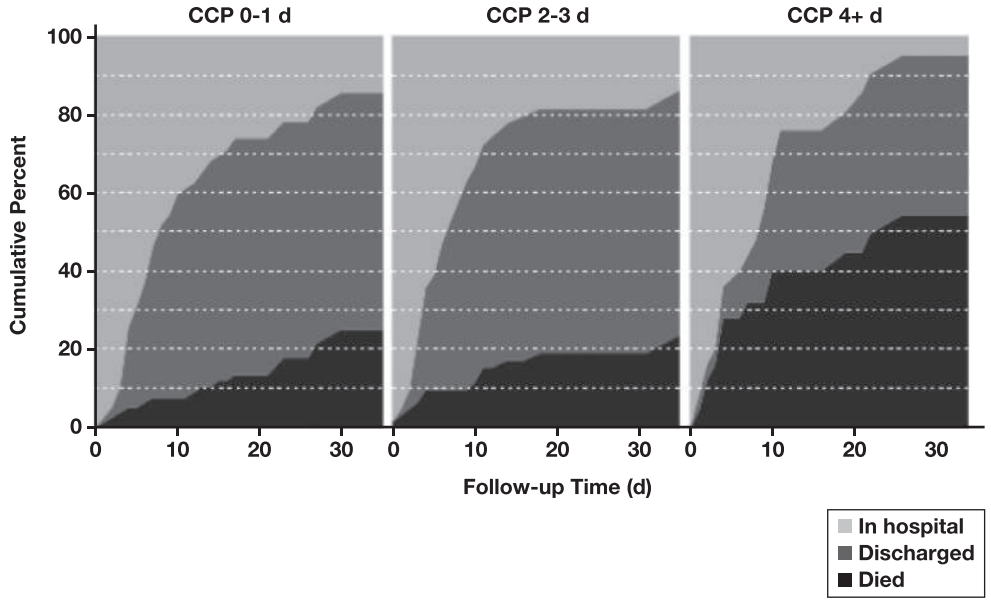


**TABLE 3.** **Results of Cox Proportional Hazard Model Assessing the Effect of Titer Level on the Risk of Death for Patients Treated with COVID-19 Convalescent Plasma Therapy**[a]

| Titer Level | Referent | RR | 95% CI | *P* Value |
|---|---|---|---|---|
| Low | High | 1.13 | 0.23–5.67 | .8804 |
| Negative | High | 3.02 | 0.95–9.67 | .0620 |
| Missing | High | 2.22 | 0.89–5.52 | .0854 |
| Likelihood ratio test: 5.13 (3 degrees of freedom) | | | | .1625 |

[a]*Survival time was calculated from when the first dose was administered until death. Survival times were censored at the time of discharge for those patients who were discharged alive. Risk ratio (RR) and 95% confidence interval (CI) are presented for each level. A high titer level was used as the referent class for these calculations.*

providing 2 units of convalescent plasma to treat COVID-19. One limitation was the predominant retrospective design of our study. We attempted to minimize the bias by collecting data concurrently with the treatment of the patient. In addition, Arkansas is a resource-constrained state, and the delivery of CCP in the state was to ensure access to life-saving therapy. In this setting, we formalized the delivery and transfusion of CCP through educational sessions with physicians at hospitals and blood collectors. Another is the potential small sample size of our study, which may have underestimated the mortality rate reduction and the ability to detect clinically significant differences. There is a potential for confounding by the heterogeneity that could not be adjusted for in the study. Furthermore, some patients in this study received other treatments in addition to CCP, which may confound the therapeutic benefit of this treatment.

Convalescent plasma can be a life-saving therapy that should be considered for COVID-19 given the demonstrated benefits in our study. Furthermore, given that it is relatively inexpensive in comparison to medications used to treat COVID-19, CCP may be utilized in resource-limited settings, including developing countries that have difficulty accessing expensive medications or lack the infrastructure to participate in research studies. In comparison to CCP, another passive immune therapy, monoclonal antibodies, have shown clinical benefit in the outpatient setting only. Studies on bamlanivimab plus etesevimab, casirivirimab/imdevimab, and sotrovimab have not demonstrated benefit in the hospitalized patient population.[10–12] Therefore, the FDA has authorized the use of these medications for nonhospitalized patients only. This therapy is also expensive compared to CCP. Hyperimmune globulin, which is purified immunoglobin G products, did not show disease progression risk reduction against COVID-19 in hospitalized patients.[13]

Presently, the FDA revised the Emergency Use Authorization (EUA) of CCP to immunocompromised patients in either the inpatient or outpatient settings based on recent studies showing benefits in this population. FDA-approved medications for COVID-19 hospitalized patients are limited. Remdesivir, an effective antiviral therapy did not demonstrate clinical benefits in studies on immunocompromised patients.[14,15] Therefore, immunocompromised patients in outpatient settings are unable to benefit from this treatment. Tixagevimab plus cilgivimab, which were shown to be efficacious against the Omicron variant, is EUA authorized but is expensive and difficult to obtain in low-resource states.[16,17]

In comparison to alternate therapies, the FDA should consider revising its CCP authorization because CCP is readily available and can be provided quickly, which may be beneficial in the setting of newly emerging variants. Furthermore, the risk of adverse events with the use of CCP appears negligible. It is also an inexpensive option.

## Conclusion

In conclusion, given that there is 1 FDA-approved treatment for hospitalized COVID-19 patients, high titer CCP should be considered a therapeutic option, especially in constrained settings such as Arkansas.


## Acknowledgments

Research reported in this publication was supported, in part, by the National Center For Advancing Translational Sciences of the National Institutes of Health under Award Number UL1 TR003107. The content is solely the responsibility of the authors and does not necessarily represent the official views of the National Institutes of Health.

We thank our OBI, UAMS, and other hospital staff who supported the provision of convalescent plasma through the FDA eIND mechanism in the state. We are grateful for the insights provided by the Office of Research and Regulatory Affairs and the Translational Research Institute.


## Disclosure

Dr Ipe is a consultant for Terumo Blood and Cell Technologies and Alexion Pharmaceuticals.

## REFERENCES


1. Ipe TS, Le T, Quinn B, et al. Provision of COVID-19 convalescent plasma in a resource-constrained state. *Transfusion.* 2020;60(12):2828–2833. doi:10.1111/trf.16118.
2. Hung IF, To KK, Lee CK, et al. Convalescent plasma treatment reduced mortality in patients with severe pandemic influenza A (H1N1) 2009 virus infection. *Clin Infect Dis.* 2011;52(4):447–456. doi:10.1093/cid/ciq106.
3. Luke TC, Kilbane EM, Jackson JL, Hoffman SL. Meta-analysis: convalescent blood products for Spanish influenza pneumonia: a future H5N1 treatment? *Ann Intern Med.* 2006;145(8):599–609. doi:10.7326/0003-4819-145-8-200610170-00139.
4. FDA. Recommendations for investigational COVID-19 convalescent plasma. https://www.fda.gov/vaccines-blood-biologics/investigational-new-drug-ind-or-device-exemption-ide-process-cber/recommendations-investigational-covid-19-convalescent-plasma. Accessed October 1, 2020.
5. FDA. Recommendations for investigational COVID-19 convalescent plasma. FDA vaccine, blood, biologics—investigational new drug (IND) or device exemption (IDE) process. www.fda.gov/vaccines-blood-biologics/investigational-new-drug-ind-or-device-exemption-ide-process-cber/revised-information-investigational-covid-19-convalescent-plasma#foot. Accessed October 1, 2020.
6. Joyner MJ, Senefeld JW, Klassen SA, et al. Effect of convalescent plasma on mortality among hospitalized patients with COVID-19: initial three-month experience. *medRxiv*. 2020. doi: 10.1101/2020.08.12.20169359.
7. Agarwal A, Mukherjee A, Kumar G, et al. Convalescent plasma in the management of moderate COVID-19 in adults in India: open label phase II multicentre randomised controlled trial (PLACID Trial). *BMJ.* 2020;371:m3939. doi:10.1136/bmj.m3939.
8. Estcourt LJ, Turgeon AF, McQuilten ZK, et al; Writing Committee for the REMAP-CAP Investigators. Effect of convalescent plasma on organ support-free days in critically ill patients with COVID-19: a randomized clinical trial. *JAMA.* 2021;236(17):1690–1702.
9. Bennett-Guerrero E, Romeiser JL, Talbot LR, et al. Severe acute respiratory syndrome Coronavirus 2 convalescent plasma versus standard plasma in Coronavirus disease 2019 infected hospitalized patients in New York: a double-blind randomized trial. *Critical Care Medicine.* 2021;49(7):1015–1025.
10. Dougan M, Nirula A, Azizad M, et al; for the BLAZE-1 Investigators. Bamlanivimab plus etesevimab in mild or moderate Covid-19. *N Engl J Med.* 2021;385(15):1382–1392. doi:10.1056/nejmoa2102685.
11. Weinreich, DM, Sivapalasingam S, Norton T, et al. REGEN-COV antibody combination and outcomes in outpatients with Covid-19. *N Engl J Med.* 2021;385(23):e81.
12. Gupta A, Gonzalez RY, Juarez E, et al, for the COMET-ICE Investigators. Early treatment for Covid-19 with SARS-CoV-2 neutralizing antibody sotrovimab. *N Engl J Med.* 2021;385(21):1941–1950.
13. ITAC (INSIGHT 013) Study Group. Hyperimmune immunoglobulin for hospitalized patients with COVID-19 (ITAC): a double-blind, placebo-controlled, phase 3, randomized trial. *Lancet.* 2022 Feb 5;399(10324):530–540.
14. Helleberg M, Neimann CU, Moestrup KS, et al. Persistent COVID-19 in an immunocompromised patient temporarily responsive to two courses of remdesivir therapy. *J Infect Dis.* 2020;222(7):1103–1107.
15. Camprubi D, Goya A, Marcos MA. Persistent replication of SARS-CoV-2 in a severely immunocompromised patient treated with several courses of remdesivir. *Case Reports Int J Infect Dis.* 2021;104:379–381. doi:10.1016/j.ijid.2020.12.050.
16. FDA letter of authorization. http://www.azpicentral.com/pi.html?product=evusheld_fda_auth. Accessed March 30, 2022.
17. Case JM, Mackin S, Errico J, et al. (year). Resilience of S309 and AZD7442 monoclonal antibody treatments against infection by SARS-CoV-2 Omicron lineage strains. Biorxiv. 2022. https://doi.org/10.1101/2022.03.17.484787.

# Prospective Validation of a Machine Learning Model for Low-Density Lipoprotein Cholesterol Estimation

*Jean Pierre Ghayad, PharmD,[1] Vanda Barakett-Hamadé, MD,[1,2,3,*] Ghassan Sleilaty, MD[3,4]*

[1]Department of Laboratory Medicine, Hôtel-Dieu de France University Hospital, Beirut, Lebanon, [2]Directorate, Department of Laboratory Medicine, Hôtel Dieu de France University Hospital, Beirut, Lebanon, [3]Faculty of Medicine, Université Saint Joseph, Beirut, Lebanon,[4]Clinical Research Center, Hôtel Dieu de France University Hospital, Beirut, Lebanon. *To whom correspondence should be addressed: vanda.barakett@hdf.usj.edu.lb.

**Keywords:** low-density lipoprotein cholesterol, machine learning, agreement study, method validation, triglycerides, clinical chemistry

**Abbreviations:** LDL-C, low-density lipoprotein cholesterol; KNN, k-nearest neighbors; ICC, intraclass correlation coefficient; ASCVD, atherosclerotic cardiovascular disease; NCEP, National Cholesterol Education Program; ATP III, adult treatment panel III; LDL-F, Friedewald formula; HDL-C, high-density lipoprotein cholesterol; VLDL-C, very-low-density lipoprotein cholesterol; TC, total cholesterol; TG, triglyceridemia; RMP, reference method procedure; BQ, beta quantification; LDL-MH, Martin/Hopkins equation; ACC, American College of Cardiology; AHA, American Heart Association; ML, machine learning; LDL-KNN, LDL-C using k-nearest neighbors; Ln, natural logarithm; CV, coefficient of variation; DNN, deep neural networks.

*Laboratory Medicine* 2022;53:629–635; https://doi.org/10.1093/labmed/lmac049

## ABSTRACT

**Objective:** We aim to prospectively validate a previously developed machine learning algorithm for low-density lipoprotein cholesterol (LDL-C) estimation.

**Methods:** We retrospectively and prospectively evaluated a machine learning algorithm based on k-nearest neighbors (KNN) according to age, sex, health care setting, and triglyceridemia against a direct LDL-C assay. The agreement of low-density lipoprotein-k-nearest neighbors (LDL-KNN) with the direct measurement was assessed using intraclass correlation coefficient (ICC).

**Results:** The analysis comprised 31,853 retrospective and 6599 prospective observations, with a mean age of 54.2 ± 17.2 years. LDL-KNN exhibited an ICC greater than 0.9 independently of age, sex, and disease status. LDL-KNN was in satisfactory agreement with direct LDL-C in observations with normal triglyceridemia and mild hypertriglyceridemia but displayed an ICC slightly below 0.9 in severely hypertriglyceridemic patients and lower in very low LDL-C observations.

**Conclusion:** LDL-KNN performs robustly across ages, genders, health care settings, and triglyceridemia. Further algorithm development is needed for very low LDL-C observations.

The accumulation and oxidization of low-density lipoprotein cholesterol (LDL-C) within the arterial intima is a major modifiable risk factor of atherosclerotic cardiovascular diseases (ASCVD), such as myocardial infarction.[1,2] The National Cholesterol Education Program (NCEP) Adult Treatment Panel III (ATP III) has therefore defined LDL-C as the main biomarker to estimate ASCVD risk and the primary target of lipid-lowering therapy.[3] Henceforth, the accuracy and reliability of LDL-C determination is a key issue in diagnostic cardiology.

In most clinical laboratories, LDL-C is calculated using the Friedewald equation (LDL-F), which subtracts high-density lipoprotein cholesterol (HDL-C) and very low-density lipoprotein cholesterol (VLDL-C) from total cholesterol (TC). As VLDL-C measurement is not readily available, LDL-F assumes that it is equal to one-fifth of triglyceridemia (TG) in a fasting state. Thus, LDL-F consists in utilizing the equation LDL-C = TC – HDL-C – TG/5 (in mg/dL).[4] LDL-F is inapplicable in cases of severe hypertriglyceridemia, defined as TG >400 mg/dL (4.52 mmol/L) and very low LDL-C (LDL-C <70 mg/dL [1.81 mmol/L]), settings in which it significantly underestimates LDL-C.[5,6] Moreover, multiple guidelines are nowadays considering nonfasting blood samples to be an at least acceptable alternative to fasting samples.[7]

The reference method procedure (RMP) to directly determine LDL-C is beta quantification (BQ), but it is inaccessible to most laboratory settings. Direct homogeneous assays that specifically measure LDL-C by an enzymatic method following a masking of non–apolipoprotein B particles have been commercialized and endorsed by the NCEP.[8] However, their lack of standardization and cost has sustained a need to estimate LDL-C at no additional expense. In an aim to improve on LDL-F's performance, numerous alternative equations to calculate LDL-C have been proposed. Many of these methods performed inconsistently across anthropometric and biochemical parameters. For instance, the Anandaraja equation (LDL-C = 0.9 × TC – 0.9 × TG/5 – 28 in mg/dL) was

deemed preferable to LDL-F in Greek children[9] with dyslipidemia but inferior to LDL-F in both normotriglyceridemic and hypertriglyceridemic Americans.[10] The Ahmadi equation (LDL-C = TC/1.19 + TG/1.19 – HDL -C/1.1 – 38 in mg/dL) seems to perform better in an Iranian population with hypercholesterolemia[11] than a normolipidemic population of the same country.[12] Nonetheless, the Martin/Hopkins equation (LDL-MH), which utilizes patient TG and non-HDL-C to modify the fixed factor of 5 in LDL-F, proved to be more reliable than LDL-F independently of the studied population, disease states, or therapeutic states.[13] LDL-MH was therefore endorsed by the 2019 American College of Cardiology (ACC)/American Heart Association (AHA) Guideline on the Primary Prevention of Cardiovascular Disease as an acceptable method to estimate LDL-C in cases of high TG (≥150 mg/dL [1.69 mmol/L]) or low LDL-C (<70 mg/dL [1.81 mmol/L]).[14]

Recently, different machine learning (ML) methods for LDL-C estimation emerged. In 2010, Chakraborty and Tudu[15] used artificial neural networks using anthropometric, clinical, and biochemical input parameters to estimate LDL-C. In 2020, Singh et al[16] validated a ML algorithm based on random forests to estimate LDL-C using the other components of the standard lipid panel (HDL-C, TG, and TC). More recently, an algorithm based on the KNN method was developed and compared with various equations for LDL-C calculation.[17]

In this study, we aim to prospectively evaluate the developed LDL-KNN ML-model[17] and critically assess its reliability in specific subgroups, namely sex, health status, age quintiles, and strata of lipid panel components, using a direct homogeneous assay as a reference method.

## Materials and Methods

### Study Design

The conduction of this study was approved by the ethics committee of Université Saint Joseph, Beirut, Lebanon (CE HDF 1748). The retrospective subsample was built between September 1, 2017, and July 31, 2019, in which the results of complete standard lipid profiles were extracted from the laboratory information system of the Hotel Dieu de France University Hospital clinical chemistry laboratories. The extracted data comprised the patient unique identification number, sex, age, date and time of phlebotomy, setting (hospitalized setting vs ambulatory setting), and the values of the directly measured LDL-C, TC, HDL-C, and TG during the same day. Any observations lacking a lipid panel measurement were excluded. All observations included in both subsamples were obtained from patients at a 12-hour fasting state. The patients who performed multiple standard lipid profile testing throughout the data collection period were included in the analysis. The prospective validation dataset was built from the observations prospectively collected between August 1, 2020, and April 30, 2021.

### Analytical Methods

Blood samples were drawn in separator tubes at a fasting state. All tubes were centrifuged (at 2500*g* for 12 minutes), and all the lipid measurements were executed on serum immediately after centrifugation. The TC, HDL-C, LDL-C, and TG assays were executed by the VITROS 5600 dry chemistry analyzer (Ortho-Clinical Diagnostics) in accordance with a previous publication.[17] Briefly, TC was measured using the CHOL VITROS Chemistry Products colorimetric assay, with a linearity of 49.88 mg/dL–324.8 mg/dL (1.29 mmol/L–8.40 mmol/L), and a total coefficient of variation (CV) of 1.4% at a mean of 143.08 mg/dL (3.7 mmol/L) and 1.6% at a mean of 247.5 mg/dL (6.4 mmol/L). TG was measured using the TRIG VITROS Chemistry Products colorimetric assay with a linearity of 9.74–525.2 mg/dL (0.11–5.93 mmol/L), and a total CV of 1.5% at a mean of 106.29 mg/dL (1.2 mmol/L) and 1.3% at means of 248 mg/dL (2.8 mmol/L) and 469.4 mg/dL (5.3 mmol/L). HDL-C was measured directly using the dHDL VITROS Chemistry Products, with a linearity of 5.03–109.82 mg/dL (0.13–2.84 mmol/L), and a total CV of 3.4% at a mean of 38.67 mg/dL (1.0 mmol/L) and 3.1% at means of 69.6 mg/dL (1.8 mmol/L) and 104.40 mg/dL (2.7 mmol/L). LDL-C was measured directly using dLDL VITROS Chemistry Products, with a linearity of 30.1–350 mg/dL (0.78–9.05 mmol/L), and a total CV of 2.9% at a mean of 65.74 mg/dL (1.7 mmol/L) and 3.3% at a mean of 146.95 mg/dL (3.8 mmol/L). The analyzer was calibrated according to manufacturer protocols.

### Statistical Analysis

Categorical variables were expressed as frequencies and percentages. Continuous variables with symmetrical distribution were expressed as mean ± standard deviation. Continuous variables with skewed distribution (assessed mainly using the QQ plots) were expressed as median with its interquartile range. LDL-C was estimated using a previously developed and published machine learning model relying on the k-nearest neighbors algorithm.[17] Briefly, the model randomly partitioned observations in the retrospective subsample into training and holdout datasets comprising 80% and 20% of observations, respectively. Ten folds were used for cross-validation. Gender was included as a factor. Covariates, which were normalized and adjusted, included age, non-HDL-C, TG, and sampling hour. The number of neighbors tested was allowed to vary between 3 and 7, and the Euclidian distance was used. The prospective subsample was used as a second external validation dataset.

In each sample, the age was symmetrically distributed, expressed as mean ± standard deviation, then divided into quintiles for analysis. The lipid panel markers were subdivided into strata for analysis. The lipid strata were chosen either on clinical grounds (the European Society of Cardiology/European Atherosclerosis Society LDL-C cardiovascular risk classes, and 3 classes for triglycerides with 2 cutoffs: 150 mg/dL [1.69 mmol/L] and 400 mg/dL [4.52 mmol/L]) or were based on distributional cutoffs defined empirically by percentiles that would create exploratory subgroups either for low LDL-C (percentiles 5, 10, and 40), or for high triglycerides (percentiles 60, 90, and 95), as these latter would be interesting with their gradually outward values and decreasing sample size. The distributional cutoffs were built on the whole sample. For agreement analysis, natural logarithm (Ln) of lipid parameters, which have symmetrical distributions, were used. An intraclass correlation coefficient type 3 (ICC3) using a 2-way mixed effects model was used to test the absolute agreement of estimated LDL-C values with the directly measured LDL-C values, performing F tests for an ICC3 true value = 0.9. The 95% confidence limits for the ICC3 were also calculated. ICCs were obtained, then assessed, in each subsample for each age and lipid marker strata, as well as each gender and disease status.

The analysis was performed using IBM SPSS software (IBM, SPSS Statistics for Windows version 26.0). The statistical code and the

deidentified dataset are available from the main author upon a reasonable scientific request.

## Results

The whole sample comprised 38,452 observations, with a mean age of 54 ± 17 years and 46.5% males. The retrospective subsample included 31,853 observations, whereas the prospective validation subsample encompassed 6599 observations. The characteristics of the 2 subsamples are shown in **TABLE 1**. The 2 subsamples exhibited similar distribution characteristics for all of the tested parameters, namely age, sex, health status, and lipid panel components. **TABLE 2** depicts specific percentiles (distributional cutoffs) and prespecified cutoffs (clinical cutoffs) for the direct homogeneous LDL-C assay and TG used for subgroup analysis. There were 2005 observations from hospitalized patients, making up 5.2% of observations. A total of 575 (1.5%) observations presented TG > 400 mg/dL (4.52 mmol/L).

The distributional cutoffs were 57.23 mg/dL (1.48 mmol/L), 68.06 mg/dL (1.76 mmol/L), and 99 mg/dL (2.56 mmol/L) for LDL-C,

**TABLE 1. Characteristics of the Subjects Included in the Total Sample and in the Retrospective and Prospective (Validation) Subsamples[a]**

| Variable | Total Sample (n = 38,452) | Retrospective Subsample (n = 31,853) | Prospective Subsample (n = 6599) |
|---|---|---|---|
| Age, mean ± SD (y) | 54.2 ± 17.2 | 54.3 ± 17.2 | 53.4 ± 17.3 |
| Age (y) | | | |
| ≤39 | 8071 (21%) | 6602 (20.7%) | 1469 (22.3%) |
| 40–51 | 8108 (21.1%) | 6701 (21%) | 1407 (21.3%) |
| 52–59 | 7105 (18.5%) | 5891 (18.5%) | 1214 (18.4%) |
| 60–70 | 8044 (20.9%) | 6656 (20.9%) | 1388 (21%) |
| 71+ | 7124 (18.5%) | 6003 (18.8%) | 1121 (17%) |
| Sex | | | |
| M | 17,883 (46.5%) | 14,755 (46.3%) | 3128 (47.4%) |
| F | 20,569 (53.5%) | 17,098 (53.7%) | 3471 (52.6%) |
| Setting | | | |
| Hospitalized | 2005 (5.2%) | 1756 (5.5%) | 249 (3.8%) |
| Ambulatory | 36,447 (94.8%) | 30,097 (94.5%) | 6350 (96.2%) |
| TC, Me (Q1–Q3) (mg/dL) | 185.0 (157.0–235.0) | 184.0 (157.0–212.0) | 188.0 (160.0–217.0) |
| HDL-C, Me (Q1–Q3) (mg/dL) | 48.0 (39.0–59.0) | 48.0 (39.0–58.0) | 48.0 (40.0–60.0) |
| LDL-D, Me (Q1–Q3) (mg/dL) | 108.0 (86.0–133.0) | 108.0 (86.0–133.0) | 107.0 (85.0–133.0) |
| LDL-C class (mg/dL) | | | |
| <40.0 | 506 (1.3%) | 419 (1.3%) | 87 (1.3%) |
| 40.0–55.0 | 1236 (3.2%) | 1021 (3.2%) | 215 (3.3%) |
| 55.0–70.0 | 2865 (7.5%) | 2339 (7.3%) | 526 (8%) |
| 70.0–100.0 | 11,333 (29.5%) | 9335 (29.3%) | 1998 (30.3%) |
| 100.0–116.0 | 6749 (17.6%) | 5586 (17.5%) | 1163 (17.6%) |
| 116.0–190.0 | 14,988 (39%) | 12,512 (39.3%) | 2476 (37.5%) |
| >190.0 | 775 (2%) | 641 (2%) | 134 (2%) |
| TG, Me (Q1–Q3) (mg/dL) | 125.0 (89.0–173.0) | 124.0 (88.0–173.0) | 129.0 (94.0–178.0) |
| TG class (mg/dL) | | | |
| TG <150.0 | 24,666 (64.1%) | 20,576 (64.6%) | 4090 (62%) |
| 150.0≤ TG <400.0 | 13,211 (34.4%) | 10,820 (34%) | 2391 (36.2%) |
| TG ≥400.0 | 575 (1.5%) | 457 (1.4%) | 118 (1.8%) |
| Non-HDL-C, Me (Q1–Q3) (mg/dL) | 133.0 (108.0–162.0) | 133.0 (107.0–161.0) | 135.0 (109.0–166.0) |
| Non-HDL-C class (mg/dL) | | | |
| <100.0 | 7383 (19.2%) | 6216 (19.5%) | 1167 (17.7%) |
| 100.0–130.0 | 10,910 (28.4%) | 9061 (28.4%) | 1849 (28%) |
| 131.0–185.0 | 15,760 (41%) | 13,087 (41.1%) | 2673 (40.5%) |
| 186.0–210.0 | 2742 (7.1%) | 2211 (6.9%) | 531 (8%) |
| >210.0 | 1657 (4.3%) | 1278 (4.0%) | 379 (5.7%) |

*HDL-C, high density lipoprotein cholesterol; LDL-C, low-density lipoprotein cholesterol; LDL-D, LDL-C obtained by direct homogeneous assay; Me (Q1–Q3), median (1st quartile–3rd quartile); TC, total cholesterol; TG, triglycerides.*
*[a]Data are given as No. (%) except where indicated otherwise.*

**TABLE 2. Intraclass Correlation Coefficients Between K-Nearest Neighbors, Derived LDL-C Values, and the Directly Measured LDL-C Values According to Clinical and Biological Parameters in the Retrospective and Prospective Subsamples**

| Factor | Retrospective Subsample | | | Prospective Subsample | | |
|---|---|---|---|---|---|---|
| | No. | ICC3 (95% CI) | *P* Value | No. | ICC3 (95% CI) | *P* Value |
| Age (y) | | | | | | |
| ≤39 | 6602 | 0.94 (0.936–0.943) | .000 | 1469 | 0.931 (0.884–0.955) | .076 |
| 40–51 | 6701 | 0.926 (0.922–0.93) | .000 | 1407 | 0.887 (0.843–0.916) | .790 |
| 52–59 | 5891 | 0.93 (0.925–0.934) | .000 | 1214 | 0.9 (0.85–0.93) | .518 |
| 60–70 | 6656 | 0.929 (0.924–0.933) | .000 | 1388 | 0.919 (0.884–0.941) | .125 |
| 71+ | 6003 | 0.934 (0.93–0.938) | .000 | 1121 | 0.92 (0.86–0.948) | .221 |
| Sex | | | | | | |
| F | 14,755 | 0.933 (0.93–0.936) | .000 | 3128 | 0.922 (0.886–0.944) | .093 |
| M | 17,098 | 0.939 (0.936–0.942) | .000 | 3471 | 0.917 (0.869–0.943) | .212 |
| Setting | | | | | | |
| Hospitalized | 1756 | 0.931 (0.923–0.937) | .000 | 249 | 0.921 (0.883–0.945) | .117 |
| Ambulatory | 30,097 | 0.935 (0.933–0.938) | .000 | 6350 | 0.918 (0.876–0.942) | .173 |
| TG (mg/dL) | | | | | | |
| TG <150 | 20,576 | 0.953 (0.951–0.954) | .011 | 4090 | 0.899 (0.823–0.935) | .550 |
| 150≤ TG <400 | 10,820 | 0.917 (0.903–0.928) | .000 | 2391 | 0.943 (0.92–0.957) | .001 |
| TG ≥400 | 457 | 0.758 (0.501–0.864) | .998 | 118 | 0.703 (0.296–0.853) | .998 |
| LDL-C class (mg/dL) | | | | | | |
| <40 | 419 | 0.04 (–0.034–0.119) | 1.000 | 87 | 0.039 (–0.05–0.151) | 1.000 |
| 40–55 | 1021 | 0.145 (–0.006–0.281) | 1.000 | 215 | 0.52 (0.107–0.732) | 1.000 |
| 55–70 | 2339 | 0.256 (0.122–0.369) | 1.000 | 526 | 0.252 (0.142–0.349) | 1.000 |
| 70–100 | 9335 | 0.615 (0.577–0.649) | 1.000 | 1998 | 0.786 (0.767–0.803) | 1.000 |
| 100–116 | 5586 | 0.296 (0.272–0.32) | 1.000 | 1163 | 0.065 (–0.043–0.18) | 1.000 |
| 116–190 | 12,512 | 0.797 (0.768–0.82) | 1.000 | 2476 | 0.207 (–0.02–0.396) | 1.000 |
| > 190 | 641 | 0.637 (0.211–0.808) | 1.000 | 134 | 0.544 (0.322–0.68) | 1.000 |
| Distributional LDL-C cutoffs | | | | | | |
| LDL-C >p5 | 30,223 | 0.939 (0.938–0.94) | 0.000 | 6252 | 0.925 (0.893–0.945) | .055 |
| LDL-C ≤p5 | 1630 | 0.309 (0.008–0.521) | 1.000 | 347 | 0.276 (–0.064–0.53) | 1.000 |
| LDL-C >p10 | 28,478 | 0.932 (0.931–0.934) | .000 | 5877 | 0.917 (0.888–0.937) | .108 |
| LDL-C ≤p10 | 3375 | 0.516 (0.221–0.684) | 1.000 | 722 | 0.436 (0.026–0.666) | 1.000 |
| LDL-C >p40 | 19,189 | 0.89 (0.883–0.897) | .998 | 3850 | 0.875 (0.859–0.889) | 1.000 |
| LDL-C ≤p40 | 12,664 | 0.8 (0.729–0.847) | 1.000 | 2749 | 0.744 (0.489–0.851) | .999 |
| Distributional TG cutoffs | | | | | | |
| TG <p60 | 19,189 | 0.953 (0.952–0.954) | .000 | 3806 | 0.943 (0.92–0.957) | .000 |
| TG ≥p60 | 12,664 | 0.91 (0.893–0.923) | .110 | 2793 | 0.888 (0.808–0.928) | .705 |
| TG <p90 | 28,711 | 0.948 (0.947–0.949) | .000 | 5856 | 0.938 (0.909–0.955) | .007 |
| TG ≥p90 | 3142 | 0.855 (0.785–0.897) | .983 | 743 | 0.809 (0.596–0.892) | .984 |
| TG <p95 | 30,294 | 0.945 (0.943–0.946) | .000 | 6218 | 0.934 (0.902–0.953) | .019 |
| TG ≥p95 | 1559 | 0.828 (0.702–0.889) | .990 | 381 | 0.767 (0.459–0.878) | .993 |

*ICC3, intraclass correlation coefficient 3; LDL-C, low-density lipoprotein cholesterol; p, percentile; TG, triglycerides.*

corresponding respectively to the 5th, 10th, and 40th percentiles of LDL-C distribution over the whole sample (**FIGURE 1A**). The distributional cutoffs were 141.72 mg/dL (1.60 mmol/L), 239.15 mg/dL (2.7 mmol/L), and 292.3 mg/dL (3.3 mmol/L) for TG, corresponding respectively to the 60th, 90th, and 95th percentiles of TG distribution over the whole sample (**FIGURE 1B**).

The ICCs describing the concordance between LDL-KNN and directly measured LDL-C across clinical and biological strata are depicted in **TABLE 2**. Overall, in both retrospective and prospective subsamples, ICCs are well above the 0.9 cutoff independently of gender, age quintiles, and health care setting. Across TG values, ICCs seem to slightly decrease in cases of severe hypertriglyceridemia, exhibiting an ICC of 0.899 in normotriglyceridemic observations (TG <150 mg/dL [1.69 mmol/L]) and 0.703 in observations with TG >400 mg/dL (4.52 mmol/L) in the prospective subsample. In both subsamples, ICCs satisfied the ICC cutoff of 0.9 in observations with

**FIGURE 1. Distribution of LDL cholesterol (A) and triglycerides (B) in the whole sample (retrospective and prospective subsamples, n = 38,452). The vertical lines represent the 5th, 10th, and 40th percentiles of low-density lipoprotein (LDL) cholesterol in panel A. In panel B, the vertical lines represent the 60th, 90th, and 95th percentiles of triglycerides. Values shown on top of the vertical lines correspond to the actual value of the percentiles. The x-axis is log-scaled.**

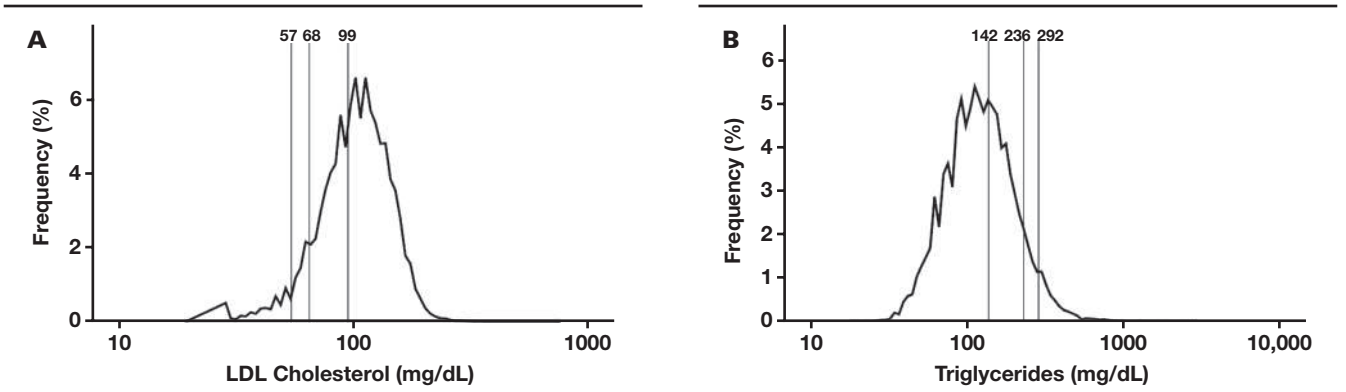


mild hypertriglyceridemia, with values of 0.943 and 0.953 in the prospective and retrospective samples, respectively. LDL-KNN showed satisfactory agreement with directly measured LDL-C at the 90th percentile of TG in both subsamples. Beyond the 95th percentile of TG, the algorithm performed noticeably better in the retrospective subsample, with an ICC of 0.828 and with a 95% confidence interval (CI) of 0.702–0.889, than the prospective validation subsample (ICC of 0.767 with a 95% CI of 0.459–0.878). In contrast with TG, agreement of LDL-KNN with the direct homogeneous assay seems to be poor in very low LDL-C observations for both subsamples. LDL-KNN performance improves as LDL-C increases. In the retrospective subsample, ICCs progress from 0.145 in the 40–55 mg/dL (1.03–1.41 mmol/L) stratum to 0.615 in the 70–100 mg/dL (1.81–2.58 mmol/L) stratum. In the prospective subsample, the ICC progresses from 0.52 in the 40–55 mg/dL (1.03–1.41 mmol/L) category to 0.786 in the 70–100 mg/dL (1.81–2.58 mmol/L) category. However, there is a dip in the agreement between LDL-KNN and direct LDL-C in the 100–116 mg/dL (2.61–3.0 mmol/L) stratum for both subsamples.

Throughout all the studied clinical and biochemical parameters without exception, agreements obtained in the prospective subsample closely shadowed those obtained in the retrospective subsample, although marginally inferior to the latter.

## Discussion

As major guidelines recommend different dyslipidemia management strategies according to patient LDL-C,[18] accurately determining LDL-C is a major issue in laboratory medicine. Because of the unavailability of BQ, the cost of direct homogeneous LDL-C measurement, and the unreliability of LDL-F, various equations have been proposed to estimate LDL-C, but most of them performed very inconsistently when evaluated in different settings. To our knowledge, this is the first study to prospectively evaluate the reliability of a KNN-based algorithm for LDL-C estimation across sexes, age strata, disease status, TG strata, and LDL-C variation in a White population.

There are 4 key findings to this study. First, LDL-KNN is in very good agreement with a direct LDL-C assay independent of sex, age, and health care setting over a very large sample of complete lipid panel observations studied retrospectively then prospectively. Second, while agreement of LDL-KNN with the direct measurement does not seem to be impacted whatsoever by mild hypertriglyceridemia (150< TG <400 mg/dL [1.69< TG <4.52 mmol/L]), it is minorly affected by severe hypertriglyceridemia (TG > 400 mg/dL [4.52 mmol/L]). Third, LDL-KNN performance is severely impacted by very low LDL-C concentrations (LDL-C <40 mg/dL [1.03 mmol/L]), and its performance tends to improve as LDL-C increases. Fourth, since the 2 subsamples only differ by size with otherwise very similar distributional characteristics, sample size seemed to play a minor role in LDL-KNN performance. Nonetheless, even the smaller prospective subsample still comprised more than 6000 observations, which can be considered a large dataset in itself.

As LDL-KNN agreement with the direct homogeneous LDL-C assay generally improves as LDL-C increases, its ICC curiously plunged in the 100–116 mg/dL (2.61–3.0 mmol/L) stratum of LDL-C. This can be explained by the tightness of the latter. As a matter of fact, we noticed that the algorithm exhibited better ICCs in larger LDL-C intervals than tighter ones. Notwithstanding, the poor performance of LDL-KNN in observations with LDL-C <40 mg/dL (1.03 mmol/L) warrants further algorithm training to assess a potential improvement of performance in very low LDL-C observations.

Recently, various data mining and ML-derived methods have shown great promise in LDL-C estimation. Çubukçu and Topcu[19] developed various ML-derived methods to estimate LDL-C and showed them to outperform the guideline-endorsed Martin-Hopkins equation, especially in low LDL-C (70 mg/dL [1.81 mmol/L]) and moderate hypertriglyceridemia (176.26–398.6 mg/dL [1.99–4.50 mmol/L]).[19] However, careful interpretation of the data provided in some studies casts doubt on the generalizability of ML models. For instance, Dansethakul et al[20] used a Pace regression data mining model to derive an LDL-C equation, finding it to outperform other equations (including LDL-F) for TG <1000 mg/dL (11.29 mmol/L) in a dataset of 1786 observations in a Thai population. Nevertheless, Dansethakul et al only used the correlation coefficient *r* to assess the equations' performances, and equations may very well correlate

with LDL-C obtained by direct homogeneous assay without being in agreement with the latter. Using such an approach, Dansethakul et al[20] found LDL-F to be usable for TG <1000 mg/dL (11.29 mmol/L), which contradicts a wealth of evidence proving that LDL-F is inapplicable for TG >400 mg/dL (4.52 mmol/L). Sarangi et al[21] also derived an LDL-C equation using an unspecified data mining approach and showed it outperformed LDL-F and the Anandaraja equation for TG <1000 mg/dL (11.29 mmol/L) using mean differences and Bland-Altman plot analysis. However, the authors' equation was derived from a very small dataset of 266 observations that is markedly skewed towards hypertriglyceridemia. Sarangi et al[21] assessed the equations' performance across arbitrarily defined TG strata, and even the lowest stratum (200 mg/dL [≤2.25 mmol/L]) included both hypertriglyceridemic among normotriglyceridemic observations. Furthermore, the standard deviation of TG is so great that it would fallaciously imply the existence of negative TG observations.[21] Singh et al[16] developed the Weill Cornell model based on random forests on a large dataset of 17,500 observations and found it to outperform LDL-F and the Martin-Hopkins equation across all predefined strata of LDL-C and TG, including very low LDL-C (<70 mg/dL [1.81 mmol/L]) and severe hypertriglyceridemia (>500 mg/dL [5.64 mmol/L]). Yet, a few remarks can be raised upon scrutiny of the provided data. The Weill Cornell model presented by the authors was trained on a dataset lacking any LDL-C values beyond 350 mg/dL (9.05 mmol/L). Having not encountered such values, it cannot perform as satisfactorily as externally validated LDL-C estimation methods in that regard. Moreover, there are concerns regarding the studied population that cast doubt over the model's generalizability: for instance, the mean HDL-C in the study was 60.5 ± 3.5 mg/dL (1.56 ± 0.09 mmol/L), higher than the 90th percentile for the US male population and around the 75th percentile for the US female population, as per the Appendix III-A of the Third Report of the NCEP/ATP III.[22] Also, the standard deviation for HDL-C seems unnaturally small, yielding an unrealistically increased lower limit of the 95% distribution interval around the 75th HDL-C percentile for US male population and around the median for the US female population.[16] Likewise, LDL-C and TG mean values are away from median values for the US population, with their increased standard deviation reflecting a hidden positive skewedness of their respective distributions.[16] Understandably, the Weill Cornell model—and any ML algorithm—can be continuously updated to ameliorate its performance. While none of the aforementioned studies used LDL-KNN to estimate LDL-C, our investigations took all of these limitations into account.

"Deep" ML algorithms, such as deep neural networks (DNN), have also been developed to estimate LDL-C with a satisfactory level of performance.[23] However, they are very computationally expensive, and Tsigalou et al[24] showed that various "shallow" ML algorithms (such as LDL-KNN, which was not tested) exhibit similar levels of performance as DNN without their informatic complexity. The works of Tsigalou et al also indicated that ML algorithms, including multivariate linear regression, support vector machine regression, extreme gradient boosting, and DNN don't perform as well when the testing dataset has different distributional characteristics than the training dataset.[24] As both of our subsamples presented equivalent distributions of population and lipid data, we could not verify this variability in performance for LDL-KNN.

The lower performance of the current KNN model in patients with LDL-C <80 mg/dL (2.09 mmol/L) is not concerning. In a previous article,[17] the current model's performance relative to that of the existing classic and newer closed-form equations (Friedewald, De Cordova, Martin-Hopkins, and Sampson) in patients with LDL-C <80 mg/dL (2.09 mmol/L) was tested. The model had none of the predicted values below the Bland-Altman 95% lower limit of agreement contrary to the closed-form equations, which is desirable, since it does not underestimate LDL values. In this respect, we might consider that the ML model shows an improvement over the existing closed-form equations.

One caveat for the low-LDL subgroups is their small group size, either in relative terms (less than 1.5% have LDL-C <40 mg/dL in the current sample, and less than 5% have LDL-C less than 55 mg/dL), or most importantly in absolute terms (506 observations and 1742 observations, respectively), limiting the learning process of ML, which is demanding in terms of observations. Nonetheless, the fact that the ICCs were preserved in the prospective subsample sends a reassuring message.

This study is not without limitations. First, it did not use the RMP of BQ following ultracentrifugation to build, train, and validate LDL-KNN, and a search of the literature could not provide an investigation tracing the assay used for the RMP. In a study evaluating 8 direct homogeneous LDL-C assays, Miller et al[25] found that none of them fulfilled the NCEP total error goals in diseased patients with dyslipidemia. While ML would have harbored better results had BQ been used for training and validating LDL-KNN, direct homogeneous assays are nonetheless well correlated with BQ, suitable for routine practice, and recommended by the 2018 AHA/ACC Multisociety Guideline on the Management of Blood Cholesterol.[2] Second, our validation of LDL-KNN only used 1 direct LDL-C assay. In fact, Rossouw et al[26] showed that the performance of LDL-C equations can significantly differ according to the analyzer chosen to measure TC, HDL-C, and TG. Therefore, further investigations are needed to evaluate whether LDL-KNN performance can vary according to the RMP used to assess it.

## Conclusion

LDL-KNN performs robustly across age strata, gender, disease status, and triglyceridemia, and poorly in very low LDL-C observations, warranting further research in this specific category.

## REFERENCES


1. Malekmohammad K, Bezsonov EE, Rafieian-Kopaei M. Role of lipid accumulation and inflammation in atherosclerosis: focus on molecular and cellular mechanisms. *Front Cardiovasc Med.* 2021;8(1):707529. doi:10.3389/fcvm.2021.707529.
2. Grundy SM, Stone NJ, Bailey AL, et al. 2018 AHA/ACC/AACVPR/AAPA/ABC/ACPM/ADA/AGS/APhA/ASPC/NLA/PCNA guideline on the management of blood cholesterol: executive summary: a report of the American College of Cardiology/American Heart Association task force on clinical practice guidelines. *J Am Coll Cardiol.* 2019;73(24):3168–3209. doi:10.1016/j.jacc.2018.11.002.
3. Expert Panel on Detection, Evaluation, and Treatment of High Blood Cholesterol in Adults. Executive summary of the third report of the national cholesterol education program (NCEP) expert panel on detection, evaluation, and treatment of high blood cholesterol in adults (adult treatment panel III). *JAMA.* 2001;285(19):2486–2497. doi:10.1001/jama.285.19.2486.
4. Friedewald WT, Levy RI, Fredrickson DS. Estimation of the concentration of low-density lipoprotein cholesterol in plasma, without use of the preparative ultracentrifuge. *Clin Chem.* 1972;18(6):499–502. doi:10.1093/clinchem/18.6.499.
5. Palmer MK, Barter PJ, Lundman P, et al. Comparing a novel equation for calculating low-density lipoprotein cholesterol with the Friedewald

equation: a VOYAGER analysis. *Clin Biochem.* 2019;64:24–29. doi:10.1016/j.clinbiochem.2018.10.011.

6. Sampson M, Ling C, Qian S, et al. A new equation for calculation of low-density lipoprotein cholesterol in patients with normolipidemia and/or hypertriglyceridemia [published correction appears in *JAMA Cardiol*. 2020;5(5):613]. *JAMA Cardiol.* 2020;5(5):540–548. doi:10.1001/jamacardio.2020.0013.
7. Farukhi Z, Mora S. The future of low-density lipoprotein cholesterol in an era of nonfasting lipid testing and potent low-density lipoprotein lowering. *Circulation.* 2018;137(1):20–23. doi:10.1161/CIRCULATIONAHA.117.031857.
8. Bachorik PS, Ross JW. National Cholesterol Education Program recommendations for measurement of low-density lipoprotein cholesterol: executive summary. The National Cholesterol Education Program Working Group on Lipoprotein Measurement. *Clin Chem.* 1995;41(10):1414–1420. doi:10.1093/clinchem/41.10.1414.
9. Garoufi A, Drakatos A, Tsentidis C, et al. Comparing calculated LDL-C with directly measured LDL-C in healthy and in dyslipidemic children. *Clin Biochem.* 2017;50(1-2):16–22. doi:10.1016/j.clinbiochem.2016.05.026.
10. Oliveira MJA, van Deventer HE, Bachmann LM, et al. Evaluation of four different equations for calculating LDL-C with eight different direct HDL-C assays. *Clin Chim Acta.* 2013;423:135–140. doi:10.1016/j.cca.2013.04.009.
11. Ahmadi S-A, Boroumand M-A, Gohari-Moghaddam K, et al. The impact of low serum triglyceride on LDL-cholesterol estimation. *Arch Iran Med.* 2008;11(3):318–321. PMID: 18426324.
12. Atabi F, Mohammadi R. Clinical validation of eleven formulas for calculating LDL-C in Iran. *Iran J Pathol.* 2020;15(4):261–267. doi:10.30699/ijp.2020.110379.2174.
13. Chung S. Update on low-density lipoprotein cholesterol quantification. *Curr Opin Lipidol.* 2019;30(4):273–283. doi:10.1097/MOL.0000000000000611.
14. Arnett DK, Blumenthal RS, Albert MA, et al. 2019 ACC/AHA guideline on the primary prevention of cardiovascular disease: a report of the American College of Cardiology/American Heart Association task force on clinical practice guidelines [published correction appears in *Circulation.* 2019;140(11):e649-e650] [published correction appears in *Circulation*. 2020;141(4):e60] [published correction appears in *Circulation*. 2020;141(16):e774]. *Circulation.* 2019;140(11):e596–e646. doi:10.1161/cir.0000000000000678.
15. Chakraborty M, Tudu B. Comparison of ANN models to predict LDL level in diabetes mellitus type 2. Paper presented at 2010 International Conference on Systems in Medicine and Biology; December 16-18, 2010; Kharagpur, India.
16. Singh G, Hussain Y, Xu Z, et al. Comparing a novel machine learning method to the Friedewald formula and Martin-Hopkins equation for low-density lipoprotein estimation. *PLoS One.* 2020;15(9):e0239934. doi:10.1371/journal.pone.0239934.
17. Barakett-Hamade V, Ghayad JP, Mchantaf G, et al. Is machine learning-derived low-density lipoprotein cholesterol estimation more reliable than standard closed form equations? Insights from a laboratory database by comparison with a direct homogeneous assay. *Clin Chim Acta.* 2021;519:220–226. doi:10.1016/j.cca.2021.05.008.
18. Mach F, Baigent C, Catapano AL, et al. 2019 ESC/EAS guidelines for the management of dyslipidaemias: lipid modification to reduce cardiovascular risk. *Eur Heart J.* 2020;41(1):111–188. doi:10.1093/eurheartj/ehz455.
19. Çubukçu HC, Topcu Dİ. Estimation of low-density lipoprotein cholesterol concentration using machine learning. *Lab Med*. 2022;53(2):161–171. doi:10.1093/labmed/lmab065.
20. Dansethakul P, Thapanathamchai L, Saichanma S, et al. Determining a new formula for calculating low-density lipoprotein cholesterol: data mining approach. *EXCLI J.* 2015;14(1):478–483. doi:10.17179/excli2015-162.
21. Sarangi R, Bahinipati J, Pathak M, et al. Is data mining approach a best fit formula for estimation of low-density lipoprotein cholesterol? *J Family Med Prim Care.* 2021;10(1):327–332. doi:10.4103/jfmpc.jfmpc_1734_20.
22. National Cholesterol Education Program (NCEP) Expert Panel on Detection, Evaluation, and Treatment of High Blood Cholesterol in Adults (Adult Treatment Panel III). Third report of the National Cholesterol Education Program (NCEP) expert panel on detection, evaluation, and treatment of high blood cholesterol in adults (adult treatment panel III): final report. *Circulation.* 2002;106(25):3143–3421. doi:10.1161/circ.106.25.3143.
23. Lee T, Kim J, Uh Y, et al. Deep neural network for estimating low density lipoprotein cholesterol. *Clin Chim Acta.* 2019;489:35–40. doi:10.1016/j.cca.2018.11.022.
24. Tsigalou C, Panopoulou M, Papadopoulos C, et al. Estimation of low-density lipoprotein cholesterol by machine learning methods. *Clin Chim Acta.* 2021;517:108–116. doi:10.1016/j.cca.2021.02.020.
25. Miller WG, Myers GL, Sakurabayashi I, et al. Seven direct methods for measuring HDL and LDL cholesterol compared with ultracentrifugation reference measurement procedures. *Clin Chem.* 2010;56(6):977–986. doi:10.1373/clinchem.2009.142810.
26. Rossouw HM, Nagel SE, Pillay TS. Comparability of 11 different equations for estimating LDL cholesterol on different analysers. *Clin Chem Lab Med.* 2021;59(12):1930–1943. doi:10.1515/cclm-2021-0747.

# Evaluation of Intra- and Interlaboratory Variations in SARS-CoV-2 Real-Time RT-PCR Through Nationwide Proficiency Testing

*Kuenyoul Park, MD,*[1] *Heungsup Sung, MD,*[1,*] *Sail Chun, MD,*[1] *Won-Ki Min, MD*[1]

[1]Department of Laboratory Medicine, Asan Medical Center, University of Ulsan College of Medicine, Seoul, Republic of Korea *To whom correspondence should be addressed. sung@amc.seoul.kr

**Keywords:** cycle threshold, external quality assessment, proficiency testing, SARS-CoV-2, COVID-19, interlaboratory variation

**Abbreviations:** Ct, cycle threshold; PCR, polymerase chain reaction; COVID-19, coronavirus disease 2019; PT, proficiency testing; KEQAS, Korean Association of External Quality Assessment Service; rRT-PCR, real-time reverse transcription polymerase chain reaction; CLSI, Clinical and Laboratory Standards Institute; *RdRp*, RNA-dependent RNA polymerase.

*Laboratory Medicine* 2022;53:636–639; https://doi.org/10.1093/labmed/lmac052

## ABSTRACT

**Objective:** This study aimed to examine the intra- and interlaboratory variations of cycle threshold (Ct) values using the nationwide proficiency testing for SARS-CoV-2.

**Methods:** Triplicated strong-positive contrived samples duplicated weak-positive contrived samples, and 2 negative samples were transported to participating laboratories in October 2021.

**Results:** A total of 232 laboratories responded. All except 4 laboratories correctly answered. Six false-negative results, including 2 false-negatives with Ct values beyond the threshold and 1 clerical error, were noted from weak-positive samples. Intralaboratory variations of Ct values of weak-positive and strong-positive samples were not acceptable (Ct > 1.66) in 17 and 7 laboratories, respectively. High interlaboratory variations of Ct values (up to 7 cycles) for the 2 commonly used polymerase chain reaction (PCR) reagents were observed.

**Conclusion:** The overall qualitative performance was acceptable; intralaboratory variation was acceptable. However, interlaboratory variations of Ct values were remarkable even when the same PCR reagents were used.

During the coronavirus disease 2019 (COVID-19) pandemic, diagnostics is an important armamentarium in dealing with COVID-19. Several reported proficiency testing (PT) programs, with up to 930 participating laboratories for SARS-CoV-2 in Austria, China, Europe, South Korea, and the US, showed excellent performance and preparedness.[1–7] Cycle threshold (Ct) values are generally accepted as semiquantitative estimates of SARS-CoV-2 in samples and clinically regarded as indicators of infectivity in the real world.[8] However, professional bodies discourage the clinical application of Ct values in qualitative testing.[9,10] Interlaboratory variation of Ct values was observed in reports from Austria and the US; therefore, caution needs to be exercised when interpreting Ct values of SARS-CoV-2 testing.[1,7,11] However, intralaboratory precision of Ct value has not yet been analyzed. Therefore, this study aimed to evaluate the status of SARS-CoV-2 reporting of laboratories in South Korea, a country with a low prevalence of SARS-CoV-2, and assess intralaboratory and interlaboratory variations of SARS-CoV-2 testing.

## Materials and Methods

### PT Scheme

Participation in the nationwide PT conducted by the Korean Association of External Quality Assessment Service (KEQAS) was mandatory for 232 laboratories performing SARS-CoV-2 real-time reverse transcription polymerase chain reaction (rRT-PCR) tests in Korea. Specimen preparation, validation and transport, and data reporting were performed as described previously.[4] The Korea Research Institute of Standards and Science (KRISS) SARS-CoV-2 Proficiency Panel was adopted. This PT panel is composed of triplicated strong-positive samples, duplicated weak-positive samples, and 2 negative samples. Two-level concentrations of the positive reference material were prepared using the entire SARS-CoV-2 genome inserted into a lentivirus vector, and the negative reference materials included the human RNase P gene. Strong-positive samples and weak-positive samples showed *E* gene Ct values of 26.74 ± 0.16 and 32.79 ± 0.39 when tested in triplicate with eMAG (bioMérieux) and Allplex SARS-CoV-2 Assay (Seegene), respectively. These samples were transported to participating laboratories in October 2021, and responses were returned within 4 days. Due to the lack of personal identifiers and patient data in this study, the

institutional review board of Asan Medical Center waived the ethics review (#2021-1772).

### Data Analysis

Only samples showing ≥80% agreed response with the expected results were submitted for qualitative evaluation as recommended by the Clinical and Laboratory Standards Institute (CLSI). Intralaboratory variations were calculated using the maximum difference in the Ct values of RNA-dependent RNA polymerase (*RdRp*) genes for strong-positive samples and weak-positive samples, tested using PCR reagents in the same laboratory. The difference from false-negative responses was discarded from this analysis. The maximum difference of >1.66, reflecting a difference of 0.5 log concentration, was considered unacceptable for strong-positive and weak-positive samples. Meanwhile, interlaboratory variations were analyzed by comparing the Ct values of *RdRp* with extraction kits and PCR reagents using the box-and-whisker plot. MedCalc 20.015 (MedCalc Software) and Excel 2016 (Microsoft) were used for the descriptive statistical analyses.

## Results

A total of 232 laboratories, including 35 public laboratories (26 laboratories operated by public health bodies, 5 army laboratories, and 4 national quarantine stations), participated. RNA extraction kits, extraction devices, PCR platforms, and PCR reagents were varied along with the protocols used by participating institutions (Supplemental Table 1).

All participating laboratories, except 4 laboratories, answered correctly. False-negative results from weak-positive samples were reported from 4 laboratories, as described in **TABLE 1**. Two laboratories using the Biosewoom Real-Q Direct SARS-CoV-2 Detection Kit incorrectly responded for 1 of the weak-positive samples; one completely missed 1 weak-positive sample for any of the target genes. Another laboratory incorrectly responded due to clerical error, and the fourth laboratory detected *E* gene with a Ct value >38 for both samples. However, the positive threshold of the Seasun Biomaterials U-TOP COVID-19 Detection Kit Plus was at Ct value 38.

Intralaboratory variations of Ct of weak-positive and strong-positive samples were not acceptable (>1.66) in 17 (7.3%) and 7 (3.0%) laboratories, respectively (**FIGURE 1**). A majority (62.9%) of the participating laboratories used PCR reagents produced by SDbiosensors STANDARD M nCoV Real-Time Detection Kit (93; 40.1%) and Seegene Allplex SARS-CoV-2 Assay (53; 22.8%), as shown in Supplemental Table 1. Interlaboratory variation for these 2 PCR reagents is depicted in **FIGURE 2**. The ranges of the Ct values of *RdRp* were 21–28 (SDBiosensors) and 25–30 (Seegene) for strong-positive samples and 28–35 (SDBiosensors) and 32–37 (Seegene) for weak-positive samples.

**TABLE 1. Six False-Negative Cases From Four Participating Laboratories**

| Laboratory | Sample | Target Gene | Reported Ct Value | Other Target Gene Ct Value | PCR Reagent Used | Extraction Kit Used |
|---|---|---|---|---|---|---|
| 1 | WPS #2 | *E* | ND | *RdRp* 35.93 | Biosewoom Real-Q Direct SARS-CoV-2 Detection Kit | Alphagene Nucleic Acid Extraction Kit |
| 2 | WPS #1 | *RdRp* | ND | *E* ND | Biosewoom Real-Q Direct SARS-CoV-2 Detection Kit | Real-Prep Viral DNA/RNA Kit |
| 2 | WPS #1 | *E* | ND | *RdRp* ND | Biosewoom Real-Q Direct SARS-CoV-2 Detection Kit | Real-Prep Viral DNA/RNA Kit |
| 3 | WPS #1 | *RdRp* | 30.78 | *E* 32.46 | SDbiosensors STANDARD M nCoV Real-Time Detection Kit | Libex Viral DNA and RNA Extraction Kit |
| 4 | WPS #1 | *E* | 38.30 | *S* 36.30, *N* 35.20, *RdRp* 33.90 | Seasun Biomaterials U-TOP COVID-19 Detection Kit Plus | Others |
| 4 | WPS #2 | *E* | 39.90 | *S* 37.00, *N* 36.50, *RdRp* 35.70 | Seasun Biomaterials U-TOP COVID-19 Detection Kit Plus | Others |

*Ct, cycle threshold;* E, *envelope;* N, *nucleocapsid; ND, not detected; PCR, polymerase chain reaction;* RdRp, *RNA-dependent RNA polymerase;* S, *spike; WPS, weak-positive sample.*

**FIGURE 1. Intralaboratory variation of cycle threshold (Ct) values of *RdRp* for strong-positive (A) and weak-positive (B) samples. Intralaboratory variation was defined as the maximum difference between Ct values of *RdRp* from the same sample in the same laboratory. Negative results for strong-positive and weak-positive samples were excluded.**

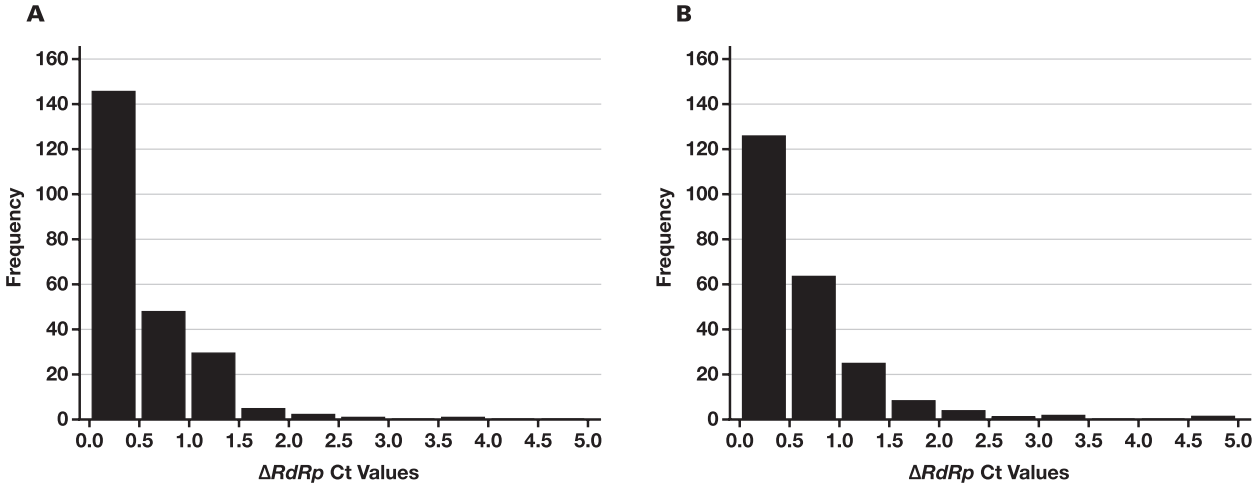

## Discussion

This PT study showed the performance of commonly used molecular assays for SARS-CoV-2 detection in laboratories in South Korea. The overall qualitative performance of the participating laboratories was acceptable, and intralaboratory variation was acceptable in the vast majority (89.7%). Considering the well-known variability of weak-positive samples, 97.0% of participating laboratories reported Ct values with acceptable intralaboratory variability.

Six false-negative results were reported in this PT. However, only 1 laboratory missed 1 weak-positive sample without positivity of any target genes; the agent used in this laboratory targeted only 2 genes, *RdRp* and *E* genes. Other cases with false-negative results of a single target could be reexamined due to positivity in another gene. In light of the continuous emergence of novel SARS-CoV-2 variants,[12] PCR reagents targeting multiple genes have advantages over those with only 2 targets considering the dropout phenomenon.[13,14] However, not only PCR reagents but also extraction and sample preparation should be rigorously reviewed for satisfactory reporting of SARS-CoV-2.

Intralaboratory variation was acceptable for most laboratories. With this finding, follow-up of the Ct value in the same institution seems reasonable. However, variability can occur even in the sample acquisition process.[10,15] Furthermore, sampling using a nasopharyngeal swab, as recommended by the Centers for Disease Control and Prevention, is very painful and difficult in some instances[16]; thus, Ct values obtained on the same day from the same patient can be varied even if the same protocol is performed in the same institution. Therefore, caution is required in monitoring patients with COVID-19 in the same institution.

Conversely, interlaboratory variation of the Ct values for the 2 commonly used PCR reagent companies were observed up to 7 cycles, as shown in **FIGURE 2**. Previous reports from the US and Austria[1,7,11] pointed to remarkable interlaboratory variation. One report from Austria demonstrated a Ct value range for *RdRp* of 25.1 to 37.7 from a single

**FIGURE 2. Interlaboratory variation of cycle threshold (Ct) values of *RdRp* gene along with extraction kits for laboratories using SDbiosensors reagents (n = 93) and Seegene reagents (n = 53). Strong-positive samples using SDbiosensors reagents (A) and Seegene reagents (B). Weak-positive samples using SDbiosensors reagents (C) and Seegene reagents (D). Extraction kits: 1, AdvanSure R (LG Chem); 2, Alphagene Nucleic Acid Extraction Kit (Alphagene); 3, EZ1 Advanced XL RNA Card (Qiagen); 4, Genolution Viral NA Kit (Genolution); 5, Libex Viral DNA and RNA Extraction Kit (Tianlong); 6, NucleiSens easyMAG (bioMérieux); 7, QIAamp Viral RNA Mini Kit (Qiagen); 8, QIAcube Kit (Qiagen); 9, QIAsymphony DSP Virus/Pathogen Kit (Qiagen); 10, RealPrep Viral DNA/RNA kit (Bioneer); 11, Seegene ProPrep (Seegene); 12, Seegene STARMag (Seegene); 13, Smart LabAssist Extraction Kit (TANBead); 14, TANBead Optipure Prep (TANBead); 15, Viral Nucleic Acid (small or large) Volume Kit (Roche); 16, other kits.**

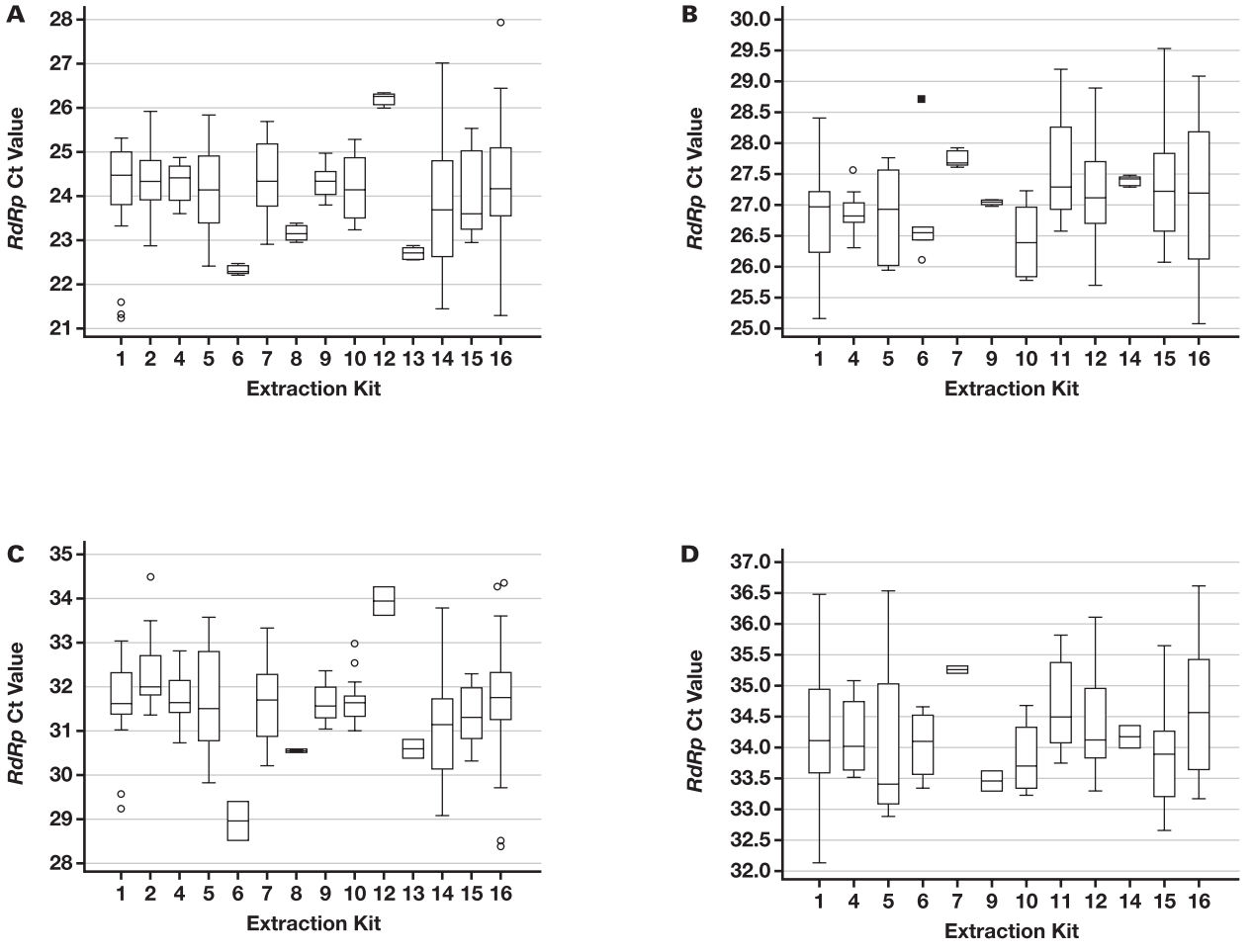

sample.[1] The study noted interassay variation, in addition to sample volume used during extractions, as a major cause for this variation.[1,11] In the present study, high interlaboratory variations between laboratories using the same reagent and extraction protocol were observed. This finding is in line with the US study,[7] which reported an interlaboratory variation of up to 14 cycles between laboratories using the same testing systems. Therefore, we discourage clinicians from interpreting the Ct values reported from other institutions, even if the same PCR reagent was used.

This study has some limitations. First, positive samples showing high viral loads were not included in this study; Ct values of all positive samples were higher than 20. Therefore, false-positives resulting from cross-contamination were not evaluated. Second, this PT was conducted in 1 country, so most laboratories used the PCR reagents from only 4 companies. International PT is required to investigate intra- and interlaboratory variations of various PCR reagents.

## Conclusion

In conclusion, this study showed that the overall performance of the participating laboratories was satisfactory. However, a few laboratories with unsatisfactory results were also noted. In addition to evaluating the performance of the participating laboratories, PT can also examine the SARS-CoV-2 rRT-PCR protocols, including reagents and extraction methods. Interlaboratory variations in SARS-CoV-2 testing were remarkable even if the same extraction method and PCR reagent were applied. Therefore, attention is needed when using the Ct value to estimate the clinical status of patients with COVID-19, including their infectivity.

## Supplementary Data

Supplemental figures and tables can be found in the online version of this article at www.labmedicine.com


## Acknowledgments

We thank all participants in this study for kindly responding to this proficiency testing and Editage (www.editage.co.kr) for English language editing.

## Funding

This work was supported by Korea Centers for Disease Control and Prevention (grant No. 4837-301) and the Korean Health Technology R&D Project through Korea Health Industry Development Institute (KHIDI), funded by Ministry of Health and Welfare, Republic of Korea (grant No. HI18C2383).


## REFERENCES


1. Buchta C, Camp JV, Jovanovic J, et al. The versatility of external quality assessment for the surveillance of laboratory and in vitro diagnostic performance: SARS-CoV-2 viral genome detection in Austria. *Clin Chem Lab Med.* 2021;59(10):1735–1744. doi:10.1515/cclm-2021-0604.
2. Edson DC, Casey DL, Harmer SE, et al. Identification of SARS-CoV-2 in a proficiency testing program. *Am J Clin Pathol.* 2020;154(4):475–478. doi:10.1093/ajcp/aqaa128.
3. Matheeussen V, Corman VM, Donoso Mantke O, et al. International external quality assessment for SARS-CoV-2 molecular detection and survey on clinical laboratory preparedness during the COVID-19 pandemic, April/May 2020. *Euro Surveill*. 2020;25(27):2001223.
4. Sung H, Han MG, Yoo CK, et al. Nationwide external quality assessment of SARS-CoV-2 molecular testing, South Korea. *Emerg Infect Dis.* 2020;26(10):2353–2360. doi:10.3201/eid2610.202551.
5. Wang Z, Chen Y, Yang J, et al. External quality assessment for molecular detection of Severe Acute Respiratory Syndrome Coronavirus 2 (SARS-CoV-2) in clinical laboratories. *J Mol Diagn.* 2021;23(1):19–28. doi:10.1016/j.jmoldx.2020.10.008.
6. Görzer I, Buchta C, Chiba P, et al. First results of a national external quality assessment scheme for the detection of SARS-CoV-2 genome sequences. *J Clin Virol.* 2020;129:104537. doi:10.1016/j.jcv.2020.104537.
7. Rhoads D, Peaper DR, She RC, et al. College of American Pathologists (CAP) Microbiology Committee perspective: caution must be used in interpreting the cycle threshold (Ct) value. *Clin Infect Dis*. 2021;72(10):e685–e686.
8. Rao SN, Manissero D, Steele VR, et al. A systematic review of the clinical utility of cycle threshold values in the context of COVID-19 [published correction appears in *Infect Dis Ther*. 2020 Aug 18]. *Infect Dis Ther.* 2020;9(3):573–586. doi:10.1007/s40121-020-00324-3.
9. American Association for Clinical Chemistry. AACC recommendation for reporting SARS-CoV-2 cycle threshold (CT) values. https://www.aacc.org/science-and-research/covid-19-resources/statements-on-covid-19-testing/aacc-recommendation-for-reporting-sars-cov-2-cycle-threshold-ct-values. Accessed December 2, 2021.
10. Infectious Disease Society of America and Association for Molecular Pathology. IDSA and AMP joint statement on the use of SARS-CoV-2 PCR cycle threshold (Ct) values for clinical decision-making. https://www.idsociety.org/globalassets/idsa/public-health/covid-19/idsa-amp-statement.pdf. Accessed December 2, 2021.
11. Buchta C, Görzer I, Chiba P, et al. Variability of cycle threshold values in an external quality assessment scheme for detection of the SARS-CoV-2 virus genome by RT-PCR. *Clin Chem Lab Med.* 2020;59(5):987–994.
12. World Health Organization. Update on Omicron. https://www.who.int/news/item/28-11-2021-update-on-omicron. Accessed December 2, 2021.
13. Amato L, Jurisic L, Puglia I, et al. Multiple detection and spread of novel strains of the SARS-CoV-2 B.1.177 (B.1.177.75) lineage that test negative by a commercially available nucleocapsid gene real-time RT-PCR. *Emerg Microbes Infect*. 2021;10(1):1148–155. 10.1080/22221751.2021.1933609.
14. Wollschläger P, Todt D, Gerlitz N, et al. SARS-CoV-2 N gene dropout and N gene Ct value shift as indicator for the presence of B.1.1.7 lineage in a commercial multiplex PCR assay. *Clin Microbiol Infect.* 2021;27(9):1353.e1–1353.e5.
15. Rabaan AA, Tirupathi R, Sule AA, et al. Viral dynamics and real-time RT-PCR Ct values correlation with disease severity in COVID-19. *Diagnostics (Basel).* 2021;11(6):1091.
16. Centers for Disease Control and Prevention. Interim guidelines for collecting and handling of clinical specimens for COVID-19 testing. https://www.cdc.gov/coronavirus/2019-ncov/lab/guidelines-clinical-specimens.html. Accessed December 2, 2021.

CASE STUDY

# Whole-Exome Sequencing Revealed a Pathogenic Nonsense Variant in the *SLC19A2* Gene in an Iranian Family with Thiamine-Responsive Megaloblastic Anemia

*Neda Mohsen-Pour, PhD,[1] Niloofar Naderi, MSc,[2] Serwa Ghasemi, PhD,[3] Mahshid Hesami, MD,[4] Majid Maleki, MD,[2] and Samira Kalayinia, PhD[2,*]*

[1]Zanjan Pharmaceutical Biotechnology Research Center, Zanjan University of Medical Sciences, Zanjan, Iran, [2]Cardiogenetic Research Center, Rajaie Cardiovascular Medical and Research Center, Iran University of Medical Sciences, Tehran, Iran, [3]Department of Biology, Science and Research Branch, Islamic Azad University, Tehran, Iran, [4]Rajaie Cardiovascular Medical and Research Center, Iran University of Medical Sciences, Tehran, Iran *To whom correspondence should be addressed. samira.kalayi@yahoo.com

**Keywords:** whole-exome sequencing, thiamine-responsive megaloblastic anemia, *SLC19A2* mutation, diabetes mellitus, hearing loss, variant

**Abbreviations:** *SLC19A2*, solute carrier family 19 member 2; THTR-1, thiamine human transporter 1; TRMA, thiamine-responsive megaloblastic anemia; WES, whole-exome sequencing; SNV, single-nucleotide variant; PCR, polymerase chain reaction.

*Laboratory Medicine* 2022;53:640–650; https://doi.org/10.1093/labmed/lmac040

## ABSTRACT

**Objective:** Solute carrier family 19 member 2 (*SLC19A2*, OMIM *603941) encodes thiamine human transporter 1 (THTR-1), which contributes to bringing thiamine (vitamin B1) into cells. Mutations in *SLC19A2* lead to a rare recessive genetic disorder termed thiamine-responsive megaloblastic anemia (TRMA) syndrome.

**Methods:** An Iranian family with TRMA was investigated by whole-exome sequencing (WES) to determine the genetic cause(s) of the disease. Accordingly, *SLC19A2* genetic variants were gathered through literature analysis.

**Results:** WES recognized a known pathogenic variant, c.697C > T (p.Q233X), within exon 2 of *SLC19A2* (NM_006996). Subsequently, the proband's parents and sister were confirmed as heterozygous carriers of the identified variant.

**Conclusion:** The diagnostic utility and affordability of WES were confirmed as the first approach for the genetic testing of TRMA to verify the diagnosis. This analysis can be used to guide future prenatal diagnoses and determine the consequences in the other family members.

Thiamine-responsive megaloblastic anemia (TRMA) syndrome, also called Rogers syndrome[1] or thiamine metabolism dysfunction syndrome-1 (THMD1), is specified by cardinal clinical findings of megaloblastic anemia, progressive sensorineural hearing loss, and non-type I diabetes mellitus.[2] The manifestation of diabetes mellitus and megaloblastic anemia occurs between infancy and adolescence, whereas deafness onset is usually observed in the toddler age group.[3] It is an autosomal recessive genetic condition caused by different pathogenic variants in solute carrier family 19 member 2 (*SLC19A2*) (OMIM: *603941, HGNC ID: 10938; NM_006996.2), encoding the high-affinity thiamine human transporter 1 (THTR-1) (UniProt/SwissProt: O60779),[4] which is the major thiamine transporter in pancreatic islet tissue and hematopoietic cells.[5,6] The *SLC19A2* gene is composed of 6 exons, spanning 22.5 kb on chromosome 1q23.3 in the 1.4 cM region.[7,8] THTR-1 encompasses 497 amino acids and owns 12 putative transmembrane domains and cytoplasmic NH2- and COOH-terminal areas.[8]

TRMA syndrome is very rare and seen in children of consanguineous parents and isolated communities.[9] Although TRMA is diagnosed based on a triad of clinical characteristics, composed of megaloblastic anemia, sensorineural deafness, and diabetes, it is also associated with various other abnormal and unspecific clinical conditions, including retinal detachment, optic atrophy, thrombocytopenia, hepatomegaly, congenital heart disease, cardiomyopathy, arrhythmia, ataxia, and stroke leading to a significant delay between the accurate time of symptom onset and a correct diagnosis. Also, differentiation diagnosis of TRMA syndrome would enable clinicians to make correlations between clinical phenotypes and molecular results. The average time from symptom presentation to diagnosis could be up to 8 years.[10–12] Residual activities of some mutants, environmental factors, and/or coinheritance of mutations in other genes seem to be associated with these variable phenotypic presentations observed in patients with TRMA.[10]

So far, research has yielded over 60 TRMA variants. Most of these variants are missense and nonsense mutations, followed by insertion and deletion mutations, for which phenotypic variabilities are restricted to help guide a molecular workup. Mutations in other genes

such as *SLC19A3*,[13] *SLC25A19*,[14] and *TPK1* are also related to thiamine metabolism.[15] The current diagnostic approach, polymerase chain reaction (PCR)-based Sanger sequencing (the gold standard to identify gene mutations), is a costly and time-consuming process. Next-generation sequencing-based assay[16] provides simultaneous analysis of known and novel mutations associated with TRMA, leading to a higher detection rate of causative variants.

In this research, the efficacy of whole-exome sequencing (WES) was explored as the first diagnostic approach to identify known and novel gene(s) causing TRMA. Accordingly, a known, albeit rare, nonsense variation—namely c.697C > T (p. Q233X)—in exon 2 of the *SLC19A2* gene was identified in a boy with consanguineous parents who suffered from anemia, diabetes mellitus, and severe deafness. Moreover, the genetic variants of patients with TRMA were reviewed to enhance the existing knowledge on this syndrome.

## Materials and Methods

### Ethics Approval and Consent to Participate

The present study complied with the Declaration of Helsinki and was approved by the Ethics Committee of Rajaie Cardiovascular Medical and Research Center (IR.RHC.REC.1400.112). Informed consent was obtained from the subjects for participation in this research and the publication of this report.

### Family Recruitment and Clinical Characteristics

**FIGURE 1** illustrates the pedigree of three generations of an Iranian family presenting with the manifestations of TRMA. Seven members of the pedigree, consisting of 2 affected (**FIGURE 1A**: II-10 and III-6) and 5 healthy individuals (**FIGURE 1A**: II-3, II-5, II-6, II-7, and III-1), who consented to participate in this study are depicted in the figure. Information regarding the clinical and demographic characteristics of the studied pedigree, including family history and related clinical symptoms, was collected from Rajaie Cardiovascular Medical and Research Center. Evidence of diabetes mellitus, stroke, several seizures, hearing loss (**FIGURE 1A**: II-8), hematological diseases (**FIGURE 1A**: II-4 and II-9), hearing loss (**FIGURE 1A**: II-10), and stroke and seizure (**FIGURE 1A**: I-4) was reported in this family. Other clinical information concerning the other family members was unavailable.

The proband (III-6) was a 2-year-old boy who was found to be deaf at 14 months. His parents stated that he showed no response to any sound. He developed diabetes mellitus at the age of 1. Based on the available reports, there was no stroke and visual impairment. Additionally, no abnormalities were seen in the limbs. The hearing aid trial failed for him, so he was planned to receive cochlear implantation. A laboratory routine blood test at the age of 2 indicated a white blood cell count of 9200/μL, a neutrophil count of 26.2%, a lymphocyte count of 61.5%, a red blood cell count of $1.50 \times 10^{12}$/L, a hemoglobin level of 8.4 g/dL, a mean corpuscular volume of 96.8 fl, and a platelet count of 259.00/μL. The hemoglobin level rose to 11 g/dL following oral treatment with iron, vitamin B12, and folic acid. Biochemistry laboratory analysis showed a fasting blood glucose level of 213 mg/dL (70–115 mg/dL) and an HbA1c level of 7.9% (4.0%–6.5%). Serum creatinine and sodium levels were below the normal range. Thiamine treatment improved diabetes and anemia to some extent. For an investigation of other coexisting clinical characteristics of the syndrome, he underwent a cardiologic examination at the age of 2. His echocardiogram was normal. Clinical possibility for the proband (III-6) being suggestive of TRMA syndrome, clinical exome sequencing was ordered for him.

The proband (**FIGURE 1A**: III-6) had a healthy sister (**FIGURE 1A**: III-1, 12 years old) and a diabetic brother (**FIGURE 1A**: III-5). The brother (III-5), who had received cochlear implants because of severe hearing loss, died at the age of 4 from sudden cardiac death due to long QT syndrome. The proband's father (**FIGURE 1A**: II-5) and mother (**FIGURE 1A**: II-6) were clinically unaffected. The proband's (III-6) mother (II-6) had a history of three miscarriages.

### WES and Bioinformatics Analysis

A family with a TRMA syndrome-affected son was referred to the Cardiogenetics Research Center of Rajaie Cardiovascular Medical and Research Center, affiliated with Iran University of Medical Sciences, Tehran, Iran. The study protocol was approved by the institutional ethics committee, and signed informed consent was obtained from the family.

DNA was extracted from blood samples of all family members. Exomes were captured with the Agilent SureSelect Human All Exon V7 kit (Agilent). Then, the sequencing of the enriched exon libraries was performed on the Illumina NovaSeq 6000 (Macrogen). The sequencing reads were aligned to the human genome reference (GRCh37 build) by using the BWA (v07.17) tool. The quality of exome data mapping to the reference genome was 98.8%, and the target region coverage was 99%. Single-nucleotide variant (SNV)/insertion and deletion (InDel) were called by applying the GATK (v4.1.4.1) tool with the result file of mapping (BAM). Duplicates were marked and removed with SAMtools (GATK package). Recalibration and SNV/InDel calling were done next. Confident variants were filtered and prioritized due to the minor allele frequency (MAF > 0.05) of 1000 Genomes Project, gnomAD (v2.1.1), and ExAc databases. Bioinformatics analysis was performed with prediction tools such as CADD,[17] SIFT,[18] PolyPhen-2,[19] PROVEAN,[19] FATHMM,[20] and GERP$^{++}$[21]to evaluate the pathogenicity of the detected variants. The variant interpreted to be pathogenic in at least four algorithms was considered for validation.

### Variant Validation

The identified candidate variant was segregated from the exome data via polymerase chain reaction (PCR)-based Sanger sequencing on an ABI Sequencer 3500XL PE (Applied Biosystems) in our center. With the use of Primer3 (v.04.0) (http://bioinfo.ut.ee/primer3-0.4.0/), the following specific primers were designed: *SLC19A2*_fwd 5′- TTGCCACAGACTACCTCCG -3′, *SLC19A2*_rev 5′- CCAGCCCCCATAGTAGCA -3′.

PCR was then performed on a SimpliAmp Thermal Cycler (Thermo Fisher Scientific) with 100 ng genomic DNA (gDNA), 200 mmol/L dNTP, 10 pmol/L primers, 1.5 mmol/L MgCl2, and 1 U of Taq DNA polymerase (Amplicon). After incubation of the entire mix at 95°C for 5 minutes, 35 amplification cycles (40 seconds at 95°C, 30 seconds at 60°C, and 30 seconds at 72°C) were performed. PCR products were then subjected to Sanger sequencing-based analysis on an ABI Sequencer 3500XL PE (Applied Biosystems). The sequences were subsequently analyzed using CodonCode Aligner v.7.1.2 (http://www.codoncode.com/aligner).

### Homology Modeling and Docking

The 3D structure of the human THTR-1 protein (SLC19A2) was not available in the Protein Data Bank (PDB [http://www.rcsb.org/pdb]).

**FIGURE 1.** *SLC19A2* **mutation in a family with an autosomal recessive pattern. A, The pedigree of the family indicates a typical autosomal recessive inheritance pattern. In the pedigree members, males are illustrated by squares and females by circles. The affected and unaffected individuals are respectively shown by shaded symbols and open symbols. The triangles represent miscarriages. The diagonal line shows a deceased family member, and the double lines indicate consanguineous mating. B, The sequences show the pathogenic c. 697C > T (p. Q233X) variant identified in exon 2 of** *SLC19A2* **(reverse sequencing results). The proband (III-6, arrow) was homozygous for the variant. The proband's father (II-5), mother (II-6), and sister (III-1) were carriers of c. 697C > T (p. Q233X). CC, wild type; CT, heterozygous for the variant; TT, homozygous for the variant.**

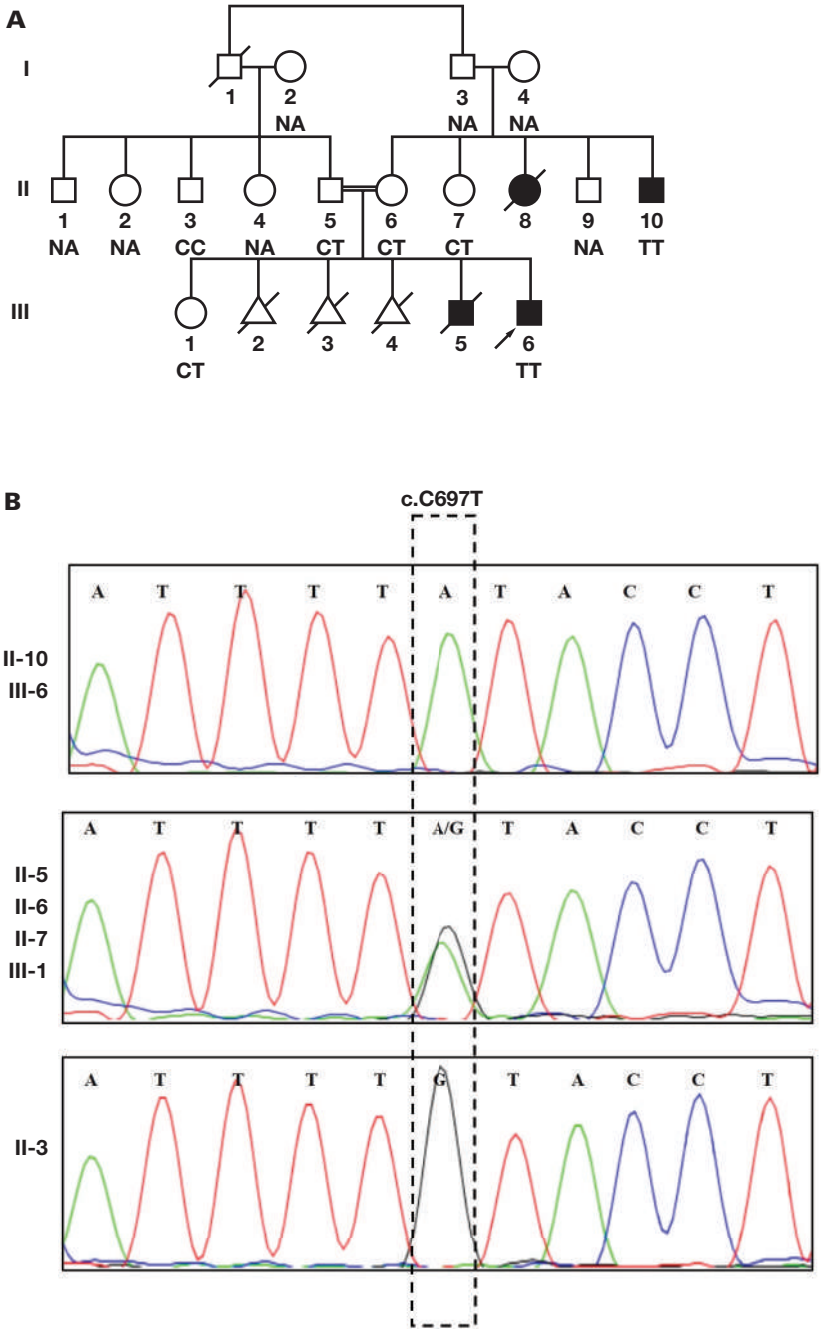


The protein sequence (FASTA format) was downloaded from the NCBI database (https://www.ncbi.nlm.nih.gov/), and the 3D structure was constructed by homology modeling via the SWISS-MODEL server (https://swissmodel.expasy.org/). For the generation of 3D structures in the SWISS-MODEL server, each of the protein sequences, normal and mutant (p.Q233X) in FASTA format, was loaded into the SWISS-MODEL server, and the molecular modeling was initiated to generate the PDB format of each protein. The 3D structure of the thiamine molecule (vitamin B1, PubChem CID: 1130) was accessed from the PubChem database (https://pubchem.ncbi.nlm.nih.gov/) and was processed into PDB format. The protein structures were corrected by ViewerLite (v.5), and polar hydrogens were added. Furthermore, energy minimization

for molecular docking was performed using the YASARA Energy Minimization Server (http://www.yasara.org/minimizationserver.htm). The 3D structures of the compounds were imported as an SCE file into the YASARA View (v.20.12.24) to deliver low-energy structures of the compounds and then saved in PDB format.

Molecular docking was carried out to evaluate the binding efficacy of the normal and mutant protein-ligand complexes using AutoDock Vina (in UCSF [University of California, San Francisco] Chimera version 1.15). Post-docking analysis was visualized using PyMOL (v.2.5.2), BIOVIA Discovery Studio (v.4.5), and LigPlus + (v.2.2.4), yielding details of the size, binding site location, and hydrogen-bond interactions of the docked ligand in various conformations.

## Results

### Molecular Analysis

WES was conducted on genomic DNA extracted from a peripheral blood sample obtained from the proband (III-6) to discover the mutated gene. A previously known but extremely rare pathogenic variant, c.697C > T, was found in the second exon of the *SLC19A2* gene. This pathogenic variant substituted glutamine at site 233 for a stop codon, which has been proposed to cause a premature THTR-1 truncated protein and/or nonsense-mediated SLC19A2 mRNA decay. The variant was validated in the proband (**FIGURE 1A**: III-6) by Sanger sequencing in the homozygous state. It was also found in the proband's father (**FIGURE 1A**: II-5), mother (**FIGURE 1A**: II-6), and sister (**FIGURE 1A**: III-1) in a heterozygous state. Accordingly, the variant was validated in the other studied pedigree members (**FIGURE 1A**: II-3, II-7, and II-10). Only one healthy individual (**FIGURE 1A**: II-3) was homozygous for the c.697C > T variant. DNA from the other family members was not available. The results are shown in **FIGURE 1B**.

Relevant English articles were identified by searching Web of Science, OMIM, Scopus, Google Scholar, ScienceDirect, MalaCards (the human disease database), Research Gate, and ClinVar databases using the following words: *SLC19A2 variants*, *the clinical importance of SLC19A2 gene mutations*, *thiamine*, *THTR-1*, *TRMA*, *anemia*, *hearing loss*, and *diabetes*. Studies on TRMA syndrome with observed variant(s) in *SLC19A2* were included. The results, consisting of several variants of *SLC19A2*, are detailed in **TABLE 1**. According to the American College of Medical Genetics and Genomics 2015 (ACMG),[22] the c.697C > T was determined to be a pathogenic variant (criteria: PVS1, PP5, PM2, and PP3). The nonsense variant was supported as the cause of the disease by CADD, SIFT, PolyPhen-2, PROVEAN, FATHMM, and GERP$^{++}$.

### Homology Modeling and Docking Findings

Molecular docking analysis was used to survey the interaction between THTR-1 (normal/mutant) and the thiamine molecule. Docking analysis was performed on THTR-1_ligand compounds in mutated and normal modes with the root-mean-square deviations of 0 and 2.538 and docking scores of –5.9 and –5.6. The normal THTR-1_ligand compound had a binding energy value of –5.6 kcal/mol and two hydrogen bonds (viz, PRO271 and ASP285) with thiamine (**FIGURE 2A**, **2B**). However, the mutant THTR-1_ligand compound had a binding energy value of –5.9 kcal/mol and no connection with thiamine (**FIGURE 2C**, **2D**). The buried surface area of the normal/mutant THTR-1 with thiamine is illustrated in **FIGURE 3**.

## Discussion

In this study, a pathogenic variant in the *SLC19A2* gene, c.697C > T (p.Q233X), was found in an Iranian family with TRMA syndrome presenting a homozygous mutation in the proband (III-6) and heterozygous mutations in his parents (II-5 and II-6) and sister (III-1). The identified genetic variant was extremely rare and had been reported in a few studies among TRMA patients.[23–26] It was located in exon 2 of the *SLC19A2* gene, which includes amino acids 69 to 269.[9] The c.697C > T (p. Q233X) pathogenic variant changes the amino acid glutamine at position 233 to a stop codon. TRMA diagnosis only relied on the proband's (III-6) typical clinical features, including diabetes mellitus, deafness, and anemia. The *SLC19A2* gene encodes the THTR-1 protein, which is capable of actively transporting thiamine. Thiamine is a vital nutrient for all tissues. It works as an important cofactor of various enzymes involved in numerous metabolic processes in mitochondria, cytosol, and peroxisomes.[27] Aside from THTR-1, thiamine can be transported by THTR-2, which specifically serves as a compensatory substitute in THTR-1 deficiency.[28–30] Although both THTR-1 and THTR-2 transporters are expressed in most tissues, THTR-1 is the sole thiamine transporter in bone marrow cells, cochlear cells, and pancreatic beta cells, and it indicates no compensatory mechanisms, which explains the cytological basis of anemia, progressive hearing loss, and diabetes mellitus as a consequence of loss-of-function variants in *SLC19A2*.[31] Molecular docking and bioinformatics studies, widely employed to predict ligand-target interactions, suggest that the truncated THTR-1 protein has no affinity with thiamine. Therefore, the mutant SLC19A2 (p.Q233X) has significantly reduced thiamine transport activity compared with the normal SLC19A2.

TRMA is a rare hereditary disorder with an extremely low incidence rate.[32] The first case of TRMA syndrome was reported in 1969 by Rogers et al.[1] Zhang et al[27] reported a high frequency of *SLC19A2* mutations in the Middle East, South Asia, and northern Mediterranean. Accordingly, the family studied in the current investigation constitutes another report of this variant in TRMA with a distinct phenotype from the Iranian population and, thus, increases the probability of discovering other TRMA patients in the future. Early genetic diagnosis of TRMA syndrome is essential to allow accurately targeted interventions and to guide clinical management. The majority of the affected individuals with follow-up data have been shown to benefit from early initiation of thiamine treatment. Exogenous thiamine therapy could reverse some of the clinical manifestations of TRMA syndrome. It has been reported that the lifelong use of oral thiamine at pharmacological doses (25–100 mg/d) can reverse anemia and delay diabetes. Its commencement through the first years of life, before 2 months of age, can also prevent hearing defects.[10,33] At high concentrations, thiamine can cross the cell membrane via passive diffusion. Therefore, patients with TRMA who lack functional THTR-1 could respond to supraphysiological doses[34] if diagnosed and treated with thiamine promptly.[26] Despite the obvious triad of clinical features, TRMA diagnosis may remain challenging.[35] Thus far, more than 60 mutations have been reported in the *SLC19A2* gene. More complexity arises from the existence of variable phenotypes in TRMA. The clinical presentations of TRMA syndrome can manifest themselves anytime from infancy to adolescence.[36] A misdiagnosis during this short time can be harmful, increasing the lag time between the onset of the symptoms and a precise diagnosis. Based on the results obtained from the present study, the application of WES, together with the presentation of the clinical triad and laboratory tests, is recommended for the clinical diagnosis and management of TRMA.

**TABLE 1.** The Reported Variants in the *SLC19A2* Gene (NM_006996.2) Related to Thiamine-Responsive Megaloblastic Anemia Syndrome

| Case No. | Nucleotide Change | Location on Chromosome 1 | Amino Acid Change | dbSNP | CADD[a] | SIFT[b] | PolyPhen-2[c] | PROVEAN[d] | Mutation Taster | ClinVar | Reference |
|---|---|---|---|---|---|---|---|---|---|---|---|
| 1 | c.95T > A | 116720508 | p. L32X | rs140765634 | 1.877 | NA | NA | NA | PO | NA | 27, 37 |
| 2 | c.121G > C | 169454884 | p. G41R | NA | 26.1 | D | PD | D | PO | NA | 27, 38 |
| 3 | c.152C > T | 169454853 | p. P51L | rs121908540 | 26.9 | D | PD | D | PO | P | 27, 38, 39 |
| 4 | c.196G > T | 169454809 | p. E66X | NA | 34 | NA | NA | NA | PO | NA | 12, 27, 40 |
| 5 | c.237C > A | 169446963 | p. Y79X | NA | 34 | NA | NA | NA | DC | NA | 12, 27 |
| 6 | c.277G > C | 169446923 | p. D93H | NA | 26.8 | D | PD | D | PO | NA | 2, 27 |
| 7 | c.314G > A | 169446886 | p. G105E | rs867811009 | 26.0 | T | PD | D | PO | NA | 27 |
| 8 | c.382G > A | 169446818 | p. E128K | NA | 25.2 | D | PD | D | DC | NA | 27 |
| 9 | c.412G > A | 169446788 | p. E138K | NA | 29.3 | T | PD | D | DC | NA | 27 |
| 10 | c.428C > T | 169446772 | p. S143F | rs761957186 | 27.5 | D | PD | D | DC | P | 2, 12, 27 |
| 11 | c.473C > G | 169446727 | p. T158R | NA | 25.0 | D | PD | D | DC | NA | 27, 41 |
| 12 | c.508A > C | 169446692 | p. T170P | NA | 25.7 | T | PD | D | DC | NA | 27 |
| 13 | c.514G > C | 169446686 | p. G172R | NA | 25.8 | D | PD | D | DC | NA | 27 |
| 14 | c.515G > C | 169446685 | p. G172A | NA | 22.3 | T | PD | D | DC | NA | 27 |
| 15 | c.602C > T | 169446598 | p. A201V | NA | 27.5 | T | PD | D | DC | NA | 27, 38 |
| 16 | c.688A > T | 169446512 | p. I230F | rs770374931 | 21.3 | T | B | N | DC | VUS | 12, 27, 38 |
| 17 | c.697C > T | 169446503 | p. Q233X | NA | 35 | NA | NA | NA | DC | P | 24, 27 |
| 18 | c.750G > A | 169446450 | p. W250X | rs74315374 | 38 | NA | NA | NA | DC | P | 4, 27 |
| 19 | c.848G > A | 169439384 | p. W283X | NA | 39 | NA | NA | NA | DC | NA | 27 |
| 20 | c.958T > G | 169439274 | p. W320G | NA | 31 | D | PD | D | DC | NA | 27 |
| 21 | c.1001G > A | 169439231 | p. G334D | rs199921604 | 28.2 | D | PD | D | DC | LP | 27, 42 |
| 22 | c.1074G > A | 169438031 | p. W358X | rs74315375 | 40 | NA | NA | NA | DC | P | 12, 27, 43 |
| 23 | c.1148T > A | 169437957 | p. V383E | NA | 19.24 | T | B | N | PO | NA | 27, 44 |
| 24 | c.1189A > T | 169437916 | p. R397X | rs371383730 | 40 | NA | NA | NA | DC | NA | 44, 45 |
| 25 | c.1213A > G | 169437892 | p. T405A | rs576208768 | 26.8 | T | PD | D | DC | NA | 46 |
| 26 | c.1322T > C | 169437392 | p. I441T | rs17847484 | 26.2 | D | PD | D | PO | B/LB | 8, 27 |
| 27 | c.1001G > A | 169439231 | p. G334D | rs199921604 | 28.2 | D | PD | D | DC | LP | 27, 42 |
| 28 | c.204 + 2T > G | 169454799 | splice variant | NA | 22 | NA | NA | NA | DC | NA | 27, 42, 47 |
| 29 | c.205G > T | 169446995 | p. V69F | rs1384006430 | 33 | T | PD | D | DC | NA | 27, 48 |
| 30 | C.1223 + 1G > A | 169437881 | G408 + 1A | rs768890368 | 34 | NA | NA | NA | DC | NA | 2, 27 |
| 31 | c.64_72delACCGCTCGG | 169454934 | p. Thr22_Arg24del | NA | 27 | NA | NA | NA | PO | NA | 49 |
| 32 | c.1002_1004delTGG | 169439228 | p. G335del | NA | 22.1 | NA | NA | NA | DC | NA | 27, 50 |
| 33 | c.1108del | 169437997_ 169437997delA | p. S370LfsTer3 | NA | 22.6 | NA | NA | NA | DC | NA | 27, 51 |
| 34 | c.1232delT | 169437481 | p. I411MfsTer12 | rs1379204044 | 34 | NA | NA | NA | DC | NA | 27 |

**TABLE 1.** (cont)

| Case No. | Nucleotide Change | Location on Chromosome 1 | Amino Acid Change | dbSNP | CADD[a] | SIFT[b] | PolyPhen-2[c] | PROVEAN[d] | Mutation Taster | ClinVar | Reference |
|---|---|---|---|---|---|---|---|---|---|---|---|
| 35 | c.1148_1149delT | 169437958 | p. V383Gfs | rs1401027751 | 31 | NA | NA | NA | DC | P | 12, 27, 42 |
| 36 | c.327_334del TGTTACAT | 169446866_ 169446873delATGTAACA | p. Ile109MetfsTer27 | NA | 32 | NA | NA | NA | DC | DC | 12, 27 |
| 37 | c.1173_1175dup | 169437930 | p. S392dup | NA | 21.1 | NA | NA | NA | NA | NA | 12, 38 |
| 38 | c.454_458delGGCATinsTA | 169446741 | p. G152X | NA | 33 | NA | NA | NA | DC | NA | 12, 27, 38 |
| 39 | c.757delA | 169446443 | p. I253Lfs*7 | NA | 24.8 | NA | NA | NA | DC | NA | 12, 38 |
| 40 | c.515G > A | 169446685 | p. G172D | rs28937595 | 27.1 | D | PD | D | DC | P | 4, 12, 27, 38 |
| 41 | c. 759dup | 169446441 | p. E254X | rs1368720035 | 27.3 | NA | NA | NA | NA | NA | 12, 38 |
| 42 | c. 242dup | 169446958 | p. Y81X | rs752104654 | 33 | NA | NA | NA | NA | P | 52 |
| 43 | c.287delG | 169446913 | p. R96Lfs*32 | NA | 32 | NA | NA | NA | DC | NA | 12, 27, 53 |
| 44 | c.484C > T | 169446716 | p. R162X | rs74315373 | 35 | NA | NA | NA | DC | P | 2, 4, 12, 27, 54 |
| 45 | c.242insA | 169446957_169446958 | p. Tyr81Ter | rs752104654 | 33 | NA | NA | NA | DC | NA | 2, 7, 27, 55 |
| 46 | c.1370delT | 169435211 | p. L457X | rs761803462 | 27.4 | NA | NA | NA | DC | NA | 27, 55 |
| 47 | c.430delT | 169446771 | p. Y144Ifs*32 | NA | 33 | NA | NA | NA | DC | NA | 7, 27 |
| 48 | c.566_567delGCinsTCT | 169446633 | p. S189IfsTer52 | NA | 32 | NA | NA | NA | DC | NA | 25, 27, 39 |
| 49 | c. 724delC | 169446475 | p. P242QfsTer18 | rs1571537544 | 23.9 | NA | NA | NA | DC | NA | 4, 7, 27 |
| 50 | c. 885delT | 169439347 | p. L296SfsTer18 | rs1571532822 | 33 | NA | NA | NA | DC | NA | 27, 29 |
| 51 | c.1409dup | 169435172 | p. L471Pfs*13 | NA | 29 | NA | NA | NA | DC | NA | 27, 30 |
| 52 | c.382 G> | 169446818 | P. E128K | NA | 25.2 | D | PD | D | DC | NA | 27, 56 |
| 53 | c.1063A > C | 169438042 | p. K355Q | rs200879349 | 24.1 | T | PD | D | DC | NA | 16 |
| 54 | c.1256G > A | 169437458 | p. R419H | rs530420883 | 32 | T | PD | D | DC | NA | 27, 57 |
| 55 | c.1052 T > C | 169438053 | p. V351A | rs748588472 | 23.6 | T | B | D | DC | NA | 27, 57 |
| 56 | c.373C > T | 169446827 | p. Q125X | NA | 35 | NA | NA | NA | DC | NA | 27, 58 |
| 57 | c.1214C > G | 169437891 | p. T405R | rs554433074 | 27.7 | T | PD | D | DC | NA | 27, 58 |
| 58 | c.336_363del | 169446837_ 169446864delCAGTCCCT GGGCATAGAGCAGCATAAAC | p. W112fs | NA | 32 | NA | NA | NA | DC | NA | 27 |
| 59 | c.358G > T | 169446842 | p. G120X | NA | 36 | NA | NA | NA | DC | NA | 27 |
| 60 | c.725delC | 169446475 | p. P242QfsX18 | rs1571537544 | 23.8 | NA | NA | NA | DC | P | 12, 59 |
| 61 | c.89G > A | 169454916 | p.Trp30* | rs1430840234 | 37 | NA | NA | NA | DC | NA | 27 |
| 62 | c.191T > C | 169454814 | p. L64P | NA | 28.4 | D | PD | D | DC | NA | 27 |
| 63 | c.239_240insA | 169446960_169446961insT | p. Y81Lfs*18 | NA | 25 | NA | NA | NA | DC | NA | 27 |
| 64 | c.241_242insA | 169446958_169446959insT | p.Y81* | NA | 24.3 | NA | NA | NA | DC | NA | 27 |
| 65 | c.262delG | 169446938 | p. V88CfsTer40 | NA | 22.4 | NA | NA | NA | DC | NA | 27 |
| 66 | c.271G > C | 169446929 | p. A91P | NA | 25.8 | D | PD | D | DC | NA | 27 |

**TABLE 1.** (cont)

| Case No. | Nucleotide Change | Location on Chromosome 1 | Amino Acid Change | dbSNP | CADD[a] | SIFT[b] | PolyPhen-2[c] | PROVEAN[d] | Mutation Taster | ClinVar | Reference |
|---|---|---|---|---|---|---|---|---|---|---|---|
| 67 | c.339del | 169446863 | p. P113LfsTer15 | NA | 32 | NA | NA | NA | DC | NA | 27 |
| 68 | c.405dupA | 169446795 | p. A136SfsTer3 | NA | 28 | NA | NA | NA | NA | NA | 27 |
| 69 | c.429_430del | 169446770 | p. I145Lfs*95 | rs1571537879 | 32 | NA | NA | NA | DC | P | 27 |
| 70 | c.581C > T | 169446619 | p. S194F | NA | 26.6 | D | PD | D | DC | NA | 27 |
| 71 | c.596C > G | 169446604 | p. S199X | NA | 37 | NA | NA | NA | DC | NA | 27 |
| 72 | c.598G > C | 169446602 | p. V200L | NA | 20.4 | T | B | N | DC | NA | 27 |
| 73 | c.623dup | 169446577 | p. L208FfsTer33 | NA | | NA | NA | NA | NA | NA | 27 |
| 74 | c.641delG | 169446559 | p. S214TfsTer14 | NA | 32 | NA | NA | NA | DC | NA | 27 |
| 75 | c.724delC | 169446475 | p. P242Qfs*18 | rs1571537544 | 23.8 | NA | NA | NA | DC | NA | 27 |
| 76 | c.726dup | 169446474 | p. A243SfsTer3 | NA | 26 | NA | NA | NA | NA | NA | 27 |
| 77 | c.759dup | 169446441 | p. E254X | rs1368720035 | 27.3 | NA | NA | NA | NA | NA | 27 |
| 78 | c.903delG | 169439329 | p. W301CfsTer13 | NA | 33 | NA | NA | NA | DC | NA | 27 |
| 79 | c.905G > A | 169439327 | p. W302X | NA | 45 | NA | NA | NA | DC | NA | 27 |
| 80 | c.993_996dup | 169439236 | p. N333LfsTer2 | NA | 23 | NA | NA | NA | NA | NA | 27 |
| 81 | c.1003G > A | 169439229 | p. G335S | NA | 24.0 | T | PD | N | DC | NA | 27 |
| 82 | c.1052T > C | 169438053 | p. V351A | rs748588472 | 23.6 | T | B | D | DC | NA | 27 |
| 83 | c.1147_1148delGT | 169437957_ 169437958delAC | p. V383Gfs*2 | rs1401027751 | 27.3 | NA | NA | NA | DC | NA | 27, 29 |
| 84 | c.1160G > A | 169437945 | p. W387X | NA | 41 | NA | NA | NA | DC | NA | 27 |
| 85 | c.1173_1175dup | 169437930 | p. S392dup | NA | 29 | NA | NA | NA | NA | NA | 27 |
| 86 | c.1201_1202delAT | 169437903 | p.M401VfsTer82 | rs1213206212 | 33 | NA | NA | NA | DC | NA | 27 |
| 87 | c.1256G > A | 169437458 | p. R419H | rs530420883 | 32 | T | PD | D | DC | NA | 27 |
| 88 | c.1265T > C | 169437449 | p. L422P | NA | 29.4 | D | PD | D | DC | NA | 27 |
| 89 | c.1409dup | 169435172 | p. L471PfsTer13 | NA | 26 | NA | NA | NA | NA | NA | 27 |

*B, benign; D, deleterious; DC, disease causing; LB, likely benign; NA: not available/not applicable; PD, possibly damaging; PO: polymorphism; T: tolerated; VUS, variant of uncertain significance.*
[a]*CADD, Phred ≤ 20: deleterious; Phred > 20: benign.*
[b]*SIFT, score ≤ 0.05: deleterious; score > 0.05: tolerable.*
[c]*PolyPhen-2, score 0.0 to 0.85: benign; score 0.85 to 1.0: possibly damaging.*
[d]*PROVEAN, score = -2.5: deleterious.*

**FIGURE 2.** The image depicts the complexes of THTR-1 and thiamine. A, B, Normal THTR-1 (green) is shown in interaction with thiamine. C, D, The mutant THTR-1 (pink) is demonstrated in interaction with thiamine. A and C were obtained by BIOVIA Discovery Studio (v.4.5) and B and D were obtained by PyMOL (v.2.5.2).

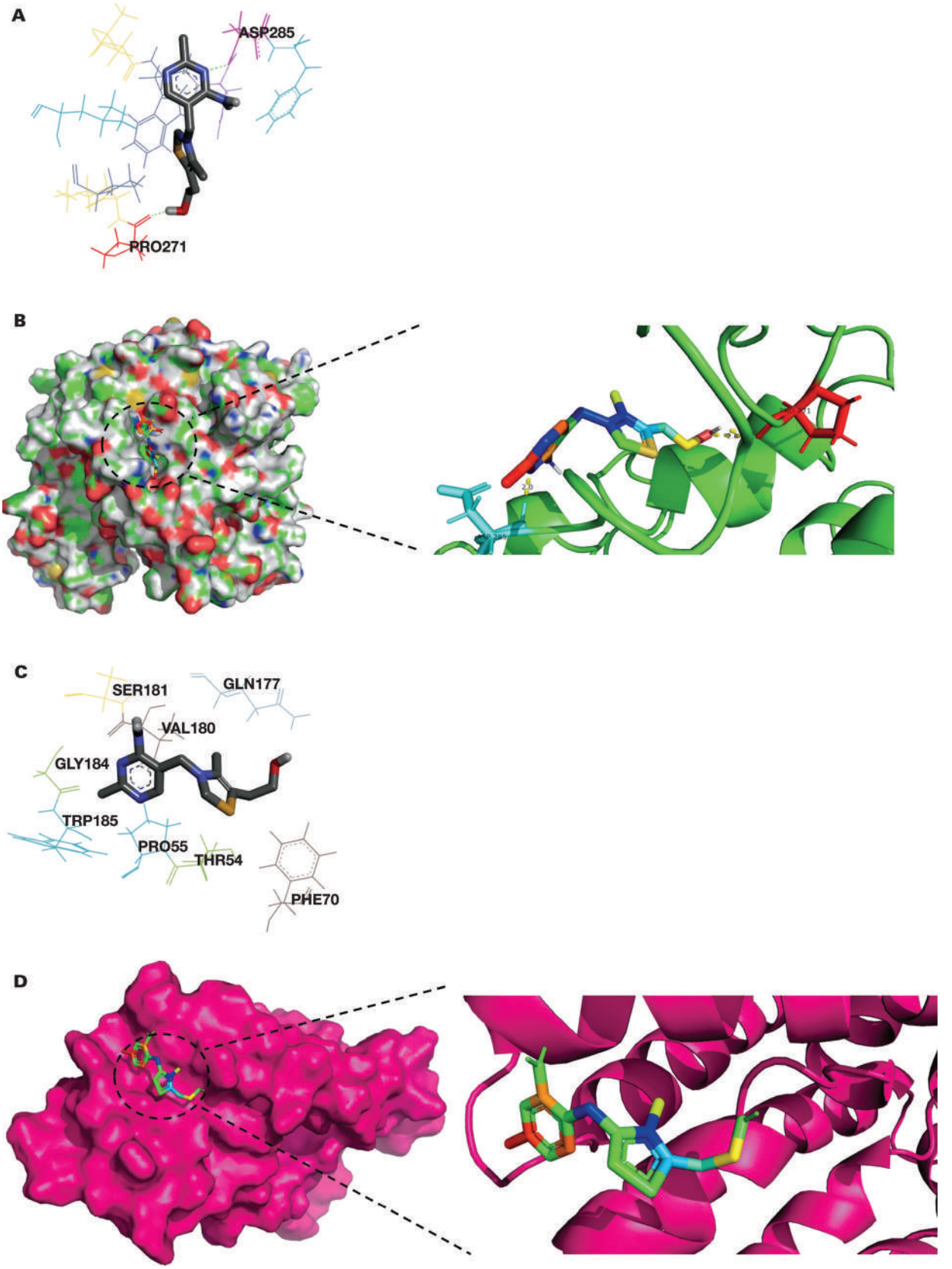

**FIGURE 3.** **The image shows the interacted surface of normal (A) and mutant (B) THTR-1 with thiamine, obtained by LigPlus+. Pink stick models present the thiamine, the green lines are hydrogen bonds, red and aqua green stick models present the important residues in the active site and dashed half-moons present non-ligand residue interactions with thiamine.**

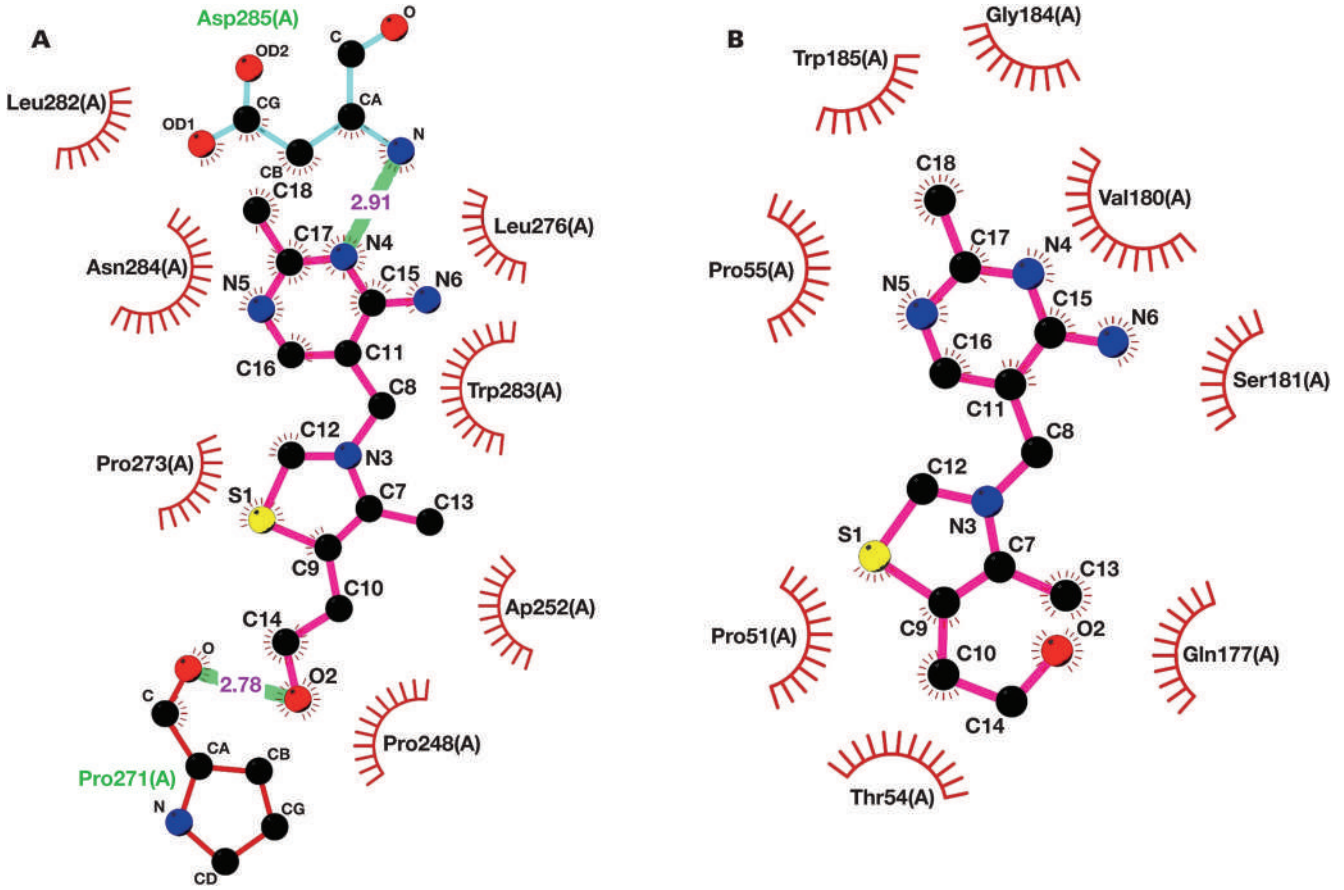


## Conclusions

WES is an appropriate approach to identify the etiology of genetic cause(s) for individuals with clinical characteristics, suspicion, or a family history of TRMA. Exogenous thiamine has been reported to reverse some of the clinical features of TRMA, hence the vital importance of an early genetic diagnosis of this syndrome. The full spectrum of TRMA clinical manifestations is still developing due to the rare incidence of this disease. Therefore, extensive cellular and clinical investigations are required to scrutinize mutation effects and the clinical utility of the genetic testing of TRMA.


## Acknowledgments

The authors thank the family members for their cooperation.


## REFERENCES


1. Rogers LE, Porter FS, Sidbury JB Jr. Thiamine-responsive megaloblastic anemia. *J Pediatr.* 1969;74(4):494–504. doi:10.1016/s0022-3476(69)80031-4.
2. Raz T, Labay V, Baron D, et al. The spectrum of mutations, including four novel ones, in the thiamine-responsive megaloblastic anemia gene SLC19A2 of eight families. *Hum Mutat.* 2000;16(1):37–42. doi:10.1002/1098-1004(200007)16:1<37::AID-HUMU7>3.0.CO;2-9.
3. Madaan P, Jauhari P, Michael SN, Sinha A, Chakrabarty B, Gulati S. Stroke as an initial manifestation of thiamine-responsive megaloblastic anemia. *Ann Indian Acad Neurol.* 2020;23(1):136–138. doi:10.4103/aian.AIAN_166_19.
4. Labay V, Raz T, Baron D, et al. Mutations in SLC19A2 cause thiamine-responsive megaloblastic anaemia associated with diabetes mellitus and deafness. *Nat Genet.* 1999;22(3):300–304. doi:10.1038/10372.
5. Mee L, Nabokina SM, Sekar VT, Subramanian VS, Maedler K, Said HM. Pancreatic beta cells and islets take up thiamin by a regulated carrier-mediated process: studies using mice and human pancreatic preparations. *Am J Physiol-Gastrointest Liver Physiol*. 2009;297(1):G197–G206.
6. Enogieru OJ, Koleske ML, Vora B, et al. The effects of genetic mutations and drugs on the activity of the thiamine transporter, SLC19A2. *AAPS J* 2021;23(2):1–8.
7. Diaz GA, Banikazemi M, Oishi K, Desnick RJ, Gelb BD. Mutations in a new gene encoding a thiamine transporter cause thiamine-responsive megaloblastic anaemia syndrome. *Nat Genet.* 1999;22(3):309–312. doi:10.1038/10385.
8. Manimaran P, Subramanian VS, Karthi S, et al. Novel nonsense mutation (p. Ile411Metfs* 12) in the SLC19A2 gene causing thiamine responsive megaloblastic anemia in an Indian patient. *Clin Chim Acta.* 2016;452:44–49. doi:10.1016/j.cca.2015.11.002.
9. Omkar P, Ravikumar KG, Gopi S, Raman T, Radha V, Mohan V. Thiamine-responsive megaloblastic anemia syndrome: a case report. *J Diabetol.* 2020;11(1):45.

10. Amr K, Pawlikowska P, Aoufouchi S, Rosselli F, El-Kamah G. Whole exome sequencing identifies a new mutation in the SLC19A2 gene leading to thiamine-responsive megaloblastic anemia in an Egyptian family. *Mol Genet Genomic Med.* 2019;7(7):e00777.
11. Naeem M, Shabaz A, Shoaib A, Usman M. A rare case of thiamine-responsive megaloblastic anaemia syndrome: a disorder of high-affinity thiamine transport. *J Ayub Med Coll Abbottabad: JAMC* 2008;20(3):146–148.
12. Shaw-Smith C, Flanagan SE, Patch AM, et al. Recessive SLC19A2 mutations are a cause of neonatal diabetes mellitus in thiamine-responsive megaloblastic anaemia. *Pediatr Diabetes.* 2012;13(4):314–321.
13. Rajgopal A, Edmondson A, Goldman ID, Zhao R. SLC19A3 encodes a second thiamine transporter ThTr2. *Biochim Biophys Acta (BBA)-Mol Basis Dis.* 2001;1537(3):175–178.
14. Lindhurst MJ, Fiermonte G, Song S, et al. Knockout of Slc25a19 causes mitochondrial thiamine pyrophosphate depletion, embryonic lethality, CNS malformations, and anemia. *Proc Natl Acad Sci USA.* 2006;103(43):15927–15932.
15. Rehman JU, AlJohani NI, Nassani Momin SM, Yousef M. Thiamine deficiency syndrome (Rogers syndrome) with recurrent thrombosis and pulmonary embolism with a novel mutation. *Oman Med J*. 2022. doi:10.5001/omj.2022.39.
16. Jungtrakoon P, Shirakawa J, Buranasupkajorn P, et al. Loss-of-function mutation in thiamine transporter 1 in a family with autosomal dominant diabetes. *Diabetes.* 2019;68(5):1084–1093. doi:10.2337/db17-0821.
17. Kircher M, Witten DM, Jain P, O'Roak BJ, Cooper GM, Shendure J. A general framework for estimating the relative pathogenicity of human genetic variants. *Nat Genet.* 2014;46(3):310–315. doi:10.1038/ng.2892.
18. Kumar P, Henikoff S, Ng PC. Predicting the effects of coding non-synonymous variants on protein function using the SIFT algorithm. *Nat Protocols.* 2009;4(7):1073–1081. doi:10.1038/nprot.2009.86.
19. Adzhubei IA, Schmidt S, Peshkin L, et al. A method and server for predicting damaging missense mutations. *Nat Methods.* 2010;7(4):248–249. doi:10.1038/nmeth0410-248.
20. Shihab HA, Gough J, Cooper DN, et al. Predicting the functional, molecular, and phenotypic consequences of amino acid substitutions using hidden Markov models. *Hum Mutat.* 2013;34(1):57–65. doi:10.1002/humu.22225.
21. Dong C, Wei P, Jian X, et al. Comparison and integration of deleteriousness prediction methods for nonsynonymous SNVs in whole exome sequencing studies. *Hum Mol Genet.* 2015;24(8):2125–2137. doi:10.1093/hmg/ddu733.
22. Richards S, Aziz N, Bale S, et al. Standards and guidelines for the interpretation of sequence variants: a joint consensus recommendation of the American College of Medical Genetics and Genomics and the Association for Molecular Pathology. *Genet Med.* 2015;17(5):405–424. doi:10.1038/gim.2015.30.
23. Argun M, Baykan A, Hatipoğlu N, et al. Arrhythmia in thiamine responsive megaloblastic anemia syndrome. *Turk J Pediatr.* 2018;60(3):348–351. doi:10.24953/turkjped.2018.03.021.
24. Ozdemir MA, Akcakus M, Kurtoglu S, Gunes T, Torun YA. TRMA syndrome (thiamine-responsive megaloblastic anemia): a case report and review of the literature. *Pediatr Diabetes.* 2002;3(4):205–209. doi:10.1034/j.1399-5448.2002.30407.x.
25. Yeşilkaya E, Bideci A, Temizkan M, et al. A novel mutation in the SLC19A2 gene in a Turkish female with thiamine-responsive megaloblastic anemia syndrome. *J Trop Pediatr.* 2009;55(4):265–267. doi:10.1093/tropej/fmn060.
26. Setoodeh A, Haghighi A, Saleh-Gohari N, Ellard S, Haghighi A. Identification of a SLC19A2 nonsense mutation in Persian families with thiamine-responsive megaloblastic anemia. *Gene* 2013;519(2):295–297. doi:10.1016/j.gene.2013.02.008.
27. Zhang S, Qiao Y, Wang Z, et al. Identification of novel compound heterozygous variants in SLC19A2 and the genotype-phenotype associations in thiamine-responsive megaloblastic anemia. *Clin Chim Acta.* 2021;516:157–168. doi:10.1016/j.cca.2021.01.025.
28. Rindi G, Ferrari G. Thiamine transport by human intestine in vitro. *Experientia* 1977;33(2):211–213. doi:10.1007/BF02124072.
29. Fleming JC, Tartaglini E, Steinkamp MP, Schorderet DF, Cohen N, Neufeld EJ. The gene mutated in thiamine-responsive anaemia with diabetes and deafness (TRMA) encodes a functional thiamine transporter. *Nat Genet.* 1999;22(3):305–308. doi:10.1038/10379.
30. Xian X, Liao L, Shu W, et al. A novel mutation of SLC19A2 in a Chinese Zhuang ethnic family with thiamine-responsive megaloblastic anemia. *Cell Physiol Biochem.* 2018;47(5):1989–1997. doi:10.1159/000491467.
31. Reidling JC, Lambrecht N, Kassir M, Said HM. Impaired intestinal vitamin B1 (thiamin) uptake in thiamin transporter-2–deficient mice. *Gastroenterology* 2010;138(5):1802–1809. doi:10.1053/j.gastro.2009.10.042.
32. Kang P, Zhang W, Wen J, Zhang J, Li F, Sun W. Case report: genetic and clinical features of maternal uniparental isodisomy-induced thiamine-responsive megaloblastic anemia syndrome. *Front Pediatr.* 2021;19(9):630329. doi:10.3389/fped.2021.630329.
33. Önal H, Baris S, Özdil M, et al. Thiamine-responsive megaloblastic anemia: early diagnosis may be effective in preventing deafness. *Turk J Pediatr.* 2009;51(3):301.
34. Habeb AM, Flanagan SE, Zulali MA, et al. Pharmacogenomics in diabetes: outcomes of thiamine therapy in TRMA syndrome. *Diabetologia.* 2018;61(5):1027–1036. doi:10.1007/s00125-018-4554-x.
35. Odaman-Al I, Gezdirici A, Yıldız M, et al. A novel mutation in the SLC19A2 gene in a Turkish male with thiamine-responsive megaloblastic anemia syndrome. *Turk J Pediatr.* 2019;61(2):257–260. doi:10.24953/turkjped.2019.02.015.
36. Li X, Cheng Q, Ding Y, et al. TRMA syndrome with a severe phenotype, cerebral infarction, and novel compound heterozygous SLC19A2 mutation: a case report. *BMC Pediatr.* 2019;19(1):1–6.
37. Agladioglu SY, Aycan Z, Bas V, Kendirci HP, Onder A. Thiamine-responsive megaloblastic anemia syndrome: a novel mutation. *Genet Couns.* 2012;23(2):149–156.
38. Bergmann AK, Sahai I, Falcone JF, et al Thiamine-responsive megaloblastic anemia: identification of novel compound heterozygotes and mutation update. *J Pediatr.* 2009;155(6):888–892.e1. doi:10.1016/j.jpeds.2009.06.017.
39. Lagarde WH, Underwood LE, Moats-Staats BM, Calikoglu AS. Novel mutation in the SLC19A2 gene in an African-American female with thiamine-responsive megaloblastic anemia syndrome. *Am J Med Genet A.* 2004;125(3):299–305.
40. Bundey S, Fielder A, Poulton K. Wolfram syndrome: mitochondrial disorder. *Lancet.* 1993;342(8878):1059–1060.
41. Ricketts CJ, Minton JA, Samuel J, et al. Thiamine-responsive megaloblastic anaemia syndrome: long-term follow-up and mutation analysis of seven families. *Acta Paediatr.* 2006;95(1):99–104.
42. Pomahačová R, Zamboryová J, Sýkora J, et al. First 2 cases with thiamine-responsive megaloblastic anemia in the Czech Republic, a rare form of monogenic diabetes mellitus: a novel mutation in the thiamine transporter SLC19A2 gene—intron 1 mutation c. 204 + 2T> G. *Pediatr Diabetes.* 2017;18(8):844–847. doi:10.1111/pedi.12479.
43. Scharfe C, Hauschild M, Klopstock T, et al. A novel mutation in the thiamine responsive megaloblastic anaemia gene SLC19A2 in a patient with deficiency of respiratory chain complex I. *J Med Genet.* 2000;37(9):669–673. doi:10.1136/jmg.37.9.669.
44. Liu G, Yang F, Han B, Liu J, Nie G. Identification of four SLC19A2 mutations in four Chinese thiamine responsive megaloblastic anemia patients without diabetes. *Blood Cells Mol Dis* 2013;52(4):203–204.
45. Tahir S, Leijssen LG, Sherif M, Pereira C, Morais A, Hussain K. A novel homozygous SLC19A2 mutation in a Portuguese patient with diabetes mellitus and thiamine-responsive megaloblastic anaemia. *Int J Pediatr Endocrinol.* 2015;2015(1):1–4.

46. Cao B, Gong C, Di Wu CL, et al. Genetic analysis and follow-up of 25 neonatal diabetes mellitus patients in China. *J Diabetes Res.* 2016;2016(2):1–9. doi:10.1155/2016/6314368.

47. Karimzadeh P, Moosavian T, Moosavian H. Recurrent stroke in a child with TRMA syndrome and SLC19A2 gene mutation. *Iran J Child Neurol.* 2018;12(1):84–88.

48. Mikstiene V, Songailiene J, Byckova J, et al. Thiamine responsive megaloblastic anemia syndrome: a novel homozygous SLC19A2 gene mutation identified. *Am J Med Genet A.* 2015;167(7):1605–1609. doi:10.1002/ajmg.a.37015.

49. Wood MC, Tsiouris JA, Velinov M. Recurrent psychiatric manifestations in thiamine-responsive megaloblastic anemia syndrome due to a novel mutation c. 63_71 delACCGCTC in the gene SLC19A2. *Psychiatry Clin Neurosci.* 2014;68(6):487–487. doi:10.1111/pcn.12143.

50. Dua V, Yadav SP, Kumar V, et al. Thiamine responsive megaloblastic anemia with a novel SLC19A2 mutation presenting with myeloid maturational arrest. *Pediatric blood & cancer* 2013;60(7):1242–1243. doi:10.1002/pbc.24529.

51. Kurtoglu S, Hatipoglu N, Keskin M, Kendirci M, Akcakus M. Thiamine withdrawal can lead to diabetic ketoacidosis in thiamine responsive megaloblastic anemia: report of two siblings. *J Pediatr Endocrinol Metab.* 2008;21(4):393–398.

52. Yaghootkar H, Abbasi F, Ghaemi N, et al. Type 1 diabetes genetic risk score discriminates between monogenic and Type 1 diabetes in children diagnosed at the age of <5 years in the Iranian population. *Diabet Med.* 2019;36(12):1694–1702. doi:10.1111/dme.14071.

53. Gritli S, Omar S, Tartaglini E, et al. A novel mutation in the SLC19A2 gene in a Tunisian family with thiamine-responsive megaloblastic anaemia, diabetes and deafness syndrome. *Br J Haematol.* 2001;113(2):508–513. doi:10.1046/j.1365-2141.2001.02774.x.

54. Haworth C, Evans D, Mitra J, Wickramasinghe S. Thiamine responsive anaemia: a study of two further cases. *Br J Haematol.* 1982;50(4):549–561.

55. Mozzillo E, Melis D, Falco M, et al. Thiamine responsive megaloblastic anemia: a novel SLC19A2 compound heterozygous mutation in two siblings. *Pediatr Diabetes.* 2013;14(5):384–387. doi:10.1111/j.1399-5448.2012.00921.x.

56. Ghaemi N, Ghahraman M, Abbaszadegan MR, Vakili R. Novel mutation in the SLC19A2 gene in thiamine-responsive megaloblastic anemia (Rogers' syndrome). *Iranian Journal of Neonatology IJN*. 2012;3(1):30–35.

57. Zhang Y, Zhang Y, Zhang VW, Zhang C, Ding H, Yin A. Mutations in both SAMD9 and SLC19A2 genes caused complex phenotypes characterized by recurrent infection, dysphagia and profound deafness–a case report for dual diagnosis. *BMC Pediatr.* 2019;19(1):1–5.

58. Uroic AS, Milenkovic D, De Franco E, Bilic E, Putarek NR, Krnic N. Importance of immediate thiamine therapy in children with suspected thiamine-responsive megaloblastic anemia—report on two patients carrying a novel SLC19A2 gene mutation. *J Pediatr Genet.* 2020. doi:10.1055/s-0040-1717136.

59. Bazarbachi A, Muakkit S, Ayas M, et al. Thiamine-responsive myelodysplasia. *Br J Haematol.* 1998;102(4):1098–1100. doi:10.1046/j.1365-2141.1998.00861.x.

CORRECTION

# Correction to: Treatment of COVID-19 Patients with Two Units of Convalescent Plasma in a Resource-Constrained State

*Laboratory Medicine* 2022;53:651; https://doi.org/10.1093/labmed/lmac118



Tina S Ipe, MD, MPH, Blessing Ugwumba, BMLS, Horace J Spencer, MS, Tuan Le, MD, Terry Ridenour, John Armitage, MD, Stefanie Ryan, APRN, Shanna Pearson, APRN, Atul Kothari, MD, Naveen Patil, MD, Ryan Dare, MD, Juan C R Crescencio, MD, Anand Venkata, MD, Jennifer Laudadio, MD, Khalid Mohammad, MD, Naznin Jamal, MD, John Thompson, MD, Hailey McNew, MHSA, McKenzie Gibbs, Steve Hennigan, MD, Stan Kellar, MD, Keith Reitzel, MD, Brandon E Walser, MD, Amanda Novak, MD, Brian Quinn, MD, Treatment of COVID-19 Patients with Two Units of Convalescent Plasma in a Resource-Constrained State, *Laboratory Medicine*, 2022;, lmac055, https://doi.org/10.1093/labmed/lmac055

In the originally published version of this manuscript, an acknowledgement of grant support was omitted:

"Research reported in this publication was supported, in part, by the National Center For Advancing Translational Sciences of the National Institutes of Health under Award Number UL1 TR003107. The content is solely the responsibility of the authors and does not necessarily represent the official views of the National Institutes of Health."

This error has been corrected online.

CASE STUDY

# Rare Case of Accelerated-Phase Chronic Myeloid Leukemia Diagnosed During Treatment for *JAK2* V617F–Positive Primary Myelofibrosis

*Jeayeon Ryu, MD,[1] Daehyun Chu, MD,[1] Bosung Park, MD,[1] Miyoung Kim, MD, PhD,[1,*] Young-Uk Cho, MD, PhD,[1] Sang-Hyun Hwang, MD, PhD,[1] Seongsoo Jang, MD, PhD,[1] Eul-Ju Seo, MD, PhD,[1] Jung-Hee Lee, MD, PhD,[2] Chan-Jeoung Park, MD, PhD[1]*

[1]Department of Laboratory Medicine, Asan Medical Center, University of Ulsan College of Medicine, Seoul, Korea, [2]Department of Hematology, Asan Medical Center, University of Ulsan College of Medicine, Seoul, Korea; *To whom correspondence should be addressed. miyoungkim@amc.seoul.kr

**Keywords:** *BCR-ABL1*, chronic myeloid leukemia, *JAK2*, primary myelofibrosis, myeloproliferative neoplasm, ruxolitinib

**Abbreviations:** MPN, myeloproliferative neoplasm; CML, chronic myeloid leukemia; PMF, primary myelofibrosis; CBC, complete blood count; WBC, white blood cell; BM, bone marrow; HPF, high-power field; PCR, polymerase chain reaction; IS-NCN, international scale-normalized copy number; PV, polycythemia vera.

*Laboratory Medicine* 2022;53:e140–e144; https://doi.org/10.1093/labmed/lmac011

## ABSTRACT

Myeloproliferative neoplasms (MPNs) are clonal hematopoietic stem cell disorders characterized by the expansion of myeloid lineage cells. Chronic myeloid leukemia (CML) is characterized by a *BCR-ABL1* fusion gene that causes constitutive tyrosine kinase activity. Polycythemia vera, essential thrombocythemia, and primary myelofibrosis (PMF) are frequently associated with driver mutations in genes such as *JAK2, CALR,* and *MPL* and are mutually exclusive of *BCR-ABL1*. Herein, we report the first case study of a patient diagnosed with accelerated-phase CML while undergoing treatment for initial *JAK2* V617F–positive, *BCR-ABL1*-negative PMF. This finding emphasizes the importance of *BCR-ABL1* testing in patients with an atypical *BCR-ABL1*-negative MPN disease course.

## Clinical History

A 58 year old Korean woman was referred to the hematology department after having experienced anemia and thrombocytosis for 6 months. Her complete blood count (CBC) showed a hemoglobin level of 9.9 g/dL, a white blood cell (WBC) count of 10.2 × $10^3$/μL with a normal differential count, and a platelet count of 547 × $10^3$/μL. A peripheral blood smear showed occasional large platelets, and bone marrow (BM) aspiration showed increased trilineage hematopoiesis with no blast increase. A BM biopsy showed hypercellular marrow (70% cellularity) with megakaryocytic hyperplasia (7.0 per high-power field [HPF]) exhibiting cluster formation. Reticulin staining showed a diffuse increase with extensive intersections and coarse bundles of thick fibers, and Masson's trichrome staining showed a diffuse connecting meshwork of collagen comprising >30% of the specimen, which was equivalent to grade 3 fibrosis. (**FIGURE 2**) Molecular genetic studies performed on the patient's BM specimen showed a *JAK2* V617F mutation but no *BCR-ABL1* rearrangement. Her BM karyotype was 46,XX[12], and her spleen was not palpable. As such, she was diagnosed with overt fibrotic primary myelofibrosis (PMF).

The patient remained untreated for the first 4 years post initial diagnosis until leukocytosis became evident. During the following 3-year treatment course with hydroxyurea, her WBC and platelet counts fluctuated, with a gradual increase in basophils. The *JAK2* inhibitor ruxolitinib was added to her treatment after marked leukocytosis with anemia, basophilia, and circulating blasts were detected (hemoglobin, 6.7 g/dL; WBCs, 88.4 × $10^3$/μL, with blasts at 1.0% and basophils at 7.0%; and platelets, 200 × $10^3$/μL). Marked splenomegaly (17.7 cm) was observed together with abdominal discomfort and weight loss.

Follow-up BM examination was performed 3 months later. The patient's CBC showed hemoglobin of 7.1 g/dL, WBCs of 18.7 × $10^3$/μL with circulating blasts at 1.0% and basophils at 7.0%, and platelets of 193 × $10^3$/μL. The BM aspirate was hemodiluted with 1.6% blasts, and BM biopsy showed hypercellular marrow (cellularity 80%) with granulocytic hyperplasia and megakaryocytes in cluster formation (2.7/HPF [0-8/HPF]). Reticulin and Masson's trichrome staining indicated grade 2 fibrosis. (**FIGURE 3**) Quantitative real-time polymerase chain reaction (PCR) of the BM specimen showed major *BCR-ABL1* rearrangement (b3a2) with an international scale-normalized copy number (IS-NCN) of 41.114. The patient was positive for the *JAK2* V617F mutation; her BM karyotype was 46,XX,t(9;22)(q34;q11.2),t(12;19)(q24.1;q13.3)[14]/46,XX[6]. Based on these findings, which included an additional clonal chromosomal abnormality on Philadelphia chromosome-positive cells, a diagnosis of accelerated-phase chronic myeloid leukemia (CML) was inferred. (**FIGURE 1**)

The CML clone remained constantly detectable for 3 months after diagnosis despite treatment with ruxolitinib and hydroxyurea, ranging from 39.663 to 59.360 IS-NCN in peripheral blood. The patient's WBCs also reached 53.4 × $10^3$/μL with circulating blasts at 1.0% and basophils

**FIGURE 1.** Time course of WBC count, basophil percentage, PLT count, *JAK2* V617F status, *BCR-ABL1* fusion transcript, and splenomegaly during the patient's disease timeline. AP; accelerated phase; CML, chronic myeloid leukemia; PLT, platelet; PMF, primary myelofibrosis.

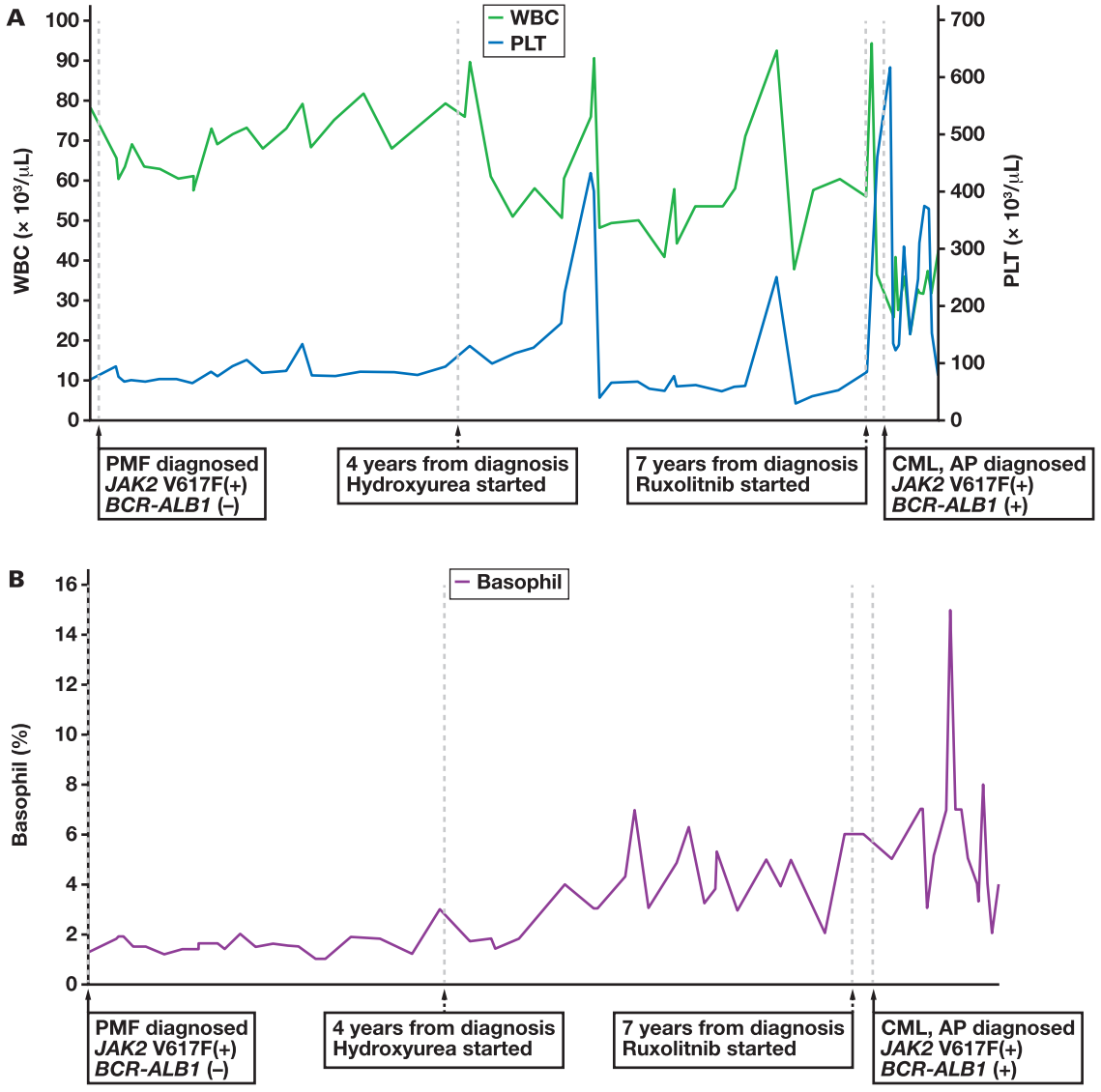


at 8.0%. To treat the CML, the tyrosine kinase inhibitor imatinib was added to ruxolitinib and hydroxyurea, but she showed an IS-NCN of 31.73 for *BCR-ABL1* rearrangement in the peripheral blood 2 weeks later. Her CBC after 1.5 months revealed hemoglobin of 8.5 g/dL, a WBC count of 11.2 × $10^3$/μL with circulating blasts at 1.0% and basophils at 4.0%, and a platelet count of 298 × $10^3$/μL.

## Discussion

Patients with concurrent *BCR-ABL1* rearrangements and *JAK2* V617F mutations have rarely been reported and can be categorized into 3 types: (i) concurrent *BCR-ABL1* rearrangement and *JAK2* V617F mutation at the initial diagnosis of myeloproliferative neoplasms (MPNs), (ii) acquisition of *JAK2* V617F mutation during the course of CML with *BCR-ABL1* rearrangement, and (iii) acquisition of *BCR-ABL1* rearrangement during the course of *BCR-ABL1*-negative MPN with *JAK2* V617F mutation.[1-11] The first and the third types seem to be more common than the second, although there remain too few patients reported to confirm this observation.[2,10]

Our patient fell under the third type, in which most MPNs are polycythemia vera (PV) or (less commonly) essential thrombocythemia with *BCR-ABL1* rearrangements acquired during the course of the original disease.[1,2,5,7-10] Only 2 patients with initially *BCR-ABL1*-negative, *JAK2* V617F–positive PMF who acquired *BCR-ABL1* rearrangements during the courses of their diseases have been reported to date, both of whom were untreated for PMF.[2,4] In a multi-institutional study from the Bone Marrow Pathology Group, only 11 of 1570 patients were tested for both *BCR-ABL1* and *JAK2* V617F, among whom only 1 had *JAK2* V617F–positive PMF and later acquired *BCR-ABL1* with a CML phenotype during the course of disease without any treatment.[2] Another patient with similar characteristics was reported by Jallades et al.[4] Ours is the third reported patient with PMF who acquired *BCR-ABL1* rearrangement but is the first to have acquired a *BCR-ABL1* rearrangement while undergoing treatment for PMF with a *JAK2* inhibitor and was determined to have

**FIGURE 2.** **Peripheral blood smear and bone marrow biopsy at the initial diagnosis of *JAK2* V617F-positive primary myelofibrosis. (A) Peripheral blood smear showing anisopoikilocytosis including tear-drop cells and occasional large platelets (Wright-Giemsa stain, ×400). (B) Bone marrow biopsy showing increased megakaryocytes, extensive fibrosis, neo-osteogenesis, and osteosclerosis (hematoxylin-eosin stain, ×200). (C) Bone marrow biopsy showing a diffuse and dense increase in reticulin with extensive intersections and coarse bundles of thick fibers consistent with collagen, corresponding to fibrosis grade 3 (reticulin stain, ×200). (D) Bone marrow biopsy showing a diffuse connecting meshwork of collagen in most of marrow spaces (Masson's trichrome stain, ×200).**

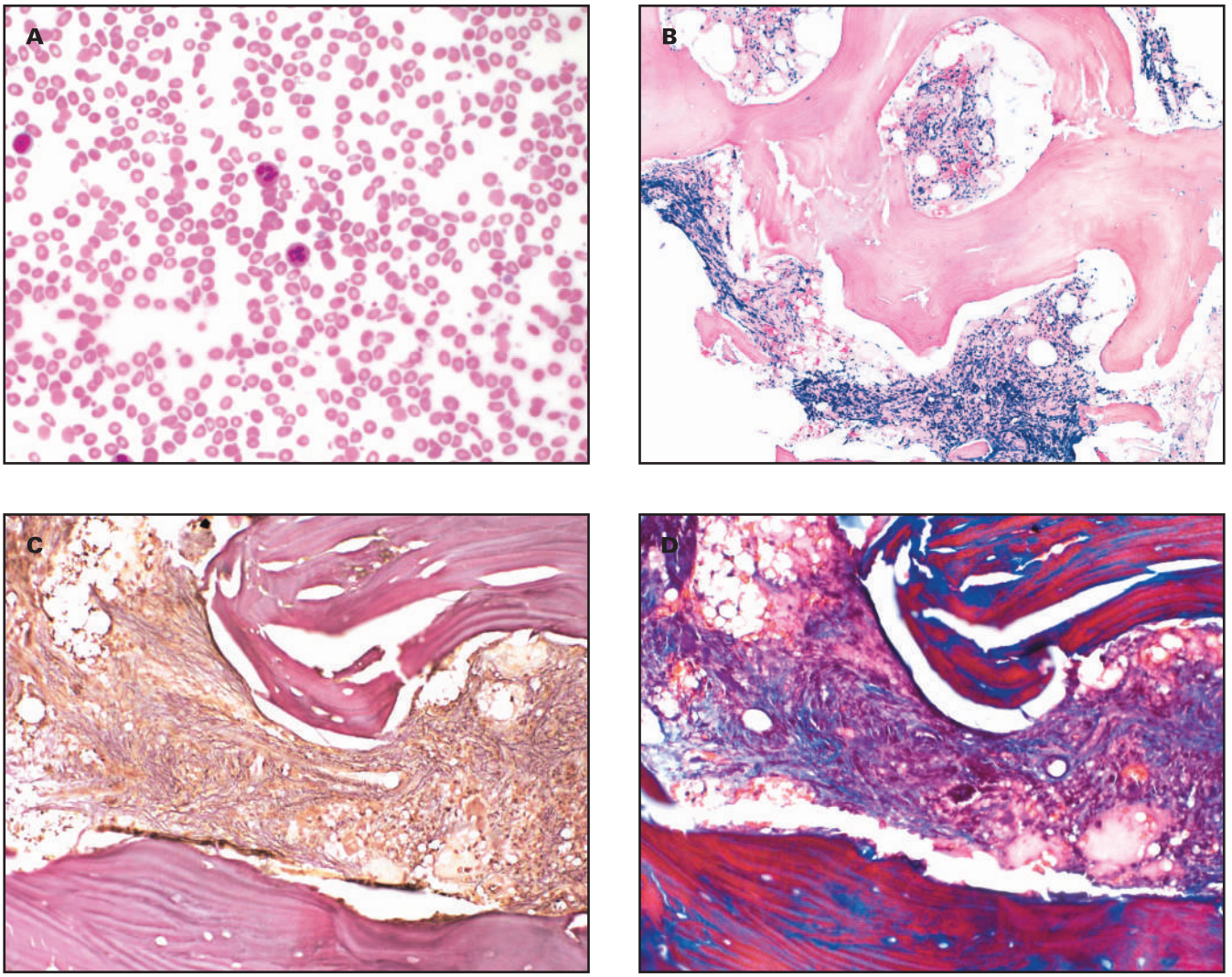


accelerated-phase CML owing to an additional chromosomal abnormality in Philadelphia chromosome–positive cells at diagnosis.[12]

The relationship between *JAK2* V617F–positive and *BCR-ABL1*-positive clones has not yet been elucidated. Wang et al[7] performed genotypic analyses of hematopoietic progenitor cells assayed from 2 patients with a history of *JAK2* V617F–positive PV who developed CML 12 and 18 years after their initial presentation, respectively; only 1 had received hydroxyurea therapy. The authors observed *BCR-ABL1* fusion only in *JAK2* V617F–positive hematopoietic colonies, but there were no such colonies with *BCR-ABL1* lacking *JAK2* V617F; this finding suggested that *BCR-ABL1* acquisition occurred after the *JAK2* V617F mutation and that the development of CML was a secondary event.

However, Cambier et al[8] could not identify any *BCR-ABL*-positive cells in the endogenous erythroid colonies of a patient with concurrent concomitant *BCR-ABL* rearrangement and *JAK2* V617F mutation at the initial presentation of CML and PV, indicating that these 2 clones were distinct. Even though the patient achieved a complete cytogenetic response after 6 months of imatinib mesylate therapy, the patient's hematocrit was not affected; this finding also suggested distinct PV and CML clones. Indeed, Bader and Dreiling[10] suggested different types of possible interactions and clones between *JAK2* V617F mutation and *BCR-ABL* transcript levels and their corresponding clonal origins after comparing the disease courses of 33 patients with concomitant *JAK2* V617F–positive MPN and CML according to therapy.

The *JAK2* V617F–positive and *BCR-ABL*-positive clones may be either the same, a component of one another, or distinct. In our patient, the *JAK2* V617F mutation was retained when accelerated-phase CML was diagnosed, and follow-up real-time PCR of the peripheral blood showed that the level of the *BCR-ABL1* fusion gene transcript decreased during treatment with ruxolitinib. Although we did not perform

**FIGURE 3.** **Peripheral blood smear and bone marrow biopsy at the time of detection of the *BCR-ABL1* fusion transcript. (A) Peripheral blood smear showing left-shifted neutrophils, circulating blasts (1%), and increased basophils (15%) (Wright-Giemsa stain, ×400). (B) Bone marrow biopsy showing increased megakaryocytes, extensive fibrosis, and osteosclerosis (hematoxylin-eosin stain, ×200). (C) Bone marrow biopsy showing a diffuse and dense increase in reticulin with extensive intersections and focal bundles of thick fibers consistent with collagen, corresponding to fibrosis grade 2 (reticulin stain, ×200). (D) Bone marrow biopsy showing paratrabecular or central deposition of collagen within a focally connecting meshwork (Masson's trichrome stain, ×200).**

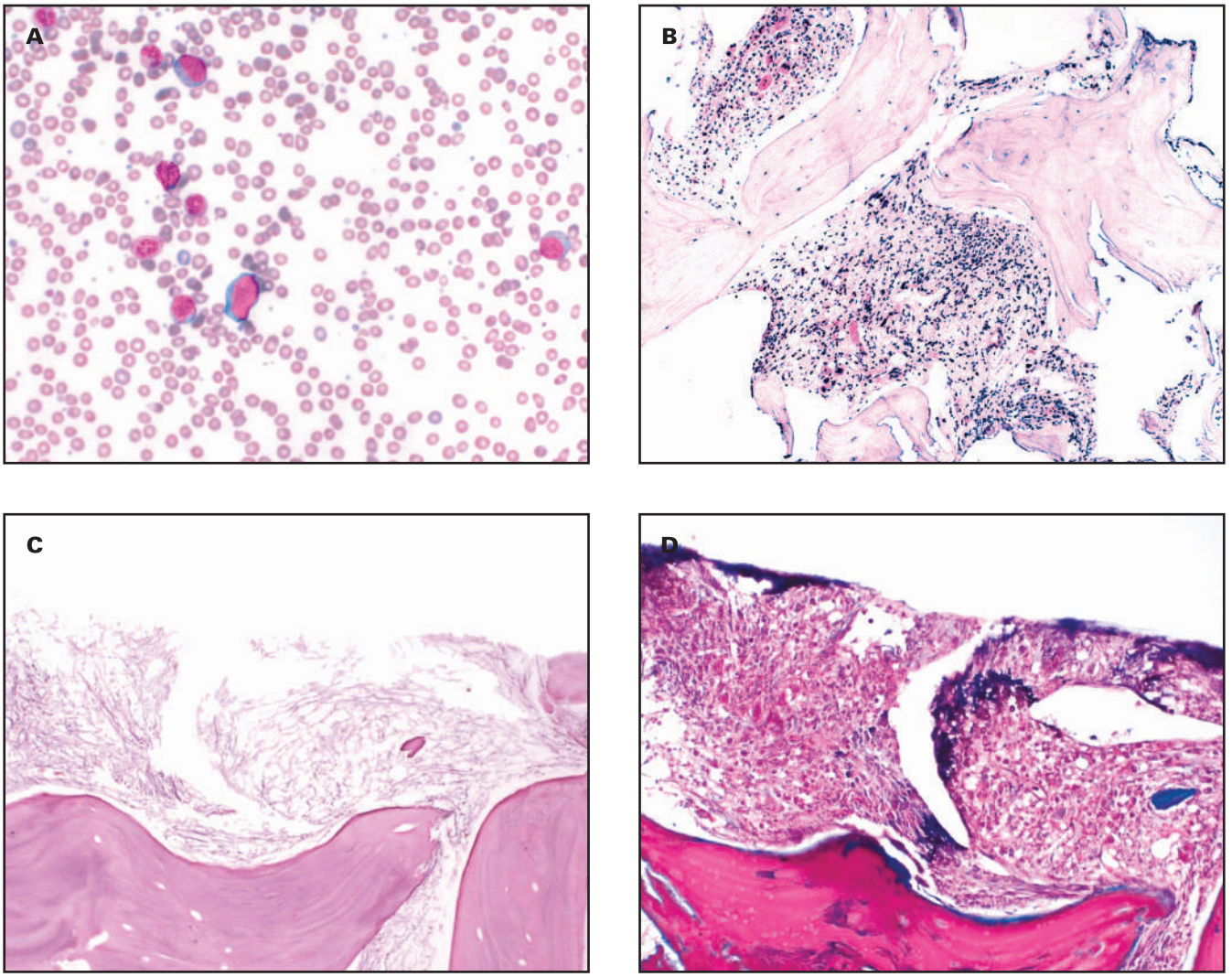


molecular analysis at the single-cell or colony level, the changes in the level of *BCR-ABL1* fusion gene transcript after ruxolitinib therapy indicated that the *BCR-ABL1* clone was at least a part of the *JAK2* V617F clone if not the same.

In summary, we have reported the first patient with accelerated-phase CML arising from *JAK2* V617F–positive PMF during *JAK2* inhibitor treatment. The emergence of the CML clone in patients with *JAK2* V617F–positive MPN may occur despite *BCR-ABL1* rearrangements and *JAK2* V617F mutations usually being mutually exclusive. It may be confused with drug resistance or relapse and can potentially be underestimated by myelosuppressive treatment. Our case study emphasizes the need to test for *BCR-ABL1* when a patient shows an atypical disease course despite treatment, particularly when accompanied by basophilia or progressive leukocytosis, to allow for the prompt readjustment of treatment.

## Acknowledgments

The patient provided informed consent for the publication of this report.

## REFERENCES

1. Lorenzo M, Grille S, Stevenazzi M. Emergence of BCR-ABL1 chronic myeloid leukemia in a JAK2-V617F polycythemia vera. *J Hematol.* 2020;9(1–2):23–29.
2. Soderquist CR, Ewalt MD, Czuchlewski DR, et al. Myeloproliferative neoplasms with concurrent BCR-ABL1 translocation and JAK2 V617F mutation: a multi-institutional study from the Bone Marrow Pathology Group. *Mod Pathol.* 2018;31(5):690–704.
3. Bocchia M, Vannucchi AM, Gozzetti A, et al. Insights into JAK2-V617F mutation in CML. *Lancet Oncol.* 2007;8(10):864–866.
4. Jallades L, Hayette S, Tigaud I, et al. Emergence of therapy-unrelated CML on a background of BCR-ABL-negative

JAK2V617F-positive chronic idiopathic myelofibrosis. *Leuk Res.* 2008;32(10):1608–1610.

5. Pingali SR, Mathiason MA, Lovrich SD, et al. Emergence of chronic myelogenous leukemia from a background of myeloproliferative disorder: JAK2V617F as a potential risk factor for BCR-ABL translocation. *Clin Lymphoma Myeloma.* 2009;9(5):E25–E29.
6. Hussein K, Bock O, Theophile K, et al. Chronic myeloproliferative diseases with concurrent BCR-ABL junction and JAK2V617F mutation. *Leukemia.* 2008;22(5):1059–1062.
7. Wang X, Tripodi J, Kremyanskaya M, et al. BCR-ABL1 is a secondary event after JAK2V617F in patients with polycythemia vera who develop chronic myeloid leukemia. *Blood.* 2013;121(7):1238–1239.
8. Cambier N, Renneville A, Cazaentre T, et al. JAK2V617F-positive polycythemia vera and Philadelphia chromosome-positive chronic myeloid leukemia: one patient with two distinct myeloproliferative disorders. *Leukemia.* 2008;22(7):1454–1455.
9. Ursuleac I, Colita A, Adam T, et al. The concomitant occurrence of JAK2V617F mutation and BCR/ABL transcript with phenotypic expression—an overlapping myeloproliferative disorder or two distinct diseases? Case report. *J Med Life.* 2013;6(1):34–37.
10. Bader G, Dreiling B. Concurrent JAK2-positive myeloproliferative disorder and chronic myelogenous leukemia: a novel entity? A case report with review of the literature. *J Investig Med High Impact Case Rep.* 2019;7:2324709619832322.
11. Bornhäuser M, Mohr B, Oelschlaegel U, et al. Concurrent JAK2(V617F) mutation and BCR-ABL translocation within committed myeloid progenitors in myelofibrosis. *Leukemia.* 2007;21(8):1824–1826.
12. Barbui T, Thiele J, Gisslinger H, et al. The 2016 WHO classification and diagnostic criteria for myeloproliferative neoplasms: document summary and in-depth discussion. *Blood Cancer J.* 2018;8(2):15.

CASE STUDY

# Acquired Thrombotic Thrombocytopenic Purpura After BNT162b2 COVID-19 Vaccine: Case Report and Literature Review

*Emna Hammami, MD,[1,*] Mathilde Lamarque, MD,[2] Olivier Aujoulat, PhD,[3] Agathe Debliquis, MD,[1] Bernard Drénou, MD,[2] Inès Harzallah, MD,[1]*

[1]Laboratory of Hematology, Groupe Hospitalier de la région Mulhouse Sud Alsace, Mulhouse, France, [2]Service d'hématologie clinique, Groupe Hospitalier de la région Mulhouse Sud Alsace, Mulhouse, France, [3]Pharmacie centrale, Groupe Hospitalier de la région Mulhouse Sud Alsace, Mulhouse, France; *To whom correspondence should be addressed. emnahammami1993@gmail.com

**Keywords:** thrombotic thrombocytopenic purpura, COVID-19, vaccine, thrombosis, thrombocytopenia, microangiopathy

**Abbreviations:** TTP, thrombotic thrombocytopenic purpura; aTTP, acquired thrombotic thrombocytopenic purpura; PE, plasma exchange; CBC, complete blood count; AIT, autoimmune thrombocytopenia; VITT, vaccine-induced immune thrombosis and thrombocytopenia; HUS, hemolytic uremic syndrome; ULVWF, ultralarge von Willebrand factor multimers.

*Laboratory Medicine* 2022;53:e145–e148; https://doi.org/10.1093/labmed/lmac016

## ABSTRACT

Thrombotic thrombocytopenic purpura (TTP) is a thrombotic microangiopathy that is deadly if not treated promptly. The treatment of choice in patients presenting with TTP is plasma exchanges. However, immunosuppressive therapy and caplacizumab have significantly improved outcomes in TTP. This microangiopathy is classically divided into 2 entities: hereditary and acquired TTP (aTTP), caused by an autoantibody against *ADAMTS 13.* We present a case study of a patient wth TTP occurring after a second dose of the BNT162b2 (Pfizer-BioNTech) COVID-19 vaccine along with a review of the literature. A 55-year-old patient presented with gastrointestinal symptoms, anemia, and severe thrombocytopenia. The blood film revealed the presence of schistocytes. A diagnosis of aTTP was established because the patient had severe *ADAMTS 13* deficiency and autoantibodies against *ADAMTS 13* were positive. This episode occurred 10 days after the patient received the COVID-19 vaccine. The patient received plasma exchanges, prednisone, rituximab, and caplacizumab and achieved complete remission. Ten patients with aTTP induced by the COVID-19 vaccine have been reported in the literature. Most of these situations occurred after the second dose of COVID-19 vaccine, and 7 patients were noted to have received the BNT162b2 vaccine. Caplacizumab was used in 6 patients, and complete remission was achieved in 8 patients.

Thrombotic thrombocytopenic purpura (TTP) is a thrombotic microangiopathy presenting in one-third of patients as a clinical pentad. Typically, this pentad is composed of fever, renal failure, neurological symptoms, thrombocytopenia, and microangiopathic hemolytic anemia. The diagnosis is suspected based on broad clinical manifestations and thrombocytopenia and hemolytic anemia of mechanical origin indicated by the presence of schistocytes. The diagnosis of TTP is confirmed by a severe deficiency of *ADAMTS 13* activity (<10%).

In France, the incidence of TTP is 1.5 cases per million per year in adults,[1] with a high mortality if treated improperly. Although the treatment of choice for TTP is plasma exchange (PE), immunosuppressive therapy has significantly improved outcomes with a reduced length of hospitalization.[2]

This microangiopathy is classically divided into 2 entities: hereditary TTP (historically known as Upshaw-Schulman syndrome) caused by a genetic mutation of the *ADAMTS 13* gene and acquired TTP (aTTP), an autoimmune disease resulting from the development of an autoantibody directed against *ADAMTS 13.*

Studies have shown that aTTP can be caused by a variety of triggers including infections, pregnancy, malignancies, autoimmune diseases, and vaccines. Vaccine-induced thrombocytopenia has been reported in the literature, including rare cases of patients with vaccine-induced aTTP.[3-5] Vaccination against COVID-19 has played an important role in controlling the pandemic. However, some adverse events have been observed, including rare cases of patients with TTP. We report a case of a patient with TTP occurring after a second dose of the BNT162b2 (Pfizer-BioNTech) COVID-19 vaccine along with a review of the literature.

## Case Report

Our patient was a 55 year old Caucasian woman. She presented to the emergency department with fatigue, nausea, and diarrhea persisting for

the previous 3 days. The patient also reported headache, and dizziness. Her background medical history included hypothyroidism, appendectomy, and amygdalotomy. Physical examination showed no particular signs aside from petechiae. A complete blood count (CBC) revealed anemia and severe thrombocytopenia (**TABLE 1**). The patient had normal hemoglobin and platelet counts with no history of hemolysis before admission.

Further tests showed an increase in lactate dehydrogenase with significantly elevated total bilirubin and indirect bilirubin (**TABLE 1**). The patient's haptoglobin level was depleted. The blood film revealed the presence of schistocytes at 2%. This finding raised suspicion for TTP.

Renal and hepatic blood panels were normal (creatinine = 62 µmol/L, alanine aminotransferase = 42 IU/L, and aspartate aminotransferase = 19 IU/L). The patient's calculated PLASMIC score[6] was 7, predicting a high risk for TTP (**TABLE 2**). The French score was 2 (creatinin < 200 >µmol/l, Platelet <30*$10^9$/l), also predicting a high risk for TTP.[7]

Cerebral MRI was performed and showed no signs of thrombosis. Laboratory investigation for other causes of microangiopathy was negative: The antinuclear antibody screen and shiga-toxin-producing *Escherichia coli* screening were negative, and the complement cascade evaluation was normal.

Lupus anticoagulant, anticardiolipin antibody, and anti-beta 2 glycoprotein I antibody assays were negative. The *ADAMTS 13* activity confirmed the diagnosis of TTP with a severe deficiency (<5%). An anti-*ADAMTS 13* antibodies screen was positive at 90 U/mL. Extensive anamnesis showed that the patient had received her second dose of BNT162b2 (Pfizer-BioNTech) COVID-19 vaccine 10 days before the onset of symptoms. Hence, the diagnosis of aTTP induced by COVID-19 vaccine was established.

We started PE right away, along with prednisone and rituximab at a dose of 375 mg/$m^2$. However, because the patient's platelet numbers continued to drop, caplacizumab was introduced at day 5 in addition to the ongoing daily PE. Platelet numbers increased to finally normalize at day 10. After 20 days of treatment, *ADAMTS 13* levels were normal and the patient was subsequently discharged. Subcutaneous caplacizumab was continued at home to total 20 doses.

**TABLE 1. Complete Blood Count and Hemolysis Panel on Admission**

| Biological Parameter (unit) | Value | Normal Range |
|---|---|---|
| Red blood cells (*$10^{12}$/L) | 3.54 | 3.92–5.08 |
| Hemoglobin (g/dL) | 10.7 | 11.9–14.6 |
| Hematocrit (%) | 30.8 | 36.6–44.4 |
| Mean corpuscular volume (fL) | 87 | 82.2–98 |
| Mean cell hemoglobin (pg) | 30.2 | 27–32.3 |
| Platelets (*$10^9$/L) | 15 | 150–450 |
| Neutrophils (*$10^9$/L) | 5.67 | 2.1–8.89 |
| Eosinophils (*$10^9$/L) | 0 | 0.01–0.07 |
| Basophils (*$10^9$/L) | 0.02 | 0.01–0.07 |
| Lymphocytes (*$10^9$/L) | 1.05 | 1.26–3.35 |
| Monocytes (*$10^9$/L) | 0.61 | 0.25–0.84 |
| Reticulocytes (*$10^9$/L) | 100.9 | 20–120 |
| Haptoglobin (g/L) | <0.02 | 0.4–2.8 |
| Lactate dehydrogenase (IU/L) | 645 | 120–246 |
| Total bilirubin (µmol/L) | 32 | 5–21 |
| Direct bilirubin (µmol/L) | 9 | 0–5 |
| Schistocytes (%) | 2 | <1 |

*The asteriks is to say that the number is multiplied bby $10^9$/L , for example it'as 5.67 * $10^9$/L for neutrophils.*

## Discussion

Since the launch of the COVID-19 vaccinations, vaccine adverse event reporting systems have been developed all over the world. Adverse events occurring after COVID-19 vaccination vary from simple events like headache, fever, and fatigue, which are described in the safety evaluation reports for COVID-19 vaccines,[8,9] to serious events like myocarditis and anaphylactic reactions.[10] Our patient presented with nausea and diarrhea 10 days after the second dose of a COVID-19 vaccine. The main laboratory finding in the initial workup was a severe symptomatic thrombocytopenia.

COVID-19 vaccine–related thrombocytopenia has been observed as an adverse event and described as various conditions, all of them involving autoimmunity.[11] Vaccine-triggered autoimmunity with vaccination has been known for decades, mainly involving epitope mimicry mechanisms.[12]

Thrombocytopenia induced by a COVID-19 vaccine can be caused by autoimmune thrombocytopenia (AIT),[11] which was the first diagnosis we considered in our patient. However, AIT is usually isolated in the CBC. In addition, the presence of schistocytes provided initial clues as to the diagnosis of TTP.

Another adverse event responsible for thrombocytopenia reported in the literature is vaccine-induced immune thrombosis and thrombocytopenia (VITT).[13] This condition has been observed more with the adenovirus-based coronavirus vaccines, and mostly after the first dose. Thrombocytopenia in VITT is caused by antibodies against platelet factor 4, in the absence of heparin. The severity of VITT is related to the occurrence of unusual-location thrombosis.

Although VITT and AIT are more frequently responsible for vaccine-induced thrombocytopenia, TTP has also been observed after COVID-19 vaccination. Most cases have been observed after BNT162b2 (Pfizer-BioNTech) COVID-19 vaccination,[14-17] but some were induced by ChAdOx1 nCov-19 (AstraZeneca)[18,19] (**TABLE 3**) and one case occurred after mRNA-1273 COVID-19 vaccine (Moderna) administration.[20]

Our patient received the second dose of the BNT162b2 (Pfizer-BioNTech) COVID-19 vaccine 10 days before the onset of symptoms. Her PLASMIC score predicted a high risk of severe *ADAMTS 13* deficiency. Hence, aTTP induced by vaccination was the most likely diagnosis.

**TABLE 2. PLASMIC Score in Patient**

| Items in PLASMIC Score | Score |
|---|---|
| Platelet count <30* $10^9$/L | 1 |
| Hemolysis; reticulocyte count >2.5%, haptoglobin undetectable, or indirect bilirubin >2.0 mg/dL (34.2 µmol/L) | 1 (haptoglobin undetectable) |
| Active cancer; treated for cancer within the past year | No: 1 |
| History of solid-organ or stem-cell transplant | No: 1 |
| MCV <9.0 × 10–14 L (<90 fL) | 1 |
| INR <1.5 | 1 |
| Creatinine <2.0 mg/dL (176.8 µmol/L) | 1 |
| PLASMIC score | 7 |

*INR, international normalized ratio; MCV, mean corpuscular volume.*

**TABLE 3. Case Reports of TTP After COVID-19 Vaccination**

| Author, Country | Vaccine | Vaccination Dose | Delay After Vaccine | Relapse/First Episode of TTP | Age (y) | Clinical Presentation | Treatment | Outcome |
|---|---|---|---|---|---|---|---|---|
| Chamarti et al, USA[22] | BNT162b2 (Pfizer-BioNTech) | Second | 2 wks | First | 80 | Weakness, malaise | PE, prednisone, rituximab | Remission |
| Waqar et al, USA, Pakistan[23] | BNT162b2 (Pfizer-BioNTech) | Second | 1 wk | First | 69 | Severe fatigue, shortness of breath | PE, prednisone, rituximab | Remission |
| Kirpalani et al, Canada[21] | BNT162b2 (Pfizer-BioNTech) | Second | 2 wks | First | 14 | Fatigue, confusion, headache, bruising | PE, rituximab, caplacizumab | Remission |
| Karabulut et al, USA[20] | mARN-1273 (Moderna) | First | 5 d | Relapse | 48 | Weakness and slurred speech | PE, rituximab, caplacizumab | Remission |
| Wang et al, Taiwan[18] | ChAdOx1 nCov-19 (AstraZeneca) | Not mentioned | 30 d | Not mentioned | 75 | Bleeding (tongue) | PE | Not mentioned |
| Lee et al, UK, Malaysia[19] | ChAdOx1 nCov-19 (AstraZeneca) | First | 12 d | First | 50 | Dysphasia and acute numbness | PE, prednisone, rituximab, aspirin, fondaparinux | Remission |
| Maayan et al, Israel[17] | BNT162b2 (Pfizer-BioNTech), case series | Second | 8 d | First | 49 | Somnolence, low-grade fever, macroscopic hematuria | PE, steroids, caplacizumab | Remission |
| | | Second | 28 d | First | 29 | Dysarthria | PE, steroids, rituximab, caplacizumab | Remission |
| | | First | 13 d | Relapse | 31 | Purpura, vaginal bleeding | PE, steroids, caplacizumab | Patient still on caplacizumab |
| | | Second | 8 d | Relapse | 30 | Purpura | PE, steroids, rituximab, caplacizumab | Remission |
| Current patient | BNT162b2 (Pfizer-BioNTech) | Second | 10 d | First | 55 | Nausea, diarrhea, headache | PE, prednisone, rituximab, caplacizumab | Remission |

*PE, plasma exchange; TTP, thrombotic thrombocytopenic purpura.*

Hemolytic uremic syndrome (HUS) was also considered in the differential diagnosis because the patient had a thrombotic microangiopathy and gastrointestinal symptoms. However, the absence of renal impairment was more in favor of a TTP diagnosis. Yet we ruled out probable causes of typical or atypical HUS because the patient had normal complement exploration and negative shiga-toxin-producing *E. coli* screening. The diagnosis of aTTP was confirmed along with a severe *ADAMTS 13* deficiency. The delay between symptom onset and COVID-19 vaccination was consistent with the literature (**TABLE 3**). All reported cases have been observed in adults except for 1 case observed in an adolescent.[21]

The patient's *ADAMTS 13* levels at admission were severely deficient. In fact, in the absence of *ADAMTS 13* (ie, TTP), uncleaved ultralarge von Willebrand factor multimers (ULVWF) are accumulated. They interact with platelets through the GpIb/IX/V complex, inducing the formation of microthrombi. Those microthrombi are responsible for the clinical manifestations and the formation of schistocytes.[24] A severe *ADAMTS 13* deficiency is necessary for the development of TTP but not sufficient. The development of TTP is abruptly precipitated by the activation of the alternative complement pathway by ULVWF. Complement activation has also been described as a pejorative prognosis factor.[25] Our patient's favorable outcome after immunosuppressive therapy can be explained by her normal C3, C4, and CH50 levels .

For decades, PE has been the cornerstone of TTP treatment. However, recent advancements in aTTP pathophysiology understanding have led to the inclusion of rituximab as a front-line treatment along with PE. More recently, caplacizumab, an antibody targeting domain A1 of von Willebrand factor was introduced. Caplacizumab showed satisfactory results, especially in patients with refractory TTP. Our patient received PE, prednisone, rituximab, and caplacizumab according to the HERCULES protocol.[26] The platelet count normalized after 10 days of treatment, and the patient is currently in complete remission.

Most patients with aTTP have been observed after receiving the second dose of a COVID-19 vaccine (**TABLE 3**). However, patients with relapse seem to be more frequently observed after receiving the first dose. Hence, the question is whether a patient should receive the COVID-19 booster. Because COVID-19 infection has also been observed as an aTTP trigger, the benefit-risk balance of vaccination should be carefully considered in such patients.

## Conclusion

This case report highlights the challenge of thrombocytopenia's etiology diagnosis after COVID-19 vaccination. Although VITT has been previously well described, aTTP related to COVID-19 may be less known and much is yet to be understood in the disease triggers, management, and prognosis. Caplacizumab seems to be an important therapy to consider and possibly include in front-line treatment in further studies.

## REFERENCES

1. Mariotte E, Azoulay E, Galicier L, et al. Epidemiology and pathophysiology of adulthood-onset thrombotic microangiopathy with severe ADAMTS13 deficiency (thrombotic thrombocytopenic

purpura): a cross-sectional analysis of the French national registry for thrombotic microangiopathy. *Lancet Haematol.* 2016;3(5):e237–e245.
2. Zheng XL. The standard of care for immune thrombotic thrombocytopenic purpura today. *J Thromb Haemost.* 2021;19(8):1864–1871.
3. Kadikoylu G, Yavasoglu I, Bolaman Z. Rabies vaccine-associated thrombotic thrombocytopenic purpura. *Transfus Med.* 2014;24(6):428–429.
4. Dias PJ, Gopal S. Refractory thrombotic thrombocytopenic purpura following influenza vaccination. *Anaesthesia.* 2009;64(4):444–446.
5. Kojima Y, Ohashi H, Nakamura T, et al. Acute thrombotic thrombocytopenic purpura after pneumococcal vaccination. *Blood Coagul Fibrinolysis.* 2014;25(5):512–514.
6. Bendapudi PK, Hurwitz S, Fry A, et al. Derivation and external validation of the PLASMIC score for rapid assessment of adults with thrombotic microangiopathies: a cohort study. *Lancet Haematol.* 2017;4(4):e157–e164.
7. Fage N, Orvain C, Henry N, et al.; Les scores PLASMIC et French ont des performances diminuées pour prédire le diagnostic de purpura thrombotique thrombocytopénique lorsqu'ils sont appliqués à une cohorte de microangiopathies thrombotiques non biaisé. *Néphrologie & Thérapeutique.* 2021;17(5):264. doi:10.1016/j.nephro.2021.07.261
8. Sadoff J, Gray G, Vandebosch A, et al.; ENSEMBLE Study Group. Safety and efficacy of single-dose Ad26.COV2.S vaccine against Covid-19. *N Engl J Med.* 2021;384(23):2187–2201.
9. Oliver SE, Gargano JW, Marin M, et al. The Advisory Committee on Immunization Practices' interim recommendation for use of Pfizer-BioNTech COVID-19 vaccine—United States, December 2020. *MMWR Morb Mortal Wkly Rep.* 2020;69(50):1922–1924.
10. Lamptey E. Post-vaccination COVID-19 deaths: a review of available evidence and recommendations for the global population. *Clin Exp Vaccine Res.* 2021;10(3):264–275.
11. Kragholm K, Sessa M, Mulvad T, et al. Thrombocytopenia after COVID-19 vaccination. *J Autoimmun.* 2021;123:102712.
12. Olivieri B, Betterle C, Zanoni G. Vaccinations and autoimmune diseases. *Vaccines*. 2021;9(8):815.
13. Klok FA, Pai M, Huisman MV, Makris M. Vaccine-induced immune thrombotic thrombocytopenia. *Lancet Haematol.* 2022;9(1):e73–e80.
14. Malayala SV, Papudesi BN, Sharma R, Vusqa UT, Raza A. A case of idiopathic thrombocytopenic purpura after booster dose of BNT162b2 (Pfizer-Biontech) COVID-19 Vaccine. *Cureus.* 2021;13(10):e18985.
15. Ruhe J, Schnetzke U, Kentouche K, et al. Acquired thrombotic thrombocytopenic purpura after first vaccination dose of BNT162b2 mRNA COVID-19 vaccine. *Ann Hematol.* 2022;101(3):717–719.
16. Yoshida K, Sakaki A, Matsuyama Y, et al. Acquired thrombotic thrombocytopenic purpura following BNT162b2 mRNA coronavirus disease vaccination in a Japanese patient. *Intern Med.* 2022;61(3):407–412.
17. Maayan H, Kirgner I, Gutwein O, et al. Acquired thrombotic thrombocytopenic purpura: a rare disease associated with BNT162b2 vaccine. *J Thromb Haemost.* 2021;19(9):2314–2317.
18. Wang Y-C, Chen T-C, Teng C-LJ, Wu C-H. ChAdOx1 nCov-19 vaccine-induced thrombotic thrombocytopenic purpura successfully treated with plasmapheresis. *Ann Hematol*. Published online October 18, 2021. doi: 10.1007/s00277-021-04701-x.
19. Lee HP, Selvaratnam V, Rajasuriar JS. Thrombotic thrombocytopenic purpura after ChAdOx1 nCoV-19 vaccine. *BMJ Case Rep.* 2021;14(10):e246049.
20. Karabulut K, Andronikashvili A, Kapici AH. Recurrence of thrombotic thrombocytopenic purpura after mRNA-1273 COVID-19 vaccine administered shortly after COVID-19. *Case Rep Hematol.* 2021;2021:4130138.
21. Kirpalani A, Garabon J, Amos K, et al. Thrombotic thrombocytopenic purpura temporally associated with BNT162b2 vaccination in an adolescent successfully treated with caplacizumab. *Br J Haematol.* 2022;196(1):e11–e14.
22. Chamarti K, Dar K, Reddy A, Gundlapalli A, Mourning D, Bajaj K. Thrombotic thrombocytopenic purpura presentation in an elderly gentleman following COVID vaccine circumstances. *Cureus.* 2021;13(7):e16619.
23. Waqar SHB, Khan AA, Memon S. Thrombotic thrombocytopenic purpura: a new menace after COVID bnt162b2 vaccine. *Int J Hematol.* 2021;114(5):626–629.
24. Sukumar S, Lämmle B, Cataland SR. Thrombotic thrombocytopenic purpura: pathophysiology, diagnosis, and management. *J Clin Med.* 2021;10(3):536.
25. Wu TC, Yang S, Haven S, et al. Complement activation and mortality during an acute episode of thrombotic thrombocytopenic purpura. *J Thromb Haemost.* 2013;11(10):1925–1927.
26. Scully M, Cataland SR, Peyvandi F, et al. Caplacizumab treatment for acquired thrombotic thrombocytopenic purpura. *N Engl J Med.* 2019;380:335–346.

SCIENCE

# High C-Reactive Protein-to-Lymphocyte Ratio Is Predictive of Unfavorable Prognosis in HBV-Associated Decompensated Cirrhosis

*Bin Ye, MD,[1] QiuMing Ding, MD,[2] Xia He, MD,[2] XiaoYun Liu, MD,[2] Jianjiang Shen, MD[2,*]*

[1]Department of Critical Care Medicine, Shengzhou People's Hospital, Shengzhou Branch of the First Affiliated Hospital of Zhejiang University, Shengzhou, China, [2]Department of Clinical Laboratory, Shengzhou People's Hospital, Shengzhou Branch of the First Affiliated Hospital of Zhejiang University, Shengzhou, China; *To whom correspondence should be addressed. sykele2021@yeah.net

**Keywords:** hepatitis B virus, decompensated cirrhosis, CRP-to-lymphocyte ratio, prognostic factors, systemic inflammation, mortality

**Abbreviations:** HBV-DeCi, hepatitis B virus–associated decompensated cirrhosis; CLR, C-reactive protein-to-lymphocyte ratio; HBV, hepatitis B virus; DeCi, decompensated cirrhosis; CRP, C-reactive protein; MELD, Model for End-Stage Liver Disease; AUC, area under the curve.

*Laboratory Medicine* 2022;53:e149–e153; https://doi.org/10.1093/labmed/lmac019

## ABSTRACT

**Objective:** Hepatitis B virus–associated decompensated cirrhosis (HBV-DeCi) is difficult to cure and has a very high risk of mortality. However, prediction of its prognosis is challenging. The C-reactive protein–to–lymphocyte ratio (CLR) is a newly discovered inflammatory indicator, but its role in HBV-DeCi remains unclear. In the present study, we sought to determine the prognostic role of the CLR in patients with HBV-DeCi.

**Materials and Methods:** This retrospective study enrolled 134 patients with HBV-DeCi. Independent prognostic markers were identified using multivariate regression analysis.

**Results:** The 30-day mortality rate was 12.7% (n = 17). The CLR was markedly higher in nonsurvivors compared with survivors. The multivariate analysis identified a high CLR as an independent risk factor for mortality.

**Conclusion:** We found that the CLR is an effective and simple prognostic marker in patients with HBV-DeCi.

Hepatitis B virus (HBV) is one of the major causes of morbidity and mortality worldwide.[1] Viral hepatitis is highly endemic in China, with HBV infection being the most common cause of cirrhosis and 3% of patients with compensated cirrhosis that develops into decompensated cirrhosis (DeCi) per year.[2] Research has shown that DeCi is an end-stage liver disease accompanied by various complications responsible for the poor prognosis, and survival markedly decreases to 15% at 5 years.[3] Currently, liver transplantation is the only effective therapeutic strategy for patients with DeCi. However, because of the lack of available donors and the lack of effective prediction for life expectancy, some patients remain on the waiting list for transplantation until they die.[4-6] Therefore, early and accurate prognostic indicators that can identify high-risk patients are very important to improve clinical management and reduce the mortality of patients with HBV-DeCi.

Systemic inflammation is recognized to play a crucial role in the pathology of advanced cirrhosis and to be associated with worse outcomes. The inflammatory response is usually evaluated by measuring leukocytes, neutrophils, lymphocytes, platelets, or C-reactive protein (CRP) in routine clinical practice. Thus, combinations of these inflammatory parameters may provide prognostic indicators for HBV-related hepatic disorders.[7,8] Furthermore, HBV-induced direct cytopathic effects and viral evasion of host immune responses are believed to contribute to disease severity.[9] It is generally acknowledged that lymphocytes play a key role in the immune response and that excessive immune activation leads to a decrease in the lymphocyte count.[9,10] Meanwhile, dysregulated immune responses have been shown to be associated with poor survival in patients with HBV infection.[11] Given that both inflammation and immunity are important for liver disease progression, the CRP-to-lymphocyte ratio (CLR), a combination of these 2 parameters measured in routine examinations, can be assumed to reflect systemic inflammatory and immune status and may serve as a convenient and accurate prognostic indicator for liver diseases.

Several recent studies have shown that a high CLR was linked to adverse outcomes in certain clinical situations. For example, the results of a meta-analysis conducted by Lagunas-Rangel[12] showed that an increased CLR reflects unfavorable outcomes in patients with COVID-19. Moreover, a high CLR has been proposed as a poor prognostic indicator in patients with malignant diseases.[13-16] Notably, Mungan et al[13] found

that the CLR was more effective than CRP alone for predicting poor prognosis after colorectal surgery. However, the relationship between the CLR and prognosis in patients with HBV-DeCi has not been determined. In the present study, we evaluated whether the CLR can be used as a predictor for clinical outcomes in patients with HBV-DeCi.

## Materials and Methods

### Patients

We enrolled patients with HBV-DeCi who were treated in our hospital between 2017 and 2020. The study was approved by the ethics committee of our hospital. We identified DeCi by the development of 1 or more major symptomatic complications of liver disease (ascites, encephalopathy, gastrointestinal bleeding, or hepatorenal syndrome).[17] All patients presented with clinical manifestations of decompensated liver disease for the first time. The exclusion criteria were concomitant infection with other hepatitis viruses or HIV, as other causes of liver diseases; malignant tumors; hematologic disorders; immunomodulatory therapy within the previous 3 months; and age >75 years. A total of 134 patients were ultimately enrolled (**FIGURE 1**). The primary endpoint was 30-day mortality.

### Data Collection

Demographic and clinical data, including hematology, coagulation, hepatic and renal parameters, and CRP, were obtained from the day of admission for all patients. Biochemical values were measured using a Hitachi 7600 analyzer (Hitachi, Tokyo, Japan) and a Sysmex CA1500 analyzer (Sysmex, Hyogo, Japan). Hematological parameters were measured using a Sysmex XE-2100 analyzer (Sysmex, Kobe, Japan). The CRP values were measured using an immunoturbidimetric assay (BN II System; Siemens, Erlangen, Germany) with a reference range of 0–10 mg/L. The CLR was calculated as CRP (mg/L) divided by lymphocytes ($\times 10^9$/L). The severity of liver disease was assessed using the Model for End-Stage Liver Disease (MELD) score.[18]

**FIGURE 1. Flow chart of the included participants. HBV-DeCi, hepatitis B virus–associated decompensated cirrhosis.**

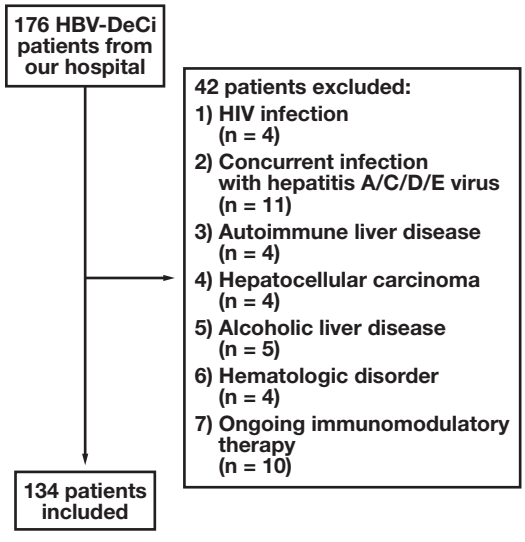


### Statistical Analysis

Variables are expressed as number or median (interquartile range). Comparisons between nonsurvivors and survivors at 30 days were carried out using the chi-square test for categorical data and the Mann-Whitney *U* test for continuous data. Univariate and multivariate analyses were performed to identify risk factors for mortality. Receiver operating characteristic curve analyses were conducted to determine the area under the curve (AUC) values for the CLR and the MELD score to evaluate their prognostic values for HBV-DeCi. Youden's index was used to identify cutoff values for the baseline CLR and the MELD score to predict clinical outcomes. Kaplan-Meier curves were used to evaluate the survival of patients with different CLR levels. All statistical analyses were performed using SPSS 21.0 (Chicago, IL) and MedCalc 14.8 software (MedCalc Software, Mariakerke, Belgium). Statistical significance was set at $P < .05$.

## Results

### Study Population

A total of 134 patients were enrolled in the study. The median age was 54.0 years, and 102 (76.1%) patients were men. The common complications for decompensation were ascites (80%), gastrointestinal bleeding (19%), hepatorenal syndrome (10%), and hepatic encephalopathy (2%).

At the 30-day follow-up, 17 of the 134 patients had died (12.7%). The causes of death were hepatic failure (n = 7), gastrointestinal bleeding (n = 5), encephalopathy (n = 2), and hepatorenal syndrome (n = 3). **TABLE 1** shows the comparisons between the survivors and nonsurvivors. There were marked differences in creatinine, international normalized ratio, MELD score, CRP, CLR, and total bilirubin between the 2 groups (**FIGURE 2**).

### Factors Associated with Poor Outcomes

The predictors associated with poor survival in the univariate analyses were CRP, the MELD score, and the CLR. The multivariate analysis identified the MELD score and the CLR as independent predictors for poor survival (**TABLE 2**). Using Youden's index, the cutoff values for the MELD score and the CLR were 17.7 (sensitivity: 82.4%; specificity: 78.6%) and 25.0 (sensitivity: 70.6%; specificity: 85.5%), respectively. As shown in **FIGURE 3**, the AUCs of the MELD score and the CLR for predicting poor outcomes were 0.845 and 0.795, respectively. The ability of the CLR to predict death was comparable to that of the MELD score ($z = 0.605$; $P = .545$). The combination of the CLR and the MELD score further improved the prognostic accuracy for poor outcomes (AUC: 0.928) compared with the CLR or the MELD score alone (both $P < .05$). Furthermore, patients with a CLR ≤25.0 had a higher 30-day survival than patients with a CLR >25.0 ($P < .001$; **FIGURE 4**).

## Discussion

Patients with HBV-DeCi are difficult to cure and have a very high risk of mortality. Therefore, early and accurate prognostic indicators are very important for clinicians to manage these patients. At present, the MELD score is a commonly used prognostic scoring system for end-stage liver disease.[18] However, in approximately 15%–20% of patients, mortality cannot be accurately predicted by the MELD score. This problem may

**TABLE 1. Patient Characteristics at Baseline**

| | All Patients (n = 134) | Nonsurviving Patients (n = 17) | Surviving Patients (n = 117) | *P* Value |
|---|---|---|---|---|
| Sex (female/male) | 32/102 | 4/13 | 28/89 | .789 |
| Age (y) | 54.0 (47.0–62.0) | 55.0 (49.8–58.0) | 53.0 (46.8–63.0) | .823 |
| Total protein (g/L) | 60.7 (56.1–66.6) | 59.4 (50.1–66.4) | 60.7 (56.4–66.6) | .297 |
| Albumin (g/L) | 29.8 (26.2–33.5) | 26.4 (22.4–33.6) | 30.1 (26.4–33.4) | .170 |
| Alanine aminotransferase (U/L) | 31.0 (18.0–56.0) | 48.0 (20.5–60.8) | 30.0 (17.8–55.3) | .654 |
| Aspartate aminotransferase (U/L) | 49.0 (31.0–80.0) | 57.0 (35.0–81.0) | 49.0 (30.5–79.3) | .493 |
| Serum creatinine (μmol/L) | 73.0 (60.0–88.0) | 104.0 (60.3–130.0) | 72.0 (60.0–84.0) | .023 |
| Total bilirubin (μmol/L) | 56.5 (26.0–117.0) | 90.0 (64.8–220.8) | 44.0 (25.0–104.0) | .010 |
| INR | 1.44 (1.24–1.68) | 1.80 (1.52–2.26) | 1.37 (1.21–1.63) | <.001 |
| MELD score | 13.4 (9.3–18.3) | 20.6 (17.9–22.6) | 11.9 (8.5–17.2) | <.001 |
| Hemoglobin (g/L) | 103.5 (86.0–120.0) | 96.0 (85.0–110.3) | 104.0 (86.5–121.0) | .221 |
| Platelets ($\times 10^9$/L) | 66.0 (40.0–108.5) | 66.0 (63.5–94.0) | 66.0 (38.8–114.3) | .854 |
| CRP (mg/L) | 8.3 (3.1–18.2) | 23.5 (13.9–69.4) | 7.5 (2.8–15.6) | <.001 |
| Leukocytes ($\times 10^9$/L) | 4.4 (2.9–6.0) | 4.8 (3.8–6.7) | 4.2 (2.9–5.9) | .198 |
| Lymphocytes ($\times 10^9$/L) | 0.90 (0.70–1.40) | 0.70 (0.50–1.15) | 0.90 (0.70–1.40) | .207 |
| CLR | 8.4 (3.4–23.0) | 32.8 (11.4–68.7) | 7.6 (3.3–11.9) | <.001 |

*CLR, CRP-to-lymphocyte ratio; CRP, C-reactive protein; INR, international normalized ratio; MELD, Model for End-Stage Liver Disease. Data are expressed as number or median (interquartile range).*

**FIGURE 2. Comparisons of MELD score, CRP, and CLR between the survivors and non-survivors among the patients with HBV-DeCi. CLR, CRP-to-lymphocyte ratio; CRP, C-reactive protein.**

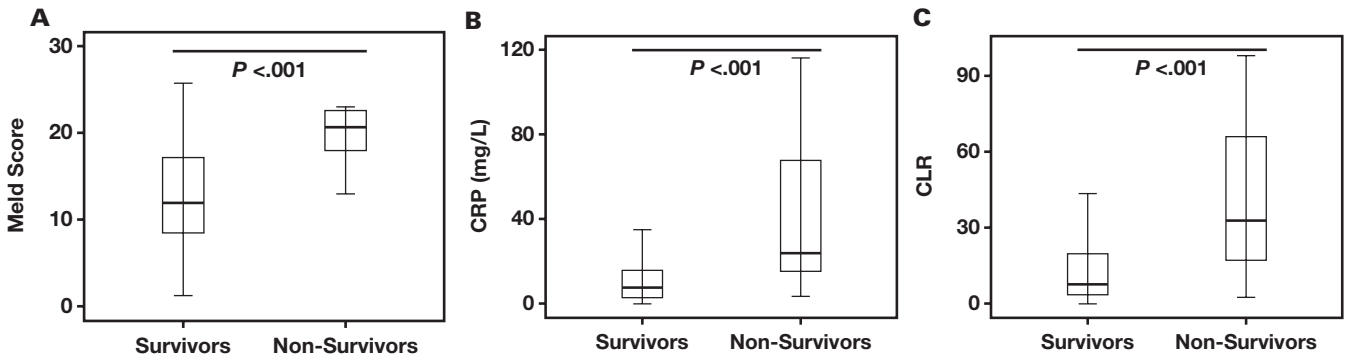


**TABLE 2. Factors Associated with Mortality of Patients wuth HBV-DeCi in Logistic Regression Analyses**

| | Univariate | | | Multivariate | | |
|---|---|---|---|---|---|---|
| | Odds Ratio | 95% CI | *P* Value | Odds Ratio | 95% CI | *P* Value |
| Albumin (g/L) | 0.939 | 0.856–1.030 | .183 | … | … | … |
| MELD score | 1.265 | 1.127–1.421 | <.001 | 1.326 | 1.129–1.556 | .001 |
| CRP (mg/L) | 1.041 | 1.017–1.065 | <.001 | … | … | … |
| Lymphocytes ($\times 10^9$/L) | 0.774 | 0.345–1.735 | .534 | … | … | … |
| CLR | 1.047 | 1.023–1.071 | <.001 | 1.048 | 1.020–1.076 | .001 |

*CI, confidence interval; CLR, CRP-to-lymphocyte ratio; CRP, C-reactive protein; MELD, Model for End-Stage Liver Disease.*

arise because certain important risk factors (gastrointestinal bleeding, hepatic encephalopathy, hepatorenal syndrome, and systemic inflammation) that affect the prognosis are not incorporated in the MELD score.[19] The present study investigated the value of the CLR as a predictor of poor prognosis in patients with HBV-DeCi and found that nonsurvivors had a higher CLR than survivors and that a high CLR predicted poor outcomes. The multivariate analysis further identified the MELD score and the CLR as prognostic predictors for poor outcomes, with the predictive power of the CLR being similar to that of the MELD score. Of note, the combination of the CLR with the MELD score improved the prognostic power to 93%. Prior studies showed that several noninvasive indices were associated with poor prognosis in patients with HBV-DeCi, including the

**FIGURE 3.** **Receiver operating characteristic curves showing the relative prognostic performances of MELD score, CLR, and their combination for prediction of 30-day mortality in patients with HBV-DeCi. AUC, area under the curve; CLR, C-reactive protein–to–lymphocyte ratio; MELD, Model for End-Stage Liver Disease.**

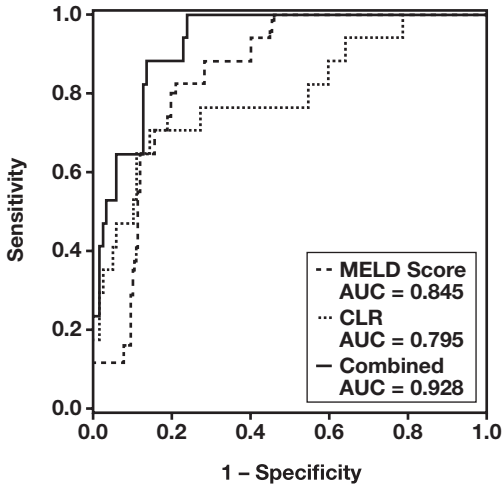


**FIGURE 4.** **Kaplan–Meier analysis of 30-day survival. The survival rate was higher in patients with CLR ≤25.0 than in patients with CLR >25.0. CLR, C-reactive protein–to–lymphocyte ratio.**

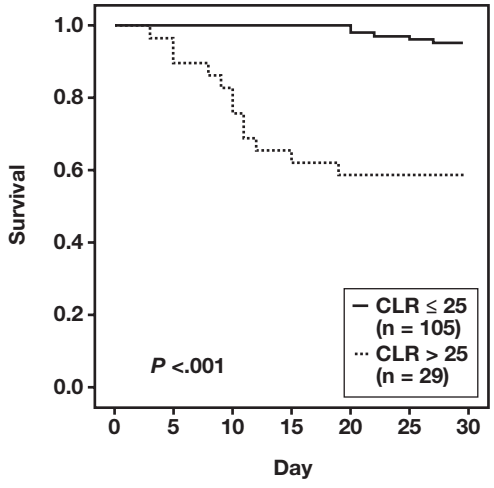


neutrophil-to-albumin ratio,[20] the lymphocyte-to-monocyte ratio,[21] and the mean platelet volume-to-lymphocyte ratio.[22] Our study complements these previous studies and suggests that a high CLR can also be used to predict the prognosis of patients with HBV-DeCi.

There are 2 reasons for using CLR as an adverse prognostic biomarker in patients with HBV-DeCi. First, accumulating evidence confirms that inflammation is relatively common in patients with advanced cirrhosis and is associated with the severity of liver disease and poor prognosis.[23,24] We found that CRP was markedly higher in nonsurvivors compared with survivors. Studies have shown that CRP is a widely accepted universal inflammatory marker, and CRP levels increase in response to cell damage or tissue injury.[25-27] Zhu et al[28] found that high CRP was a convenient negative predictor of prognosis in patients with HBV-DeCi. However, in the present study, CRP was associated with poor survival in the univariate analyses but was not identified as an independent risk factor in the multivariate analysis. It is possible that insomnia, depression, smoking, and high body mass index can all contribute to elevations in CRP.[29] Thus, CRP may not effectively reflect the inflammatory status of the liver and the disease severity, or the prognosis of patients.

Second, slightly lower lymphocyte counts were found in nonsurvivors compared with survivors in the present study. Lymphocytes play critical roles in the pathogenesis of different clinical scenarios and in immune defense.[30] Lymphocytes represent the outcome of controlled immune responses, and a decrease in the lymphocyte count may be related to apoptosis and dysfunction of immune cells.[31] A previous study showed that lymphopenia is associated with malnutrition or poor immune response in liver diseases, and the occurrence of advanced cirrhosis may be linked to a gradual decrease in the lymphocyte count.[32] Moreover, previous studies showed that the pretransplant lymphocyte count was a prognostic factor for liver transplant recipients.[33,34] However, the lymphocyte count was not identified as an independent prognostic indicator of unfavorable outcomes in our univariate and multivariate analyses. Thus, we propose that the CLR, a new compound biomarker that integrates data for CRP and the lymphocyte count, can reflect the systemic inflammatory, nutritional, and immune status of patients and may be useful to predict the prognosis of patients with HBV-DeCi. Compared with each single indicator, it has higher stability, sensitivity, and specificity. In future studies, the underlying mechanisms will require further investigation.

The present study had some limitations. First, it was retrospectively conducted and may have some selective bias. Second, it was a single-center study, and the number of patients with HBV-DeCi was small. Third, the 2 parameters were not measured dynamically; thus, it remains unclear whether they exhibited stepwise changes when the patient condition deteriorated. Finally, the results lacked external verification. Therefore, the present findings need to be validated by a large-scale study in the future.

## Conclusion

The present results show that a high CLR is associated with poor short-term prognosis in patients with HBV-DeCi. The CLR is readily available and inexpensive, and it is a novel candidate biomarker. The combination of the CLR and the MELD score may help clinicians achieve early assessment of prognosis and adjust treatment disciplines.


## Acknowledgments

This work was supported by the Health Department of Zhejiang Province (grant no. 2019KY735). None of the authors have any commercial or other association that might pose a conflict of interest.


## REFERENCES


1. Xiao J, Wang F, Wong NK, et al. Global liver disease burdens and research trends: analysis from a Chinese perspective. *J Hepatol*. 2019;71:212–221.
2. Asrani SK, Kamath PS. Natural history of cirrhosis. *Curr Gastroenterol Rep*. 2013;15:308.

3. European Association for the Study of the Liver. EASL Clinical Practice Guidelines for the management of patients with decompensated cirrhosis. *J Hepatol.* 2018;69(2):406–460.
4. D'Amico G. The clinical course of cirrhosis. Population based studies and the need of personalized medicine. *J Hepatol.* 2014;60(2):241–242.
5. Tsochatzis EA, Bosch J, Burroughs AK. Liver cirrhosis. *Lancet*. 2014;383:1749–1761.
6. Cárdenas A, Ginès P. Management of patients with cirrhosis awaiting liver transplantation. *Gut*. 2011;60:412–421.
7. Karagoz E, Ulcay A, Tanoglu A, et al. Clinical usefulness of mean platelet volume and red blood cell distribution width to platelet ratio for predicting the severity of hepatic fibrosis in chronic hepatitis B virus patients. *Eur J Gastroenterol Hepatol*. 2014;26:1320–1324.
8. Liu H, Zhang H, Wan G, et al. Neutrophil-lymphocyte ratio: a novel predictor for short-term prognosis in acute-on-chronic hepatitis B liver failure. *J Viral Hepat*. 2014;21:499–507.
9. Twu YC, Gold MR, Teh HS. TNFR1 delivers pro-survival signals that are required for limiting TNFR2-dependent activation-induced cell death (AICD) in CD8 + T cells. *Eur J Immunol*. 2011;41:335–344.
10. Baumann S, Dostert A, Novac N, et al. Glucocorticoids inhibit activation-induced cell death (AICD) via direct DNA-dependent repression of the CD95 ligand gene by a glucocorticoid receptor dimer. *Blood*. 2005;106:617–625.
11. Li X, Liu X, Wang W. IL-35: a novel immunomodulator in hepatitis B virus-related liver diseases. *Front Cell Dev Biol*. 2021;9:614847.
12. Lagunas-Rangel FA. Neutrophil-to-lymphocyte ratio and lymphocyte to-C-reactive protein ratio in patients with severe coronavirus disease 2019 (COVID-19): a meta-analysis. *J Med Virol*. 2020;92:1733–1734.
13. Mungan İ, Bostancı EB, Türksal E, et al. The predictive power of C-reactive protein-lymphocyte ratio for in-hospital mortality after colorectal cancer surgery. *Cancer Rep*. 2021;15:e1330.
14. Lu LH, Zhong C, Wei W, et al. Lymphocyte-C-reactive protein ratio as a novel prognostic index in intrahepatic cholangiocarcinoma: a multicentre cohort study. *Liver Int*. 2021;41:378–387.
15. Han YY, Chen KH, Guan Y, et al. Predictive value of some inflammatory indexes in the survival and toxicity of nasopharyngeal carcinoma. *Cancer Manag Res*. 2020;12:11541–11551.
16. Fan Z, Luo G, Gong Y, et al. Prognostic value of the C-reactive protein/lymphocyte ratio in pancreatic cancer. *Ann Surg Oncol*. 2020;27:4017–4025.
17. Liaw YF, Tai DI, Chu CM, et al. The development of cirrhosis in patients with chronic type B hepatitis: a prospective study. *Hepatology*. 1988;8:493–496.
18. Freeman RB Jr, Wiesner RH, Harper A, et al. The new liver allocation system: moving toward evidence-based transplantation policy. *Liver Transpl*. 2002;8:851–858.
19. Stewart CA, Malinchoc M, Kim WR, et al. Hepatic encephalopathy as a predictor of survival in patients with end-stage liver disease. *Liver Transpl*. 2007;13:1366–1371.
20. Han Z, He X, Peng S. Neutrophil count to albumin ratio as a prognostic indicator for HBV-associated decompensated cirrhosis. *J Clin Lab Anal*. 2021;35:e23730.
21. Qi X. Peripheral blood lymphocyte-to-monocyte ratio predicts mortality in patients with HBV-related decompensated cirrhosis. *Clin Lab.* 2019;65(1). doi: 10.7754/Clin.Lab.2018.180717.
22. Zhang J, Qiu Y, He X, et al. Platelet-to-white blood cell ratio: a novel and promising prognostic marker for HBV-associated decompensated cirrhosis. *J Clin Lab Anal*. 2020;34:e23556.
23. Behroozian R, Bayazidchi M, Rasooli J. Systemic inflammatory response syndrome and MELD score in hospital outcome of patients with liver cirrhosis. *Middle East J Dig Dis*. 2012;4:168–172.
24. Abdel-Khalek EE, El-Fakhry A, Helaly M, et al. Systemic inflammatory response syndrome in patients with liver cirrhosis. *Arab J Gastroenterol*. 2011;12:173–171.
25. Ma LN, Liu XY, Luo X, et al. Serum high-sensitivity C-reactive protein are associated with HBV replication, liver damage and fibrosis in patients with chronic hepatitis B. *Hepatogastroenterology*. 2015;62:368–372.
26. Atta M, Cabral M, Santos G, et al. Inflammation biomarkers in chronic hepatitis C: association with liver histopathology, HCV genotype and cryoglobulinemia. *Inflamm Res*. 2012;61:1101–1106.
27. Sjöwall C, Cardell K, Boström EA, et al. High prevalence of autoantibodies to C-reactive protein in patients with chronic hepatitis C infection: association with liver fibrosis and portal inflammation. *Hum Immunol*. 2012;73(4):382–388.
28. Zhu SM, Waili Y, Qi XT, et al. Serum C-reactive protein predicts early mortality in hospitalized patients with HBV-related decompensated cirrhosis. *Medicine (Baltimore)*. 2017;96(4):e5988.
29. Pearson TA, Mensah GA, Alexander RW, et al. Markers of inflammation and cardiovascular disease: application to clinical and public health practice: a statement for healthcare professionals from the Centers for Disease Control and Prevention and the American Heart Association. *Circulation*. 2003;10:499–511.
30. Wang W, Wang Y, Qu C, et al. The RNA genome of hepatitis E virus robustly triggers an antiviral interferon response. *Hepatology*. 2018;67:2096–2112.
31. Kwon JH, Jang JW, Kim YW, et al. The usefulness of C-reactive protein and neutrophil-to-lymphocyte ratio for predicting the outcome in hospitalized patients with liver cirrhosis. *BMC Gastroenterol*. 2015;15:146.
32. O'Keefe SJ, El-Zayadi AR, Carraher TE, et al. Malnutrition and immuno-incompetence in patients with liver disease. *Lancet*. 1980;2:615–617.
33. Nagai S, Yoshida A, Kohno K, et al. Peritransplant absolute lymphocyte count as a predictive factor for advanced recurrence of hepatitis C after liver transplantation. *Hepatology*. 2014;59:35–45.
34. Nierenberg NE, Poutsiaka DD, Chow JK, et al. Pretransplant lymphopenia is a novel prognostic factor in cytomegalovirus and noncytomegalovirus invasive infections after liver transplantation. *Liver Transpl*. 2014;20:1497–1507.

ONLINE ONLY - SPECIAL REPORT

# ASCP Board of Certification Survey of Medical Laboratory Science Education 2020: Programs

*Karen Brown, MS, MLS(ASCP)CM,[1] Dana Duzan, MLS(ASCP)CM, Karen Fong, BA,[2,3,*] Vicki S. Freeman, PhD, MASCP, MLS(ASCP)CM, SCCM,[3] Jonathan Genzen, MD, PhD, FASCP,[4] Nancy Goodyear, PhD, MLS(ASCP)CM,[5] Susan M. Harrington, PhD, D(ABMM), MLS(ASCP)CM,[6] Teresa Taff, MA, MT(ASCP)SMCM,[7] Patricia A. Tanabe, MPA, MLS(ASCP)CM2*

[1]University of Utah Department of Pathology, Salt Lake City, Utah, USA, [2]American Society for Clinical Pathology Board of Certification, Chicago, Illinois, USA [3]University of Texas Medical Branch Department of Clinical Laboratory Sciences, Galveston, Texas, USA, [4]ARUP Labortories, University of Utah Department of Pathology, Salt Lake City, Utah, USA, [5]University of Massachusetts Lowell Department of Biomedical and Nutritional Sciences, Lowell, Massachusetts, USA [6]Cleveland Clinic Laboratory Medicine, Cleveland, Ohio, USA, [7]Mercy Hospital St. Louis School of Clinical Laboratory Science, Aurora, Missouri, USA.*To whom correspondence should be addressed. karen.fong@ascp.org

**Abbreviations:** BOC, board of certification; R&D, research and development; MLS, medical laboratory science; GPA, grade point average; MLT, medical laboratory technician; NAACLS, National Accrediting Agency for Clinical Laboratory Sciences.

*Laboratory Medicine* 2022;53:e154–e158; https://doi.org/10.1093/labmed/lmac032

The ASCP Board of Certification (BOC) Research and Development (R&D) committee launched 2 surveys of medical laboratory science (MLS) education programs. These questionnaires were a follow-up to the survey of MLS education programs conducted in 2016. Two publications in 2019 reported results of the 2016 study.[1,2] The recent surveys were divided into 2 questionnaires. One survey was designed for participation by program directors of university/college and hospital MLS programs. (Note that, for purposes of this paper, "university/college" will be referred to as just "university"). Another survey targeted faculty in MLS university and hospital programs. The purpose of the surveys was to gather information to support MLS program directors and faculty in educating students, especially to clarify current issues and reveal trends that may impact future program resources and the quality of MLS education. Specifically, the surveys were designed to provide data to support strategic planning, funding requests, evidence for grant applications, workforce issues, and policy assessment. Topics in the surveys included demographics, educational level and rank, certification patterns, experience, responsibilities, salaries, retirement, and program-specific areas, such as minimum grade point averages (GPAs) for acceptance, vacancies, capacity, and clinical sites.

## Methods

The BOC staff and R&D committee members drafted, reviewed, and edited the survey questions. The surveys were distributed as electronic invitations via Key Survey (an online survey tool) on May 14, 2020, and surveys were closed on August 14, 2020. A total of 60 program directors from universities and 51 from hospital programs responded. Responses were received from 84 university faculty and 76 hospital faculty. This is the first of 2 papers reporting results of the surveys.

## Results

### Minimum Educational Level Requirements for Program Director and Faculty

The majority of both university and hospital programs require a minimum of a master's degree for program directors. The situation differs slightly for faculty, where the majority of university programs requires a minimum of a master's degree for faculty while the majority of hospital programs requires a bachelor's degree (**TABLE 1**).

### Duration of MLS Programs (Length of University and Hospital Programs) and Acceptance of Online Students

University programs were more varied than hospital programs in regard to length, with 31.7% lasting 12 months or less and 40% lasting 24 months or more. The majority of hospital programs (96.1%) were 12 months or less in duration.

Of the 25 university programs reported offering online programs, 68% provided bridge courses (medical laboratory technician (MLT) to MLS), 40% offered the entire MLS program (85% or more) online, and 68% provided individual courses (50% or more) online. Ten hospital programs reported offering online courses, with 70% of these being individual courses. No hospital-based programs reported bridge programs or the entire MLS program online.

### Student GPAs

The majority of both university and hospital programs require a minimum GPA between 2.5 and 2.9 for admission (**TABLE 2**).

There is a difference in the minimum science GPA for admission with majority of university programs requiring a minimum GPA of 3.0–3.4, and a majority of hospital programs requiring 2.5–2.9.

When looking at overall GPAs for enrolled students, the majority of both university and hospital programs have students averaging GPAs in the 3.0–3.4 range, above the required minimums for most programs.

**TABLE 1. Minimum Educational Level of Requirements for Program Director and Faculty**

| | University (n = 60) | | Hospital (n = 51) | |
|---|---|---|---|---|
| | Program director | Faculty | Program director | Faculty |
| Associate degree | 0.0% | 0.0% | 0.0% | 9.8% |
| Bachelor's degree | 3.3% | 23.3% | 9.8% | 90.2% |
| Master's degree | 83.3% | 63.3% | 90.2% | 0.0% |
| Doctorate | 13.3% | 13.3% | 0.0% | 0.0% |

**TABLE 2. Minimum GPA**

| | GPA | University (n = 60) | Hospital (n = 51) |
|---|---|---|---|
| Minimum required overall GPA to be accepted into MLS program | | | |
| | 2.0–2.4 | 20.5% | 5.9% |
| | 2.5–2.9 | 66.7% | 88.2% |
| | 3.0–3.4 | 13.3% | 5.9% |
| | 3.5–4.0 | 0.0% | 0.0% |
| Minimum required science GPA to be accepted into MLS program | | | |
| | 2.0–2.4 | 1.7% | 3.9% |
| | 2.5–2.9 | 11.7% | 88.2% |
| | 3.0–3.4 | 80.0% | 7.8% |
| | 3.5–4.0 | 6.7% | 0.0% |
| Average GPA of students currently enrolled | | | |
| | 2.0–2.4 | 1.7% | 0.0% |
| | 2.5–2.9 | 11.7% | 0.0% |
| | 3.0–3.4 | 80.0% | 83.3% |
| | 3.5–4.0 | 6.7% | 16.7% |

**TABLE 3. Capacity to Add More Students (Face-to-Face and/or Online)**

| | University (n = 60) | Hospital (n = 51) |
|---|---|---|
| Able to add more face-to-face students | 50.0% | 22.6% |
| Able to add more online students | 24.3% | 1.9% |
| Program is at full capacity | 25.7% | 75.5% |

## Student Numbers (Applicants and Graduates) and Student Capacity (Face-to-Face and Online)

The majority of programs reported a 5-year average of 20 to 29 applicants (university: 25%, hospital: 28.6%). Cumulatively, 65% of university programs and 76.1% of hospital programs averaged at most 39 applicants over the last 5 years.

In terms of graduation, 20% of university programs graduated 30 or more students per year, while all hospital programs graduated fewer than 30 students per year.

Most university programs would be able to take more students either face-to-face or online. Most hospital programs are at capacity, and few would be able to take additional online students (**TABLE 3**).

## Clinical Sites and Rotations

Of all hospital programs, 90.2% reported that they utilize 1–9 clinical training sites. University programs had a wider range of responses, with an equal 28% reporting 1–9 clinical sites, 10–19 sites, and 20–29 sites. Two university programs utilized 100 or more clinical sites. The number of clinical sites positively correlated with the number of graduates reported by universities (**FIGURE 1**).

The combined length of time spent on all clinical rotations was quite variable, particularly among hospital programs. One-third of hospital program directors selected 40–49 weeks as the length of the clinical rotation, but the length of clinical rotations varied between 10 and 59 weeks. Clinical rotations associated with most university programs (56%) were 10–19 weeks in length, and students were typically on site for 30–49 hours each week (**TABLE 4**).

There were large differences in the laboratory disciplines available as clinical training sites. In general, university program directors responded that adequate numbers of clinical sites were available for chemistry, coagulation, hematology, immunology, phlebotomy, specimen processing, and urinalysis training. However, university program directors indicated the top 3 programs with difficulty obtaining clinical sites were microbiology (55%), blood bank (35%), and molecular diagnostics (28%). Hospital program directors did not experience the same level of difficulty but indicated the top 3 programs with difficulty obtaining clinical sites were molecular diagnostics (7.8%), blood bank (5.9%), and microbiology (3.9%).

The greatest barriers to obtaining adequate clinical sites identified by both university and hospital program directors were staffing, competition with other programs, and time. Other common obstacles were geographic location, increase in workload, lack of physical space, budget, administrative support, and personal reasons. Additional challenges noted by university program directors included contracts, regulatory limitations, and the value of the program not being recognized.

Taking steps to overcome these barriers was common among university programs and included sending students to multiple clinical sites (72%) and sharing clinical sites among multiple students (53%). Rescheduling clinical training, simulation labs, scheduling students during evenings/weekends, splitting rotations among sites, and expanding clinical rotation sites to small facilities were other approaches employed by over 22% to as many as 37% of university programs. Some hospital programs also relied on these means, but no single tactic was used by more than 8% of programs.

Replacing the training experience in clinical laboratories with a laboratory experience simulated in the university setting was reported by 35% of university programs. Although more common for microbiology (20%) and blood bank (22%), simulation labs were incorporated for clinical training in each of the other laboratory disciplines as well.

An additional approach to obtaining clinical sites for students has been to provide incentives to the training sites. Both university and hospital programs encouraged participation through recognition awards/certificates of appreciation, small gifts such as lunch or candy, providing for continuing education offerings, and faculty and staff appointments. Less than 5% of university programs provided any financial compensation,

**FIGURE 1. Correlation between number of graduates and number of clinical sites for university programs.**

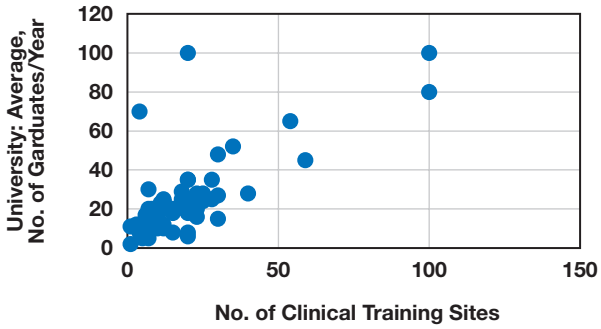


**TABLE 4. Length of All Clinical Rotations**

| Combined length of all rotations (weeks) | University (n = 59) | Hospital (n = 51) |
|---|---|---|
| 1–9 | 5.1% | 0 |
| 10–19 | 55.9% | 17.6% |
| 20–29 | 20.3% | 13.7% |
| 30–39 | 13.6% | 15.7% |
| 40–49 | 3.4% | 33.3% |
| 50–59 | 1.7% | 19.6% |

and one-third of university programs indicated that no incentives were provided.

### Students in Categorical Programs

There has been an increase in the percentage of university and hospital programs accepting categorical students between 2016 and 2020 (**TABLE 5**). The most common categorical program is microbiology, followed by chemistry and hematology (**TABLE 6**).

### Number of Program Faculty

The majority of university programs (70.0%) and hospital programs (72.6%) reported having 0–5 faculty members and have no open positions (**TABLE 7**). Only a minority of university and hospital programs have open faculty positions (**TABLE 8**). To fill open positions, university programs generally take a longer time than hospital programs (**TABLE 9**).

University program directors expressed more difficulty in recruiting faculty across specialty areas than did hospital program directors. The most common difficulties in recruiting faculty for university programs were educational requirements (61.7%), salary (45.0%), certification requirements (41.7%), geographic location (23.3%), and other considerations to include teaching load, research expectations, and unspecified additional reasons. For hospital programs, the most common difficulties were salary (13.7%), educational requirements (9.8%), geographic location (5.9%), and other areas, such as teaching load and personal/family considerations (33.4%).

## Discussion

The minimum educational requirement for university program directors is higher than hospital program directors. This is consistent with the findings of the 2016 survey. The number of university programs requiring a doctoral degree decreased from 19.7% in the 2016 survey (n = 76) to 13.3% in 2020. Possible reasons for the decrease include the significant administrative demands of the position, resulting in a change to a master's degree and/or a nontenure track position or may be due to a lack of doctorally educated MLS candidates and difficulty recruiting those candidates into academia. Hospital program director data showed a slight decrease in the master's degree as the minimum requirement, from 97% in 2016 to 90.2% in 2020. The National Accrediting Agency for Clinical Laboratory Sciences (NAACLS) requires that program directors have a master's degree. However, some individuals may be hired provisionally prior to obtaining the master's, and thus, the minimum requirement for a master's degree can be variable.[3]

The minimum educational level requirements for MLS program faculty are higher for university programs than for hospital programs, which is consistent with the 2016 findings. There was a slight decline in the minimum educational levels for hospital programs with an increase in the number of programs requiring a minimum of an associate degree, from 0% to 9.8% in 2020. One possible explanation is the retirement of faculty and difficulty recruiting MLS candidates. Conversely, there is a slight increase in the number of university programs requiring a doctoral degree from 5.3% in 2016 to 13.3% in 2020.

The number of online courses and programs offered by universities has substantially increased since 2016, from 20% to 41.7% of programs. Hospital online course offerings increased notably from 1 in 2016 to 10 in 2020; however, hospital programs still lag behind university programs. Survey comments indicated COVID-19 had an impact on the increase of online programs. It will be interesting to track this over the next few years.

Most programs appear to enroll students with higher overall GPAs than are required, indicating applicants are well-qualified. This is particularly true for hospital programs, none of which reported average overall GPAs less than 3.0, compared to 13.4% of university programs.

Hospital programs are generally much smaller than university programs, however, relative to class size, hospital programs appear to have larger applicant pools. This may contribute to the higher overall GPAs for enrolled students in hospital programs.

The length of MLS programs was largely unchanged from 2016 to 2020. Hospital programs are generally shorter than university programs, with a slight decrease from 100% of programs reporting 12 months or less in 2016 to 96.1% in 2020. University programs lasting 12 months or less increased from 28.4% in 2016 to 31.7% in 2020. This slight increase in shorter duration may reflect adjustments made due to COVID-19 and may or may not reflect an ongoing trend.

The data demonstrate that the number of clinical sites needed by university programs correlates to the number of graduates. Universities continue to be challenged to secure clinical rotation sites which is, thereby, a major factor limiting the number of graduates. As determined in the 2016 survey of MLS programs, sites for clinical rotations in microbiology, blood bank, and molecular diagnostics rotations continue to be in greatest demand. These results are consistent with a 2015 Summary Report from the Minnesota Laboratory Professionals Workforce Summit, which detailed microbiology and blood bank as areas most limited in clinical capacity. This report also indicated that student enrollment had decreased, and graduation times delayed due to lack of capacity for clinical rotation sites.[4] Interestingly, the number of respondents indicating inadequate numbers of clinical sites decreased by more than 10% for both blood bank and microbiology in comparison

**TABLE 5.** Percent of Programs Accepting Categorical Students in Any Discipline, 2016 Survey vs 2020 Survey

| | 2016 | | 2020 | |
|---|---|---|---|---|
| | University (n = 75) | Hospital (n = 62) | University (n = 60) | Hospital (n = 51) |
| Yes | 29.0 | 27.4 | 59.6 | 45.9 |
| No | 70.0 | 72.6 | 40.4 | 54.1 |

**TABLE 6.** Disciplines in Which Categorical Students Are Accepted

| | 2016 | | 2020 | |
|---|---|---|---|---|
| | University (n = 75) | Hospital (n = 62) | University (n = 60) | Hospital (n = 51) |
| Microbiology | 27.6 | 21.0 | 28.8 | 26.5 |
| Chemistry | 23.7 | 17.7 | 23.7 | 26.5 |
| Blood Bank | 23.7 | 16.0 | 16.9 | 17.6 |
| Hematology | 26.3 | 16.0 | 23.7 | 20.6 |
| Molecular | 2.6 | 8.1 | 6.8 | 8.8 |

**TABLE 7.** Size of Programs by Faculty Number

| University (n = 60) | | Hospital (n = 51) | |
|---|---|---|---|
| Total no. of positions | Percentage | Total no. of positions | Percentage |
| 0–5 | 70.0% | 0 | 9.8 |
| 6–10 | 23.3% | 1 | 27.5% |
| 11–15 | 6.7% | 2–3 | 35.3% |
| 16–20 | 0.0% | 4–6 | 13.7% |
| 21+ | 0.0% | 7–9 | 5.9% |
| | | 10+ | 7.8% |

**TABLE 8.** Program Faculty Member Open Positions

| No. of open positions | University (n = 60) | Hospital (n = 51) |
|---|---|---|
| 0 | 73.3% | 80.4% |
| 1 | 18.3% | 7.8% |
| 2 | 6.7% | 3.9% |
| 3 | 0.0% | 2.0% |
| 4 | 1.7% | 3.9% |
| 5 | 0.0% | 0.0% |
| 6 | 0.0% | 2.0% |

**TABLE 9.** Time to Fill Open Faculty Positions

| No. of open positions | University (n = 55) | Hospital (n = 29) |
|---|---|---|
| < 3 mo | 7.3% | 55.2% |
| >3 to <6 mo | 25.5% | 20.7% |
| >6 to <12 mo | 36.4% | 17.2% |
| >12 mo | 30.9% | 6.9% |

to 2016. Whether this is due to greater innovation in ways to overcome the challenges in obtaining clinical sites or greater participation on the part of clinical laboratories is not clear. Limitations in the number of laboratories available as a result of consolidation of laboratory services is likely the root cause of discipline-specific clinical site shortages.[5] This trend leads to greater competition between training programs for sites and fewer available hospital laboratories in some geographic locations. However, as in 2016, greater demands on time, staffing shortages, and an increased workload in hospitals were also identified as key factors impacting training of MLS students.

The length of time students spend in clinical rotations was highly variable for hospital programs, ranging from 10 to 59 weeks. This may reflect the diversity in hospital program structures. For some programs, students are in the clinical setting throughout the entire length of the program; and for others, didactic and clinical portions are separated. NAACLS does not specify program structure.[3] For about 75% of university programs, the clinical rotation lasts 10–29 weeks, reflecting a structure wherein students spend specific time at the university followed by rotations in hospitals or other clinical laboratory settings.

University programs generally have greater capacity for expansion than hospital programs, both face-to-face and online. Few hospital programs have the ability to take online students, probably reflecting a lack of infrastructure (online teaching platform), staff time, experience, skill in online teaching, and the ability to manage hands-on experience remotely.

More programs are accepting categorical students, perhaps reflecting both staffing shortages and qualified postbaccalaureate applicants with non-MLS science degrees. The most notable changes in disciplines are the increase in chemistry and hematology categoricals at hospital programs, the decrease in blood bank categoricals, and the increase in molecular categoricals at university programs.

The size of programs by total number of faculty remained largely unchanged between the 2016 and 2020 surveys. Also largely unchanged, is the number of open faculty positions in university programs. Hospital programs with open faculty positions decreased from 2016, from 24.1% to 19.6%. Consistent with the 2016 survey, university programs have slightly higher ongoing demand for faculty than hospital programs.

Similar to the 2016 findings, it takes university programs much longer than hospital programs to fill open faculty positions, with more than 60% of university programs taking 6 months or more while more than 70% of hospital programs report taking less than 6 months.

Hospital program directors indicated fewer reasons for difficulty in recruiting faculty, consistent with the shorter times to fill vacant positions in hospital programs as noted above. However, the most common reasons for difficulty in recruiting faculty included educational

requirements, salary, and geographic location for both program types. The increased difficulty in recruiting university faculty in specific specialty areas may reflect the different expectations for university faculty compared to hospital faculty, as well as a lack of qualified candidates. These difficulties, as well as existing university structures, likely influence the greater use of adjunct faculty at university programs.

## REFERENCES


1. Brown K, Fenn JP, Fong K, et al. ASCP Board of Certification Survey of Medical Laboratory Science Faculty. *Lab Med* 2019;50(4): e75–e81. doi:10.1093/labmed/lmz024.
2. Brown K, Fenn JP, Fong K, et al. ASCP Board of Certification Survey of Medical Laboratory Science Programs. *Lab Med.* 2019;50(4):e70–e74. doi:10.1093/labmed/lmz019.
3. NAACLS Standards for Accredited and Approved Programs, Adopted 2012, Revised 2021. NAACLS website: https://www.naacls.org/ Accessed November 8, 2021.
4. HealthForce Minnesota. Minnesota laboratory professionals workforce summit summary report. 2015. HealthForce Minnesota website: http://www.healthforceminnesota.org/assets/files/SummaryReports.pdf. Accessed November 8, 2021.
5. The American Society for Clinical Laboratory Science. Addressing the clinical laboratory workforce shortage. 2020. ASCLS website: https://ascls.org/addressing-the-clinical-laboratory-workforce-shortage/ Accessed November 8, 2021.

ONLINE ONLY - SPECIAL REPORT

# ASCP Board of Certification Survey of Medical Laboratory Science Education 2020: Faculty

*Karen Brown, MS, MLS(ASCP)CM,[1] Dana Duzan, MLS(ASCP)CM,[2,3] Karen Fong,[3] Vicki S. Freeman, PhD, MASCP, MLS(ASCP)CM, SCCM,[4] Jonathan Genzen, MD, PhD, FASCP,[5] Nancy Goodyear, PhD, MLS(ASCP)CM,[6] Susan M. Harrington, PhD, D(ABMM), MLS(ASCP)CM,[7] Teresa Taff, MA, MT(ASCP) SMCM,[8] Patricia A. Tanabe, MPA, MLS(ASCP)CM[3]*

[1]University of Utah Department of Pathology, Salt Lake City, Utah, USA, [2], [3]American Society for Clinical Pathology Board of Certification, Chicago, Illinois, USA, [4]University of Texas Medical Branch Department of Clinical Laboratory Sciences, Galveston, Texas, USA, [5]ARUP Laboratories University of Utah Department of Pathology, Salt Lake City, Utah, USA, [6]University of Massachusetts Lowell Department of Biomedical and Nutritional Sciences, Lowell, Massachusetts, USA, [7]Cleveland Clinic/ Lab Medicine, Cleveland, Ohio, USA, [8]Mercy Hospital St. Louis School of Clinical Laboratory Science, Aurora, Missouri, USA. *To whom correspondence should be addressed. karen.fong@ascp.org

**Abbreviations:** ASCP, American Society for Clinical Pathology; BOC, board of certification; (R&D), research and development; MLS, medical laboratory science; NAACLS, National Accrediting Agency for Clinical Laboratory Science; ASCP-BOC, American Society for Clinical Pathology Board of Certification; MT/MLS, Medical Technologist/Medical Laboratory Scientist; PD, program director.

*Laboratory Medicine* 2022;53:e159–e163; https://doi.org/10.1093/labmed/lmac044

The ASCP Board of Certification (BOC) Research and Development (R&D) Committee launched 2 surveys of Medical Laboratory Science (MLS) education programs. These questionnaires were in follow-up to a survey of MLS education programs that was conducted in 2016. Two publications in 2019 reported results of the 2016 study.[1,2] The recent surveys were divided into 2 questionnaires. One survey was designed for participation by program directors of university/college and hospital MLS programs. (Note that for purposes of this paper, "university/college" will be referred to as just "university.") Another survey targeted faculty in MLS programs to include university and hospital. The purpose of the surveys was to gather information to support MLS program directors and faculty in educating students, especially to clarify current issues and reveal trends that may impact future program resources and the quality of MLS education. Specifically, the surveys were designed to provide data to support strategic planning, funding requests, evidence for grant applications, workforce issues, and policy assessment. Topics in the surveys included demographics, educational level and rank, certification patterns, experience, responsibilities, salaries, retirement, and program-specific areas such as minimum grade point averages to be accepted, vacancies, capacity, and clinical sites.

## Methods

The BOC staff and R&D Committee members drafted, reviewed, and edited the survey questions. The surveys were distributed as electronic invitations via Key Survey (an online survey tool) on May 14, 2020, and surveys were closed on August 14, 2020. A total of 60 directors from universities and 51 from hospital programs responded. Responses were received from 84 university faculty and 76 hospital faculty. In total, 37 states, 1 territory, and the District of Columbia were represented in the survey.

The education level, certification type and agency, clinical and teaching experience, and teaching-related and other responsibilities were compared by university and hospital faculty and by university and hospital program directors. This paper is the second of 2 papers reporting the results of the survey.

## Results

### Demographic Information

Of the university respondents, 75% identified as female and 25% identified as male. The ethnicity distributions for university programs were 81.1% White/Caucasian, 8.1% Asian, 5.4% Hispanic/Latino, 4.1% Black or African American, and 1.4% Mixed Race.

Of the hospital respondents, 83% identified as female and 17% identified as male. The ethnicity distributions for hospital programs were 8% White/Caucasian, 5.6% Asian, 4% Black or African American, 43.% Hispanic/Latino, and 1.4% Mixed Race.

### Education Level and Rank

Although all university faculty, regardless of gender, were more likely to have a doctoral degree than hospital faculty, male respondents were more likely to have postdoctorate experiences regardless of whether they were employed in a university or hospital program. When the doctorate and postdoctorate categories are combined, the percentage of males with doctoral degrees outnumbered the percentage of females with doctoral degrees at university programs by 9.5% (**FIGURE 1**) and at hospital programs by 5.1% (**FIGURE 2**). When university program directors and faculty were asked to select their academic rank, the percentage of males at an advanced academic rank (ie, professor or associate professor) was higher than for females. The results should be interpreted with caution as the total sample for males (n = 57) is significantly smaller than for females (n = 210).

### Certification

All program directors are required by the National Accrediting Agency for Clinical Laboratory Science (NAACLS)[3] to have ASCP-BOC

generalist certification or ASCP$^{i}$-BOC certification as a Medical Laboratory Scientist/Medical Technologist. The majority of university and hospital program directors and faculty have only an MT/MLS certification, and another small fraction also hold a specialist certification (eg, SBB, SC, SH, SM, DLM, etc.). University personnel are more likely than their hospital counterparts to hold an additional specialist certification (**TABLE 1**).

**FIGURE 1.** Comparison of university educational levels by gender.

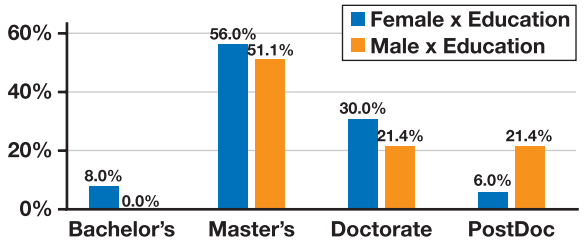


**FIGURE 2.** Comparison of hospital educational levels by gender.

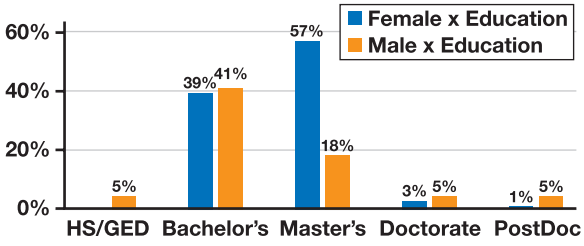


## Education and Clinical Laboratory Experience

In general, program directors (PDs) have more teaching and clinical laboratory experience than faculty. Faculty in university and hospital programs showed similar years of teaching and clinical laboratory experience (**TABLE 2**). These data were similar to the 2016 data for program directors, but for university faculty, the years of clinical laboratory experience in 2020 was slightly less (17 in 2020 vs 23 in 2016).

## Academic Year Schedule and Average Number of Credit Hours Taught Each Term

The academic year is the semester for 88% of the 84 respondents, 9.5% use the trimester, and 2.4% utilize the quarter in the university setting.

Of the 84 university faculty, 34.5% reported teaching 4–6 credit hours; 25% taught 10–12 hours; 19% taught 13 + hours; 14.3% taught 7–9 hours; and 7.1% taught 1–3 hours.

### Teaching Preparation Time

In the recent survey, 78.6% of the hospital faculty indicated they are allocated teaching preparation time. The majority of hospital faculty indicted they felt the time was adequate (72.0%). Up to 88.7% of hospital program directors specified they were allocated time for teaching preparation.

In terms of teaching preparation time, it appears that program directors and faculty in hospital and university programs experienced a contrasting trend. Program directors reported an increase, while university faculty spent less time preparing for teaching per week. Hospital program directors reported less time preparing for teaching per week over the past years, while hospital faculty spent more time preparing for teaching (**TABLE 3**).

## Nonteaching Responsibilities

Of the university program directors, 46.6% spent more than half of their time on job responsibilities other than teaching in 2016. The percentage

**TABLE 1.** Certifications of program directors and faculty.

| | University | | Hospital | |
|---|---|---|---|---|
| | Program director (n = 60) | Faculty (n = 84) | Program director (n = 51) | Faculty (n = 76) |
| MT/MLS only | 56.7% | 58.3% | 80.4% | 71.1% |
| MT/MLS + Specialist (eg, SC, DLM, etc.) | 28.3% | 22.6% | 13.7% | 13.2% |
| MT/MLS + Technologist (eg, BB, C, H, etc.) | 3.3% | 8.3% | 5.9% | 0.0% |
| MT/MLS + Technician (eg, MLT, HT, etc.) | 5.0% | 2.4% | 0.0% | 2.6% |
| Specialist and/or categorical | 5.0% | 2.4% | 0.0% | 3.9% |
| other (ie, non-ASCP certifications) | 0.0% | 0.0% | 0.0% | 1.3% |
| None | 1.7% | 6.0% | 0.0% | 7.9% |

*MT/MLS, medical technologist/medical laboratory scientist; SC, Specialist in Chemistry; DLM, Diplomate in Laboratory Management; BB, Technologist in Blood Banking; C, Technologist in Chemistry; H, Histotechnician; MLT, Medical Laboratory Technician; and HT, Histotechnologist*

**TABLE 2.** Years of Experience

| Institution | | Teaching | | Clinical laboratory | |
|---|---|---|---|---|---|
| *University* | N | Mean (SD) | Range | Mean (SD) | Range |
| Program director | 60 | 19 (10) | 4–10 | 22 (14) | 3–50 |
| Faculty | 84 | 13 (10) | 1–40 | 17 (13) | 1–40 |
| *Hospital* | | | | | |
| Program director | 51 | 20 (11) | 1–40 | 28 (10) | 4–40 |
| Faculty | 76 | 11 (10 | 1–40 | 20 (12) | 2–40 |

*SD, standard deviation.*

rose to 71.7% in 2020. Additional duties for program directors included primarily program administration.

Of hospital program directors, 66.1% utilized more than half of their time on job responsibilities other than teaching. The percentage increased to 80.4% in 2020. The majority of hospital faculty indicated up to 39% of their job responsibilities are related to teaching. In addition to teaching, the remaining job responsibilities include primarily clinical bench work but also laboratory administration, continuing education, quality assurance, and safety.

## Retirement Plans

Information on retirement/career changes was compared to the 2016 data. In 2020, 35% of university program directors indicated they plan to retire or change careers within the next 5 years compared to 32.9% in 2016. Of those who plan to retire, 57.1% currently have a plan for their replacement. For hospital program directors in 2020, 31.4% indicated that they plan to retire or change careers within the next 5 years, as compared to 30.6% in 2016, and 50% indicated they currently have a plan for their replacement.

## Salaries

**TABLES 3–9** show salary data for 2020, which are compared to 2016 data in the text.

Based on the data collected, salaries for both program directors and faculty increased in the 4 years between surveys with a greater increase in the program directors' salaries. University program director salaries increased by 17.3% compared to hospital program directors, which increased 14.7%. University faculty salaries increased by 11% compared to the hospital faculty salary increase of 8.3% (**TABLE 4**).

As reported in 2016, individuals, in general, who had advanced degrees reported higher salaries in 2020. For university program directors and faculty, those who have a master's or doctoral degree reported a higher median salary. There was no substantial difference in median salary for hospital program directors based on level of education, but the median salary difference for hospital faculty mirrored the university faculty salary increases (**TABLE 5**). With only 1 PhD hospital program director salary reported, there is not enough data to provide meaningful information.

Salaries of program directors and faculty at both university and hospital programs from 2016 to 2020 were compared based on certification status. Both university program directors and faculty who hold an additional specialist certification have a higher median salary. Although this same trend was not seen with hospital program directors, hospital faculty who hold a specialist certification had a higher median salary than those without the certification. (**TABLE 6**)

Both university program director and faculty salaries based on tenure and academic rank have risen 15% over the last 4 years. As reported in 2016, individuals with tenure or who are on a tenure track have higher median salaries than those who are not tenured or are not on a tenure track (**TABLE 7**).

**TABLE 3. Hours Spent on Teaching Preparation Per Week**

| | University | | Hospital | |
|---|---|---|---|---|
| | Program director (n = 60) | Faculty (n = 84) | Program director (n = 51) | Faculty (n = 76) |
| 2020 | 12.62 | 7.98 | 8.60 | 13.51 |
| 2016 | 10.25 | 13.75 | 21.8 | 8.80 |

**TABLE 4. Base Salary in Dollars ($) of University vs Hospital Program Directors and Faculty**

| Institution | Program directors | | | | Faculty members | | | |
|---|---|---|---|---|---|---|---|---|
| | N | Median | Mean (SD) | Range | N | Median | Mean (SD) | Range |
| University | 56 | 87,500 | 91,741 (39815) | 48,000–295,000 | 71 | 78,000 | 79,000 (16926) | 51,000–150,000 |
| Hospital | 51 | 86,860 | 87,629 (15218) | 63,500–135,000 | 43 | 68,000 | 69,943 (15862) | 48,000–130,000 |

**TABLE 5. Salary in Dollars ($) of University vs Hospital Program Directors and Faculty by Education**

| Institution | Program directors | | | | Faculty members | | | |
|---|---|---|---|---|---|---|---|---|
| | N | Median | Mean (SD) | Range | N | Median | Mean (SD) | Range |
| University | | | | | | | | |
| Bachelor's | 2 | 76,500 | 76,500 (4950) | 73,000–80,000 | 5 | 65,000 | 62,343 (10557) | 51,000–72,259 |
| Master's | 32 | 85,000 | 83,641 (16923) | 48,000–115,000 | 37 | 75,000 | 76,609 (15521) | 55,000–120,000 |
| Doctorate/postdoc | 25 | 95,000 | 105,790 (46251) | 58,000–295,000 | 26 | 84,500 | 87,034 (17343) | 64,000–150,000 |
| Hospital | | | | | | | | |
| High School or GED | NA | NA | NA | NA | 1 | 84,000 | 84,000 (0) | 84,000 |
| Bachelor's | 4 | 85,000 | 85,000 (5773) | 80,000–90,000 | 45 | 68,000 | 69,167 (16349) | 35,000–130,000 |
| Master's | 46 | 86,930 | 87,980 (15926) | 63,500–135,000 | 22 | 75,500 | 77000 (11710) | 48,000–94,000 |
| Doctorate/postdoc | 1 | 82,000 | 82,000 (0) | 82,000 | 3 | 180,000 | 218,000 (71077) | 174,000–300,000 |

*SD, standard deviation; GED, general equivalency diploma; NA, not applicable*

**TABLE 6.** Salary in Dollars ($) of University vs Hospital Program Directors and Faculty by Certification

| Institution | Program directors | | | | Faculty members | | | |
|---|---|---|---|---|---|---|---|---|
| | N | Median | Mean (SD) | Range | N | Median | Mean (SD) | Range |
| University | | | | | | | | |
| MT/MLS | 33 | 85,000 | 86,233 (17479) | 48,000–130,000 | 42 | 78,000 | 77,999 (14,822) | 51,000–110,000 |
| MT/MLS + Specialist | 17 | 92,000 | 96,151 (24045) | 70,000–92,000 | 15 | 85,000 | 84,250 (15354) | 62,000–120,000 |
| Hospital | | | | | | | | |
| MT/MLS | 41 | 86,200 | 87,591 (16561) | 63,500–135,000 | 53 | 68,000 | 69,456 (15640) | 35,000–130,000 |
| MT/MLS + Specialist | 7 | 82,000 | 87,286 (9962) | 79,000–105,000 | 10 | 80,000 | 79,035 (13120) | 48,000–94,000 |

*SD, standard deviation; MT/MLS, medical technologist/medical laboratory scientist.*

**TABLE 7.** Salary in Dollars ($) of University Program Directors and Faculty by Tenure Track

| Institution | University program directors | | | | University faculty | | | |
|---|---|---|---|---|---|---|---|---|
| | N | Median | Mean (SD) | Range | N | Median | Mean (SD) | Range |
| Tenured or tenure track | 29 | 94,000 | 103,647 (42909) | 69,000–295,000 | 30 | 85,000 | 82786 (19747) | 56,000–150,000 |
| Clinical track/nontenure/other | 30 | 82,000 | 82,284 (18000) | 48,000–119,000 | 41 | 75,000 | 75,806 (13555) | 51,000–120,000 |

**FIGURE 3.** Comparison of 2016 to 2020 university salaries in dollars ($) by rank.

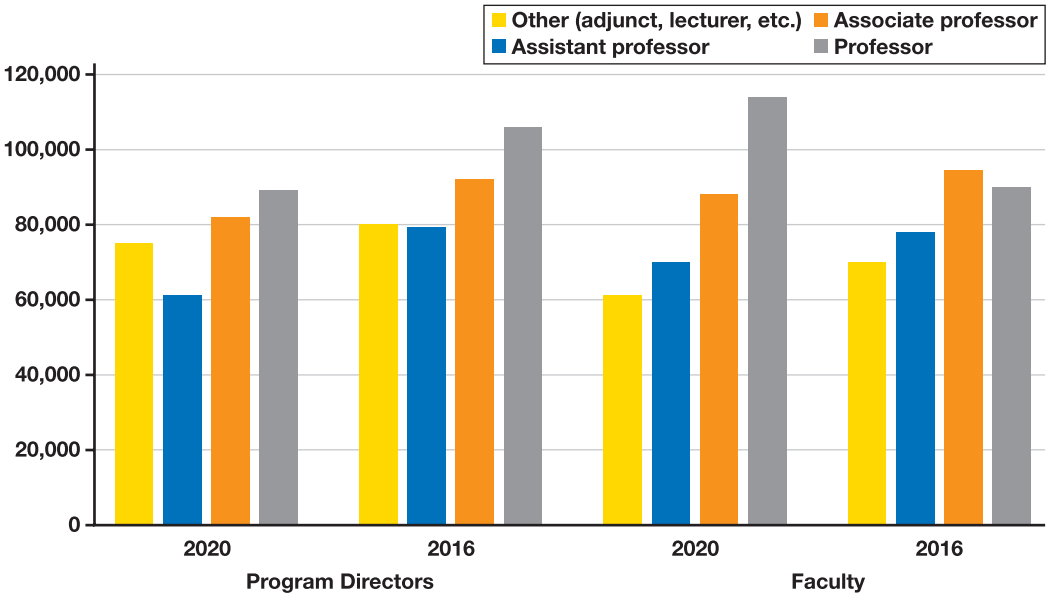


**TABLE 8.** Salary in Dollars ($) of University Program Directors and Faculty by Academic Rank

| Institution | University program directors | | | | University faculty | | | |
|---|---|---|---|---|---|---|---|---|
| | N | Median | Mean (SD) | Range | N | Median | Mean (SD) | Range |
| Other (adjunct, lecturer, etc.) | 14 | 80,000 | 80,237 (17736) | 48,000–110,000 | 13 | 70,000 | 67,808 (9314) | 51,000–80,000 |
| Assistant professor | 13 | 79,206 | 79,784 (15790) | 49,500–101,000 | 34 | 78,000 | 76,342 (12211) | 55,000–109,887 |
| Associate professor | 25 | 92,000 | 93,560 (18633) | 58,000–135,000 | 18 | 94,500 | 90,000 (16620) | 55,000–120,000 |
| Professor | 7 | 106,000 | 139,250 (73863) | 82,000–295,000 | 3 | 90,000 | 104,000 (40841) | 72,000–150,000 |

*SD, standard deviation.*

As shown in **FIGURE 3**, an individual's salary increases as they progress in rank. However, the greatest variability in salary for both program directors and faculty was at the professor rank, where salaries ranged from $82,000 to $295,000 and $72,000 to $150,000, respectively (**TABLE 8**). These data should be viewed with caution, as the numbers reported in this category are small.

## Gender

Gender comparisons of salary information for program directors and faculty were performed (**TABLE 9**). Male program directors had approximately $5,000 higher salaries than female program directors. The data showed small differences in the salaries based on faculty genders.

**TABLE 9. Comparison of Salary in Dollars ($) by Gender**

| Institution | Program Directors | | | | Faculty Members | | | |
|---|---|---|---|---|---|---|---|---|
| | N | Median | Mean (SD) | Range | N | Median | Mean (SD) | Range |
| University | | | | | | | | |
| Female | 44 | 86,500 | 88,760 (21838) | 48,000–156,751 | 48 | 78,000 | 79,839 (17208) | 51,458–150,000 |
| Male | 14 | 91,000 | 105,987 (58150) | 65,000–295,000 | 18 | 81,500 | 80,133 (18165) | 51,000–109,887 |
| Hospital | | | | | | | | |
| Female | 45 | 86,860 | 87,524 (14817) | 63,711–135,000 | 51 | 73,000 | 78,671 (37541) | 50,000–300,000 |
| Male | 6 | 91,000 | 88,417 (19566) | 63,500–110,000 | 14 | 74,000 | 81236 (31968) | 48,000–180,000 |

*SD, standard deviation.*

## Discussion

The respondents of the survey matched the demographics of the laboratory workforce with 75% being female and 80% White/Caucasian. Responses from the 2020 survey were compared to the 2016 survey data. Both PDs and faculty at universities and hospitals have similar years of teaching experience. As in 2016, hospital PDs and faculty tend to have more experience in the clinical laboratory than university PDs and faculty. The salaries for both university and hospital program directors and faculty have increased at a greater rate than inflation over the last 4 years (cumulative inflation rate from 2016 to 2020 was 7.84%[4]). In general, individuals who have an advanced degree, are at a higher academic rank, tenured or on the tenure track, or hold a specialist certification in addition to MT/MLS certification, receive a higher salary.

Survey data showed that male faculty were more likely to have completed a postdoctorate degree and outnumbered the number of females at the doctorate level (when combined with the postdoctorate) and held a higher academic rank than female faculty. In both university and hospital programs, male program directors had a slightly higher median salary than females, but this may be skewed because of the small number of males who responded to the survey and the large range reported in university salaries. When comparing faculty salaries, males and female salaries were similar.

Interesting to note, when compared to 2016 data, there is a decrease in the percentage of faculty, for both genders, at the higher academic ranks. This may indicate more junior faculty have joined the faculty ranks. With approximately one-third of university and hospital program directors indicating that they plan to retire in the next 5 years, and with only around 50% having replacement plans, there is a need to grow faculty members to take on the program director role. With younger, less experienced faculty members, this may present a challenge to programs in the next few years.

In the conclusion, the ASCP Research and Development Committee plans to continue this survey on a regular basis and to expand it to other programs.

## REFERENCES


1. Brown K, Fenn JP, Fong, K, et al. ASCP Board of Certification Survey of Medical Laboratory Science Faculty. *Lab Med* 2019;50(4):e75–e81. doi:10.1093/labmed/lmz024.
2. Brown K, Fenn JP, Fong K, et al. ASCP Board of Certification Survey of Medical Laboratory Science Programs. *Lab Med*. 2019;50(4):370–e74. doi:10.1093/labmed/lmz019 Accessed November 8, 2021.
3. *NAACLS Standards for Accredited and Approved Programs. Adopted 2012, Revised 5/2021*. Website: http//www.naacls.org.
4. US Bureau of Labor Statistics CPI Inflation Calculator. Website: http//www.bls.gov/cpi Accessed November 8, 2021.

EDITORIAL

# Call for Emergency Action to Limit Global Temperature Increases, Restore Biodiversity, and Protect Health

## *Wealthy nations must do much more, much faster*[†]

*Lukoye Atwoli,[1] Abdullah H. Baqui,[2] Thomas Benfield,[3] Raffaella Bosurgi,[4] Fiona Godlee,[5] Stephen Hancocks,[6] Richard Horton,[7] Laurie Laybourn-Langton,[8,*] Carlos Augusto Monteiro,[9] Ian Norman,[10] Kirsten Patrick,[11] Nigel Praities,[12] Marcel G. M. Olde Rikkert,[13] Eric J. Rubin,[14] Peush Sahni,[15] Richard Smith,[16] Nick Talley,[17] Sue Turale,[18] Damián Vázquez[19]*

[1]Editor in Chief, East African Medical Journal; [2]Editor in Chief, Journal of Health, Population and Nutrition; [3]Editor in Chief, Danish Medical Journal; [4]Editor in Chief, PLOS Medicine; [5]Editor in Chief, The BMJ; [6]Editor in Chief, British Dental Journal; [7]Editor in Chief, The Lancet; [8]Senior Adviser, UK Health Alliance on Climate Change; [9]Editor in Chief, Revista de Saúde Pública; [10]Editor in Chief, International Journal of Nursing Studies; [11]Interim Editor in Chief, CMAJ; [12]Executive Editor, Pharmaceutical Journal; [13]Editor in Chief, Dutch Journal of Medicine; [14]Editor in Chief, NEJM; [15]Editor in Chief, National Medical Journal of India; [16]Chair, UK Health Alliance on Climate Change; [17]Editor in Chief, Medical Journal of Australia; [18]Editor in Chief, International Nursing Review; [19]Editor in Chief, Pan American Journal of Public Health; *To whom correspondence should be addressed. laurie.laybourn@ukhealthalliance.org

[†]This editorial is being published simultaneously in many international journals. Please see the full list here: https://www.bmj.com/content/full-list-authors-and-signatories-climate-emergency-editorial-september-2021

*Laboratory Medicine* 2022;53:e164–e166; https://doi.org/10.1093/labmed/lmab077

The UN General Assembly in September 2021 will bring countries together at a critical time for marshalling collective action to tackle the global environmental crisis. They will meet again at the biodiversity summit in Kunming, China, and the climate conference (COP26) in Glasgow, UK. Ahead of these pivotal meetings, we—the editors of health journals worldwide—call for urgent action to keep average global temperature increases below 1.5°C, halt the destruction of nature, and protect health.

Health is already being harmed by global temperature increases and the destruction of the natural world, a state of affairs health professionals have been bringing attention to for decades.[1] The science is unequivocal; a global increase of 1.5°C above the pre-industrial average and the continued loss of biodiversity risk catastrophic harm to health that will be impossible to reverse.[2,3] Despite the world's necessary preoccupation with COVID-19, we cannot wait for the pandemic to pass to rapidly reduce emissions.

Reflecting the severity of the moment, this editorial appears in health journals across the world. We are united in recognizing that only fundamental and equitable changes to societies will reverse our current trajectory.

The risks to health of increases above 1.5°C are now well established.[2] Indeed, no temperature rise is "safe." In the past 20 years, heat-related mortality among people aged over 65 has increased by more than 50%.[4] Higher temperatures have brought increased dehydration and renal function loss, dermatological malignancies, tropical infections, adverse mental health outcomes, pregnancy complications, allergies, and cardiovascular and pulmonary morbidity and mortality.[5,6] Harms disproportionately affect the most vulnerable, including among children, older populations, ethnic minorities, poorer communities, and those with underlying health problems.[2,4]

Global heating is also contributing to the decline in global yield potential for major crops, falling by 1.8–5.6% since 1981; this, together with the effects of extreme weather and soil depletion, is hampering efforts to reduce undernutrition.[4] Thriving ecosystems are essential to human health, and the widespread destruction of nature, including habitats and species, is eroding water and food security and increasing the chance of pandemics.[3,7,8]

The consequences of the environmental crisis fall disproportionately on those countries and communities that have contributed least to the problem and are least able to mitigate the harms. Yet no country, no matter how wealthy, can shield itself from these impacts. Allowing the consequences to fall disproportionately on the most vulnerable will breed more conflict, food insecurity, forced displacement, and zoonotic disease—with severe implications for all countries and communities. As with the COVID-19 pandemic, we are globally as strong as our weakest member.

Rises above 1.5°C increase the chance of reaching tipping points in natural systems that could lock the world into an acutely unstable state. This would critically impair our ability to mitigate harms and to prevent catastrophic, runaway environmental change.[9,10]

## Global Targets Are Not Enough

Encouragingly, many governments, financial institutions, and businesses are setting targets to reach net-zero emissions, including targets for 2030. The cost of renewable energy is dropping rapidly. Many countries are aiming to protect at least 30% of the world's land and oceans by 2030.[11]

These promises are not enough. Targets are easy to set and hard to achieve. They are yet to be matched with credible short and longer term plans to accelerate cleaner technologies and transform societies. Emissions reduction plans do not adequately incorporate health considerations.[12] Concern is growing that temperature rises above 1.5°C are beginning to be seen as inevitable, or even acceptable, to powerful members of the global community.[13] Relatedly, current strategies for reducing emissions to net zero by the middle of the century implausibly assume that the world will acquire great capabilities to remove greenhouse gases from the atmosphere.[14,15]

This insufficient action means that temperature increases are likely to be well in excess of 2°C,[16] a catastrophic outcome for health and environmental stability. Critically, the destruction of nature does not have parity of esteem with the climate element of the crisis, and every single global target to restore biodiversity loss by 2020 was missed.[17] This is an overall environmental crisis.[18]

Health professionals are united with environmental scientists, businesses, and many others in rejecting that this outcome is inevitable. More can and must be done now—in Glasgow and Kunming—and in the immediate years that follow. We join health professionals worldwide who have already supported calls for rapid action.[1,19]

Equity must be at the centre of the global response. Contributing a fair share to the global effort means that reduction commitments must account for the cumulative, historical contribution each country has made to emissions, as well as its current emissions and capacity to respond. Wealthier countries will have to cut emissions more quickly, making reductions by 2030 beyond those currently proposed[20,21] and reaching net-zero emissions before 2050. Similar targets and emergency action are needed for biodiversity loss and the wider destruction of the natural world.

To achieve these targets, governments must make fundamental changes to how our societies and economies are organized and how we live. The current strategy of encouraging markets to swap dirty for cleaner technologies is not enough. Governments must intervene to support the redesign of transport systems, cities, production and distribution of food, markets for financial investments, health systems, and much more. Global coordination is needed to ensure that the rush for cleaner technologies does not come at the cost of more environmental destruction and human exploitation.

Many governments met the threat of the COVID-19 pandemic with unprecedented funding. The environmental crisis demands a similar emergency response. Huge investment will be needed, beyond what is being considered or delivered anywhere in the world. But, such investments will produce huge positive health and economic outcomes. These include high-quality jobs, reduced air pollution, increased physical activity, and improved housing and diet. Better air quality alone would realize health benefits that easily offset the global costs of emissions reductions.[22]

These measures will also improve the social and economic determinants of health, the poor state of which may have made populations more vulnerable to the COVID-19 pandemic.[23] But, the changes cannot be achieved through a return to damaging austerity policies or the continuation of the large inequalities of wealth and power within and between countries.

## Cooperation Hinges on Wealthy Nations Doing More

In particular, countries that have disproportionately created the environmental crisis must do more to support low- and middle-income countries to build cleaner, healthier, and more resilient societies. High-income countries must meet and go beyond their outstanding commitment to provide $100bn a year, making up for any shortfall in 2020 and increasing contributions to and beyond 2025. Funding must be equally split between mitigation and adaptation, including improving the resilience of health systems.

Financing should be through grants rather than loans, building local capabilities and truly empowering communities, and should come alongside forgiving large debts, which constrain the agency of so many low-income countries. Additional funding must be marshalled to compensate for inevitable loss and damage caused by the consequences of the environmental crisis.

As health professionals, we must do all we can to aid the transition to a sustainable, fairer, resilient, and healthier world. Alongside acting to reduce the harm from the environmental crisis, we should proactively contribute to global prevention of further damage and action on the root causes of the crisis. We must hold global leaders to account and continue to educate others about the health risks of the crisis. We must join in the work to achieve environmentally sustainable health systems before 2040, recognizing that this will mean changing clinical practice. Health institutions have already divested more than $42bn of assets from fossil fuels; others should join them.[4]

The greatest threat to global public health is the continued failure of world leaders to keep the global temperature rise below 1.5°C and to restore nature. Urgent, society-wide changes must be made and will lead to a fairer and healthier world. We, as editors of health journals, call for governments and other leaders to act, marking 2021 as the year that the world finally changes course.

## Conflict of Interest

We have read and understood BMJ policy on declaration of interests and F.G. serves on the executive committee for the UK Health Alliance on Climate Change and is a Trustee of the Eden Project. R.S. is the chair of Patients Know Best, has stock in UnitedHealth Group, has done consultancy work for Oxford Pharmagenesis, and is chair of the Lancet Commission of the Value of Death. None further declared.

Provenance and peer review: Commissioned; not externally peer reviewed.

## REFERENCES

1 In support of a health recovery. https://healthyrecovery.net

2 Intergovernmental Panel on Climate Change. Summary for policymakers. In: *Global warming of 1.5°C. An IPCC special report on the impacts of global warming of 1.5°C above pre-industrial levels and related global greenhouse gas emission pathways, in the context of strengthening the global response to the threat of climate change, sustainable development, and efforts to eradicate poverty*. 2018. https://www.ipcc.ch/sr15/

3 Intergovernmental Science-Policy Platform on Biodiversity and Ecosystem Services. Summary for policymakers: the global assessment report on biodiversity and ecosystem services. 2019. https://ipbes.net/sites/default/files/2020-02/ipbes_global_assessment_report_summary_for_policymakers_en.pdf

4 Watts N, Amann M, Arnell N, et al. The 2020 report of the Lancet Countdown on health and climate change: responding to converging crises. *Lancet.* 2021;397:129–170.

5 Rocque RJ, Beaudoin C, Ndjaboue R, et al. Health effects of climate change: an overview of systematic reviews. *BMJ Open.* 2021;11:e046333. doi:10.1136/bmjopen-2020–046333

6 Haines A, Ebi K. The imperative for climate action to protect health. *N Engl J Med.* 2019;380:263–273.

7 United Nations Environment Programme and International Livestock Research Institute. *Preventing the next pandemic: zoonotic diseases and how to break the chain of transmission*. 2020. https://72d37324-5089-459c-8f70-271d19427cf2.filesusr.com/ugd/056cf4_b5b2fc067f094dd3b2250cda15c47acd.pdf

8 IPCC. 2019: Summary for policymakers. In: *Climate change and land: an IPCC special report on climate change, desertification, land degradation, sustainable land management, food security, and greenhouse gas fluxes in terrestrial ecosystems*. Forthcoming.

9 Lenton TM, Rockström J, Gaffney O, et al. Climate tipping points—too risky to bet against. *Nature.* 2019;575:592–595.

10 Wunderling N, Donges JF, Kurths J, Winkelmann R. Interacting tipping elements increase risk of climate domino effects under global warming. *Earth Syst Dyn.* 2021;12:601–619.

11 High Ambition Coalition. https://www.hacfornatureandpeople.org

12 Global Climate and Health Alliance. Are national climate commitments enough to protect our health? https://climateandhealthalliance.org/initiatives/healthy-ndcs/ndc-scorecards/

13 Climate strikers: Open letter to EU leaders on why their new climate law is 'surrender.' Carbon Brief 2020. https://www.carbonbrief.org/climate-strikers-open-letter-to-eu-leaders-on-why-their-new-climate-law-is-surrender

14 Fajardy M, Köberle A, MacDowell N, Fantuzzi A. *"BECCS deployment: a reality check."* Grantham Institute briefing paper 28, 2019. https://www.imperial.ac.uk/media/imperial-college/grantham-institute/public/publications/briefing-papers/BECCS-deployment---a-reality-check.pdf

15 Anderson K, Peters G. The trouble with negative emissions. *Science.* 2016;354:182–183.

16 Climate action tracker. https://climateactiontracker.org

17 Secretariat of the Convention on Biological Diversity. *Global biodiversity outlook 5*. 2020. https://www.cbd.int/gbo5

18 Steffen W, Richardson K, Rockström J, et al. Sustainability. Planetary boundaries: guiding human development on a changing planet. *Science.* 2015;347:1259855. doi:10.1126/science.1259855

19 UK Health Alliance. Our calls for action. http://www.ukhealthalliance.org/cop26/

20 Climate Action Tracker. *Warming projections global update: May 2021*. https://climateactiontracker.org/documents/853/CAT_2021-05-04_Briefing_Global-Update_Climate-Summit-Momentum.pdf

21 United Nations Environment Programme. *Emissions gap report 2020*. UNEP, 2020.

22 Markandya A, Sampedro J, Smith SJ, et al. Health co-benefits from air pollution and mitigation costs of the Paris Agreement: a modelling study. *Lancet Planet Health.* 2018;2:e126–e133. doi:10.1016/S2542-5196(18)30029-9

23 Paremoer L, Nandi S, Serag H, Baum F. Covid-19 pandemic and the social determinants of health. *BMJ.* 2021;372:n129.

# On labmedicine.com

Several articles featuring practical information are now available on labmedicine.com.

This month, the website features a paper by Ye et al regarding the CRP-to-lymphocyte ratio in patients with cirrhosis. In "Acquired Thrombotic Thrombocytopenic Purpura After BNT162b2 COVID-19 Vaccine: Case Report and Literature Review," Hammami et al present a case study of a patient with TTP occurring after a second dose of the BNT162b2 (Pfizer-BioNTech) COVID-19 vaccine. And finally, two surveys of MLS programs and faculty performed by ASCP give readers a picture of today's educational landscape.

Check out these articles and more on labmedicine.com.

**Lablogatory**

Recent contributions to the blog for medical laboratory professionals includes information on monkeypox, tick identification, and laboratory safety. To see why over half a million readers visited Lablogatory in 2021, visit labmedicineblog.com.



Published by Oxford University Press on behalf of American Society for Clinical Pathology, 2022.